CELLULAR MECHANISMS IN PRION-MEDIATED NEURODEGENERATION

A thesis submitted in partial fulfilment for the degree of Doctor of Philosophy to the University of London

by

Pelagia Deriziotis BSc (Hons) MSc

University College London

Declaration

I, Pelagia Deriziotis, confirm that the work presented in this thesis is my original research work. Where contributions of others are involved, this has been clearly indicated in the thesis.

Acknowledgements

First and foremost, I would like to thank my supervisor Dr Sarah Tabrizi for her teaching, advice and enthusiasm. My gratitude also goes out to Prof Parmjit Jat, my secondary supervisor. I would also like to acknowledge all past and current members of the MRC Prion Unit/Department of Neurodegenerative disease at the UCL Institute of Neurology for their intellectual and practical help over the last three years. I am also grateful to Ray Young for his assistance with figures.

My gratitude goes out to the members of 'Team Tabrizi': Dr Ralph André, Samira Rabbanian, Dr Rob Goold, Dr Kerri Kinghorn, Christine Butler-Cole, Anna Magnusson and Julie Moonga, for providing an inspiring and fun environment in which to learn and develop, as well as for being awesome friends! I wouldn't have made it without Sami's ever-lasting positive nature and friendship, whereas 'The *Ralphinator*' was the best lifestyle guru anyone could ask for! I would also like to thank my Prion Unit mates who got me through the drama associated with a PhD, especially Hazel Urwin for understanding and for always trying to get me out for a drink or two, Ilaria Mirabile for calming me down, Dr Malin Sandberg for listening, and of course my fellow TCG members, Laura D' Castro and Alex Swales! Thanks also to Dr Adrian Isaacs (2007 cook-off King) for passing on knowledge and wisdom! Last, but not least, thanks to Kevin Williams for always making me smile and Kate Perry for teaching me to accept certain words of the English language!

I also would like to thank Prion Unit scientists who have moved onto pastures new: Dr Liza Sutton, Dr Tim Szeto and Dr Melanie White. Also, thanks to Robert Cheyne for being a funny little crab! A special thank you goes out to Dr Mark Kristiansen, who taught me a great deal about science, is a good friend and helped me keep my sanity (for the most part)!

Above all, I would like to thank my parents and my brother, Giannis, for their constant support and understanding, as well as for their patience, encouragement and love. I also want to thank Sofia K., Anna N., Irene T., Tony E.K., Jason G., for always being there for me, even from far away, when I needed them most. Particular thanks to P.R.C for your *immense* patience, friendship, support and advice- words are not enough.

For my parents

'I decided that it was not wisdom that enabled [poets] to write their poetry, but a kind of instinct or inspiration, such as you find in seers and prophets who deliver all their sublime messages without knowing in the least what they mean.'

Socrates, in *"Apology"*, sct 21, by Plato

The most exciting phrase to hear in science, the one that heralds new discoveries, is not 'Eureka!', but 'That's funny...'

Isaac Asimov, US science fiction novelist and scholar

Abstract

Prion diseases are fatal neurodegenerative disorders of both humans and other animals. The cause of prion-mediated neurodegeneration by conversion of the normal cellular prion protein (PrP^{C}) to the disease-related isoform (PrP^{Sc}) remains unknown. Increasing evidence suggests a role for the ubiquitin proteasome system (UPS) in prion disease. PrP^{C} and PrP^{Sc} isoforms have been shown to accumulate in cells after proteasome inhibition, leading to increased cell death. The aim of this thesis was to investigate the role of cellular degradation systems, such as the UPS and autophagy, in prion-mediated cell death.

In UPS-mediated degradation poly-ubiquitinated substrates get degraded by the 26S proteasome, which comprises a 20S hydrolytic core and a 19S regulatory particle. Using a variety of biochemical methods, I report that abnormal β-sheet-rich PrP isoforms inhibit the catalytic activity of the 26S proteasome, by specifically inhibiting its β_1 and β_5 proteolytic subunits. Pre-incubating these PrP isoforms with an antibody raised against aggregation intermediates abrogates the inhibitory effect seen, consistent with an 'oligomeric' inhibitory species. Using open-gated yeast 20S proteasome mutants and conserved 19S ATPase C-terminal peptides containing an essential motif for gate-opening, this thesis describes findings supporting an inhibitory effect on proteasomal gating rather than a direct inhibitory effect on the active sites of the 20S proteasome. These C-terminal peptides open the gate in a 'key in a lock' fashion by docking into inter-subunit pockets in the α-ring of the 20S proteasome. In this system, the inhibitory effect of the β-sheet-rich PrP isoforms may be due to abnormal PrP competing with the C-terminal peptides for the inter-subunit pockets, thereby preventing gate-opening.

Proteins are also degraded by autophagy, a degradation pathway that has not been adequately characterised in prion disease. This thesis investigates potential roles autophagy may play in prion disease. Data presented here suggest that a) prions are cleared by autophagy, b) prion-infected cells have higher numbers of autophagosomes compared to uninfected controls, c) induction of autophagy ameliorates cell death after

proteasome inhibition, indicating cross-talk between the two protein-degradation pathways, and d) it is up-regulated *in vivo* at end-stage prion disease.

Table of Contents

Index of figures and tables

Abbreviation List

°C – degrees Celsius

Ab – antibody

AD – Alzheimer's disease

AEBSF – 4-(2-aminoethyl)benzenesulphonyl fluoride

Atg – autophagy related

ATP – adenosine 5'-triphosphate

ATPase – ATP hydrolyzing enzyme

AP – alkaline phosphatase

BCA – bicinchoninic acid

BSA – bovine serum albumin

BSE – bovine spongiform encephalopathy

cDNA – complementary deoxyribose nucleic acid

CJD – Creutzfeld-Jakob disease

CNS – central nervous system

CWD – chronic wasting disease

DAPI – 4',6-diamidinobenzidine

dH_20 – distilled water

ddH_20 – de-ionised distilled water

DMSO – dimethyl sulfoxide

DNA – deoxyribonucleic acid

dNTP – deoxynucleotide triphosphates

DTT – dithiotreitol

ECL – enhanced chemiluminescence

EDTA – ethylene diamine tetra-acetic acid

EPOX – epoxomicin

ER – endoplasmic reticulum

ERAD – endoplasmic reticulum associated degradation

FCS – foetal calf serum

FFI – Fatal familial insomnia

FITC – fluorescein isothiocyanate

FTIR – Fourier Transform Infrared Spectroscopy

FVB – Friend Virus B-type (mouse)

g – gravity (acceleration due to)

g – gram

GAPDH – glyceraldehyde-3-phosphate dehydrogenase

GFAP – glial fibrillary acidic protein

GFP – green fluorescent protein

GSCN – guanidinium thiocyanate

GSS – Gerstmann-Straussler-Scheinker syndrome

h – hour(s)

HD – Huntington's disease

HEPES – 4-(2-hydroxyethyl)-1-piperazineethanesulfonic acid

HRP – horseradish peroxidase

Hz – hertz

kDa – kilodalton

KO – knockout

LAMP-1 – lysosomal associated membrane protein-1

LDH – lactate dehydrogenase

M – molar

MEM – minimum essential medium

mg – milligrams

min – minute(s)

ml – milliliters

mM – millimolar

mRNA – messenger ribonucleic acid

MW – molecular weight

ng - nanogram

NGS – normal goat serum

PAGE – polyacrylamide gel electrophoresis

PBS – phopho-buffered saline

PBST – phosphate buffered saline with 0.5% Tween-20

PCR – polymerase chain reaction

PD – Parkinson's disease

PFA – paraformaldehyde

pH – hydrogen ion concentration

PK – proteinase K

PMSF – phenylmethylsuphonyl fluoride

PRNP – prion protein gene (human)

Prnp – prion protein gene (mouse)

PrP – prion protein

PrP^{C} – normal isoform of the prion protein

PrP^{Sc} – disease-associated prion protein

PVDF – polyvinylidene difluoride

RAP – rapamycin

RML – Rocky Mountain laboratory

RNA – ribonucleic acid

RNase – ribonuclease

rpm – revolutions per minute

ROS – reactive oxygen species

RT – room temperature

RT – reverse transcription

SCA – scrapie cell assay

sCJD – sporadic Creutzfeldt-Jakob disease

SD – standard deviation

SDS – sodium dodecyl sulphate

SEM – standard error of the mean

SOD – superoxide dismutase

TME – transmissible mink encephalopathy

UPS – ubiquitin proteasome system

UV – ultraviolet

v/v – volume in volume

vCJD – variant Creutzfeldt-Jakob disease

WT – wild-type

w/v – weight in volume

μg – micrograms

μl– microliters

μM – micromolar

1 INTRODUCTION

Prion diseases, also known as transmissible spongiform encephalopathies (TSEs), comprise a family of fatal neurodegenerative disorders. They affect both humans (i.e., Creutzfeldt-Jakob disease; CJD) and other animals (i.e., bovine spongiform encephalopathy; BSE), and can be transmitted within or between mammalian species by inoculation with, or dietary exposure to infected tissues. Although they are relatively rare - it is estimated that they affect one person per million worldwide annually - they remain in the spotlight due to the unique biology of the transmissible agent. According to the protein-only hypothesis, the main pathogenic event in prion disease is associated with a conformational re-arrangement of the normal cellular prion protein, PrP^{C} (C for cellular), to an abnormal isoform, PrP^{Sc} (Sc for scrapie). At the microscopic level, prion diseases share four principal neuropathological features, specifically spongiform vacuolation, marked neuronal loss, astrocytic and microglial proliferation, as well as an accumulation of the disease-associated isoform of the prion protein in the brain, sometimes accompanied by the formation of amyloid deposits. To date, the exact cause of prion-mediated neurodegeneration remains unclear and a major gap exists in the understanding of how the conversion of PrP^{C} to PrP^{Sc} ultimately kills neurones.

1.1 Animal prion diseases

The first prion disease, scrapie, was described in the 18^{th} century in Europe. Although it was not shown to be transmissible until 200 years later, it was believed that flocks of sheep could be infected by this disease. Descriptions of other animal prion diseases include chronic wasting disease of deer and elk, transmissible mink encephalopathy, BSE in cattle, and feline transmissible encephalopathies.

1.1.1 Scrapie

Scrapie is a naturally-occurring, common disease of sheep and goats, and is present worldwide. Its name is derived from the predominant clinical symptom, whereby the animal will scrape its fleece off due to an itching sensation caused by the disease. Symptoms include gait disorders and wool loss; death usually occurs between 6 weeks to 6 months after symptom onset. At present, its routes of transmission remain unclear; however, a hereditary link has been suspected because of a strong genetic element (Parry, 1979). In the 19th century, it was demonstrated that neuronal vacuolation was a characteristic neuropathological feature of the disease, but initial transmissibility studies of scrapie infection were negative. The failure to recognise the long incubation times of the disease was overcome by the inoculation of scrapie into goats (Cuillé and Chelle, 1936). The transmissibility of the infectious agent was further confirmed after scrapie was accidentally transmitted into sheep when a Scottish herd was inoculated against a virus with a brain, spleen and spinal cord extract from an infected animal (Gordon, 1946). Since then, scrapie has effectively been transmitted experimentally into other species including laboratory mice (Chandler, 1961), demonstrating that it can cross the 'species barrier' (**Section 1.4.6**). Scrapie has never been shown to pose a threat to human health (Brown and Bradley, 1998).

1.1.2 Chronic wasting disease

Chronic wasting disease (CWD) is a TSE affecting mule deer and elk, predominantly in the USA (Sigurdson and Aguzzi, 2007). It is the only TSE of free-ranging wildlife, affecting white deer, white-tailed deer, Rocky Mountain elk (Williams and Miller, 2002) and moose (Williams, 2005). Symptoms include weight loss and excessive drinking, and disease duration ranges from days to months. Experimental evidence has confirmed neuronal vacuolation (Williams and Young, 1980), the accumulation of aggregated prion protein (Spraker *et al.*, 2002) and prion infectivity in the brain (Browning *et al.*, 2004). Moreover, prion protein aggregates are not only found in the central nervous system (CNS), but also in lymphoid tissues, skeletal muscles and other organs. The origin and routes of

transmission are unclear (Miller and Williams, 2003; Mathiason *et al.*, 2006). As yet, there is no evidence for CWD transmission to humans.

1.1.3 Transmissible mink encephalopathy

Transmissible mink encephalopathy (TME) has been described in captive animals mainly in the USA and is believed to be an acquired prion disease (Marsh, 1992). Symptoms include aggression and loss of muscle coordination; following symptom onset animals die within 6 weeks. TME epidemics have occurred infrequently among ranched mink and it is thought they originated from scrapie-infected sheep or TSE-infected cattle in feeds (Marsh *et al.*, 1991). TME has been experimentally transmitted to hamsters (Kimberlin and Marsh, 1975) and although not thought to be related to BSE in cattle (**Section 1.1.4**), a study by Baron and colleagues noted similarities between TME and BSE in a mouse model (Baron *et al.*, 2007).

1.1.4 Bovine spongiform encephalopathy

BSE is a fatal neurodegenerative disorder in cattle. 'Mad cow disease', as it is also colloquially known, first appeared in the UK in the mid 1980s and evolved into a major epidemic (Wilesmith *et al.*, 1988; Anderson *et al.*, 1996). Since then, BSE cases have been recognised in many European countries, the US, Canada, Israel and Japan (www.BSEreview.org.uk). Epidemiological studies identified meat-and-bone-meal (MBM), a high protein supplement, which originates from tissue waste from various species, as the linking feature in all UK farms with BSE-positive cattle. Clinical symptoms include changes in temperament and movement disorders. Since 1986, approximately 180,000 cattle have developed the disease, with a one to three million thought to be infected prior to slaughter for human consumption (Anderson *et al.*, 1996; Donnelly *et al.*, 2002).

Two hypotheses have been put forward regarding the origin of BSE. First, neuropathological findings in BSE are similar to those seen in scrapie, so BSE may have arisen from either a scrapie-like agent from sheep or from cattle infected with a scrapie-

like agent (Wilesmith *et al.*, 1988; Wilesmith *et al.*, 1991; Smith and Bradley, 2003). However, the BSE strain is molecularly and biologically different to the strain causing scrapie, arguing against this hypothesis (Bruce *et al.*, 1994). Alternatively, perhaps a sporadic case of BSE arose by chance and was incorporated in MBM, which could have then seeded the epidemic (Weissmann and Aguzzi, 1997). Control measures, which were applied in 1988, but that were not always properly enforced, resulted in a steady decline of BSE in the UK. Nonetheless, BSE cases were still identified after the 1988 ban, and following the emergence of variant CJD in 1996 (Will *et al.*, 1996; Collinge and Rossor, 1996), the ban was re-enforced. The route of BSE transmission is thought to be oral. European countries enforced the 1996 UK ban in 2001 and due to the long incubation time of the disease (usually 5 years), further cases are likely to be identified.

1.1.5 Other animal prion diseases

In addition to the animal TSEs described above, prion diseases with links to BSE have been described in other species, such as in domestic and captive exotic cats. Feline TSE was first reported in domestic cats in the UK (Leggett *et al.*, 1990). Reports of prion disease have also been described in greater kudu, tiger, and cheetah. These TSEs appeared during or after the emergence of BSE, and studies have confirmed that some are caused by a BSE-like strain (Bruce *et al.*, 1994; Collinge *et al.*, 1996a).

1.2 Human prion diseases

Human prion diseases are rare and fatal disorders, and include CJD, Gerstmann-Sträussler-Scheinker disease (GSS), fatal familial insomnia (FFI) and kuru (Wadsworth and Collinge, 2007). Uniquely, they may arise spontaneously, be genetically inherited, or acquired *via* infection, and they all have the potential to be transmissible. Clinical features comprise rapidly progressive dementia accompanied by cerebellar ataxia and myoclonus. Definitive diagnosis can be made from post-mortem examination of brain tissue showing the classical histopathological triad: spongiform change, severe neuronal loss and marked astrogliosis; these are sometimes accompanied by PrP^{Sc}-containing amyloid plaque deposits. Inherited forms of prion disease support the protein-only hypothesis of prion propagation (**Section 1.4**) and highlight the importance of PrP^{C} in disease. A polymorphism at amino acid residue 129 of the prion protein [which encodes methionine (M) or valine (V)] confers genetic susceptibility for development of prion disease. Thirty-eight per cent of Europeans are homozygous for M at codon 129, 51% are heterozygous and 11% are homozygous for V (Palmer *et al.*, 1991). Methionine homozygotes (codon 129MM) are at a higher risk of developing prion disease, which may be explained by the increased propensity of PrP to form PrP^{Sc}-like structures *in vitro* (Tahiri-Alaoui *et al.*, 2004), whereas heterozygosity (codon 129MV) is thought to confer resistance to disease by inhibiting homologous PrP protein-protein interactions (Palmer *et al.*, 1991).

1.2.1 Sporadic prion disease

Sporadic CJD (sCJD) affects one per million population per year worldwide (Caramelli *et al.*, 2006). It is a rapidly progressive multifocal dementia with an age of onset between 45-75 years and a mean duration of 5 months (Brown *et al.*, 1984; Collins *et al.*, 2006). Individuals initially experience insomnia, depression and ill-defined pain sensations, as well as manifesting movement disorders. Definitive diagnosis of sCJD is by post-mortem or brain biopsy. PrP amyloid plaques are not typically present in sCJD, but PrP immunohistochemistry is nearly always positive (Budka, 2003). sCJD accounts for 85% of human prion disease cases, all of which have been documented in patients with no family

history of prion disease and no known exposure to prions. Therefore, although a genetic or infectious cause cannot be excluded in all cases, the aetiology of sCJD is uncertain. The two main possible causes are either spontaneous somatic *PRNP* mutation (Brown *et al.*, 1987; Collinge, 1997; Wadsworth *et al.*, 2006), or spontaneous conversion of PrP^{C} to PrP^{Sc} as a rare stochastic event (Collinge, 1997). Interestingly, two case-control studies have reported prior surgery as a risk factor for sCJD and therefore raise the possibility that sCJD may be an acquired illness (Collins *et al.*, 1999; Ward *et al.*, 2002). As aforementioned, susceptibility to human prion disease is influenced by a polymorphism at residue 129 of human PrP (Mead, 2006), and homozygosity predisposes to sporadic and acquired forms of CJD. Moreover, genetic studies have revealed polymorphisms upstream of exon 1 of the *PRNP* gene (Mead *et al.*, 2001) and an 129MV independent polymorphism in the 5' un-translated region (UTR) of the *PRNP* gene (Vollmert *et al.*, 2006), both of which have been associated with sCJD.

1.2.2 Inherited prion disease

Around 15% of human prion disease cases are associated with autosomal dominant mutations of the *PRNP* gene (Masters *et al.*, 1981b; Windl *et al.*, 1999). Inherited prion diseases comprise GSS, FFI and familial CJD (fCJD), and confer strong evidence for the protein-only hypothesis of prion propagation (**Section 1.4**). The first reports of *PRNP* mutations described insertion and missense mutations in families with dominantly inherited neurodegenerative diseases (Owen *et al.*, 1989; Hsiao *et al.*, 1989). There are three types of *PRNP* mutation: point mutations leading to amino acid substitutions or premature stop codons, or octapeptide repeat insertions (OPRI). Over thirty distinct mutation types have been documented (Mead, 2006) (**Figure 1.1**) and *PRNP* analysis allows for pre-symptomatic diagnosis of inherited prion disease (Collinge, 2005). Clinical symptoms and neuropathology differ depending on the type of mutation involved, and occasionally variation occurs even within the same PrP mutation (Chapman *et al.*, 1993; Barbanti *et al.*, 1996; Wadsworth *et al.*, 2006). The fact that a single *PRNP* mutation can elicit different phenotypes highlights the importance of additional environmental and

epigenetic factors in prion disease pathogenesis. So far, it is unclear how *PRNP* mutations cause disease. It has been hypothesised that they may favour the tendency of the normal prion protein, PrP^{C}, to form abnormal infectious isoforms (PrP^{Sc}). Nonetheless, studies have reported that pathogenesis in inherited prion diseases may not only be due to a decreased thermodynamic stability of mutated PrP^{C} and indicated that subtle structural differences in the mutant proteins may affect inter-molecular signalling in various ways (Riek *et al.*, 1998; Swietnicki *et al.*, 1998). Moreover, spontaneous disease without any detectable protease-resistant PrP in experimental models with *PRNP* mutations has been described (Muramoto *et al.*, 1997; Hegde *et al.*, 1998).

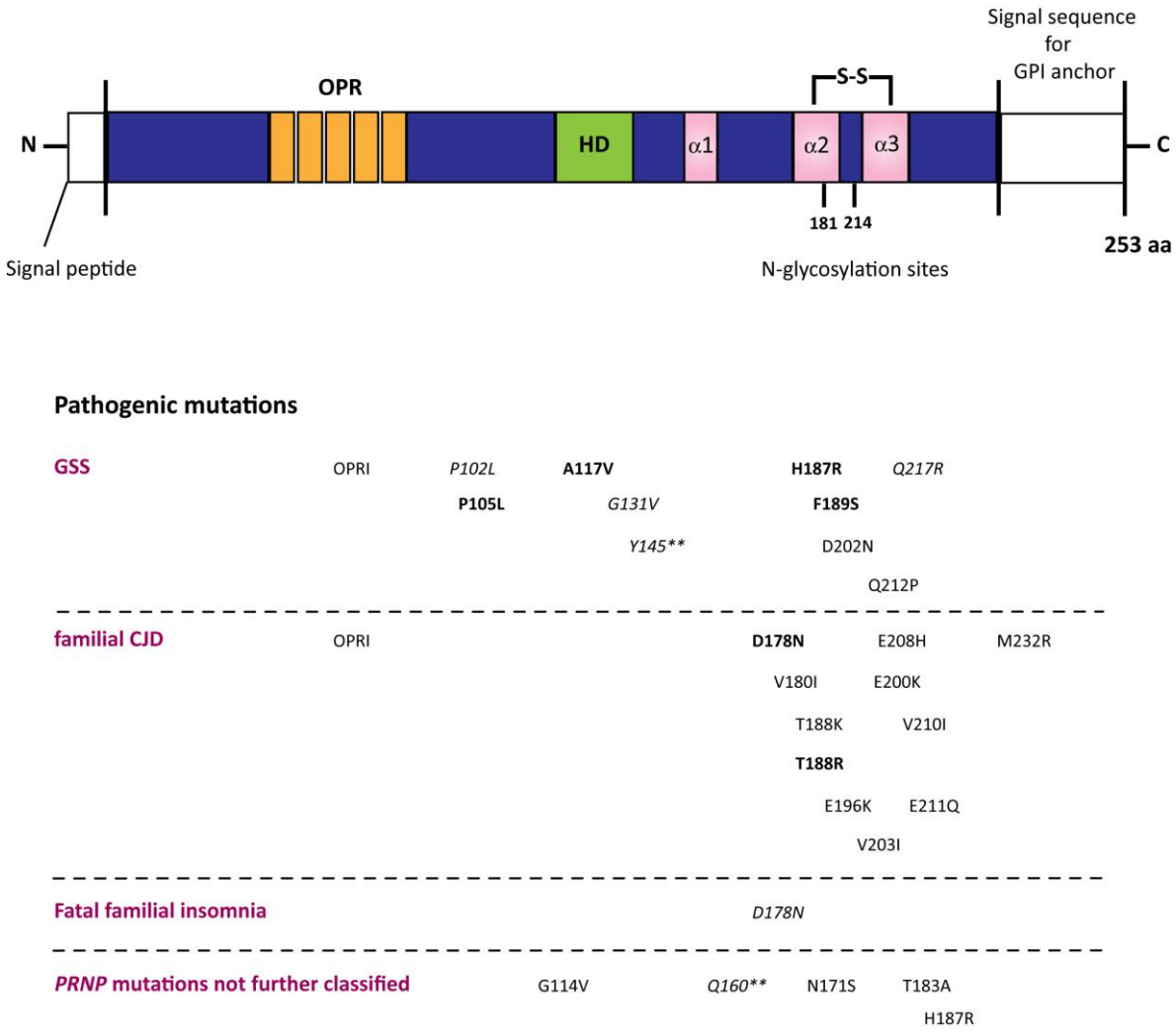

Figure 1.1 The human prion protein and pathogenic mutations[1]

Human PrP comprises two signal peptides (white), an octapeptide repeat region (OPR) (orange), a hydrophobic domain (HD) (green), three α-helices (pink), one di-sulphide bond (S-S) between cysteine residues 179 and 214, and two potential N-glycosylation sites. Included in this figure are point mutations and insertions found in *PRNP* in patients with prion disease. The associated polymorphisms at codon 129 are indicated in italics for methionine and bold for valine. ** denotes a stop codon, which results in truncated PrP.

1 Adapted and reprinted, with permission from Ann. Rev. Neurosci. Aguzzi, A., *et al.*, The Prion's elusive reason for being, Vol 31, pp 439-477, © 2008 by Annual Reviews http://www.annualreviews.org

1.2.3 Acquired prion disease

Kuru

Kuru was the first known human acquired prion disease, which emerged as a major epidemic in the 1950s as a result of endo-cannibalism in the Fore linguistic tribe of the Eastern Highlands of Papua New Guinea (Mead *et al.*, 2003). Kuru represents the only known example of a human prion disease epidemic and has provided much of the knowledge we have regarding acquired human prion disease. Kuru predominantly affected women and children who practised cannibalism as a sign of respect and mourning for deceased relatives (Alpers M, 1987). The epidemic is thought to have started when an individual with sCJD was consumed at one of these ritual feasts. Thereafter, prion recycling is the most likely reason for the extent of the epidemic. Following the ban of cannibalism by the Australian government in the late 1950s, there have been no new kuru cases (Lindenbaum, 1979). Clinically, kuru is a cerebellar syndrome with an almost complete absence of dementia (Alpers M, 1987). Disease onset ranges from 5->60 years, whilst its duration can last from 3 months to 3 years. Kuru incubation periods vary, from as little as 4.5 years to over 50 years (Collinge *et al.*, 2006). The residue 129 genotype has a profound effect on incubation period and susceptibility to kuru, with the MM genotype having the shortest incubation period (Lee *et al.*, 2001a), followed by VV homozygotes; MV heterozygotes (the most resistant genotype) have been reported to show incubation times >50 years (Collinge *et al.*, 2006). Strikingly, 129 homozygotes have been essentially eliminated as kuru imposed a strong balancing selection on the Fore population. Elderly women survivors of the kuru epidemic, who were previously exposed to mortuary feasts, are predominantly *PRNP* 129 heterozygotes (Lee *et al.*, 2001a; Mead *et al.*, 2003).

Iatrogenic CJD

Although transmissible in the laboratory, human prion disease is not contagious. Cases of acquired prion disease are limited to cannibalism (kuru) and accidental exposure to human prions. Routes of unintentional inoculation documented include: a) use of inappropriately sterilised surgical instruments or intra-cerebral electroencephalogram

(EEG) electrodes, b) dura mater grafts, c) corneal grafting, and d) use of human cadaveric pituitary-derived growth hormone or gonadotrophin. The two most frequent causes of iatrogenic CJD (iCJD) are from dura mater grafts and hormone administration (Brown *et al.*, 1992; Brown *et al.*, 2000). Interestingly, cases in which prion disease was acquired *via* an intra-cerebral or optic route clinically present with a rapidly progressive dementia, similar to sCJD (Heath *et al.*, 2006). In contrast, cases from peripheral inoculation manifest with progressive ataxia as a prominent early symptom, rather than dementia, in a manner similar to kuru (Wadsworth and Collinge, 2007).

Variant CJD

A novel human prion disease, variant CJD (vCJD), emerged in 1995 in the UK (Will *et al.*, 1996; Collinge and Rossor, 1996) and has affected ~ 170 individuals in the UK to date (www.cjd.ed.ac.uk/figures.htm). Suspicions of a link between BSE and vCJD were raised because they arose at the same time. In agreement, a plethora of experimental evidence at the clinical, neuropathological and molecular level has shown that vCJD is caused by the same prion strain as BSE in cattle (Collinge *et al.*, 1996b; Bruce *et al.*, 1997; Hill *et al.*, 1997; Asante *et al.*, 2002). This raised the possibility that an epidemic could occur in the UK and other countries as a result of dietary or other exposure (Ghani *et al.*, 1998; Collinge, 1999). Human infection with BSE involves cross-species transmission and this may confer a substantial prolongation of incubation time. Therefore, vCJD poses a potentially serious threat to public health. Moreover, a considerable number of people may have already been infected and are incubating the disease with the potential to pass it on *via* blood transfusion, blood products, organ and tissue transplantation, or other iatrogenic routes (Collinge, 1999; Wadsworth *et al.*, 2001; Peden *et al.*, 2005). This has already been highlighted by the efficient secondary transmission of infection by blood transfusion (Llewelyn *et al.*, 2004; Peden *et al.*, 2004; Wroe *et al.*, 2006), and at present there is no screening test to ensure the safety of blood products. Furthermore, subclinical forms of prion disease have also been recognised in animals that do not develop clinical disease during a normal life-span, but have high levels of infectivity and PrP^{Sc} (Hill and

Collinge, 2003a; Hill and Collinge, 2003b). Therefore, although the number of confirmed vCJD cases is small in relation to the number of individuals who have been potentially exposed, the actual number of infected people remains unknown. Epidemiological estimates of subclinical infection, which were based on archived surgical instruments, currently predict that a relatively high number of individuals (>1000) may be subclinically infected (Hilton *et al.*, 2004).

Clinically, vCJD is characterised predominantly by behavioural and psychiatric disturbances (Spencer *et al.*, 2002). Individuals initially present with progressive cerebellar symptoms and, unlike sCJD, develop dementia later. Age of onset ranges between 16-51 years and disease duration varies from 9-35 months (Knight, 2006). At the neuropathological level, vCJD is characterised by widespread spongiosis of the brain, accompanied by marked gliosis and neuronal loss (Will *et al.*, 1996) (**Figure 1.2A**). In sharp contrast to sCJD, immunohistochemistry has shown that PrP^{Sc}-positive 'florid amyloid plaques' are present in high numbers both in the cerebrum and cerebellum (Will *et al.*, 1996). These florid plaques are reminiscent of those usually seen in scrapie and in kuru (Alpers M, 1987). Moreover, unlike in other human prion diseases, PrP^{Sc} has been detected in non-CNS tissues such as in the lymporeticular system, ocular tissue and skeletal muscle (Wadsworth *et al.*, 2001; Peden *et al.*, 2006). Recently, a study also demonstrated the transmission of vCJD from human rectal tissue to transgenic mice (Wadsworth *et al.,* 2007).

As mentioned above, there is very strong evidence that dietary exposure to BSE is the cause of vCJD, as vCJD-infected individuals were resident in the UK during the BSE epidemic (Will *et al.*, 1996; Collinge and Rossor, 1996). Moreover, transmission studies in transgenic mice have demonstrated a close correlation between BSE and vCJD (Bruce *et al.*, 1997; Hill *et al.*, 1997). A further line of evidence supporting the link between BSE and vCJD comes from molecular strain-typing analysis of the disease-associated prion protein (**Section 1.4.6**). This involves analysis of SDS-PAGE PrP migration patterns following proteinase K (PK) digestion, which is used to distinguish the normal cellular isoform from the disease-related PrP as they display different sensitivities to enzymatic digestion (**Section 1.4.1 and 1.4.4 and Figure 1.3**). Such studies have demonstrated that vCJD prions

are a distinct prion strain compared to other CJD forms (types 1-3), designated type 4 (**Figure 1.2B**; **Section 1.4.6**). Migration patterns of vCJD show the same migration patterns as the BSE strain (Collinge *et al.*, 1996b). Firm diagnosis of vCJD, both ante- and post-mortem, is achieved by tonsil biopsy (for presence of type 4 PrP^{Sc}); the presence of PrP^{Sc} in tonsil is only detectable in vCJD, suggestive of a distinct pathogenesis (**Figure 1.2B**).

To date, no study has identified unusual occupational or dietary exposure of vCJD-affected individuals to BSE, suggesting that genetic susceptibility factors may be important. All clinical vCJD cases documented have been homozygous for methionine at codon 129 (Collinge *et al.*, 1996a; Hill *et al.*, 1999). This represents the strongest association of a genotype with a disease, but it is not the only genetic locus shown to be associated with prion disease. Mouse quantitative trait locus studies have shown that regions unrelated to *Prnp* play a role in the inconsistent incubation periods in prion disease, including in BSE (Stephenson *et al.*, 2000; Lloyd *et al.*, 2001; Lloyd *et al.*, 2002). Furthermore, a genome-wide association study by Mead and colleagues has recently identified two novel candidate loci, *RARB* and *STMN2*, as potential vCJD risk factors (Mead *et al.*, 2009).

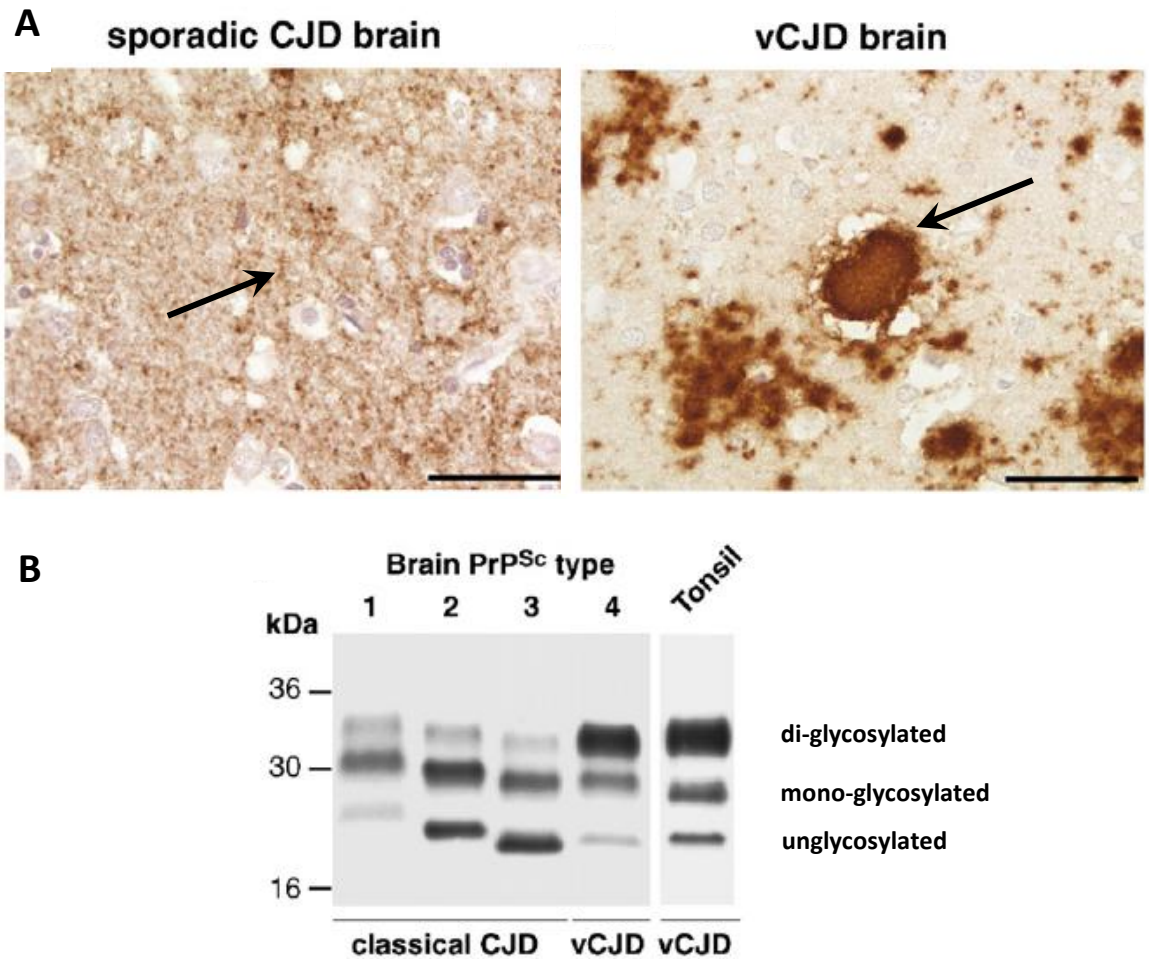

Figure 1.2 Characterisation of disease related prion protein in human prion disease[2]

(A) Brains from patients with sporadic CJD or vCJD show abnormal immunoreactivity following immunohistochemistry using anti-PrP monoclonal antibody ICSM35. Abnormal PrP deposition in sporadid CJD brain most commonly presents as diffuse, synaptic staining, whereas vCJD brain is distinguished by the presence of florid PrP plaques consisting of a round amyloid core of PrP surrounded by a ring of spongiform vacuoles (black arrows). **(B)** Immunoblot of PK-digested tissue homogenate with anti-PrP monoclonal antibody 3F4 showing PrP types 1-4 in human brain and PrP^{Sc} type 4t in vCJD tonsil. Types 1-3 PrP^{Sc} are seen in the brain of classical forms of CJD (either sporadic or iatrogenic CJD), while type 4 PrP^{Sc} and type 4t PrP^{Sc} are uniquely seen in vCJD brain or tonsil, respectively. Scale bars 50 μm.

2 Reprinted from BBA Molecular Basis of Disease, Vol. 1772, Wadsworth, J.D.F. and Collinge, J., Update on human prion disease, pp 598-609, © 2007 with permission from Elsevier.

1.3 Neuropathology and diagnosis of human prion disease

Prion disease is diagnosed clinically and confirmed at post-mortem by histopathological examination of brain tissue, with the accumulation of the conformationally abnormal isoform of the prion protein, PrP^{Sc}, a consistent marker of disease (Kubler *et al.*, 2003). To date, there is no diagnostic test to detect prion disease in humans, thus neuropathological profiles are the most significant tools for definitive diagnosis (Budka, 2003). The hallmark of prion disease comprises the classical histopathological triad, which includes spongiform change, marked neuronal loss and glial proliferation. As a rule, samples are collected from various brain areas of a suspected case. However, one tissue specimen showing the hallmark histological changes or that stains positive for PrP is adequate for diagnosis.

Grey matter is predominantly affected, but cases where white matter is affected too have also been described (Park *et al.*, 1980). Spongiform change is the most characteristic change in prion disease, and is distinguished by disperse or clustered vacuoles in the cerebellum or subcortical grey matter (Budka, 2001). Spongiform change may be mild, moderate or severe, is found rarely in the brainstem and spinal cord (although both stain positive for PrP^{Sc}), and occasionally may not even be present (Almer *et al.*, 1999). Despite their supposed specificity to prion disease, such spongiform changes have also been reported in Alzheimer's disease (AD) and diffuse Lewy body diseases (Budka *et al.*, 1995). Moreover, spongiform change distribution may vary according to the size of PrP^{Sc} fragments, *PRNP* genotype and glycoform ratio (Parchi *et al.*, 1999; Hill *et al.*, 2003).

In cases where spongiform change is ambiguous or absent, other diagnostic tools, such as *PRNP* genotyping and positive PrP^{Sc} immunohistochemistry are necessary to confirm a suspected prion disease case. Although immunohistochemistry is an invaluable tool for prion disease diagnosis, occasionally prion diseases, such as FFI, may be negative for PrP staining (Brown *et al.*, 1994b). It is also important to note that PrP^{Sc} quantity and localisation does not always correlate with the type and severity of local tissue damage, and that PrP^{Sc} does not always associate with infectivity, and *vice versa*. Crucially, PrP^{Sc} deposition and infectivity are found predominantly in the CNS of sCJD, iatrogenic CJD and

genetic prion disease cases, in contrast to vCJD where peripheral tissues are also affected, especially in the lymphoid system (Hilton *et al.*, 2002). Neuropathological criteria for the diagnosis of human prion disease are summarised in **Table 1.1**.

Prion disease	Criteria
CJD *Sporadic* *Iatrogenic* *Familial*	Spongiform encephalopathy in cerebral and/or cerebellar cortex and/or subcortical grey matter; and/or encephalopathy with PrP immunoreactivity (plaque and/or diffuse synaptic and/or patchy/perivacuolar types)
vCJD	Spongiform encephalopathy with abundant PrP deposition, particularly multiple fibrillary plaques surrounded by a halo of spongiform vacuoles ('florid') and other PrP plaques, and amorphous pericellular and perivascular PrP deposits especially prominent in the cerebellar molecular layer
GSS	Encephalo(myelo)pathy with multicentric PrP plaques
FFI	Thalamic degeneration with variably spongiform change in the cerebrum
Kuru	Spongiform encephalopathy in the Fore population in Papua New Guinea

Table 1.1 Neuropathological criteria for diagnosis of human prion disease[3]

3 From the World Health Organisation, http://www.WHO.int

1.4 Protein-only hypothesis of prion transmission

1.4.1 Biochemical properties of the infectious agent

Prion diseases have been termed as 'transmissible dementias' because of the successful transmission of such disease in laboratory animals. As aforementioned, scrapie has been transmitted experimentally in mice and studies by C. Gajdusek in 1966 showed transmission of kuru to monkeys (Gajdusek *et al.*, 1966). Subsequently, CJD and GSS have also been transmitted to monkeys (Gibbs *et al.*, 1968; Masters *et al.*, 1981a). The nature of the causative agent has been the focus of intense research. The isolation of the infectious particle has been costly and time consuming, as much of the early work was originally done in sheep or goats. Since the development of the mouse/hamster bioassay however, there is now ample information about the physico-chemical properties of the infectious agent. For example, it has been shown to associate with cellular membranes (Mould *et al.*, 1965; Hunter and Millson, 1967), co-purify with microsomes (Semancik *et al.*, 1976), detach from membranes following ultracentrifugation regimes (Malone *et al.*, 1978), and have different densities in sucrose and NaCl (Siakotos *et al.*, 1976; Brown *et al.*, 1978). The infectious agent is also aggregation-prone and hydrophobic in nature (Prusiner *et al.*, 1978; Prusiner *et al.*, 1980a), and has a remarkable resistance to procedures which modify nucleic acids, such as ultraviolet and ionizing radiation, nucleases, hydroxylamine and zinc ions (Alper *et al.*, 1967; Alper *et al.*, 1978; Prusiner, 1982). Furthermore, conditions that are non-denaturing to proteins allow for its separation from other cellular components (Prusiner *et al.*, 1977; Prusiner *et al.*, 1980b). These and other studies showing that it has partial resistance to nuclease digestion and to some forms of protease treatment (Prusiner *et al.*, 1980c), formed the basis for further purification methods.

1.4.2 Proteinaceous infectious particle

Physicist J.S. Griffith first raised the possibility in 1967 that the material responsible for prion disease transmission might be a protein able to replicate in the body (Griffith, 1967). In order to confirm a protein-like agent, the protein had to be purified and

characterised. Experimental evidence that a protein could also be infectious came from the transmission of scrapie into Syrian golden hamsters (Prusiner *et al.*, 1980b; Prusiner *et al.*, 1982b). In 1981, Stanley B. Prusiner's work culminated in a partial purification protocol for the infectious agent, which included ultracentrifugation and PK treatments (Prusiner *et al.*, 1981). These results provided firm evidence against the pathogen being a slow virus, as was originally proposed due to its long incubation period characteristics (Cho, 1976), and to date no evidence supports the notion that a nucleic acid is associated with prion infection. The term 'prion' was first coined by Prusiner in 1982 to distinguish the infectious agent in prion disease as a pathogen from bacteria, fungi, parasites and viruses, and refers to a 'small, proteinaceous infectious particle that resists inactivation by procedures which modify nucleic acids' (Prusiner, 1982). Later, Prusiner and colleagues adapted their previous purification protocols by the addition of a sucrose gradient step and were able to isolate the major constituent of infective fractions from hamster brain homogenates (Prusiner *et al.*, 1982a). Subsequent experiments showed that the major constituent was a 27-30 kDa protease-resistant protein designated PrP^{27-30} (Bolton *et al.*, 1982). A protein of similar size was identified in uninfected brain, but unlike the disease-associated protein it was digested by PK treatment (Bolton *et al.*, 1982). The identity of the disease-associated protein as a component of the infectious agent, rather than a product of disease, has been confirmed by studies showing a correlation of infectivity and PrP^{27-30} concentration (Bolton *et al.*, 1982; Prusiner *et al.*, 1982a; Hope *et al.*, 1986; Safar *et al.*, 1990). PrP^{27-30} originates from a protein with a molecular weight of 33-35 kDa, designated PrP^{Sc}. Identification of the amino acid sequence of the prion protein allowed for further analysis and the production of anti-PrP antibodies (Bendheim *et al.*, 1984), which do not however distinguish between normal and disease-associated material.

1.4.3 Prion protein gene

Following purification of the prion protein, the gene encoding PrP was identified. Amino acid sequencing of the N-terminus of PrP^{27-30} was used to derive a cDNA clone encoding a host protein, which subsequently demonstrated that PrP^{27-30} was encoded by a

single-copy chromosomal gene (Oesch *et al.*, 1985; Basler *et al.*, 1986). The presence of PrP mRNA in the brains of both infected and unaffected animals (Barry *et al.*, 1986) provided evidence that PrP could exist in two different forms: the normal cellular isoform termed PrP^{C} and the disease-associated form, PrP^{Sc}. To date, there is no proof to support the notion that the PrP gene undergoes re-arrangement during disease, and there has been no genetic basis for alternative splicing (Basler *et al.*, 1986). Additionally, studies have demonstrated that PrP mRNA does not increase during the course of prion disease (Oesch *et al.*, 1985). Amino acid sequencing studies of the N-terminus of PrP^{C} and PrP^{Sc} reported vast similarities between the two and raised the possibility that the observed difference(s) are due to post-translationals events (Turk *et al.*, 1988). Sequencing of the PrP open reading frames (ORF) from various species has demonstrated that they encode a highly conserved protein of about 250 amino acids. Its presence in mammals, but also other vertebrates such as birds, marsupials and amphibians, suggests an important role that is evolutionary conserved (Windl *et al.*, 1995; Wopfner *et al.*, 1999; Calzolai *et al.*, 2005).

1.4.4 Biochemical properties of PrP^{Sc}

Purified full-length PrP^{Sc} is insoluble in non-ionic detergents and has partial protease resistance, with only the N-terminal third of the sequence being cleaved leaving a protease-resistant core, $PrP^{27\text{-}30}$, which retains infectivity (Riesner, 2003). The increased propensity of PrP^{Sc} to aggregate correlates with its resistance to PK digestion (**Figure 1.3**). The C-terminus of PrP^{Sc} can be digested by cathepsin D, which liberates the glycosylphosphatidylinositol (GPI) anchor, but retains prion infectivity (Lewis *et al.*, 2006). Moreover, transgenic mice expressing PrP lacking a GPI anchor can propagate prions (Chesebro *et al.*, 2005), thereby suggesting that the GPI anchor is not a prerequisite component of the infectious prion. Unlike PrP^{C}, which can be readily cleaved from membranes by treatment with phosphatidylinositol-specific phospholipase C (PIPLC) (Stahl *et al.*, 1987), PrP^{Sc} is resistant to such treatment (Caughey *et al.*, 1990; Borchelt *et al.*, 1993) suggesting a conformational change prevents accessibility of PIPLC. Indeed,

evidence suggests the conversion of PrP^{C} to PrP^{Sc} does not involve a covalent modification (Stahl *et al.*, 1993), but is conformational in nature (Pan *et al.*, 1993; Cohen *et al.*, 1994).

Insight into the native conformation has been hindered by the insolubility and aggregation state of PrP^{Sc}. Nonetheless, Fourier Transform Infrared Spectroscopy (FTIR) and circular dichroism studies have demonstrated that unlike PrP^{C}, which is predominantly α-helical, PrP^{Sc} is β-sheet-rich dominant (Gasset *et al.*, 1993; Pan *et al.*, 1993). β-sheet content in PrP^{Sc} comprises 45% compared to 3% in PrP^{C}. The protease-resistant core of PrP^{Sc} has been shown to re-arrange into amyloid rods, which stain with Congo red and show green-gold birefringence, typical of amyloids (Prusiner *et al.*, 1983). Interestingly, PrP^{Sc} deposits of varying size and morphology, including amyloid plaques, have been identified in scrapie-infected animal brain tissue (Merz *et al.*, 1981). Nonetheless, no experimental evidence supports the presence of fibrils in human prion disease (Budka, 2003), although studies using synthetic fibrils have provided some insight into prion conformation (Baskakov *et al.*, 2002; Tattum *et al.*, 2006). Furthermore, although the nature of the self-propagating infectious agent is unknown, recent studies have demonstrated that small PrP oligomers of 14-28 molecules were maximally infective when compared to monomeric or fibrillar PrP (Silveira *et al.*, 2005).

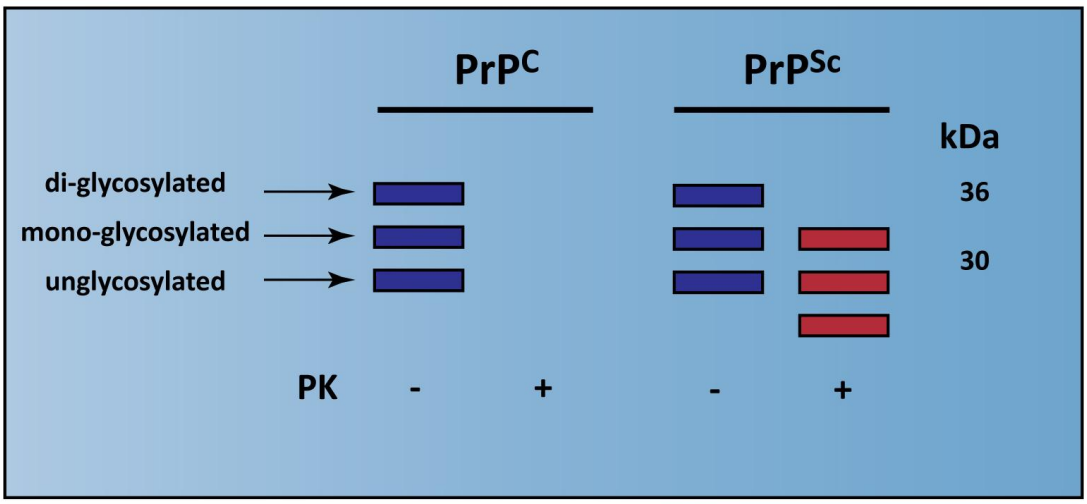

Figure 1.3 Proteinase K resistance of PrP

Schematic of a characteristic Western blot of SDS-electrophoresis of PrP^{C} and PrP^{Sc} without and with PK digestion. The characteristic three PrP bands (with two, one or none glycosyl groups; blue) are visible and disappear completely after PK digestion of PrP^{C}. In the case of PrP^{Sc}, the bands remain nearly undiminished in intensity although shifted to lower molecular weight (red) and represent the N-terminally truncated forms of PrP^{Sc}, called PrP^{27-30}.

1.4.5 Models of PrP^{Sc} replication

Following the discovery that PrP is host-encoded, much research has focused on elucidating differences between PrP^{C} and PrP^{Sc}. Although it is now known that the two isoforms share the same amino acid sequence, they have diverse biochemical properties (Prusiner, 1998). Therefore, the differences between the two isoforms appear to be due to post-translational modifications or simply conformational change. Research has focused on the refolding properties of recombinant PrP to either the normal or the disease-related isoform.

The protein-only hypothesis, which postulates that prion propagation results from a change in PrP conformation whereby PrP^{Sc} recruits endogenous PrP^{C} in order to replicate (Griffith, 1967; Prusiner, 1982), is well established. Some of the strongest supporting evidence comes from findings that inherited prion diseases are linked to mutations in the *PRNP* gene (Collinge, 2001), indicating that a genetic disease may be able to propagate in an infectious way. Another important line of evidence comes from PrP^{C} knockout (KO) mice, which are resistant to scrapie prions (Bueler *et al.*, 1993). Furthermore, infectious prions have been shown to consist mainly or exclusively of PrP^{Sc}, as indicated by a large body of experimental data. Using an *in vitro* amplification system Kocisko *et al.* showed *de novo* PrP^{Sc} production using radio-labelled PrP^{C} and a PrP^{Sc} seed (Kocisko *et al.*, 1994). However, these *in vitro* conversion methods were inefficient in transmission barrier studies, as large amounts of PrP^{Sc} seed were required (Bessen *et al.*, 1995; Raymond *et al.*, 1997). The development of the protein misfolding cyclic amplification (PMCA) assay (Castilla *et al.*, 2005) has improved such *in vitro* amplification systems both with regards to amplification and infectivity, and has helped demonstrate that infectious material can be produced in a cell-free system, which when inoculated into mice leads to a scrapie-like disease (Supattapone, 2004; Castilla *et al.*, 2005). Additionally, synthetic prions that polymerise into fibrils *in vitro* have also been shown to be infectious *in vivo* (Legname *et al.*, 2004).

A protein-only mechanism of replication and inheritance may have wider relevance in biology, and these mechanisms have been extensively investigated in yeast and fungi

(Wickner, 1997; Serio and Lindquist, 2000; Wickner *et al.*, 2007). However, the exact molecular events involved in the conversion of PrP^{C} to PrP^{Sc} remain unclear. The current model of prion replication proposes that PrP fluctuates between a native state, PrP^{C}, and a series of minor conformations, a subset of which can self-associate to form a stable supra-molecular structure, PrP^{Sc}, composed of misfolded PrP monomers. Studies using a recombinant protein mimetic of PrP^{Sc}, β-PrP, have shown that β-PrP aggregation occurs until it reaches a critical size at which a stable 'seed' structure is formed. Following this, the recruitment of unfolded PrP and/or β-PrP monomers can lead to an explosive, auto-catalytic formation of PrP^{Sc} (**Figure 1.4**). Such a mechanism could explain all three aetiologies (sporadic, inherited and acquired) of human prion disease. Initiation of this pathogenic self-propagating conversion reaction, with accumulation of aggregated β-PrP, may be induced following exposure to a 'seed' of aggregated β-PrP following prion inoculation, as a rare stochastic conformational change, or as an inevitable result of expression of a pathogenic mutant PrP^{C} form, which is prone to form β-PrP (Collinge, 2005). Whether such alternative conformational states of the protein are enough to adopt PrP^{Sc} conformation and cause prion disease alone in the absence of a cellular co-factor still remains to be seen.

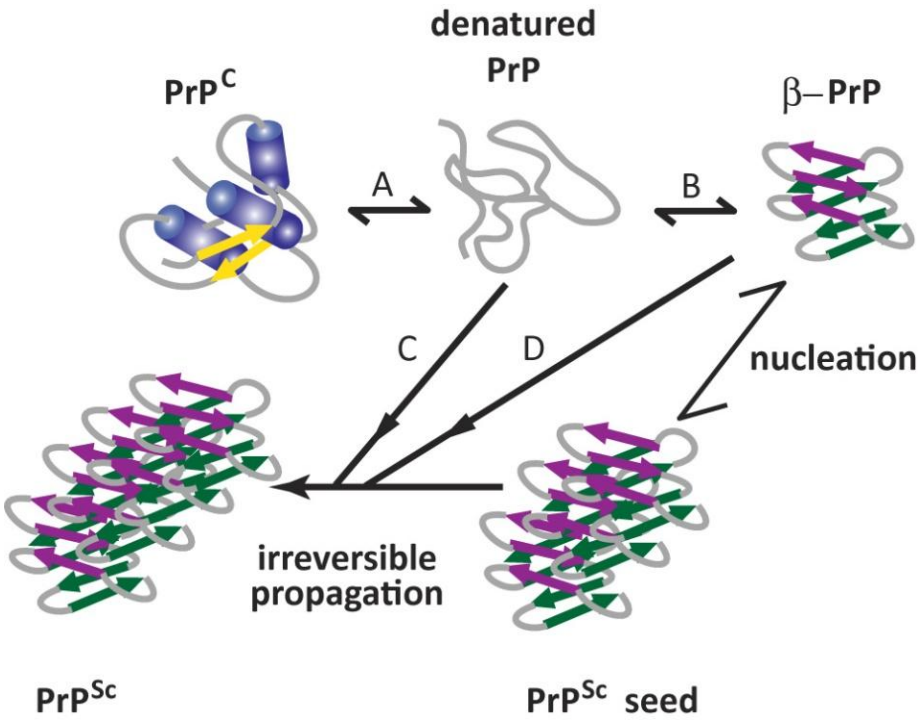

Figure 1.4 Possible mechanism for prion propagation[4]

Largely α-helical PrP^C proceeds *via* an unfolded state (**A**) to re-fold into a largely β-sheet form, β-PrP (**B**). β-PrP is prone to aggregation in physiological salt concentrations. Prion replication may require a critical 'seed' size. Further recruitment of unfolded PrP (**C**) or β-PrP monomers (**D**) then occurs as an essentially irreversible process driven thermodynamically by inter-molecular interactions.

4 Reproduced from the J. Neurol. Neurosurg. Psychiatry, Collinge, J., Vol 76, pp 906-919, © 2005 with permission from BMJ Publishing Group Ltd.

1.4.6 Prion strains and transmission barriers

The prion strain phenomenon has presented one of the most challenging problems for the protein-only hypothesis (Chesebro, 1998; Soto and Castilla, 2004). Prion strains are distinct isolates, which when transmitted to susceptible animals produce distinctive neuropathology patterns and consistent incubation periods. To comply with the criteria of the protein-only hypothesis of prion propagation, PrP^{Sc} would need to contain all the information necessary to encode strain formation. At first it was assumed that the various phenotypes found in animals were attributed to genetic information contained within the TSE-causing agent. However, unlike virus and bacterial strains, there is no experimental support that prion strains are encoded by a nucleic acid genome. The first evidence of PrP^{Sc}-encoded strain specificity came from the serial passage of two different TME strains in hamsters, which demonstrated that they are associated with different physico-chemical properties of PrP^{Sc} (Bessen and Marsh, 1992; Bessen and Marsh, 1994). Prion strains can be serially propagated in lines of inbred mice with the same *Prnp* genotype (Scott *et al.*, 1997), suggesting that strains are not encoded by differences in the primary sequence of PrP. At present, the general consensus is that the main disparities between strains arise from alternative PrP^{Sc} conformations and glycosylation patterns (Bartz *et al.*, 2000; Peretz *et al.*, 2001a). *In vivo*, distinct prion strains can be distinguished by differences in clinical signs, profile of histological damage, incubation time, and disease length (Morales *et al.*, 2007). The infectious protein of each prion strain is specifically linked to a precise set of biochemical characteristics: differential mobility on SDS-PAGE following PK-digestion (Parchi *et al.*, 1996), glycosylation patterns (Khalili-Shirazi *et al.*, 2005), and the extent of PK-resistance (Bessen and Marsh, 1992) (**Figure 1.5**). Furthermore, distinct ratios of three main PrP^{Sc} glycoforms (di-, mono- and unglycosylated) are also seen with prion strains (Collinge *et al.*, 1996b; Hill AF *et al.*, 2003). However, definitive proof for the structural nature of differences between prion strains remains obscure.

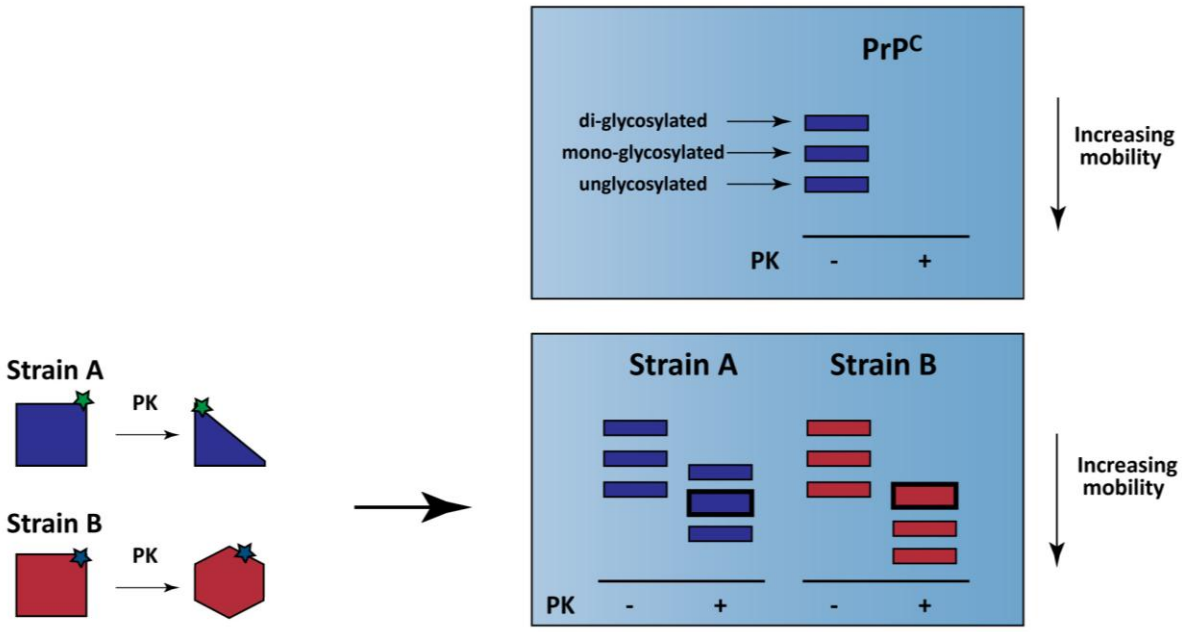

Figure 1.5 Molecular analysis of prion strains

Molecular prion strain typing is assessed by Western blotting of PK-treated brain homogenates. PK-digestion completely digests PrP^{C} but it only removes ~70 amino acid residues from the N-terminus of PrP^{Sc}. Distinct prion strains are represented by different PrP^{Sc} conformers and have different cleavage sites, which result in strain-specific migration patterns on SDS-PAGE electrophoresis. The relative intensities of the three PrP^{Sc} bands (representing the three different PrP glycoforms) are also strain-specific.

Particular strains of the infectious agent have a characteristic ability to infect some species but not others, a phenomenon recognised as the 'species barrier'. This is manifested in cases where prions from species A are used to infect species B and not all animals from species B develop the disease (those that do present with prolonged and variable incubation periods) (Moore *et al.*, 2005). Nonetheless, on secondary passage of infectivity from species B to other members of the same species all animals succumb to disease, displaying short and consistent incubation times.

Species-specific variations in the primary sequence of PrP have been suggested to be the cause of both the species barrier and the existence of different PrP^{Sc} conformations (Palmer *et al.*, 1991; Vanik *et al.*, 2004). Support for the existence of a species barrier came from studies in transgenic mice, which express human PrP, and which readily succumb to disease after infection with human prion disease, unlike their wild-type (WT) counterparts (Collinge *et al.*, 1995). On the contrary, studies in which vCJD was used to infect WT and human PrP-expressing transgenic mice have demonstrated that vCJD transmits to both (Hill *et al.*, 1997). BSE has been shown to transmit to a wide range of hosts and in doing so maintains its transmission characteristics after passage though an intermediate species. Indeed, inter-species transmission from cattle to human is the most relevant problem in terms of public health (Smith and Bradley, 2003), with a general acceptance that vCJD resulted from consumption of BSE-infected material (Bruce *et al.*, 1997; Hill *et al.*, 1997). Taken together, these findings highlight the fact that the term 'transmission-barrier', rather than 'species barrier', may be more appropriate to explain the transmissibility of prion strains and various models have been put forward to explain the transmission barrier (Hill and Collinge, 2003a; Collinge and Clarke, 2007) (**Figure 1.6**).

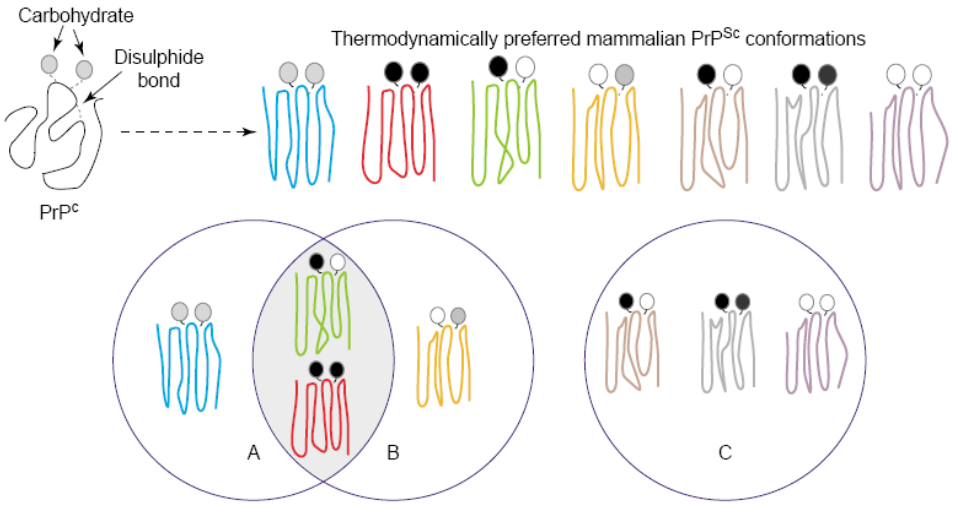

Figure 1.6 Conformational selection model of prion transmission barriers[5]

Mammalian PrP genes are highly conserved, and this hypothesis suggests that only a restricted number of different PrP^{Sc} conformations are thermodynamically permissible and constitute the range of observed prion strains. Although a significant number of different PrP^{Sc} conformations might be possible across the range of mammalian PrPs, only a subset of these would be allowed within a given mammalian species. Substantial overlap between the favoured conformations for PrP^{Sc} derived from species A and species B might therefore result in relatively easy transmission of prion diseases between these two species, whereas two species with no preferred PrP^{Sc} conformations in common would have a large barrier to transmission. According to this model of a prion transmission barrier, BSE would represent a thermodynamically highly favoured PrP^{Sc} conformation that is permissive for PrP expressed in a wide range of different species, accounting for the remarkable promiscuity of this strain in mammals. In this Figure, there is overlap between the allowable PrP^{Sc} conformers between species A and species B. This overlap facilitates transmission between these species involving the 'green' and 'red' strains. However, inoculation with the 'blue' or 'yellow' strains would only result in propagation if a strain switch to red or green occurred. There is no overlap or allowed conformers between species A or B with species C resulting in a substantial transmission barrier between species C and A, or C and B. Passage of strains through an intermediate host might allow the adaptation of a particular strain to a new host.

---

5 Reprinted from Trends Microbiol., Vol 11, Hill A.F. and Collinge J., Subclinical prion infection, pp 578-584, © 2003, with permission from Elsevier.

1.5 Cell biology of prion disease

1.5.1 Prion protein: structure

The normal cellular isoform of the prion protein, PrP^C, is a highly conserved, approximately 250 amino acid glycoprotein that is widely expressed in the body. This 30-35 kDa protein is abundant in the neurones and glia of the CNS, and can also be found in several peripheral tissues and leukocytes (Dodelet and Cashman, 1998; Aguzzi and Polymenidou, 2004). In humans, PrP^C is encoded by a single exon of the *PRNP* gene located on the short arm of chromosome 20 (20p).

PrP^C has two N-glycosylation sites and is GPI-anchored to the outer leaflet of the plasma membrane (Stahl *et al.*, 1987). Studies on purified hamster PrP^C and PrP^{Sc} have demonstrated that there are at least fifty different sugar chains capable of attaching to the glycosylation sites, with differences between the two isoforms (Endo *et al.*, 1989; Somerville and Ritchie, 1990; Rudd *et al.*, 1999; Rudd *et al.*, 2001). The C-terminal domain of PrP^C is folded largely into α-helices stabilised by a single di-sulphide bond and nuclear magnetic resonance (NMR) shows it exists in a monomeric state (Riek *et al.*, 1996). Furthermore, studies into the crystal structure of the C-terminus of PrP reveal that it has three α-helices and a short anti-parallel β-sheet (Knaus *et al.*, 2001; Eghiaian *et al.*, 2004; Haire *et al.*, 2004).

Unlike the C-terminus, structural information about the N-terminal segment of PrP^C is incomplete. The N-terminus is the most highly conserved PrP region and contains an octapeptide repeat, which may be involved in the cellular function of PrP^C. The octapeptide repeats have been shown to have tight binding sites for Cu^{2+} and Zn^{2+}, suggesting a possible role in ion regulation/signalling (Riek *et al.*, 1998; Hosszu *et al.*, 1999; Jackson *et al.*, 2001). Mutations in the N-terminal segment of PrP have been identified as the cause of some human prion diseases, raising the possibility that it may be an important factor in some PrP^{Sc} conformations and/or disease manifestation (Mead, 2006; Mead *et al.*, 2006; Hill *et al.*, 2006).

The highly conserved hydrophobic region in the middle of the protein has been shown not to serve as a transmembrane domain at the cell surface (Stahl *et al.*, 1990).

Nonetheless, studies using synthetic systems have demonstrated that peptides from this region can span membranes and suggest that this could occur as part of PrP^C function during cellular trafficking (Forloni *et al.*, 1993; Glover *et al.*, 2001). Small peptides from this region that have been refolded can adopt an apoptosis-inducing conformation suggesting that the hydrophobic domain may be an important part of an infectious prion (Gasset *et al.*, 1992; Forloni *et al.*, 1993; Goldfarb *et al.*, 1993). In agreement, PrP mutants characterised by a deleted internal hydrophobic domain, PrPΔHD, cause severe ataxia and neuronal death limited to the granular layer of the cerebellum in transgenic mice as early as 1-3 months after birth (Shmerling *et al.*, 1998; Baumann *et al.*, 2007; Li *et al.*, 2007b). More recent studies have shown that this hydrophobic domain promotes dimer formation of PrP and that PrP dimerisation is linked to a stress-protective activity (Rambold *et al.*, 2008). At present, there is little known about the structure of PrP^{Sc}, mainly because of its highly insoluble and aggregated nature (**Section 1.4.4**).

Recombinant purified PrP^C has been produced in *E. coli*. Original attempts to achieve this were hindered by low expression levels, low purification efficiency, instability and insolubility of the protein and failure to form the di-sulphide bond which is required for correct PrP^C folding (Riesner, 2003). These problems were finally overcome, and after purification recombinant PrP^C is re-constituted by denaturation in 8 M urea or 5 M guanidinium hydrochloride, whereas the di-sulphide bond is formed under oxidising conditions. Following this, PrP^C is re-natured by dialysing out the denaturant (Mehlhorn *et al.*, 1996).

1.5.2 Prion protein: localisation and trafficking

In order to further understand prion disease pathogenesis, insight into the synthesis, localisation and metabolism of both PrP^{C} and PrP^{Sc} is essential. PrP^{C} is synthesised in the endoplasmic reticulum (ER) where it undergoes post-translational modifications, which include N-terminal glycosylation, signal peptide removal, sulphide bond formation, and GPI anchor attachment (Stahl *et al.*, 1987; Turk *et al.*, 1988; Haraguchi *et al.*, 1989).

Localisation

Characterising the precise cellular localisation of PrP^{C} and PrP^{Sc} is essential in order to identify the intracellular compartment and the mechanisms that underlie prion formation. At present, there is conflicting data with regards to the exact localisation of PrP^{C} in neurones, perhaps due to the variety of techniques used. Putative sites of PrP^{C} localisation include: the ER (Sarnataro *et al.*, 2004), the Golgi (Magalhaes *et al.*, 2002), endolysosomes (Magalhaes *et al.*, 2002), exosomes (Fevrier *et al.*, 2004), the plasma membrane (Sarnataro *et al.*, 2002), the nucleus (Mange *et al.*, 2004) and the cytosol (Mironov, Jr. *et al.*, 2003). At present there is a significant gap in our understanding of PrP^{Sc} localisation as there are no PrP^{Sc}-specific antibodies. However, studies to date suggest a wide cellular distribution, in particular at the plasma membrane (Caughey and Raymond, 1991; Jeffrey *et al.*, 1992a) and in the endolysosomal compartment (McKinley *et al.*, 1991; Arnold *et al.*, 1995). Under certain conditions, PrP^{Sc}-like conformers have been reported to accumulate in the cytosol (Ma and Lindquist, 2002) and there is also evidence for cytosolic PrP^{Sc}-containing aggresomes in prion-infected cells following proteasome inhibition (Kristiansen *et al.*, 2005).

Trafficking: pathways for PrP^{C} endocytosis

Following its synthesis in the ER, PrP^{C} is trafficked *via* the Golgi to the cell surface, where it constitutively cycles between the plasma membrane and early endosomes (Shyng *et al.*, 1993). Various mechanisms have been proposed to explain how PrP^{C} is internalised

(**Figure 1.7**). For example, PrP^C has been shown to recycle from the cell surface to endosomes *via* clathrin-coated pits both in primary cultures of sensory neurones, as well as in neuroblastoma N2a and SH-SY5Y cells (Shyng *et al.*, 1994; Sunyach *et al.*, 2003; Taylor *et al.*, 2005). Furthermore, a basic amino acid motif in the N-terminal region of PrP^C has been shown to be required for localisation of PrP^C in clathrin-coated pits and subsequent internalisation (Shyng *et al.*, 1993; Lee *et al.*, 2001b; Sunyach *et al.*, 2003). These findings suggested that PrP^C may be binding, *via* its N-terminal region, to a transmembrane protein containing a localisation signal for coated pits. Another putative mechanism of internalisation has been proposed following PrP^C localisation studies in various cell models that showed that PrP^C clusters in caveolae or caveolae-like domains (Vey *et al.*, 1996; Kaneko *et al.*, 1997). Moreover, PrP^C has been found in caveolae, but not in clathrin-coated pits and vesicles, in Chinese hamster ovary cells, which express caveolin-1 (Peters *et al.*, 2003). However, the role of caveolae in prion trafficking on neurones is irrelevant, as caveolae have not been shown to occur on adult mammalian neurones (Morris *et al.*, 2006). A further possible mechanism of PrP^C internalisation involves lipid rafts. In rafts, lipids of specific chemistry can associate with one another in a dynamic manner to form platforms that segregate various membrane proteins, including GPI-anchored proteins (Simons and Ikonen, 1997). In neurones, PrP^C is found on lipid rafts that are different both chemically and spatially from those containing the major neuronal GPI-anchored protein, Thy-1 (Madore *et al.*, 1999; Sunyach *et al.*, 2003; Brugger *et al.*, 2004). In order for a GPI-anchored protein to be internalised through clathrin-coated pits it needs to translocate out of its lipid rafts into non-raft regions of the membrane. Indeed, using primary cultures of neurones as well as neuroblastoma N2a cells, Sunyach *et al.* demonstrated that PrP^C leaves its rafts to traverse detergent-soluble (non-raft) membrane, following which it enters coated pits for endocytosis, and cycles back to the cell surface *via* perinuclear sorting compartments (Sunyach *et al.*, 2003).

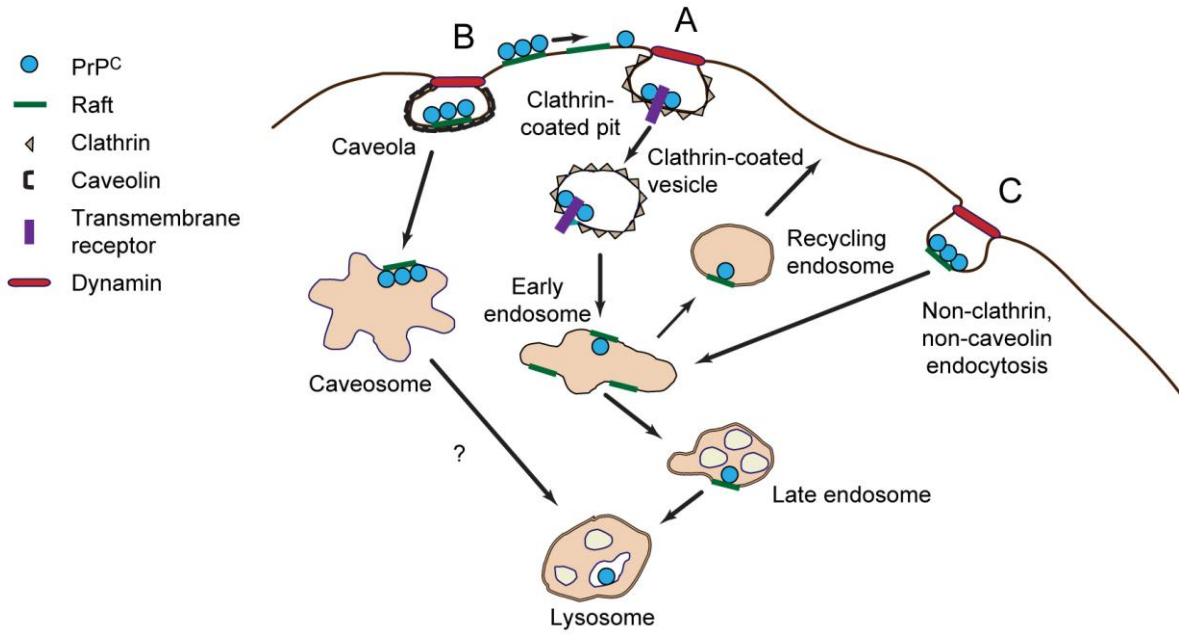

Figure 1.7 Pathways of PrP^C internalisation[6]

At the plasma membrane, PrP^C can be constitutively internalised and its endocytosis can be increased by extracellular copper ions (not shown). A chief pathway of PrP^C internalisation in neuronal cells seems to depend on clathrin-mediated endocytosis (**A**). Caveolin-related endocytosis and trafficking have been implicated in PrP^C transport in Chinese hamster ovary and glial cells (**B**). Rab5-positive endosomes and recycling endosomes involving Rab4 have also been implicated in the endocytic transport of PrP^C. Finally, non-clathrin and non-caveolin but raft-dependent endocytosis has been proposed to participate in the internalisation and conversion of prion protein (**C**).

[6] Adapted from Trends Cell Biol., Vol 15, Campana, V., *et al.*, The highways and byways of prion protein trafficking, pp 102-111, © 2005, with permission from Elsevier.

Trafficking: endocytic partner(s)

Various proteins have been proposed to bind to and act as endocytic partners for PrP^C (Morris *et al.*, 2006; Linden *et al.*, 2008). For example, the ^{NH2}-KKRPKP- amino acid residues of the N-terminal domain of PrP^C, which are essential for coated pit endocytosis (Morris *et al.*, 2006), have been identified as a major heparin sulphate/glycosoaminoglycan binding site of PrP^C (Pan *et al.*, 2002; Warner *et al.*, 2002). These basic residues also serve as binding motifs for extracellular cargo binding to the low density lipoprotein (LDL) receptor-related protein (LRP1), which has been shown to require heparin sulphate glycosoaminoglycans as co-receptors (Wang *et al.*, 2004). Furthermore, binding of a GPI-anchored protein, urokinase plasminogen activator receptor, by its basic residues to LRP1 has been shown to allow for its internalisation *via* clathrin-coated pits (Horn *et al.*, 1998). Recently, Parkyn *et al.*, showed that LRP1 associates with endogenous PrP^C on the neuronal cell surface to internalise it, and that LRP1 binds to PrP^C to facilitate its trafficking to the neuronal surface (Parkyn *et al.*, 2008). Cu^{2+} has also been demonstrated to draw PrP^C out of its rafts prior to its endocytosis in SH-SY5Y cells (Taylor *et al.*, 2005), and more recently it was shown that LRP1 is required for Cu^{2+}-dependent endocytosis of exogenous PrP^C in the same cell model (Taylor and Hooper, 2007). The laminin receptor precursor and the laminin receptor have also been shown to bind recombinant PrP^C (Rieger *et al.*, 1997; Gauczynski *et al.*, 2001; Hundt *et al.*, 2001), suggesting these receptors may be acting as cell-surface receptors for PrP^C, but more work is needed to assess whether this is also true for endogenously expressed PrP^C.

Trafficking: role in the conversion of PrP^C to PrP^{Sc}

One of the main questions in prion research is where the conversion of PrP^C to PrP^{Sc} occurs, and numerous pathways have been proposed (Campana *et al.*, 2005). First, studies suggest that PrP^C mutants, which are associated with familial forms of CJD, are retained by chaperones in the ER (Drisaldi *et al.*, 2003; Campana *et al.*, 2006), thereby indicating that in inherited prion disease the conversion process could be occurring early in the biosynthesis of PrP^C. Furthermore, PrP molecules have been shown to undergo retrograde transport toward the ER, and stimulation of this translocation leads to an

accumulation of PrP^{Sc} (Beranger *et al.*, 2002). Second, direct surface contact has also been implicated in the conversion process, as studies have shown it is required for the transfer of infection in cell models of scrapie (Kanu *et al.*, 2002). These findings are also supported by reports of transfer of infection by adherence to stainless steel wires (Flechsig *et al.*, 2001). Third, exosomes have been implicated to carry infection when released from scrapie-infected cells (Fevrier *et al.*, 2004). Fourth, increasing evidence indicates that the endocytic pathway could be involved in the conversion of PrP^{C} to PrP^{Sc} (Borchelt *et al.*, 1992; Taraboulos *et al.*, 1992). For example, blocking the endocytosis and internalisation of PrP^{C} inhibits the formation of PrP^{Sc} (Borchelt *et al.*, 1992), and studies have also shown that PrP^{Sc} is partially digested at its N-terminus in an acidic compartment following its synthesis and that it accumulates in late endosomes (McKinley *et al.*, 1991; Taraboulos *et al.*, 1992; Arnold *et al.*, 1995). Furthermore, it is also possible that prions use lipid rafts to enter cells and to initiate and/or propagate the conversion of PrP^{C} to PrP^{Sc} (Campana *et al.*, 2005). Studies have demonstrated that both PrP^{C} and PrP^{Sc} are present in rafts extracted from prion-infected mouse cells and brain (Taraboulos *et al.*, 1992; Taraboulos *et al.*, 1995; Naslavsky *et al.*, 1997; Baron *et al.*, 2002; Baron and Caughey, 2003; Botto *et al.*, 2004). Conversely, there is also evidence supporting a protective role of rafts in the conversion process. For example, it has been suggested that the GPI anchor stabilises the conformation of PrP^{C} within rafts to block the conversion of PrP^{C} to PrP^{Sc} (Baron *et al.*, 2002; Baron and Caughey, 2003), whereas disrupting lipid raft composition leads to increased scrapie infection in neuroblastoma cells (Naslavsky *et al.*, 1999) and enhanced cellular levels of misfolded PrP^{C} in the ER (Sarnataro *et al.*, 2004; Campana *et al.*, 2006). These findings, which indicate a neuroprotective role for rafts, can be explained by density gradient studies showing that PrP^{C}- and PrP^{Sc}-associated rafts have distinct characteristics (Vey *et al.*, 1996; Naslavsky *et al.*, 1997), suggesting that either the rafts associated with each isoform are different, or that the membrane association of each isoform has distinct characteristics.

Further work in defining the internalisation pathway of PrP^{C} and PrP^{Sc} and their endocytic receptor(s) is required to help our understanding of the conversion process. **Figure 1.8** summarises possible pathways of PrP^{Sc} formation.

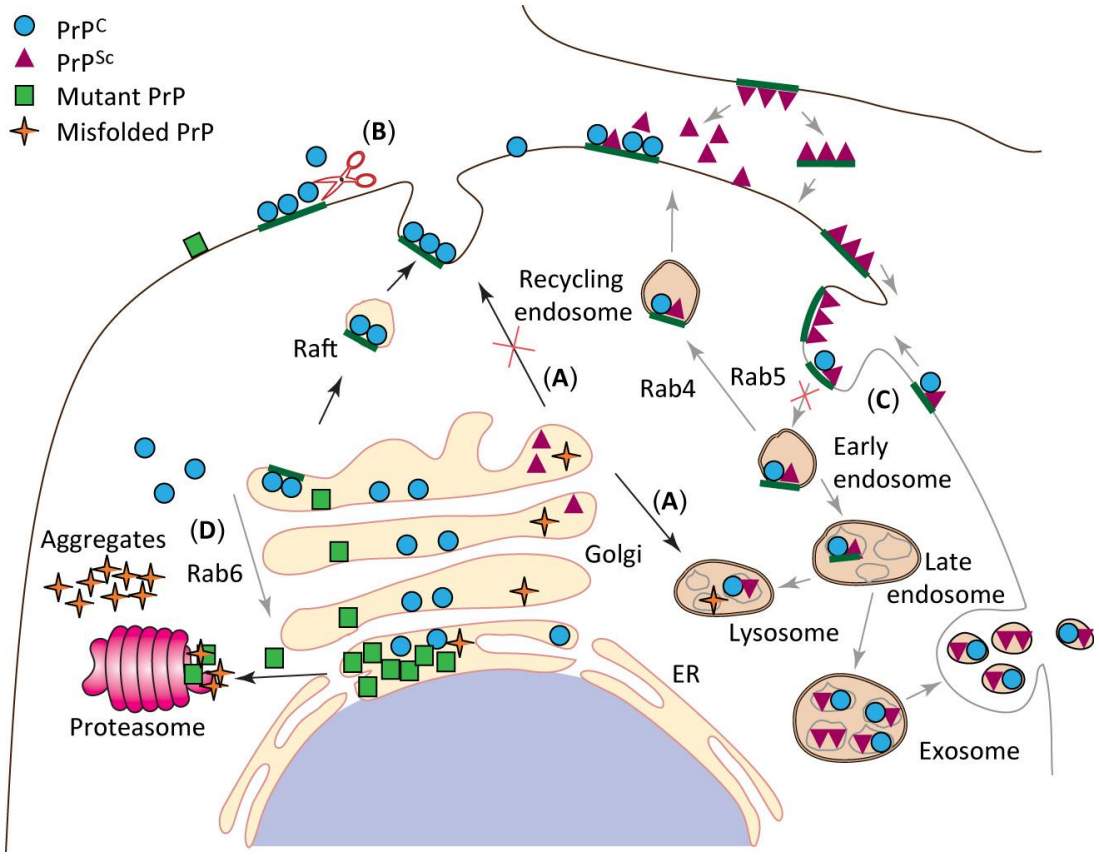

Figure 1.8 Possible pathways of PrP^{Sc} formation[7]

After its synthesis and ER quality control, PrP^{C} is transported through the Golgi apparatus to the cell surface, where it associates with rafts and is internalised by clathrin- and/or caveolin-dependent mechanisms. Blocking transport of PrP^{C} to the plasma membrane and rerouting it to lysosomes for degradation (**A**), and releasing nascent PrP^{C} from the cell surface (**B**) prevent the formation of PrP^{Sc}. A reduction in PrP^{C} internalisation (**C**) also decreases PrP^{Sc} formation. Both PrP isoforms are found in Rab5-positive early endosomes, pass through late endosomes and are totally (PrP^{C}) or partially (PrP^{Sc}) degraded in acidic lysosomes. Moreover, part of the PrP^{C} pool is recycled back to the plasma membrane in a Rab4-dependent pathway, and both PrP^{C} and PrP^{Sc} are found associated with exosomal membranes in the extracellular medium of infected cells. Finally, the ER has been postulated to have a role in prion conversion by amplifying PrP^{Sc} formation after the Rab6-dependent retrograde transport of PrP^{C} (**D**).

[7] Adapted from Trends Cell Biol., Vol 15, Campana, V., *et al.*, The highways and byways of prion protein trafficking, pp 102-111, © 2005, with permission from Elsevier.

1.5.3 Prion protein: function

The amino acid sequence of mammalian PrP^C is highly conserved between species and implies an important cellular function. Loss of PrP^C expression shows no overt phenotype in both embryonic PrP^C-null mice and adult-onset knockout models (Bueler *et al.*, 1992; Mallucci *et al.*, 2002). However, embryonic PrP^C-null mice have been shown to develop abnormalities in synaptic physiology, circadian rhythm and sleep patterns (Collinge *et al.*, 1994; Tobler *et al.*, 1996).

The function of PrP^C remains unknown, although a number of roles have been proposed (Westergard *et al.*, 2007) (**Table 1.2**). Putative functions for PrP^C are based on its localisation (**Section 1.5.2**) and on molecules that interact with it, and include cell adhesion (Graner *et al.*, 2000; Schmitt-Ulms *et al.*, 2001; Santuccione *et al.*, 2005), synaptogenesis (Kanaani *et al.*, 2005), signalling (Mouillet-Richard *et al.*, 2000), copper homeostasis (Vassallo and Herms, 2003), and neuroprotection (Kuwahara *et al.*, 1999; Bounhar *et al.*, 2001; Roucou *et al.*, 2003; Khosravani *et al.*, 2008). PrP^C has also been implicated in the self-renewal of hematopoietic stem cells during serial transplantation (Zhang *et al.*, 2006). A link between AD and prion disease has also been proposed, as PrP^C was shown to regulate neurotoxic Amyloid β (Aβ) production by inhibiting β-secretase cleavage of the amyloid precursor protein (APP) (Parkin *et al.*, 2007). Endogenous PrP^C was reported to associate with LRP1 on the cell surface, which allows for its internalisation (Parkyn *et al.*, 2008). Furthermore, the same study showed that PrP^C binds to LRP1 in biosynthetic compartments to enable its trafficking to the neuronal surface.

Putative interactor	Putative function
Growth factor receptor-bound protein 2	Signal transduction
Prion protein interacting protein 1	Unknown
Synapsin 1b	Synaptic vesicle trafficking
TREK-1	Two-pore K^+ channel
Tubulin	Microtubule subunit
NRAGE **N**eurotrophin **R**eceptor-interacting M**AGE** homologue	Activator of apoptosis
Laminin receptor precursor	Extracellular matrix interactions
Stress inducible protein 1	Heat shock protein
Hsp60	Chaperone
NCAM	Cell adhesion
Bcl-2	Multi-domain anti-apoptotic regulator
Caveolin-1	Caveolar coat
LDL receptor-related protein 1	PrP^C endocytosis
BACE-1	β-secretase cleavage of APP

Table 1.2 Putative PrP interactors

1.6 Prion-mediated neurodegeneration

The molecular basis of prion-mediated neurotoxicity is poorly understood and a major gap exists in the understanding of how the conversion of PrP^{C} to PrP^{Sc} ultimately leads to neurodegeneration. At present, there is ongoing debate about the nature of the neurotoxic species in prion disease.

1.6.1 Loss of function of PrP^{C}

Even though the precise function of PrP^{C} remains unclear (**Section 1.5.3**), a loss of its putative physiological role(s) could lead to the characteristic pathology seen in prion disease. It is known that PrP^{C} is essential for the development of prion disease (Bueler *et al.*, 1993), as PrP^{C}-null mice do not succumb to disease when inoculated with prions; prion-infected heterozygous mice show longer incubation times compared to WT mice (Bueler *et al.*, 1993). These results suggested that PrP^{Sc}, incubation time and disease progression are inversely related to PrP^{C} levels. However, loss of function of PrP^{C} is unlikely to be the cause of pathology because neither embryonic nor adult KO of PrP^{C} results in neurodegeneration (Bueler *et al.*, 1992; Manson *et al.*, 1994; Mallucci *et al.*, 2002).

Currently, there is conflicting evidence with respect to the role of abnormal PrP^{C} processing. PrP^{C}-null primary neurones *in vitro* have been shown to be more sensitive to oxidative stress (Brown *et al.*, 1997; White *et al.*, 1999). Exposure of cells to the synthetic peptide PrP106–126, which has been used as a model for PrP^{Sc} (Forloni *et al.*, 1993), has been shown to result in microglial activation and the production of reactive oxygen species (ROS) (Combs *et al.*, 1999). Furthermore, the expression of N-terminally truncated PrP^{C} in PrP^{C}-null mice has been reported to lead to rapid degeneration of cerebellar neurones, which can be rescued by co-expression of WT PrP^{C} (Shmerling *et al.*, 1998). PrP^{C} has also been reported to confer cytoprotection against the deleterious effects of the pro-apoptotic protein Bax (Bounhar *et al.*, 2001). N-terminally truncated PrP^{C} mutants have been shown to activate both Bax-dependent and independent neurotoxic pathways,

suggesting that this region could be crucial for the putative cytoprotective activity of PrP^{C} (Li *et al.*, 2007a).

1.6.2 PrP^{Sc} as the neurotoxic entity

It is widely hypothesised that an unknown toxic gain of function of PrP^{Sc}, or its precursor, is more likely to underlie cell death than a loss of PrP^{C} function. Studies have suggested that both full-length PrP^{Sc} (Hetz *et al.*, 2003) and shorter PrP peptides are toxic to primary neuronal cultures *in vitro* (Forloni *et al.*, 1993), but their relevance to *in vivo* pathogenesis is under debate. Primary neurones have been shown to undergo apoptosis when exposed to low concentrations of PrP106-126 (Forloni *et al.*, 1993). However, as there is no evidence for the occurrence of PrP106-126 *in vivo*, its relevance to the actual disease pathogenesis is unclear. Moreover, purified full-length PrP^{Sc} has also been demonstrated to cause apoptotic cell death in neuroblastoma cells *via* caspase 12 activation and ER stress (Hetz *et al.*, 2003).

Conversely, although PrP^{Sc} is thought to be associated with neuropathological features and with prion infectivity, strong evidence suggests that PrP^{Sc} itself may not be the toxic entity. For example, PrP^{C}-null tissue remains healthy and free of pathology when exposed to PrP^{Sc} (Brandner *et al.*, 1996; Mallucci *et al.*, 2003). Brandner and colleagues showed that when neural tissue over-expressing WT PrP^{C} is grafted into PrP^{C}-null mice, prion infection of the mice leads to increased levels of PrP^{Sc} and neurodegeneration only in the PrP^{C}-expressing graft (Brandner *et al.*, 1996). Furthermore, depletion of endogenous neuronal PrP^{C} in prion-infected mice has been demonstrated to reverse early spongiform change and prevent neuronal loss and progression to clinical disease, despite the presence of extra-neuronal PrP^{Sc} (Mallucci *et al.*, 2003). Another line of evidence arguing against direct PrP^{Sc} toxicity comes from CJD cases, as no direct correlation between PrP^{Sc} plaques and neuronal loss has been demonstrated in the brains of CJD patients (Parchi *et al.*, 1996). In addition, prion diseases where PrP^{Sc} levels are barely detectable have been described (Collinge *et al.*, 1995; Lasmezas *et al.*, 1997; Piccardo *et al.*, 2007). For example, although mice inoculated with BSE prions exhibit neuronal death,

biochemical analysis shows no detectable PrP^{Sc} (Lasmezas *et al.*, 1997); PrP^{Sc} levels are also barely detectable in brain homogenates from FFI patients and transgenic FFI mice (Collinge *et al.*, 1995). Conversely, Piccardo *et al.* recently showed an accumulation of PrP in a GSS patient, and in transgenic mice inoculated with brain homogenate from the same case, in the absence of any spongiform degeneration (Piccardo *et al.*, 2007). Furthermore, subclinical infection, where high levels of PrP^{Sc} accumulate in the absence of clinical symptoms, has also been described (Hill *et al.*, 2000; Race *et al.*, 2001; Race *et al.*, 2002; Hill and Collinge, 2003a). Moreover, prion-infected transgenic mice expressing PrP^{C} without a GPI anchor produce infectious prions, accumulate extracellular PrP amyloid plaques, but do not succumb to disease (Chesebro *et al.*, 2005). It has also been suggested that PrP^{Sc} needs to interact with cell surface PrP^{C} to exert a neurotoxic effect *via* aberrant signalling cascades (Solforosi *et al.*, 2004).

1.6.3 Aberrant PrP^{C} trafficking

Studies have suggested that PrP^{C} may be neuroprotective (**Section 1.5.3**) and that aberrantly processed or atypical topological PrP^{C} variants perhaps induced by PrP^{Sc}, might be neurotoxic (Hegde *et al.*, 1998; Hegde *et al.*, 1999; Yedidia *et al.*, 2001; Ma *et al.*, 2002). Studies in cell-free translation/translocation systems have shown that PrP can be found in more than one topologic forms (Hay *et al.*, 1987). Following translocation in the ER (**Section 1.5.2**), PrP^{C} can assume two different transmembrane topologies (^{Ctm}PrP- C transmembrane PrP with an extracellular C-terminus and ^{Ntm}PrP- N transmembrane PrP with an extracellular N-terminus) (Hegde *et al.*, 1998). Both isoforms are thought to represent a small amount of total PrP^{C} (about 10%), but elevated ^{Ctm}PrP has been associated with neurotoxicity (Hegde *et al.*, 1998; Hegde *et al.*, 1999). Hegde *et al.* showed *in vivo* that the expression of PrP with the A117V mutation, which is linked to GSS, leads to neurodegeneration with a prion disease phenotype (Hegde *et al.*, 1998). The authors showed increased levels of ^{Ctm}PrP, but low levels of PrP^{Sc} accumulation, in the transgenic mice carrying the A117V mutation, as well as in a patient carrying the same mutation. More recently, it has been shown that neurodegeneration in ^{Ctm}PrP transgenic mice

depends on the co-expression of endogenous WT PrP^{C} (Stewart *et al.*, 2005). ^{Ctm}PrP is thought to be a critical intermediate in the pathway of prion-mediated neurodegeneration, by means of escaping ER quality control mechanisms (Hegde *et al.*, 1998; Hegde *et al.*, 1999).

It has also been suggested that the accumulation of PrP^{C} in the cytosol may be neurotoxic (Ma *et al.*, 2002). During ER-associated degradation (ERAD), ER-resident proteins in an unassembled or misfolded form undergo retrograde transport to the cytosol, where they get ubiquitinated and degraded by the proteasome (Meusser *et al.*, 2005) (**Figure 1.9**) and misfolded, mutant and WT forms of PrP have been shown to be degraded by ERAD (Zanusso *et al.*, 1999; Jin *et al.*, 2000; Ma and Lindquist, 2001; Yedidia *et al.*, 2001; Ma *et al.*, 2002; Cohen and Taraboulos, 2003). Under normal physiological conditions, PrP^{C} in the cytosol would be degraded by the proteasome. However, following proteasome inhibition, cytosolic PrP^{C} has been shown to aggregate, acquire partial resistance to proteases and the ability to self-replicate (Ma and Lindquist, 2001; Ma and Lindquist, 2002; Cohen and Taraboulos, 2003). Whilst cytoplasmic PrP^{C} aggregates have not be shown to be toxic themselves (Ma and Lindquist, 2001; Yedidia *et al.*, 2001), expression of a PrP mutant, which lacks signal sequences and the GPI anchor, cyPrP, that remains in the cytoplasm leads to neurodegeneration both *in vitro* and *in vivo* (Ma *et al.*, 2002). Recently, evidence of ER stress and decreased translocation into the ER of nascent PrP was reported during prion infection (Rane *et al.*, 2008). The authors suggested that PrP^{Sc} accumulation could cause ER stress, forcing nascent PrP^{C} to retro-translocate to the cytosol, where putative toxic PrP molecules accumulate (Rane *et al.*, 2008). At present there is debate concerning the role of ERAD in the intracellular trafficking of PrP^{C} and whether cytoplasmic PrP^{C} is involved in prion-mediated neurotoxicity (**Section 1.9.1**). Cytoplasmic PrP^{C} may be the normal outcome of PrP^{C} trafficking, which would rapidly be degraded by the proteasome. However, functional impairment of the ubiquitin proteasome system (UPS) may account for the accumulation of cytoplasmic PrP^{C} and the ensuing toxicity (**Section 1.9.1**).

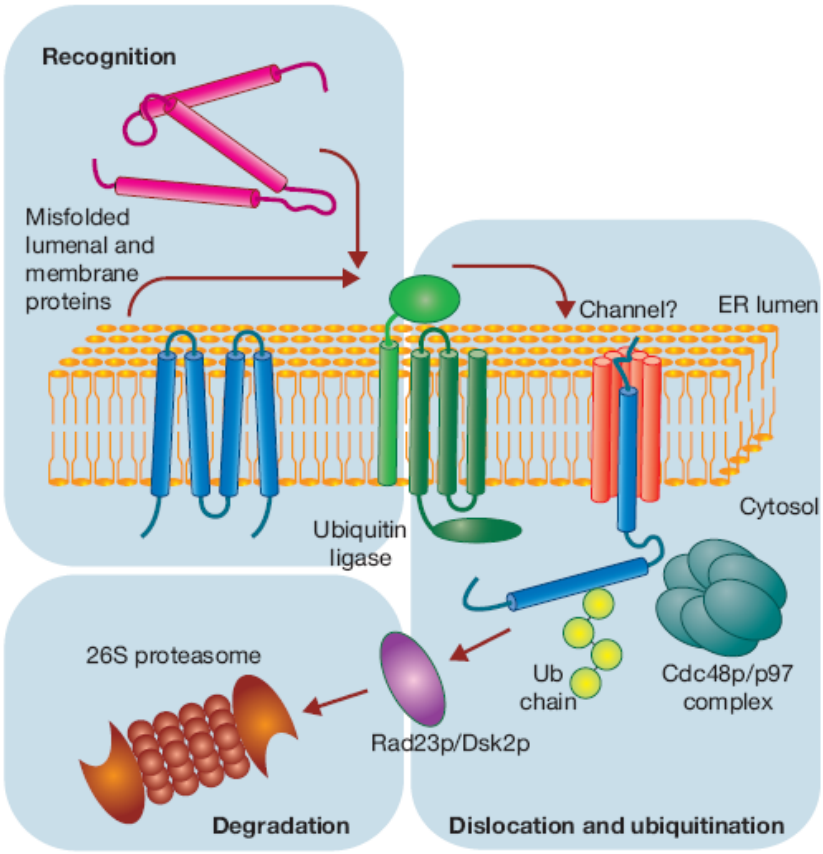

Figure 1.9 Proteasomal degradation of ERAD targets[8]

Aberrant proteins are recognised in the ER lumen by different quality control mechanisms, which escort terminally misfolded polypeptides to a putative channel that facilitates their export from the ER. Cytoplasmically exposed lysine residues are ubiquitinated by ubiquitin ligases. Dislocation is completed with the help of Cdc48p/p97 complex and membrane-extracted substrates are conveyed to the proteasome by accessory factors such as Rad23p and Dsk2p.

8 Reprinted by permission from Macmillan Publishers Ltd. Nat. Cell Biol., Meusser *et al.*, Vol 7, pp 766- 772, © 2005.

1.6.4 Intermediate PrP species

An alternative explanation for the experimental observation that both PrP^{C} and PrP^{Sc} are required for toxicity (**Sections 1.6.1, 1.6.2, 1.6.3**), is that accumulation of high intracellular levels of disease-associated PrP, or an intermediate species, is required for cytotoxicity. For example, it has been suggested that a neurotoxic intermediate molecule, PrP^{L} (L for lethal), might be formed during the conversion of PrP^{C} to PrP^{Sc} (Hill *et al.*, 2000; Hill and Collinge, 2003a), with PrP^{L} adopting a transient structure or conformation in the conversion of one to the other. However, the precise nature, or even the existence, of such a species remains unclear.

1.6.5 Neuronal death in prion disease

The exact mechanism of prion-mediated neurotoxicity is poorly understood. Cell death is thought to be caused *via* apoptosis as evidenced by *in vitro* and *in vivo* studies, as the presence of apoptotic neurones has been confirmed in both naturally-occurring and experimental models of prion disease (Dorandeu *et al.*, 1998; Liberski *et al.*, 2008) (**Figure 1.10**). Prion infection-induced neuronal apoptosis has been shown to occur in prion-infected primary neurones (Cronier *et al.*, 2004) and treatment of various primary cell cultures of brain origin with the peptide PrP106-126 has been shown to induce neuronal apoptotic death (Forloni *et al.*, 1993; Brown *et al.*, 1994a; Brown *et al.*, 1996; Jobling *et al.*, 1999; Thellung *et al.*, 2000); *in vivo* PrP106-126 injection in mouse retina has also been shown to induce apoptosis (Ettaiche *et al.*, 2000). The exact mechanism by which PrP106-126 treatment leads to apoptosis is unclear. Possibilities include increased production of ROS (Brown *et al.*, 1996; Turnbull *et al.*, 2003), or disruption of mitochondrial membranes with subsequent release of cytochrome C and caspase activation (O'Donovan *et al.*, 2001). Carimalo *et al.* reported that exposure of primary cultures to PrP106-126 directly induces apoptosis, including early production of ROS and late activation of caspase 3, highlighting the involvement of the JNK-c-Jun pathway in PrP106-126-mediated neuronal death (Carimalo *et al.*, 2005). Caspase-12 activation has been detected in neuroblastoma cells treated with nanomolar concentrations of full-length PrP^{Sc} from mouse scrapie brain, to

induce apoptosis (Hetz *et al.*, 2003). Furthermore, prion-infected neuronal cells have been shown to become apoptotic following mild proteasome inhibition (Kristiansen *et al.*, 2005). The authors showed that proteasome impairment in prion-infected cells resulted in formation of large, cytosolic aggresomes, which was directly associated with activation of caspase 3 and 8, resulting in apoptosis (Kristiansen *et al.*, 2005) and implying the possibility that proteasome dysfunction is involved in prion pathogenesis (**Section 1.9.1**).

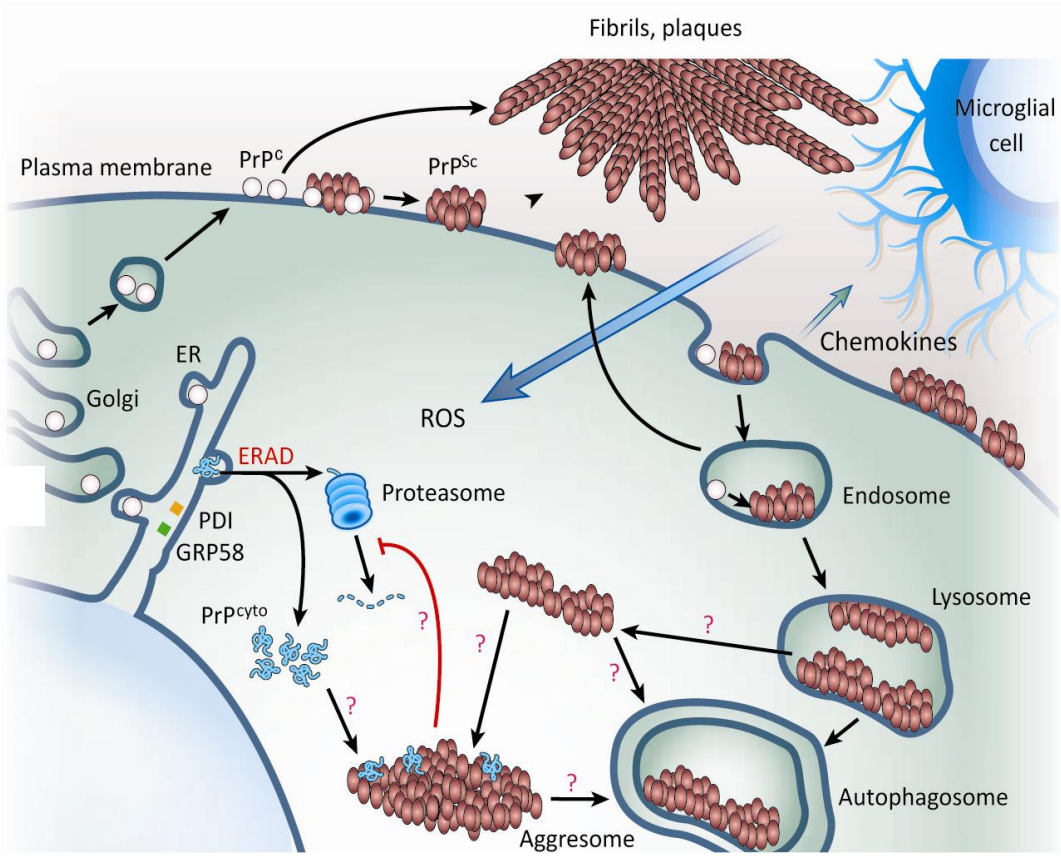

Figure 1.10 Hypothetical mechanisms for prion neurotoxicity[9]

Misfolded PrP^{C} can be subject to the ERAD pathway. Under conditions of proteasome inhibition, cytoplasmic forms of PrP aggregates have been associated with neurotoxicity (such as PrP^{cyto} and aggresomes). The mechanisms by which these aggregates are generated (for example the retro-translocation of PK-resistant PrP from the lumen of the endocytic and lysosomal vesicles into cytosolic aggresomes, and the cause of proteasome inhibition) are unknown. The release of ROS from chemokine-activated microglial cells could contribute to ER stress and/or the ERAD process by inactivation of ER chaperones (for example protein disulphibe isomerase (PDI) and GRP58), one of which has been shown to protect against prion neurotoxicity. Excessive levels of misfolded prion proteins in the cytosol might impair proteasome function, either directly or after incorporation into aggresomes.

[9] Adapted by permission from Macmillan Publishers Ltd. Nature, Caughey, B., and Baron, G.S., Vol 443, Prions and their partners in crime, pp 803-810, © 2006.

1.7 Therapeutic strategies in prion disease

Prion diseases are currently incurable and there are no available effective drugs for individuals who are already infected (Mallucci and Collinge, 2005). If prion propagation depends on the conversion of PrP^{C} to PrP^{Sc}, then the prevention of this conversion should prevent disease progression and early neuronal changes should be reversed. Prion therapeutics should therefore aim for the design of compounds that prevent disease onset and/or alter progression, or for the use of neuronal precursor cells. To date, therapeutic approaches include the use of compounds such as Congo red, polyanionic compounds, amphotericin B, porphyrins and quinacrine, each of which has been shown to reduce accumulation of PrP^{Sc} in prion-infected cell models (Trevitt and Collinge, 2006). However, such models are not stringent screens and these compounds have produced only modest effects *in vivo* (Aguzzi *et al.*, 2001). Targeting endogenous PrP^{C} in mice with early prion infection reverses spongiform change and prevents clinical symptoms, neuronal loss, cognitive and behavioural deficits (Mallucci *et al.*, 2003; Mallucci *et al.*, 2007). Strategies to prevent the conversion process may also include the use of antibodies to bind and stabilise PrP^{C} (Enari *et al.*, 2001; Heppner *et al.*, 2001; Peretz *et al.*, 2001b; White *et al.*, 2003), but the use of large quantities of anti-PrP antibodies in the CNS is not feasible as yet as they have been reported to lead to marked neurodegeneration in mice (Solforosi *et al.*, 2004). The use of RNA interference (RNAi) has been demonstrated to inhibit PrP^{C} expression in neuroblastoma cells (Tilly *et al.*, 2003) and to prevent PrP^{Sc} accumulation in scrapie-infected cells (Daude *et al.*, 2003). In a recent study using a single administration of lentivirus-expressing shRNA targeting PrP into each hippocampus of mice with established prion disease resulted in significantly prolonged survival times compared to control mice (White *et al.*, 2008).

1.8 Cellular degradation systems

Protein turnover is critical for the removal of misfolded or damaged proteins and in contributing to the amino acid pool required for protein synthesis, especially in conditions in which there are limited amounts of nutrients. The majority of cellular functions are regulated by changes in cellular protein levels, which are obtained by altering the delicate balance between protein synthesis and breakdown. The role of protein degradation systems in protecting cells from aberrant, misfolded proteins has been in the spotlight due to its emerging relevance to human neurodegenerative disease. For the purposes of the work described in this thesis, the two major degradation pathways in eukaryotic cells, the UPS and the autophagy-lysosomal system, will be discussed in detail. The UPS targets short-lived and/or aberrant ubiquitinated proteins, whereas autophagy is responsible for the degradation of long-lived proteins, organelles and for maintaining steady amino acid pools when the cell is starved.

1.8.1 The ubiquitin proteasome system

The UPS is the primary cellular quality control system in eukaryotes for selecting and degrading proteins that are either incomplete, missense, or misfolded, and that could potentially form toxic aggregates (Goldberg, 2003). In this highly complex and selective pathway, proteins destined for degradation are firstly covalently attached to ubiquitin, and subsequently recognised and degraded by the 26S proteasome in an ATP-driven process (Hershko and Ciechanover, 1998; Glickman and Ciechanover, 2002). The UPS is also responsible for the degradation of a vast number of crucial cellular factors, making it an imperative regulator in cellular functions ranging from the cell cycle to organelle biogenesis (Glickman and Ciechanover, 2002). Aberrations in the UPS have been implicated in the pathogenesis of many diseases, including neurodegenerative diseases such as Parkinson's disease (PD), Huntington's disease (HD), AD and prion disease (Ciechanover and Brundin, 2003).

The proteolytic process: ubiquitin meets the 26S

Degradation of proteins by the UPS involves two discrete steps: a) covalent attachment of a poly-ubiquitin chain to the substrate, which serves as a tag for its recognition by the 19S regulatory particle, and b) 26S-mediated substrate degradation with the release of free and recyclable ubiquitin (Hershko and Ciechanover, 1998). Ubiquitin is a highly conserved 76 amino acid protein ubiquitously expressed in cells of all eukaryotes. During ubiquitination an isopeptide bond is formed between a lysine residue on the substrate and the carboxyl terminus of ubiquitin (**Figure 1.11**). The biochemical steps in ubiquitination involve three different types of enzyme: E1 (ubiquitin-activating enzyme), E2 (ubiquitin-conjugating enzyme) and E3 (ubiquitin ligase) (Hershko and Ciechanover, 1998). The first step activates ubiquitin by its ATP-dependent conjugation to an E1 enzyme, followed by its transfer to an E2 enzyme. Ubiquitin is then transferred from the E2 to the substrate by the action of an E3 ligase, which can further elongate the ubiquitin chain by creating isopeptide bonds between ubiquitin moieties. E3 enzymes confer target recognition, through physical interactions with the substrate. Indeed, there is a vast number of E3 genes in eukaryotic genomes (Ardley and Robinson, 2005), which reflects the precise nature of substrate recognition in UPS-mediated degradation (Semple, 2003). Moreover, mass spectrometry studies have demonstrated that all seven lysine residues in ubiquitin (lys 6, lys 11, lys 27, lys 29, lys 33, lys 48, lys 63) are used for chain elongation (Peng *et al.*, 2003), but currently the importance of different ubiquitination patterns is poorly understood (Kuhlbrodt *et al.*, 2005). The most abundant chains are lys 48-linked and result in 26S-mediated substrate degradation, whereas the less frequent lys 63-linked chains have been suggested to mediate other biological functions, such as marking proteins for endocytosis (Tai and Schuman, 2008).

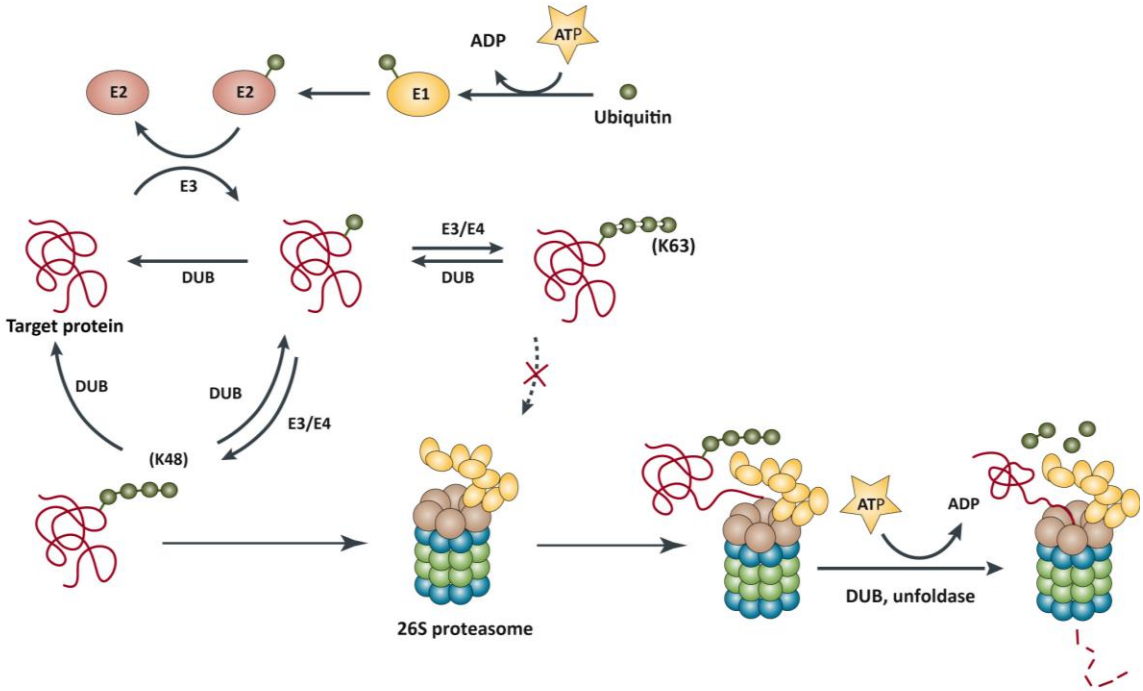

Figure 1.11 Overview of ubiquitination in the ubiquitin proteasome system[10]

An isopeptide bond forms between a lysine residue on the target protein and ubiquitin (ub) during ubiquitination, which consists of 4 different classes of enzymes: E1–E4. First, ub is covalently conjugated to the ub-activating E1 enzyme in an ATP-dependent reaction, and then it is transferred to the ub-conjugating E2 enzyme. The E3 ub–protein ligase transfers the ub from the E2 to the substrate. After the first ub has been attached, the E3 can elongate the ub chain by creating ub–ub isopeptide bonds. The E4 enzymes (chain elongation factors) are a subclass of E3-like enzymes that only catalyse chain extension. K48 chains lead to 26S proteasome-mediated degradation, whereas monoubiquitylation and K63 chains do not specify degradation. Several classes of UPS factors are involved in presenting substrates to the proteasome including ubiquitylating enzymes (E1–E4) and deubiquitylating enzymes (DUBs). The organization of these factors can differ for each substrate, and only one potential configuration is represented. The figure shows an example of how a protein's ubiquitylation pattern can be dynamically edited by E3s, E4s and DUBs. When K48-polyubiquitylated, the protein can reach the proteasome by diffusion or with the assistance of chaperones and shuttling factors.

---

10 Adapted by permission from Macmillan Publishers Ltd. Nat. Rev. Neurosci., Tai and Shuman, Vol 9, pp 826-838, © 2008.

The 26S proteasome

The 26S proteasome is an essential, 2.4 MDa, ATP-dependent enzyme complex, resident in both the nucleus and the cytosol of eukaryotic cells (Coux *et al.*, 1996). It is made up of at least thirty-two different subunits and consists of a 20S proteolytic core capped at one or both ends by a 19S complex (also known as PA700) (**Figure 1.12**). The 20S is a cylinder-shaped multi-protein complex possessing a central cavity where hydrolysis proceeds without interference from the cytosol; the 19S contributes various functions to the 26S proteasome. The structural instability of the 26S proteasome makes it very hard to conduct detailed structural analyses and therefore insights into the 26S proteasome structure come from studies on the structure, assembly and function of the 20S proteasome as well as on properties of the 19S.

The 20S proteasome has a molecular weight of about 700 kDa, a diameter of 11 nm and height of 15 nm. 20S proteasomes exist in all pro- and eukaryotes (Dahlmann *et al.*, 1992) and it is EM studies of *Thermoplasma* 20S proteasomes that have shown that these enzymes are arranged as cylinders (Puhler *et al.*, 1992). In eukaryotes, 20S proteasomes are essential and ubiquitously expressed (Zwickl *et al.*, 2000). The eukaryotic 20S proteasome is composed of fourteen α and fourteen β subunits arranged in four stacked rings. Immuno-EM studies demonstrated that the β subunits form two rings, which are located between two rings of α subunits (Zwickl *et al.*, 1992). X-ray crystallography revealed that each ring consists of seven subunits with an overall highly conserved architecture arranged as α(1-7)β(1-7)β(1-7)α(1-7) (Lowe *et al.*, 1995; Voges *et al.*, 1999). Like archaea, eukaryotic 20S proteasomes share this common subunit architecture, but eukaryotic 20S have seven different α and β subunits in two copies per 20S, thereby resulting in a pseudo-seven-fold symmetry (Groll *et al.*, 1997). In reality, the 20S proteasome has a two-fold axis of symmetry (Groll *et al.*, 1997; Groll *et al.*, 2000).

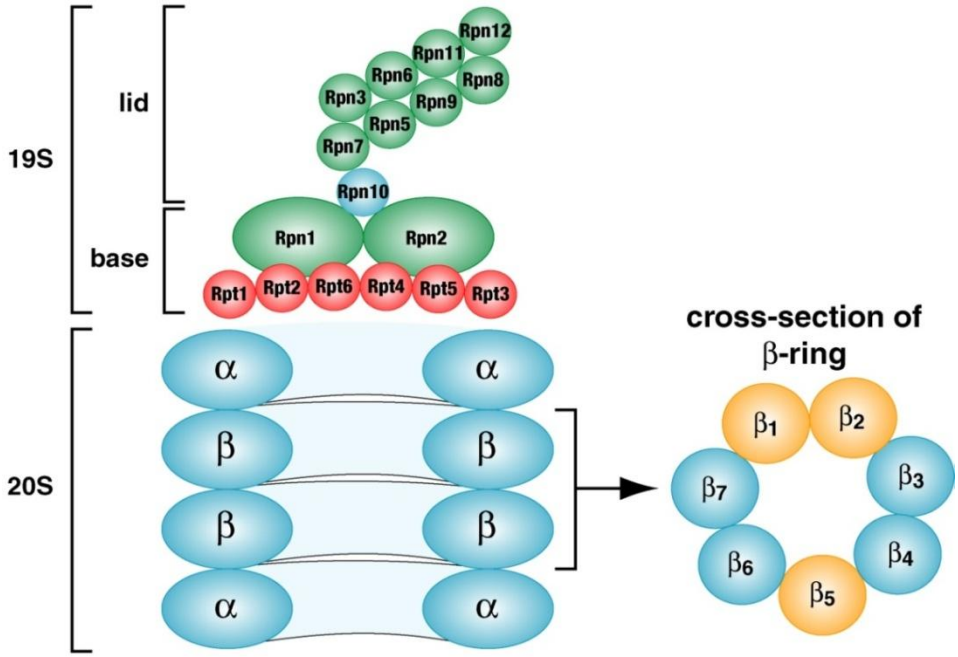

Figure 1.12 Subunit composition of the 26S proteasome[11]

Schematic of the 26S proteasome in *Saccharomyces cerevisiae*, showing the 20S proteolytic core and one 19S regulatory particle. The 19S is made up of two sub-complexes termed lid and base, the latter consisting of six homologous members of the ATPase family (Rpt1-6; shown in red) and two larger, non-ATPase subunits (Rpn1 and Rpn2). The C-termini of the ATPases dock into inter-subunit pockets in the α rings of the proteasome and open the gate for substrate hydrolysis by the 20S β subunits. Cross section of the β ring reveals the positions of the caspase-like (β_1), trypsin-like (β_2) and chymotrypsin-like (β_5) subunits (all shown in yellow). Rpn= regulatory particle non-ATPase; Rpt= regulatory particle ATPase.

11 Reprinted from BBA Molecular Basis of Disease, Vol 1782, Deriziotis P. And Tabrizi S., Prions and the proteasome, pp 713-722, © 2008 with permission from Elsevier.

The 20S proteasome is where hydrolysis of polypeptides occurs. The proteolytic activity of the 20S proteasome resides in its two β-rings and only three of the seven different β subunits in eukaryotes contain functional active sites, resulting in only six active sites per proteasome (Groll *et al.*, 1997). Studies using synthetic peptide substrates have demonstrated that the 20S proteasome comprises three distinct catalytic activities termed β_1 (caspase-like; cleaving after acidic residues), β_2 (trypsin-like; cleaving after basic residues), and β_5 (chymotrypsin-like; cleaving after hydrophobic peptides) (Orlowski, 1990). Mutational and biochemical studies of the specificity of the proteasomal subunits have revealed that all proteolytic activities can be assigned to β_1, β_2 and β_5 subunits, rejecting the existence of other active sites (Dick *et al.*, 1998). Moreover, comparisons of cleavage of enolase 1 between WT and mutant 20S proteasomes showed that product length is not dependent on the number of active sites (Nussbaum *et al.*, 1998). Nonetheless, as there is mutual allosteric regulation of the chymotrypsin-like and caspase-like sites, it has been suggested that 20S proteolysis proceeds in a 'bite and chew' fashion (Kisselev *et al.*, 1999). Unfolded polypeptides have been shown to be processively cleaved by the proteolytic active sites of the 20S in *Thermoplasma*, yeast and rabbit muscle (Nussbaum *et al.*, 1998; Kisselev *et al.*, 1998; Kisselev *et al.*, 1999). The resulting fragments range from 3-30 amino acids in length, with the average peptide comprising 7-8 residues, and which may be further degraded by cytosolic endopeptidases and aminopeptidases (Kisselev *et al.*, 1999; Venkatraman *et al.*, 2004; Bhutani *et al.*, 2007).

The use of inhibitor (Fenteany *et al.*, 1995), deletion and mutation (Seemuller *et al.*, 1995) studies have confirmed the 20S as a threonine protease, whereby the secondary alcohol of the N-terminal threonine of the active β subunit acts as the nucleophilic species (Lowe *et al.*, 1995). Only three of the seven eukaryotic β subunits have an N-terminal threonine, namely β_1, β_2 and β_5, thereby resulting in the six active sites per proteasome (Groll *et al.*, 1997). Interestingly, mutational and crystallographic studies in yeast 20S found that the inactive subunits β_3, β_6 and β_7 cannot be rendered active by introducing canonically active residues, including Thr1 (Groll *et al.*, 1999; Zwickl *et al.*, 2000).

The precise structural organisation of the 20S proteasome functions to isolate proteolytic compartments from the cytoplasm, thereby preventing unwanted degradation, and more importantly to impose constraints on substrate entry. This is achieved by the two α-rings, which form gated channels through which substrates enter and peptides exit the 20S proteasome. Structural studies in free eukaryotic 20S proteasomes have shown that the N-termini of the seven α subunits assume unique conformations while pointing inwards to the centre of the ring (Groll *et al.*, 1997; Groll *et al.*, 2000); the N-termini of the α subunits keep the pore, or 'gate', of the proteasome in a closed state (**Figure 1.13**). Activation of the 20S reflects the opening of a channel, which allows substrate access (Groll *et al.*, 2000). This is achieved by the re-arrangement of the N-terminal segments of various α subunits, which normally keep the gate sealed. Evidence for a gated channel into the proteolytic core came from crystallographic studies by Groll and colleagues, who compared WT yeast 20S proteasome with the α3ΔN mutant, which lacks the nine N-terminal residues of the α3 subunit. Even though each of the seven tails is remarkably conserved, they differ from one another and it is the α3 N-terminal segment that projects directly across the pseudo-seven-fold symmetry. The α3ΔN 20S proteasome demonstrates increased rates of hydrolysis of small peptides compared to its WT 20S counterpart (Groll *et al.*, 2000; Kohler *et al.*, 2001). This is because neighbouring α subunit tails are significantly disordered (in the absence of the nine N-terminal residues of the α3 subunit) and the α3ΔN 20S proteasome mutant is constitutively in an open state (**Figure 1.13**).

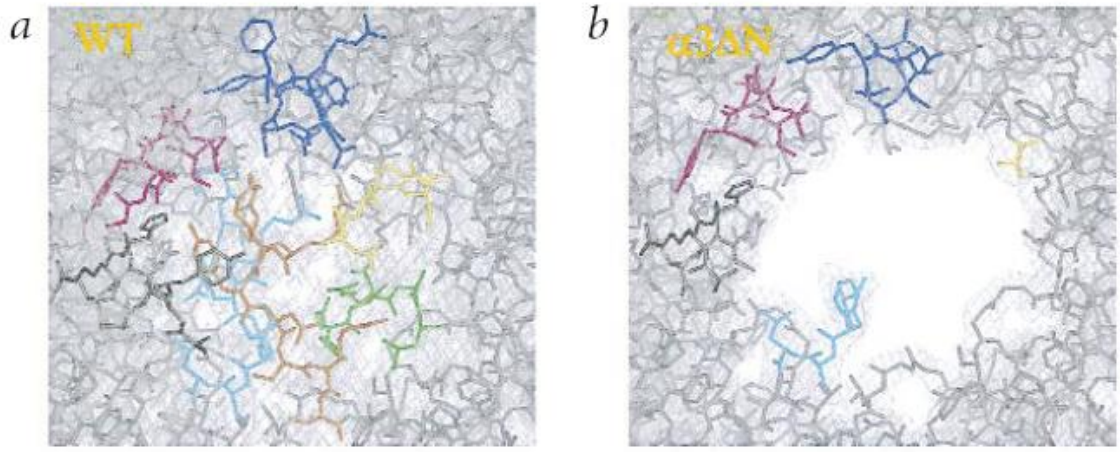

Figure 1.13 The gated channel of the 20S proteasome[12]

Electron density maps of the α ring of the yeast core particle from a) WT and b) α3ΔN cells. The N-terminal segments of the seven α subunits (shown in different colours) seal the central channel in the 20S core particle (WT). The deletion of nine residues of the α3 subunit (shown in yellow in a) and the loss of order in 20 residues from the other subunits, each of which directly contacts the α3 tail in the WT complex, results in a loss of electron density in the α3ΔN core particle compared to WT.

[12] Reprinted by permission from Macmillan Publishers Ltd. Nat. Struct. Biol., Groll *et al.*, A gated channel into the proteasome core particle, Vol 7, © 2000.

20S activation can be achieved in various ways, the most prominent of which is the attachment of regulatory particles (Chu-Ping *et al.*, 1994; Hoffman and Rechsteiner, 1994). The 20S proteasome can degrade short or unstructured polypeptides, and it has been shown to degrade proteins with misfolded or hydrophobic patches (Orlowski and Wilk, 2003; Forster and Hill, 2003). In an ATP-driven reaction, the 19S binds substrates, unfolds them, removes the poly-ubiquitin chain and translocates the polypeptide into the 20S for degradation (Pickart and Cohen, 2004) (**Figure 1.14**). The C-termini of the six 19S ATPases (Rpt1-Rpt6) (**Figure 1.12**) contain a conserved HbYX (hydrophobic amino acid residue-tyrosine-X amino acid residue) motif that docks into the pockets between the adjacent α subunits of the 20S (Smith *et al.,* 2007). Peptides seven residues or longer that correspond to these ATPases' C-termini and contain the HbYX motif, such as CtRpt5, which corresponds to the Rpt5 ATPase, dock into the same pockets and induce gate-opening (Smith *et al.*, 2007; Gillette *et al.*, 2008). When the ATPases bind a nucleotide, these C-termini function like a 'key in a lock' to open the gate.

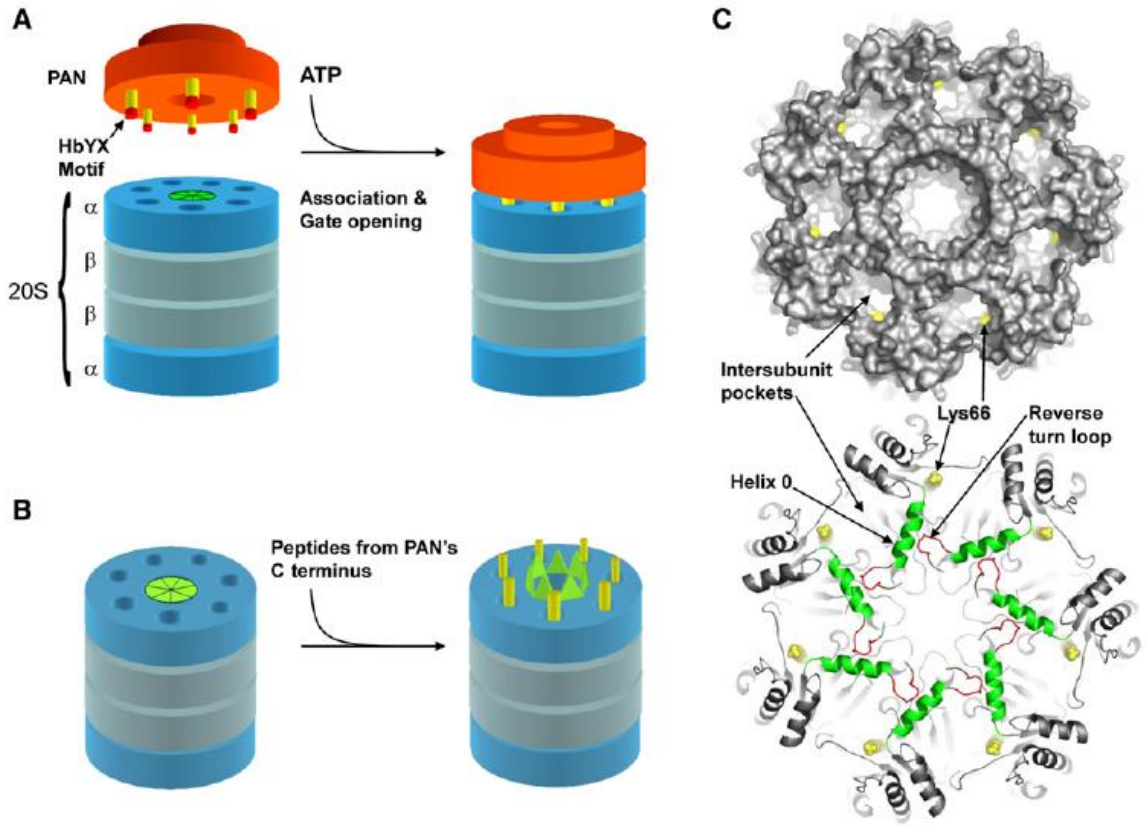

Figure 1.14 Model depicting the association of PAN with the α-ring of the 20S proteasome[13]

(**A**) The C-termini (yellow) of PAN (orange) dock into the inter-subunit pockets in the top of the 20S. (**B**) Schematic model for gate opening in the 20S upon binding of peptides derived from PAN's C-terminus to the inter-subunit pockets in the 20S. (**C**) (Top) Top view of the 20S a ring demonstrating the inter-subunit pockets and location of Lys66 (yellow). (Bottom) Ribbon representation of the α ring. The N-terminal gating residues are not resolved in this crystal structure.

[13] Reprinted from Mol. Cell, Vol 27, Smith, D.M. *et al.,* Docking of the proteasomal ATPases' carboxyl termini in the 20S proteasome's α ring opens the gate for substrate entry, pp 731-744. © 2007 with permission from Elsevier.

1.8.2 Autophagy

Autophagy, which literally means 'self-eating', is a process in which cellular constituents, such as organelles and proteins, are degraded by the lysosomal system. This degradation system is highly conserved from yeast to humans and studies in yeast have identified over twenty different autophagy-related genes (*Atg*) (Reggiori, 2006). Unlike the UPS, which targets mostly short-lived proteins (Ciechanover *et al.*, 2000), autophagy is primarily responsible for the catabolism of long-lived proteins and for maintaining steady amino acid pools during starvation. Apart from its role in protein degradation, autophagy is also involved in various cellular functions ranging from antigen presentation to the regulation of development and cell death (Mizushima, 2005). Initially, autophagy was thought to be associated with the 'bulk', non-selective degradation of proteins, but recent molecular advances have revealed specialised forms of autophagy that differ in the way cytosolic constituents reach the lysosomal compartment.

The three types of autophagy are: microautophagy, chaperone-mediated autophagy (CMA) and macroautophagy (**Figure 1.15**). The molecular mechanism of microautophagy is unknown, but the process itself involves the direct engulfment of cytosol by lysosomes (Ahlberg *et al.*, 1982). CMA is a regulated, selective process, which entails the receptor-mediated translocation of proteins that contain a pentapeptide motif into the cytosol (Dice, 1990). Macroautophagy is responsible for the degradation of long-lived proteins, and requires the formation of double-membraned vesicles called autophagosomes and their subsequent fusion with lysosomes in which their cargo is degraded. In mammalian cells, autophagosomes fuse with late endosomes and multivesicular bodies to form 'amphisomes' (Berg *et al.*, 1998), which then fuse with lysosomes. Macroautophagy (hereafter referred to as autophagy) can also be selective; autophagic processes have been shown to be specific for mitochondria (mitophagy), peroxisomes (pexophagy), ribosomes (ribophagy), protein aggregates (aggrephagy) (Kundu *et al.*, 2003).

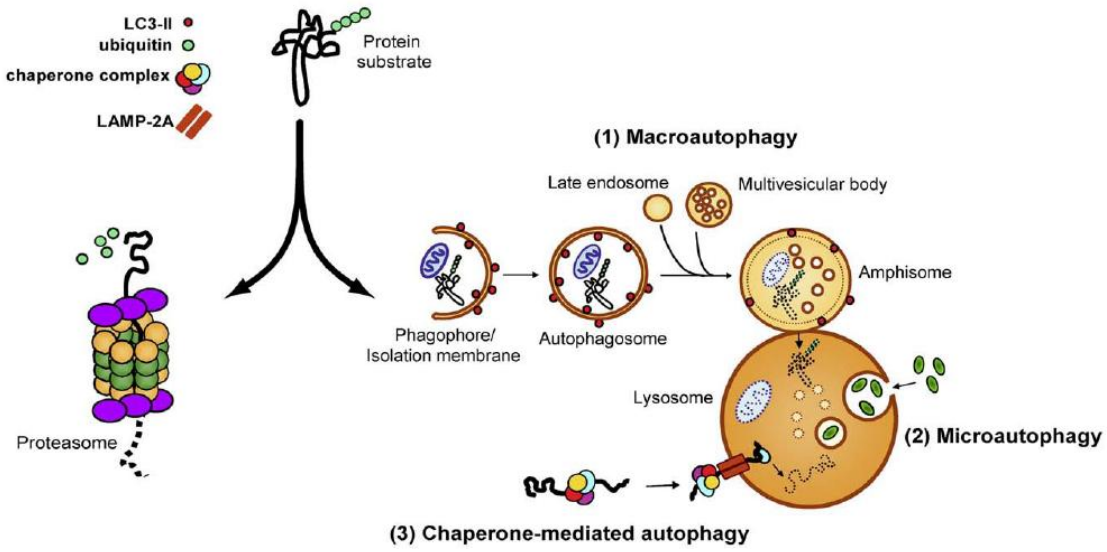

Figure 1.15 Autophagy, a cellular degradation system[14]

Proteins that are tagged with poly-ubiquitin chains are generally considered to be substrates for the UPS, which feeds unfolded proteins through the barrel of the 26S proteasome and generates small digested peptides. Recent evidence suggests that some ubiquitinated substrates can also be degraded *via* the autophagy-lysosomal system. This system comprises **(1)** macroautophagy in which cytosolic components are engulfed and delivered to the lysosome in bulk, **(2)** microautophagy, in which small volumes of cytosol are directly engulfed by lysosomes, and **(3)** chaperone-mediated autophagy (CMA), in which soluble substrates associated with a specific chaperone complex translocate into the lysosome *via* the lysosomal-associated membrane protein 2A (LAMP-2A) lysosomal receptor. Macroautophagy involves a series of maturation steps. First, a portion of cytoplasm is surrounded by an expanding isolation membrane or phagophore. Second, the phagophore seals to form an autophagosome, which in mammals fuses with late endosomes and multivesicular bodies to form an amphisome. Third, the amphisome then fuses with a lysosome to form an autolysosome, in which cytosolic cargo is degraded by lysosomal hydrolases. LC3-II is a protein that associates with the inner and outer surfaces of autophagic membranes, and provides a marker of autophagic vacuoles.

---

14 Reprinted from BBA Molecular Basis of Disease, Nedelsky *et al.*, Autophagy and the UPS: Collaborators in neuroprotection, Vol 1782, pp 691-699, © 2008 with permission from Elsevier.

Autophagy occurs at a basal level during growth and development, but can be up-regulated in conditions of cellular stress, such as during starvation. Autophagy induction is regulated by the target of rapamycin (TOR) kinase, which acts as a sensor for nutrient levels. Inactivation of TOR in yeast or mammalian cells leads to the induction of autophagy, even in nutrient-rich growth medium, indicating that TOR negatively controls starvation-induced autophagy (Blommaart *et al.*, 1995; Noda and Ohsumi, 1998). Shortly after induction, the expansion of an isolation membrane, or phagophore, engulfs a portion of the cell and eventually fuses to form the autophagosome (**Figure 1.15**). The induction, selection and packaging of cargo, formation of autophagosomes and completion, recycling of autophagy regulators, fusion of the autophagosome with the lysosome and cargo degradation are all dependent on the function of key *Atg* genes and two highly conserved ubiquitin-like conjugation reactions (**Figure 1.16**). One involves the formation of the Atg12-Atg5 complex, which can additionally bind Atg16, and the other involves the association of Atg8 (microtubule-associated protein 1 light chain in mammals, LC3) with phosphatidylethanolamine (PE). The function of the former 300 kDa complex is important in autophagosome membrane formation and has been shown to stabilise the Atg8-PE complex. The conjugation reaction between LC3 and PE allows for the lipidation of the cytosolic LC3I, forming the autophagosome-bound LC3II; LC3II is the only known protein that remains attached to the autophagosomal membrane and thus is a marker for autophagosome number (Kabeya *et al.*, 2000; Tanida *et al.*, 2005). After they are formed, autophagosomes proceed stepwise to eventually fuse with lysosomes.

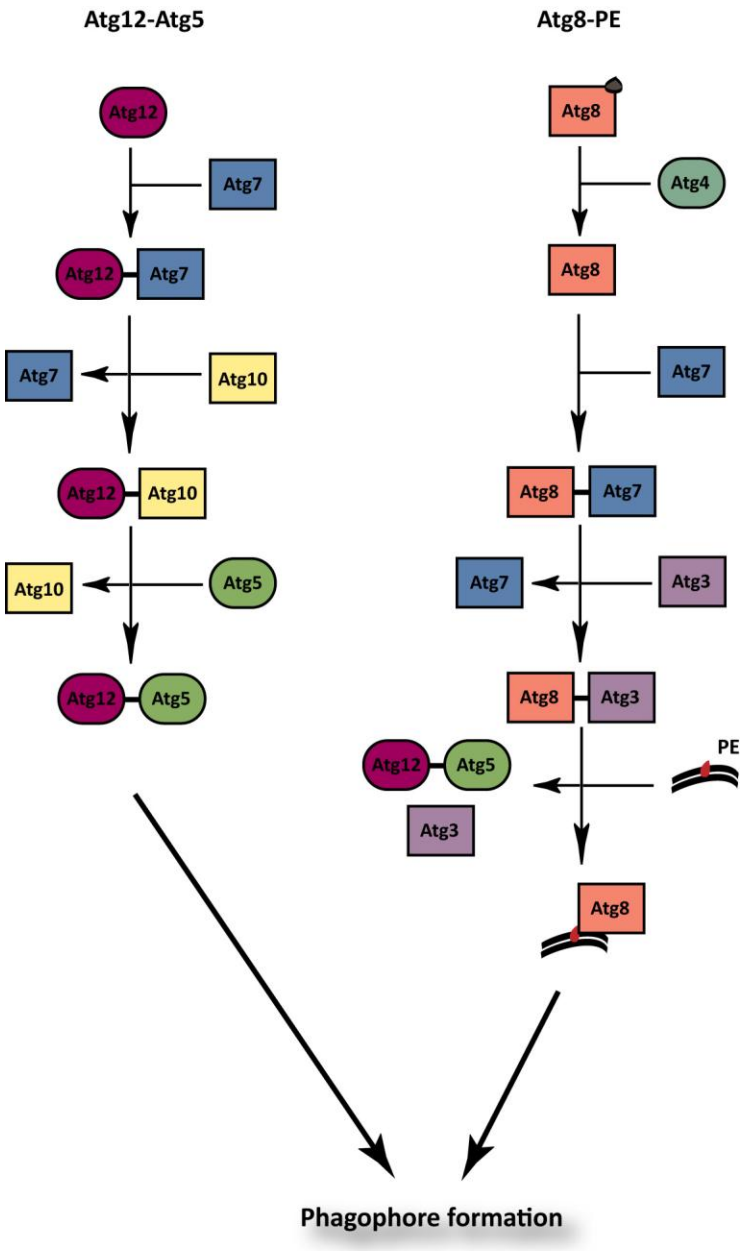

Figure 1.16 Atg conjugation pathways

In the Atg12-Atg5 pathway, the E1-like Atg7 associates with Atg12, which is then transferred to the E2-like Atg10 and finally conjugated to Atg5. In the Atg8-PE pathway, Atg8 associates with the E1-like Atg7, is then transferred to the E2-like Atg3, and subsequently conjugated to PE *via* the E3 action of the Atg12-Atg5 complex.

1.9 Cellular degradation systems and neurodegenerative diseases

Accumulating evidence in neurodegenerative diseases such as AD, PD, HD, amyotrophic lateral sclerosis (ALS) and prion disease suggests that they share cellular and molecular mechanisms such as protein misfolding and aggregation (Ross and Poirier, 2004). These 'proteinopathies' are characterised by the formation of protein aggregates, which usually include ubiquitinated deposits (Tai and Schuman, 2008). Indeed, abnormalities of four proteins, namely TAR DNA binding protein-43 (TDP-43), α-synuclein, tau and amyloid β have been linked to 90% of dementias (Tai and Schuman, 2008). The nature of the neurotoxic species in neurodegenerative disease has been a matter of increased debate and ambiguity (Taylor *et al.*, 2002; Ross and Poirier, 2005). Whether soluble monomers, oligomers, or larger amyloid fibrils are responsible for the neuropathology of neurodegenerative disease, the general consensus is that it is the capacity of abnormal proteins to aggregate *per se* that correlates with toxicity. Genetic and transgenic studies support the notion that mutations in the relevant proteins in neurodegenerative disease confer a toxic gain-of-function, thereby causing disease. Therefore, an understanding of cellular processes such as protein degradation, which coupled to protein synthesis regulates protein levels, is critical. Both proteasomes and lysosomes have been reported around ubiquitin-positive aggregates, but an unanswered question remains as to how neurodegeneration is linked to protein degradation impairment; is degradation impairment responsible for disease (and aggregate formation secondary), or is it that protein aggregation is toxic and subsequently interferes with the degradation of other proteins?

1.9.1 The UPS and neurodegenerative disease

Dysfunction of the UPS and the autophagy-lysosomal pathway have been implicated in neurological diseases (Rubinsztein, 2006; Levine and Kroemer, 2008). In sporadic PD, studies have reported loss of α subunits of 20S/26S and reduced 20S proteolytic activities (McNaught *et al.*, 2003), but whether this is a cause or late effect of the disease is poorly understood. The discovery of UPS mutations associated with familial

PD has provided the strongest support for a primary role of the UPS in the pathogenesis of neurodegenerative disease. Mutations in the E3 ubiquitin ligase parkin cause one of the more common types of familial PD, characterised by early onset, loss of dopaminergic neurones in the substantia nigra, usually in the absence of Lewy bodies (Shimura *et al.*, 2000). Mutations in UCHL1, a de-ubiquitinating enzyme, have also been implicated with familial and sporadic PD, but there are conflicting data (Belin and Westerlund, 2008). Recently, studies using novel conditional genetic mouse models showed that targeted conditional disruption of Rpt2 (19S ATPase; **Figure 1.12**) in the substantia nigra and forebrain results in neurodegeneration and Lewy body-like pathology, directly confirming that 26S dysfunction in neurones is involved in the pathology of neurodegenerative disease (Bedford *et al.*, 2008).

A significant subset of proteins that cause proteinopathies are partly dependent on the UPS for their degradation (Ravikumar *et al.*, 2002; Webb *et al.*, 2003), but proteasomes cannot efficiently degrade proteins when they are aggregated (Verhoef *et al.*, 2002). Moreover, the proteasome's enzymatic machinery is not able to cleave between successive polyQ residues, which characterise polyQ diseases such as HD (Venkatraman *et al.*, 2004). In polyQ disease there is conflicting evidence regarding the role of the UPS. Studies have shown impaired UPS function in both HD patient brain and HD-patient-derived fibroblasts (Seo *et al.*, 2004). However, in a spinocerebellar ataxia 7 mouse model, polyQ pathogenesis has been described in the absence of marked proteasome impairment (Bowman *et al.*, 2005). Additionally, in the R6/2 transgenic mouse model of HD there was no detectable impairment of proteasome catalytic function (Bett *et al.*, 2006). In a recent study, global changes to the UPS were reported in HD, early in the disease course in both the R6/2 transgenic mouse model as well as in HD patients (Bennett *et al.*, 2007), suggesting that the impairment may be occurring at the level of ubiquitin turnover rather than impairment of proteolytic function *per se*. Furthermore, recent findings of UPS impairment in the synapses of transgenic HD mice, which contribute to early synaptic dysfunction, underscore the importance of investigating proteasome activity in various sub-cellular regions (Wang *et al.*, 2008).

The UPS and prion disease

Cytosolic PrP^C

There is increasing data for a role of the UPS in prion disease. The UPS is involved in ERAD where ER-resident proteins, in unassembled or misfolded forms, undergo retrograde transport to the cytosol, get ubiquitinated and are degraded by the proteasome (Meusser *et al.*, 2005) (**Figure 1.9**). Both WT and misfolded forms of PrP^C undergo ERAD (Ma and Lindquist, 2001; Yedidia *et al.*, 2001). A pathogenic PrP^C mutant (Y145stop) associated with an inherited prion disease, GSS, is degraded *via* ERAD (Zanusso *et al.*, 1999), whereas another GSS-associated PrP^C mutant (Q217R), remains bound to BiP, an ER chaperone, for an unusually long period of time prior to proteasomal degradation (Jin *et al.*, 2000). More importantly, WT PrP^C molecules undergoing ERAD have been shown to accumulate in the cytosol when the proteasome is inhibited (Ma and Lindquist, 2001; Yedidia *et al.*, 2001). Yedidia *et al.* showed that cells treated with proteasome inhibitors accumulate both detergent-soluble and insoluble PrP^C species, with the latter containing a protease-resistant core and ubiquitin (Yedidia *et al.*, 2001). In a separate study, Ma and Lindquist showed that inhibition of the proteasome in cells leads to a significant fraction of endogenous PrP^C accumulation in the cytoplasm (Ma and Lindquist, 2001). The authors suggest that PrP^C accesses the cytoplasm *via* retrograde transport from the ER. Electron microscopy of mouse brain sections shows that cytosolic PrP^C is localised in the neurones of the hippocampus, neo-cortex and thalamus, supporting the fact that cytosolic PrP^C occurs *in vivo* (Mironov, Jr. *et al.*, 2003). It has been reported that UPS impairment may allow the conversion of this cytosolic PrP^C to an abnormal, 'PrP^{Sc}-like' form, with partial protease resistance and detergent insolubility (Ma and Lindquist, 2002). Proteasome inhibition has been shown to cause the accumulation of PrP^C aggregates in the cytosol of neurones with some PrP^{Sc} like properties, such as self-sustaining replication and partial PK-resistance (Ma and Lindquist, 2002). It is possible that if the quantity of PrP^C exceeds the degradative capacity of the UPS, then some PrP^C may be able to convert to a protease-resistant pathogenic form as removal of the proteasome inhibitor does not affect the abnormal PrP generation process once it starts (Ma and Lindquist, 2002).

The relationship between UPS inhibition, cytosolic PrP^C accumulation and neurotoxicity in prion disease has been investigated. Studies indicate that cytosolic PrP^C accumulation appears toxic to neurones (Ma *et al.*, 2002; Rane *et al.*, 2004; Rambold *et al.*, 2006). Cells with higher levels of PrP^C expression have been shown to be selectively killed by treatment with proteasome inhibitors (Ma *et al.*, 2002). In the same study, Ma *et al.* showed that unglycosylated PrP^C lacking a signal peptide, and hence the ability to traffic to the ER, accumulates in the cytosol and is neurotoxic. In agreement with these findings, it has been shown that cytosolic PrP^C accumulates in cells when the function of the PrP^C signal sequence is compromised (Rane *et al.*, 2004). More evidence for a toxic role of cytosolic PrP^C comes from a yeast model in which during post-translational targeting of PrP^C to the ER, PrP^C is mis-sorted to the cytosol and interferes with cell viability (Heller *et al.*, 2003). Additionally, toxicity has been linked to cytosolic PrP^C accumulation, when PrP^C co-aggregates with the anti-apoptotic protein Bcl-2 with toxicity abrogated after over-expression of heat shock proteins Hsp70 and Hsp40 (Rambold *et al.*, 2006). *In vivo*, mice expressing a PrP^C mutant lacking the N-terminal ER targeting signal (cytoPrP) develop normally, but are severely ataxic, with cerebellar degeneration and gliosis; they also accumulate an insoluble form of PrP^C (Ma *et al.*, 2002).

Despite the experimental data described above, the neurotoxic nature of cytosolic PrP^C in prion pathogenesis is under debate. The absence of toxicity when cytosolic PrP^C accumulates in human primary neurones treated with proteasome inhibitors has been reported; paradoxically, it protects against Bax-mediated cell death (Roucou *et al.*, 2003). Importantly, it has been observed that neither mutant or WT PrP^C undergo retrograde transport prior to proteasome degradation in various cell models (Drisaldi *et al.*, 2003; Fioriti *et al.*, 2005). Furthermore, it has been argued that cytosolic PrP^C accumulation may be a result of elevated levels of PrP^C expression from the cytomegalovirus (CMV) promoter used in many of the experiments. Drisaldi *et al.* show that proteasome inhibition results in the accumulation of unglycosylated cytosolic PrP^C in cells over-expressing PrP^C under the CMV promoter, but not in un-transfected or Tg mice-derived primary neurones, which express PrP^C from the endogenous promoter (Drisaldi *et al.*, 2003). Similarly, Fioriti *et al.* show that UPS inhibition in transfected cells expressing mutant mouse PrP

homologues associated with inherited human prion diseases causes accumulation of an unglycosylated, aggregated form of PrP^C in transfected cells that is not toxic (Fioriti *et al.*, 2005). In agreement with previous findings (Drisaldi *et al.*, 2003), the authors show that elevated PrP^C expression leads to cytosolic PrP^C accumulation and suggest this is due to impaired degradation of abortively translocated, signal peptide-bearing molecules synthesised from the CMV promoter.

Furthermore, the occurrence of PrP^C retrograde transport has been challenged, as antibodies against the signal peptide show that PrP^C accumulates in the cytosol as a result of failed translocation into the ER. *In vivo*, accumulation of unglycosylated cytosolic PrP^C does not cause any overt phenotype in aged, gene-targeted mice (Cancellotti *et al.*, 2005). These lines of evidence suggest that some PrP^C undergoes ERAD, but this proportion is most likely rapidly broken down and is a short-lived species (Yedidia *et al.*, 2001). Despite conflicting data, aberrant PrP^C trafficking to the cytosol, which does appear to occur *via* ERAD (Ma and Lindquist, 2001; Yedidia *et al.*, 2001), may play a role in prion pathogenesis, but as yet, is not fully defined.

The UPS and PrP aggresomes

A correlation between elevated levels of ubiquitin protein conjugates and reduced proteasome function in prion-infected mouse brain has been reported (Kang *et al.*, 2004), indicating that proteasome impairment may indeed be important in prion disease pathogenesis. Large, intracellular, peri-centrosomal structures termed aggresomes are thought to be a precise cellular response when cells try to cope with increased levels of misfolded and aggregated proteins, evidenced by the active recruitment of proteasome components and molecular chaperones to these aggregates (Olzmann *et al.*, 2008).

PrP^C and PrP^{Sc} aggresome formation has been reported in prion disease models *in vitro* (Cohen and Taraboulos, 2003; Mishra *et al.*, 2003; Kristiansen *et al.*, 2005; Grenier *et al.*, 2006; Goggin *et al.*, 2008). WT cells treated with cyclosporine A, an immunosuppressant, accumulate proteasome-resistant, 'prion-like' PrP species in aggresomes (Cohen and Taraboulos, 2003). Following proteasome inhibition pathogenic

PrP^{C} mutants have also been reported to accumulate in aggresomes (Cohen and Taraboulos, 2003). *In vitro*, green fluorescent protein (GFP)-tagged PrP mutants associated with familial prion disease accumulated in cytosolic, aggresome-like structures after proteasome inhibition, whereas GFP-tagged WT PrP^{C} did not (Mishra *et al.*, 2003). Moreover, the formation of cytosolic PrP^{C} aggresomes after transient cytoplasmic PrP^{C} expression appears to be toxic in both neuronal and non-neuronal cells (Grenier *et al.*, 2006). Recently, cytoplasmic PrP^{C} aggresomes were shown to induce cell death in various cell models by modifying the cell stress response *via* the activation of the RNA-dependent protein kinase and the induction of poly$(A)^{+}$ RNA aggregation (Goggin *et al.*, 2008).

Prion-infected mouse neuronal cell lines have been shown to be more susceptible to cell death following proteasome inhibition (Kristiansen *et al.*, 2005). In their cell system Kristiansen *et al.* used mild levels of proteasome inhibition, which is suggested to mimic the loss of proteasome activity associated with either the ageing process (Keller *et al.*, 2002; Ding *et al.*, 2003), or that may be seen in prion disease *in vivo* (Kang *et al.*, 2004). They showed that mild proteasome inhibition induced prion-infected cells to form cytosolic aggresomes containing PrP^{Sc}, Hsp70, ubiquitin and proteasome subunits (Kristiansen *et al.*, 2005). This work also showed that PrP^{Sc} aggresome formation was temporally associated with caspase 3 and 8 activation, and subsequent apoptosis in prion-infected cells and that cell death was abrogated after treatment with microtubule inhibitors, which prevent aggresome formation (Kristiansen *et al.*, 2005). Evidence for PrP^{Sc} aggresome-like structures in prion-infected mouse brain was described. Granular deposits of disease-related PrP have been previously reported in neuronal perikarya from post-mortem sporadic CJD cases, suggesting intra-neuronal prion aggregates may play a role in disease pathogenesis (Kovacs *et al.*, 2005).

At present, PrP^{Sc} trafficking is poorly-defined due to the lack of PrP^{Sc}-specific antibodies and hence the route by which PrP^{Sc} may enter the cytoplasm to form aggresomes has not been established (Caughey and Baron, 2006). Possibilities include retro-translocation from the ER (Ma and Lindquist, 2001; Yedidia *et al.*, 2001) or *via* endolysosomal membrane destabilisation and leakage into the cytosol, as described for $A\beta_{1\text{-}42}$ (Ji *et al.*, 2006). Furthermore, a recent paper by Wadia and colleagues reported that

some PrP may escape macropinosomes and leak into the cytosol (Wadia *et al.*, 2008). Consequently, UPS impairment due to the aging process or during prion infection *in vivo*, may allow for PrP^{Sc} accumulation into toxic aggresomes. These aggresomes could further inhibit the proteasome leading to impairment of PrP^{C} degradation and accumulation of PrP^{C} in the cytosol, in agreement with previous observations, underscoring that ERAD may contribute to neurodegeneration in prion diseases.

Although UPS impairment appears to cause accumulation of PrP^{C} in the cytosol, PrP^{Sc}-aggresome formation and lead to ER stress and subsequent cell death (Ma *et al.*, 2002; Hetz *et al.*, 2003; Kristiansen *et al.*, 2005), several unanswered questions remain. For example, does prion infection cause proteasome impairment *in vivo*, and if so, what is the mechanistic link between the two? Furthermore, the nature of the prion protein species responsible for proteasome inhibition and subsequent cellular stress is still unclear.

1.9.2 Autophagy and neurodegenerative disease

Autophagy has been implicated in the pathogenesis of a number of diseases, including cancer, myopathies, infectious disease and neurodegeneration (Kundu and Thompson, 2008). As neurones are highly active, post-mitotic cells, they are especially vulnerable to the intracellular accumulation of aberrant proteins, explaining the frequency with which proteopathies affect the nervous system (Nedelsky *et al.*, 2008).

The suggestion that autophagy plays a role in neurodegenerative disease initiation or progression resulted from increasing observations of autophagic vacuoles in affected brain regions of AD, PD, polyQ diseases and prion diseases (McCray and Taylor, 2008). In AD, autophagic vacuoles have been observed in neocortical and pyramidal neurones (Nixon *et al.*, 2005), whereas in HD, remnants of polyQ-expanded huntingtin have been shown to accumulate in cathepsin D positive vacuoles in patient-derived lymphoblasts (Sapp *et al.*, 1997). In PD, autophagic vacuoles have been described in melanised neurones of the substantia nigra (Anglade *et al.*, 1997). These observations at the histopathological level have been corroborated in respective disease models. Interestingly, exogenous

expression of polyQ-expanded disease-related proteins results in an augmentation in biochemical and morphological markers of autophagy both *in vitro* (Taylor *et al.*, 2003; Ravikumar *et al.*, 2004) and *in vivo* in fly and mouse models of polyQ diseases (Petersen *et al.*, 2001; Pandey *et al.*, 2007).

It is possible that the increased frequency of autophagic vacuoles in the diseased brain is due to the induction of autophagy as a response to cell stress or death, or due to impaired autophagy flux. In other words, the accumulation of autophagic vacuoles may be caused by either the induction of autophagosome formation, or a defect in autophagosome clearance when fusion of autophagosome to lysosome is impaired. Furthermore, the accumulation of autophagosomes in dying neurones has raised a number of important questions (Kundu and Thompson, 2008). For example, is autophagy cytoprotective or does it mediate cell death? Is it induced as a secondary effect in cells already committed to dying? Insight into the role of autophagy in neurodegenerative disease has come from studies which have collectively shown that a) aberrant proteins are degraded by autophagy, b) autophagy impairment leads to neurodegeneration in animal models and human disease, and c) manipulating autophagy alters the disease phenotype in animal models (Kundu and Thompson, 2008).

Accumulating evidence supports the degradation of some disease-related proteins by autophagy. *In vitro* studies in which autophagy was either pharmacologically induced or impaired have demonstrated changes in the turnover rate of mutant polyQ protein, mutant polyA protein, as well as WT and mutant α-synuclein (Webb *et al.*, 2003; Ravikumar *et al.*, 2004). At the ultra-structural level, immuno-electron microscopy has revealed that disease-related proteins, such as expanded polyQ, are delivered to autophagosomes (Kegel *et al.*, 2000; Taylor *et al.*, 2003). Moreover, some Atg proteins, such as LC3 and the Atg5/Atg12/Atg16 complex, have been shown to be recruited into mutant huntingtin aggregates suggesting that autophagy is taking place close to protein inclusions (Iwata *et al.*, 2005b; Yamamoto *et al.*, 2006).

A neuroprotective role conferred by autophagy in the context of proteopathies is supported by animal studies in which impairment of autophagy by genetic manipulation

leads to neurodegeneration. Specifically, cathepsin D KO mice and *Drosophila* mutants show a neurodegenerative phenotype coupled with the accumulation of autophagosomes and lysosomes (Koike *et al.*, 2000; Koike *et al.*, 2005; Myllykangas *et al.*, 2005; Shacka *et al.*, 2007). Moreover, conditional Atg-null mice die prematurely as a result of neurodegeneration and exhibit extensive ubiquitin staining (Hara *et al.*, 2006), and induction of autophagy by rapamycin treatment in fly and mouse models of HD has been shown to ameliorate the phenotype of the disease (Ravikumar *et al.*, 2004; Berger *et al.*, 2006; Pandey *et al.*, 2007). TOR independent methods of autophagy induction such as the use of lithium (Sarkar *et al.*, 2008) or trehalose (Tanaka *et al.*, 2004; Davies *et al.*, 2006; Sarkar *et al.*, 2007) also ameliorate neurodegeneration in fly and mouse models of HD (Tanaka *et al.*, 2004; Sarkar *et al.*, 2008) and clear aggregate-prone protein *in vitro* (Sarkar *et al.*, 2007).

Data on the role of autophagy in prion disease are confined to a number of electron microscopy studies, which show the presence of autophagic vacuoles in the neurones of experimental models of human and animal prion disease (Boellaard *et al.*, 1989; Boellaard *et al.*, 1991; Liberski *et al.*, 1992a), as well as in naturally occurring BSE (Liberski *et al.*, 1992b). However, unlike in other neurodegenerative diseases, the role of autophagy in prion disease has not been investigated using molecular and/or biochemical approaches. Therefore, it is unclear whether increases in autophagosome numbers, by PrP^{Sc} formation, correlate with increased levels of autophagy or impaired autophagosome turnover. Furthermore, it is yet unclear how this relates, if at all, to prion disease pathogenesis.

1.10 Aims of the thesis

A. Role of the UPS in prion disease pathogenesis

- To evaluate the role of the UPS in prion disease pathogenesis and investigate the relationship between the two
- To test whether disease-related, β-sheet-rich prion protein directly and specifically impairs neuronal cellular function by inhibiting the 26S proteasome *in vitro* as well as in prion-infected mouse brain
- To examine the nature of the PrP^{Sc} species responsible for neurotoxicity using recombinant prion protein species
- To define the biochemical mechanism by which aggregated β-sheet-rich prion protein could be inhibiting the proteasome
- To investigate whether there is a physical interaction between the aggregated prion species and the proteasome

B. Role of autophagy in prion disease pathogenesis

- To investigate the role of autophagy in prion disease by biochemical analysis, both *in vitro* and in prion-infected mouse brain
- To evaluate whether autophagy is acting as a compensatory protein degradation system when the proteasome is impaired
- To test whether induction of autophagy can ameliorate the deleterious effects seen in prion-infected cells where the proteasome is inhibited
- To examine whether induction of autophagy clears PK-resistant prion protein

2 MATERIALS AND METHODS

All chemicals were purchased from Sigma-Aldrich Ltd unless otherwise specified.

2.1 Cell culture

Work with mouse cell lines was carried out in a designated tissue culture facility using strict aseptic technique. All media and solutions were bought pre-sterilised and sterile plastic-ware was used. All procedures, including preparation of media, were performed in a tissue culture hood with a laminar flow unit. All solutions and media were pre-warmed to 37°C prior to use.

2.1.1 Cell lines

N2a

N2a mouse neuroblastoma cells were purchased from the American Type Tissue Collection (ATCC CCL131). The N2aPK-1 cell line was a kind gift from Dr Peter Klöhn (MRC Prion Unit, Institute of Neurology, UCL).

GT-1-7

GT-1-7 cells are a subcloned cell line of immortalized mouse hypothalamic GT-1 cells. They were a kind gift from Professor Hermann Schatzl (Institute of Virology, Technical University, Munich) and from Dr Andrew Hill (University of Melbourne, Australia).

Cerebellar granule neurones

Murine cerebellar granule neurones (CGN) were prepared by Ms Heike Naumann from 6 day old Friend Virus B-type (FVB) mice as previously described (Schousboe and Pasantes-Morales, 1989).

2.1.2 Propagation of cell lines

Cell growth

N2aPK-1 and GT-1 cells grew in Opti-MEM standard growth medium (Invitrogen) supplemented with 50 U/ml penicillin (Invitrogen), 50 μg/ml streptomycin (Invitrogen) and 10 % v/v foetal calf serum (FCS; Invitrogen). Cell lines were maintained in sterile 10 cm tissue culture plates (VWR) in a humidified CO_2 incubator, in an atmosphere of 5-7 % CO_2 at 37°C. Growth medium was regularly changed 2-3 times weekly. Prior to the addition of fresh medium, cells were washed with sterile phosphate buffered saline (PBS; Invitrogen) (137.9 mM NaCl, 2.7 mM KCl, 1.5 mM KH_2PO_4, 8.1 mM Na_2HPO_4, pH 7.4) to remove debris. All cell work was carried out in a Class II microbiological safety cabinet.

Cell harvesting

When cells reached confluence they were harvested and sub-cultured. First, cells were washed with PBS and subsequently incubated for 3-5 min at 37°C with 1 ml trypsin (25 g/L trypsin, 8.5 g/L NaCl; Invitrogen). Cells were then dislodged by gently tapping the plate. Following this, 6 ml of fresh Opti-MEM supplemented with FCS were added to the plate to stop the enzymatic action. The medium was then lightly triturated to ensure equal cell dispersal. The cells were then split into numerous plates ranging from 1:3 to 1:10 to continue growing.

Cryopreservation of cell lines

Confluent plates of cells were harvested in blue Falcon™ tubes and spun for 5 min at 160 x *g* at 22°C. They were then washed with ice-cold sterile PBS and spun for 5 min at 160 x *g* at 22°C. The resulting pellet was re-suspended in 1 ml of sterile freezing medium consisting of 50% FCS and 8 % sterile dimethyl sulfoxide (DMSO) and transferred to a cryo-vial. Cryo-vials were then placed in Nalgene® freezing boxes and subsequently into the -70°C freezer to gradually bring down cell temperature. The following day cryo-vials were placed in liquid nitrogen for long term storage and their location was noted in the tissue culture notebook for future reference.

Defrosting of cell lines

Cells were rapidly defrosted by thawing the cryo-vial in a 37°C water bath for 30 seconds. The cell suspension was then transferred to 9 ml of pre-warmed growth medium in a blue Falcon™ tube and spun for 5 min at 160 x *g* at 4°C. Following centrifugation, the supernatant was discarded and the pellet was re-suspended in 1 ml fresh pre-warmed growth medium. The cell suspension was then transferred to a 10 cm plastic tissue culture plate and topped up to 7 ml with growth medium. The next day cells were washed with sterile PBS and fresh medium was added.

Prion infection of cell lines

Mouse-adapted Rocky Mountain laboratory (RML) prions or WT CD-1 mouse brain homogenate were used to infect N2aPK-1 and GT-1 neuronal cells. The brains of scrapie-sick mice infected with RML mouse adapted prions or of WT CD-1 mice were homogenized by passing eight times each through a 21-gauge needle and adjusted to 10 % (w/v) with PBS. Following a 5 min centrifugation at 800 x *g* at RT, supernatants were removed and stored at -70°C. 5000 or 15000 cells were seeded into 96-well plates and maintained in culture for 24 hours (h) prior to being exposed to either 0.1 % RML-infected mouse brain in standard growth medium or to 0.1 % WT CD-1 mouse brain in standard growth medium. Three days later the inoculum was removed and cells split 1:8; cells were split 1:8 twice more in 3 day intervals. The presence of PrP^{Sc} was then tested by the scrapie cell assay (SCA). Cells were maintained in standard growth medium at 37°C in 5 % CO_2.

Curing cells of prion infection

Both ScN2aPK-1 and ScGT-1 cells were cured of PrP^{Sc} with 0.5 μg/ml anti-PrP antibody ICSM18 (D-Gen Ltd., London, UK) in standard growth medium for 14 days.

2.1.3 Scrapie cell assay

A sterile Elispot plate (MultiScreen Immobilon®-P 96-well Filtration Plates, Millipore) was activated by suctioning through with 70 % ethanol and then washing twice with PBS (by suction). Following cell counting, 5000 cells were plated in each of 12 wells (in 200 μl

standard growth medium). The plate was dried for 1 h at 50°C. Elispot plates were incubated at 37°C for 90 min with 50 μl proteinase K (PK; Roche) in 1 X lysis buffer (50 mM Tris.HCl, pH 8.0, 150 mM NaCl, 0.5 % Na deoxycholate, 0.5 % Triton-X); the liquid was then removed by suctioning, and wells washed twice with PBS (by suction). Following a 10 min RT exposure to phenylmethylsuphonyl fluoride (PMSF; 2 mM) to stop PK action, each well was incubated with 160 μl 3M guanidinium thiocyanate (GSCN) in 10 mM Tris.HCl (pH 8) at RT for 10 min to expose PrP^{Sc} epitopes. After discarding the supernatant, the plate was washed four times with PBS and the wells were incubated for 1 h at 37°C with 160 μl Superblock blocking buffer (Pierce). After suctioning the liquid off, wells were incubated with 50 μl anti-PrP antibody (ICSM-18; 1:5000) in 1 X TBST (10 mM Tris.HCl, pH 8.0, 150 mM NaCl, 0.1 % Tween-20) and 1 % milk powder (Marvel) for 1 h at RT. Following this, wells were washed 7 times with 160 μl 1 X TBST by suctioning and then incubated with 50 μl anti-IgG1 alkaline phosphatase (1:4500 in 1 X TBST/ 1 % milk powder; Southern Biotechnology; AP) for 1 h at RT. Wells were washed seven times with 160 μl 1 X TBST by suction. After being left to dry, wells were incubated with 50 μl AP conjugate substrate (prepared as recommended by BIORAD) and incubated until a clear colour change was seen in positive controls. Following this wells were washed twice with double distilled water and stored at -20°C until analysis.

2.1.4 Semi-purification of PrP^{Sc}

From RML prion-infected mouse brain

One whole RML-infected mouse brain was homogenised in 9 X volumes of lysis buffer (100 mM Tris.HCl, pH 7.4, 300 mM NaCl, 4 mM EDTA, 1 % Triton-X-100, 1 % deoxycholate) and later spun at 500 x *g* for 10 min at 4°C. Supernatants were incubated with 50 U/ml benzonase (Merck) for 20 min on ice and subsequently with PK (5 μg/ml protein) at 37°C for 30 min. PK activity was stopped by incubating lysates with AEBSF (8 mM; Merck) for 10 min at 37 °C. Lysates were then centrifuged at 100,000 x *g* for 45 min and sonicated (three

cycles of 10 x 0.5 second pulses). Protein content was measured using the BCA™ assay. After being snap-frozen, semi-purified PrP^{Sc} was kept at -70°C.

From RML prion-infected GT-1-7 cells

Ten 10 cm plates of ScGT-1 cells were pre-treated for 24 h with 1 μM lactacystin (Calbiochem) at 37°C. Cells were then harvested and gently washed in ice-cold PBS before being freeze-thawed three times in liquid nitrogen and centrifuged at 1000 x *g* for 10 min at 4°C to remove cellular debris. The supernatant was then collected and adjusted with an equal volume of 2 X lysis buffer (100 mM Tris, pH 7.4, 300 mM NaCl, 4 mM EDTA, 1 % Triton-X-100, 1 % deoxycholate) followed by incubation with benzonase (50 U/ml) for 20 min on ice. Lysates were then incubated with PK at 1 μg/mg protein (37°C, 90 min) followed by treatment with AEBSF (8 mM) to stop action of PK for 10 min at 37°C. Lysates were centrifuged at 100,000 x *g* for 45 min and then sonicated (3 cycles of 10 x 0.5 second pulses). Protein content was measured using the BCA™ assay. The pellet was diluted to a final concentration of 1 mg/ml; after being snap-frozen, semi-purified PrP^{Sc} aggresomes were kept at -70°C.

2.2 Methods for the detection of proteins

2.2.1 Western blotting of proteins

Preparation of lysates (no proteinase K digestion required)

Cells were harvested on ice and spun twice at 4°C (160 x *g*, 5 min) in ice-cold PBS to eliminate any FCS. The resulting pellet was then re-suspended in minimal volume of ice-cold PBS on ice. Cells were lysed by freeze-thawing in liquid nitrogen (3 times). Lysates were benzonase-treated for 20 min on ice (50 U/ml). Ice-cold PBS was added to acceptable viscosity and an aliquot was taken off for protein assay to ensure equal loading. The remaining supernatant was frozen at –70°C.

Preparation of lysates (proteinase K digestion required)

Cells were harvested on ice and spun twice at 4°C (160 x *g*, 5 min) in ice-cold PBS to eliminate FCS. The resulting pellet was then re-suspended in minimal volume of ice-cold PBS on ice. Cells were lysed by freeze-thawing in liquid nitrogen (3 times). Lysates were benzonase-treated for 20 min on ice. Ice-cold PBS was added to acceptable viscosity and an aliquot was taken off for protein assay to ensure equal loading. The remaining supernatant was frozen at –70°C. Upon thawing cells were treated by adding PK to a final concentration of 50 μg/ml for 30 min at 37°C. Samples were then centrifuged at 16,000 x *g* for 1 min to pellet cellular debris; digestion was ended in samples by adding 8 mM AEBSF in an equal volume of 2 X reducing sample buffer (125 mM Tris, pH 6.8, 20 % glycerol, 0.05 % bromophenol blue, 4 % SDS).

Quantification of protein by BCA

The bicinchoninic acid (BCA™) protein assay reagent kit (Pierce) was used for the detection and quantitation of total protein in lysates. This method is based on the ability of proteins to reduce Cu^{+2} to Cu^{+1} in an alkaline environment. The purple reaction product is water soluble and readily detected at 562 nm. To conserve lysates, the microplate procedure was used. A fresh set of protein standards was prepared for each assay by using bovine serum albumin (BSA) in the same diluent as the unknown sample. The range of standards was 0, 25, 125, 250, 500, 750, 1000, 1500 and 2000 μg. Preparation of BCA working reagent (WR) was according to manufacturer's instructions. 25 μl of each standard or unknown sample was pipetted into 96 well plates. This was done in duplicate for standards and triplicate for unknown samples. 200 μl WR was then added to each well and the plate was mixed thoroughly on a plate shaker for 30 seconds. The plate was then covered and incubated at 37°C for 30 min. After briefly cooling down, the plate was read at 570 nm on a Tecan plate reader (Sunrise). A standard curve was prepared and unknown protein concentrations calculated using a statistical analysis program (GraphPad Instat Version 3.02, GraphPad Software).

SDS –polyacrylamide gel electrophoresis (SDS-PAGE)

Reducing sample buffer was added to 1 X concentration and samples were boiled at 100°C for 10 min. Samples were then spun at 16,000 x *g* for 1 min, briefly vortexed and finally spun at 16,000 x *g* for 1 min before loading onto 16% Tris-Glycine mini gels (Invitrogen). Gels were electrophoresed vertically in Tris/Glycine SDS running buffer (National Diagnostics) in a X-Cell *SureLock™* Mini-Cell system (Invitrogen) for 80 min at 200V (or until the dye front run off at the end of the gel). Pre-stained Seeblue® Protein Standard (Invitrogen) was used as a molecular weight marker.

Coomassie staining of gels

After electrophoresis, gels were soaked in fixing solution (40 % v/v methanol, 10 % v/v acetic acid) for 20 min at RT with gentle agitation to fix proteins onto the gels. The gels were then covered with 0.02 % w/v R-250 Coommassie stain (in 40 % v/v methanol, 10 % v/v acetic acid) and incubated overnight with gentle agitation. Gels were de-stained using 8 % v/v acetic acid for 3-4 h, changing the de-stain solution every 30 min. When the protein bands were visible without background staining, a photograph of the gels was taken.

Electroblotting of gels

Protein was transferred onto PVDF membranes (Millipore). PVDF membrane was pre-cut at the same size as the gels and pre-soaked in 100 % methanol for 2 min to ensure even hydration prior to transfer into blotting buffer (National Diagnostics). Protein was transferred from the gel to the membrane in Novex X-Cell II™ Blot modules (Invitrogen) at either 35V for 90 min, or 14V overnight.

Immunoblotting of gels

After electroblotting, membranes were transferred to square tissue culture petri dishes and washed in PBS containing 0.05 % v/v Tween-20 (1 X PBST). Blots were then blocked for 1 h at RT with gentle agitation using either 5 % BSA or 5 % non-fat milk powder (Marvel). Blocking solution was made in 1 X PBST. Membranes were washed briefly with 1 X PBST before overnight incubation with the appropriate primary antibody at RT with

gentle agitation. The membranes were then washed in 1 X PBST for a minimum of 45 min changing buffer 5 times. Secondary detection was performed by incubating with the appropriate secondary antibody (diluted in 1 X PBST) for 45 min at RT. Detection of bound antibody was performed with SuperSignal® West Pico chemiluminescent substrate (Pierce) according to manufacturer's instructions. Excess reagents were poured off and the membranes were placed between acetate films and transferred to a photographic cassette. Biomax® MR films (Kodak™ from Anachem) were developed using Kodak™ developer and fixer by hand or by using a Xograph imaging machine (Xograph Imaging Systems). Developed films were scanned using an Epson scanner for electronic format and densitometry of digital images was achieved by using a Kodak Image Station 440 CF.

Determination of equal protein loading

The *Re-Blot™ Plus* Western Blot Strong Antibody Stripping Solution (Chemicon) consists of specially formulated solutions that quickly and effectively remove antibodies from Western blots without significantly having an effect on the immobilized proteins. Blots were washed in 1 X PBST buffer for 10 min before being incubated for 15 min with 1 X *Re-Blot™ Plus* Strong Antibody Stripping solution. Following this, blots were briefly washed with 1 X PBST and subsequently blocked with 5 % milk powder in 1 X PBST for 1 h. Mouse monoclonal anti-β-actin antibody (1:10,000; Sigma) was used to probe for the control loading protein.

Densitometry

Densitometry on immunoblots was performed using the Kodak™ Digital Science Image station 440CF (IS440CF) system and analysed using the Kodak™ ID Image Analysis Software (PerkinElmer Life Sciences).

2.2.2 Co-Immunoprecipitation experiments

Magnetic tosyl-activated beads (Dynal) were coated with mouse monoclonal antibody to PrP (ICSM35; D-GEN; at 24 μg/reaction). Five μg of human 20S proteasome were incubated with 3 μg aggregated β-PrP (**Section 2.3**) or 3 μg aggregated α-PrP (**Section 2.3**)

for 1h at 37°C. Samples were incubated with either ICSM35- or uncoated-coated beads overnight on a rotator at 4°C. Beads were concentrated, washed with PBS, re-suspended in SDS sample buffer and boiled. The supernatant was analyzed by SDS-PAGE and immunoblotted with a rabbit polyclonal antibody to the 'core' 20S subunits (BIOMOL; 1:2,000).

2.3 Preparation of recombinant proteins

Full-length (23-231aa) recombinant mouse PrP in either the oxidised form (α-PrP) or the reduced form (β-PrP) was prepared by a modification of the method as described (Jackson *et al.*, 1999) and was prepared by Mr Mark Batchelor (MRC Prion Unit, London, UK). Protein concentration was determined by UV absorption using a calculated molar extinction coefficient of 56,120 M^{-1} cm^{-1} at 280 nm. Both α- and β-PrP underwent buffer exchange, i.e. from their mother buffer to water. Like α-PrP, β-PrP was buffer exchanged in water by ultra-filtration.

Aggregation methods for recombinant PrP

Aggregation of β-PrP was initiated by the addition of NaCl to a final concentration of 150 mM. The reaction was allowed to proceed for 1 h at 37°C until aggregation was visible. Aggregation of α-PrP was achieved by thermal denaturation (heating at 70°C for 10 min). Moreover, NaCl was added to a sample of α-PrP at a similar final concentration to aggregated β-PrP (150 mM) as a control for salt-aggregated β-PrP.

Denaturation of recombinant PrP

Denaturation of recombinant β-PrP was achieved by 10 cycles of freeze (liquid nitrogen)-boiling.

PrP amyloid fibrils

Amyloid fibrils of recombinant murine PrP were prepared by Dr Howard Tattum (MRC Prion Unit, London, UK) using a protocol adapted from that of Baskakov *et al.* and were a kind gift from Dr Graham Jackson (MRC Prion Unit, London, UK) (Baskakov *et al.*, 2002).

Briefly, recombinant α-PrP was transferred into 20 mM sodium acetate, pH 3.7, and was denatured by the addition of 10 M urea. Recombinant protein was then dialysed in 1.3 M urea and 1 M GuHCl pH 6.0. 800 μl of 0.8 mg/ml protein was aliquoted into a 1.5 ml microcentrifuge tube and shaken at 600 rpm (Eppedorf Thermomixer™) at 37°C to stimulate assembly of α-PrP monomers. Amyloidogenesis was complete after a reaction time of 10 h. The presence of fibrils was confirmed by electron microscopy performed by Dr Howard Tattum (MRC Prion Unit, London, UK). Fibrils were assayed at a final concentration of 1 mg/ml.

Preparation of aggregated non-prion recombinant proteins

Lysozyme was aggregated by the addition of 50 mM DTT and the reaction was allowed to proceed for 1 h; it was assayed at a final concentration of 1 mg/ml. Amyloid β_{1-40} ($A\beta_{1-40}$) was aggregated immediately by the addition of water and assayed at a final concentration of 100 μg/ml. SOD1 WT and SOD1 mutant recombinant proteins were prepared by Dr Ruth Chia; they were aggregated in PBS and assayed at a final concentration of 1 mg/ml. Carboxy-methylated α-lactalbumin was prepared in water and assayed at a final concentration of 1 mg/ml.

2.4 Ubiquitin-proteasome system activity assays

2.4.1 Proteasomal β subunit activity probes

In their 2005 paper in Nature Methods, Berkers *et al.* described novel β subunit activity probes that were used to define the *in vivo* specificities of the proteasome inhibitor bortezomib (Berkers *et al.*, 2005). This dansylAhx3LVS activity probe was a kind gift from Dr Huib Ovaa (Netherlands Cancer Institute, Netherlands).

Protein extraction from cells and mouse brain

Confluent 10 cm plates of N2aPK-1 cells were washed with ice-cold sterile PBS and cells were harvested by trituration. The cell pellet was then washed twice at 160 x *g* for 5 min at 4°C with ice-cold sterile PBS and then lysed by vortexing for 30 min at 4°C at 1,400 rpm

(Eppendorf Thermomixer®) in an equal volume of freshly-made homogenisation buffer (50 mM Tris.HCl, pH 7.4, 250 mM sucrose, 5 mM $MgCl_2$, 2 mM ATP) and glass beads (<106 microns, acid washed). 1 mM DTT was added fresh to the lysates after a small aliquot was taken for protein determination by the BCA™ assay. The lysates were further centrifuged for 5 min at 4°C at 16,000 x *g* to remove beads, nuclei, membrane fractions and cellular debris. Subsequently 100 μg of protein were incubated with 1 μM of the dansyl-sulfonamidohexanoyl activity probe for 1 h at 37°C at 1,400 rpm (Eppendorf Thermomixer®) before assaying by immunoblotting. For GT-1 cells, the activity probe was used at a concentration of 10 μM in culture for 1 h at 37°C; cells were then harvested as described above.

Immunoblotting to assay specific β subunit activities

To assay for specific β subunit activities equal amounts of protein (100 μg) were denatured in reducing sample buffer for 10 min at 100°C and then separated by SDS PAGE on 12 % Tris Glycine mini gels for 80 min at 200V. Protein was transferred onto PVDF membranes at 35V for 90 min. Membranes were then blocked using 5 % BSA in 1 X PBST for 1 h at RT and then immunoblotted using a rabbit antibody against the dansyl-sulfonamidohexanoyl hapten tag (1:1,000 in 1 X PBST; Molecular Probes) incubated overnight at RT. Secondary detection was performed by incubating with a donkey anti rabbit horse radish peroxidase (1:5,000 in 1 X PBST; HRP; Amersham Biosciences) for 45 min at RT followed by enhanced chemiluminescence. To ensure equal protein loading PVDF membranes were stripped using *Re-Blot™ Plus* Western Blot Strong Antibody Stripping Solution and re-probed with a mouse monoclonal anti-β-actin antibody (1:10,000 in 1 X PBST).

Incubation of disease-related PrP isoforms with aggregation intermediates-specific antibody

Either 500 ng/ml aggregated β-PrP or 500 ng/ml PrP^{Sc} was incubated for 1 h at RT with 5 μg/ml or 150 μg/ml of a rabbit polyclonal antibody raised against oligomeric protein species (Kayed *et al.*, 2003) (kind gift from Dr. Glabe, Department of Molecular Biology

and Biochemistry, University of California) or 150 μg/ml of mouse monoclonal anti-PrP antibodies (ICSM18, ICSM4, or ICSM35; these antibodies were a kind gift from Dr Azy Khalili-Shirazi, MRC Prion Unit, Institute of Neurology, UCL). These mixtures were incubated with 100 μg of cytosolic fraction from N2aPK-1 cell lysates for 1 h at 37°C with 2 mM ATP on a shaker before addition of 1 μM probe (1 h at 37°C). Samples were denatured in reducing sample buffer by boiling for 10 min and then separated by SDS PAGE on 12 % Tris Glycine mini gels for 80 min at 200V. Protein was transferred onto PVDF membranes at 35V for 90 min. Membranes were then blocked using 5 % BSA in 1 X PBST for 1 h at RT and then immunoblotted using a rabbit antibody against the dansyl-sulfonamidohexanoyl hapten tag (1:1,000 in 1 X PBST) incubated overnight at RT. Secondary detection was performed by incubating with a donkey anti rabbit HRP (1:5,000 in 1 X PBST;) for 45 min at RT followed by enhanced chemiluminescence. To ensure equal protein loading PVDF membranes were stripped using *Re-Blot™ Plus* Western Blot Strong Antibody Stripping Solution and re-probed with a mouse monoclonal anti-β-actin antibody (1:10,000 in 1 X PBST).

2.4.2 Fluorogenic assays for proteasome activity

Proteasome catalytic activities in cell and mouse brain lysates

Minor modifications were made to protocols already described (Dantuma *et al.*, 2000; Kisselev and Goldberg, 2005; Berkers *et al.*, 2005). Cells were washed twice with ice-cold PBS at 4°C for 5 min at 160 x *g* and then pelleted and lysed in an equal volume of glass beads (<106 microns, acid washed) and freshly-made homogenization buffer (50 mM Tris.HCl, pH 7.4, 2 mM ATP, 5mM $MgCl_2$, 250 mM sucrose). 1 mM DTT was added to the lysates after a small aliquot was taken for protein content determination using the BCA™ assay. Following this lysates were vortexed for 30 min at 4°C at 1,400 rpm (Eppendorf Thermomixer®) and further spun at 16,000 x *g* for 5 min at 4°C to remove beads, nuclei, membrane fractions and cellular debris from the supernatant. To measure the rate of hydrolysis 10 μg of protein was incubated with 100 μM of either of the following

fluorogenic substrates: Ac-nLPnLD-AMC (assays caspase-like activity; Bachem), Suc-LLVY-AMC (assays chymotrypsin-like activity; Biomol) Boc-LRR-AMC (assays trypsin-like activity; Biomol) in 100 μl reaction buffer (50 mM Tris.HCl, pH 7.4, 5 mM $MgCl_2$, 2 mM ATP, 1 mM DTT). Samples were incubated for 30 min at 37°C and the release of 7-amino-4-methylcoumarin (AMC) was monitored continuously every minute for 30 min using a TECAN 96-well reader at 360nm excitation and 465nm emission.

Proteasome activities in pure proteasome preparations

Human 26S and 20S assays

Minor modifications were made to protocols already described (Dantuma *et al.*, 2000; Kisselev and Goldberg, 2005; Berkers *et al.*, 2005). 0.1 μg of pure human 26S proteasome (BIOMOL) or 0.1 μg of pure human 20S proteasome (BIOMOL) activated with 32 ng PA28α/β activator (BIOMOL) or CtRpt5 (250μM) were added to 100 μl reaction buffer (50 mM Tris.HCl, pH 7.4, 10 mM $MgCl_2$, 1 mM DTT; plus 2mM ATP for 26S assays) and incubated with 100 μM of either of the following fluorogenic substrates: Ac-nLPnLD-AMC (assays caspase-like activity), Suc-LLVY-AMC (assays chymotrypsin-like activity); Boc-LRR-AMC (assays trypsin-like activity) to measure the rate of hydrolysis. Samples were incubated at 37°C and the release of 7-amino-4-methylcoumarin (AMC) was monitored continuously every minute for 60 min using a TECAN 96-well reader at 360nm excitation and 465nm emission.

Yeast 26S and 20S assays

625 ng of WT yeast 20S proteasome or 0.1 μg of WT yeast 26S proteasome (both kind gifts from Dr Michael Glickman, The Technion, Israel) were added to 100 μl reaction buffer (50 mM Tris.HCl, pH 7.4, 10mM $MgCl_2$, 1 mM DTT; plus 2mM ATP for 26S assays) and incubated with 100 μM of either of the following fluorogenic substrates: Ac-nLPnLD-AMC (assays caspase-like activity), Suc-LLVY-AMC (assays chymotrypsin-like activity); Boc-LRR-AMC (assays trypsin-like activity) to measure the rate of hydrolysis. 625 ng of α3ΔN yeast 20S proteasome (kind gift from Dr Alexei Kisselev, Dartmouth Medical School, New Hampshire, USA) were added to 100 μl reaction buffer (50 mM Tris.HCl, pH 7.4, 10mM

$MgCl_2$, 1 mM DTT) and incubated with 100 μM of either of the following fluorogenic substrates: Ac-nLPnLD-AMC (assays caspase-like activity), Suc-LLVY-AMC (assays chymotrypsin-like activity); Boc-LRR-AMC (assays trypsin-like activity) to measure the rate of hydrolysis. 625 ng of α3/α7ΔN yeast 20S proteasome or 0.1 μg of α3/α7 ΔN yeast 26S proteasome (both kind gifts from Dr Michael Glickman, The Technion, Israel) were added to 100 μl reaction buffer (50 mM Tris.HCl, pH 7.4, 10mM $MgCl_2$, 1 mM DTT; plus 2mM ATP for 26S assays) and incubated with 100 μM of either of the following fluorogenic substrates: Ac-nLPnLD-AMC (assays caspase-like activity), Suc-LLVY-AMC (assays chymotrypsin-like activity); Boc-LRR-AMC (assays trypsin-like activity) to measure the rate of hydrolysis. Samples were incubated for 60 min at 30°C and the release of 7-amino-4-methylcoumarin (AMC) was monitored continuously every minute using a TECAN 96-well reader at 360nm excitation and 465nm emission.

2.4.3 Native- polyacrylamide gel electrophoresis (Native-PAGE™)

Chymotrypsin substrate overlay

Pure 26S proteasome samples were topped up to 25 μl with 4 X NativePAGE™ sample buffer (final concentration 1 X; Invitrogen) and loading buffer (30 mM Tris.HCl, pH 7.4, 5 mM $MgCl_2$, 2 mM ATP) and run on 3-12 % NativePAGE™ Bis-Tris gels (Invitrogen) in 1 X NativePAGE™ running buffer (50 mM Bis.Tris, 50 mM Tricine, pH 6.8; Invitrogen) for 1 h at 150V before changing to 200V and running for another hour. Gels were then incubated at 4°C for 15 min in developing buffer (50 mM Tris.HCl, pH 7.4, 5 mM $MgCl_2$, 2 mM ATP). Following this, gels were overlaid with 100 μM Suc-LLVY-AMC and visualized on the BIORAD Gel Doc 1000 using the Quantity One 4.5.1 (Basic) software.

Immunoblotting

Cell lysates or pure 26S proteasome samples were topped up to 25 μl with 4 X NativePAGE™ sample buffer (final concentration 1 X; Invitrogen) and loading buffer (30 mM Tris.HCl, pH 7.4, 5 mM $MgCl_2$, 250 mM sucrose, 2 mM ATP) and run on 3-12 % NativePAGE™ Bis-Tris gels in 1 X NativePAGE™ running buffer (50 mM Bis.Tris, 50 mM

Tricine, pH 6.8) for 1 h at 150V before changing to 200V and running for another hour. Gels were immunoblotted onto PVDF membranes at 25 V for 1 h in 1X NativePAGE™ transfer buffer (Invitrogen) in the blotting chamber and double distilled water in the outside chamber. Following transfer, PVDF membranes were incubated for 20 min with 8 % acetic acid (WVR) to fix the proteins and then blocked with 5 % marvel in 1 X PBST for 1 h before overnight incubation with mouse monoclonal α4 subunit antibody (1:1,000; BIOMOL) and mouse monoclonal Rpt1 (S7) subunit antibody (1:5,000; BIOMOL) in 1X PBST. The following day blots were washed in 1X PBST and incubated with secondary antibody (goat anti mouse AP 1:10,000 in 1X PBST; BIOSOURCE) for 45 min before washing in 1X PBST for 1 h changing buffer every 5 min. Blots were developed using the CDP-Star® (Tropix) system.

2.4.4 Assaying proteasome subunit levels by immunoblotting

To assay levels of proteasome subunits, immunoblotting was performed using antibodies against the α_4, β_2 or β_5 subunits of the proteasome. All three mouse monoclonal antibodies were from BIOMOL and were used at a concentration of 1:10,000 in 1 X PBST; antibodies were incubated with blots overnight at RT. Goat anti-mouse alkaline phosphatase was used as a secondary antibody (Biosource) at 1:10,000 in 1 X PBST. Secondary antibody was incubated with blots for 45 min at RT. This was followed by enhanced chemiluminescence (Pierce) and visualisation on Biomax MR film (Kodak™).

2.4.5 Methods to measure protein degradation by the proteasome

Fluorimetric assays of fluorescently-labelled casein

The SensoLyte™ Green Protease Assay Kit (Anaspec) is extensively used for the detection of generic cellular protease activities. It uses a casein derivative, which is greatly labelled with a rhodamine derivative, resulting in almost total quenching of the conjugate's fluorescence. Protease-catalysed hydrolysis relieves this quenching conjugate, yielding brightly green fluorescent dye-labelled peptides. The increase in fluorescence intensity is

directly proportional to protease activity. WT yeast 20S or 26S (20 μg) proteasome was incubated with or without aggregated β-PrP or aggregated α-PrP for 1 h at 30°C. HiLyte™-488 casein conjugate was then added to each reaction as per manufacturer's instructions. Fluorescence was measured every five minutes for 60 min on a TECAN 96-well plate reader (λex/λem= 492:535).

2.4.6 Ub^{G76V}-GFP reporter assays

N2aPK-1 transfection with Ub^{G76V}-GFP

The Ub^{G76V}-GFP construct was a kind gift from Dr Nico Dantuma (Department of Cell and Molecular Biology, Karolinska Institutet, Sweden), made as described previously (Dantuma *et al.*, 2000). The ubiquitin ORF was amplified by PCR from the Ub-Pro-bGal plasmid with the sense primer 5'-GCG**GAATTC**ACCATGCAGATCTTCGTGAAGACT-3' and the anti-sense primer 5'-GCG**GGATCC**TGTCGACCAAGCTTCCCCACCACACCTCTGAGACGGAGTAC-3' for Ub^{G76V}-GFP and was cloned in the EcoR1 and BamH1 sites of the EGFP-N1 vector (Clontech). Restriction sites are shown in bold. Transfection of this vector into N2aPK-1 cells was carried out using Genejammer lipofection transfection reagent (Stratagene). Cells were seeded at 30-50 % density in 6 well plates in standard growth medium. The DNA transfection reagent was prepared by mixing 100 μl Opti-MEM (un-supplemented) and 18 μl Genejammer. Following a 10 min incubation at RT, 3 μg plasmid DNA were added to the mixture and incubated for a further 10 min at RT. Nine hundred microliters of fresh, pre-warmed Opti-MEM supplemented with 10% v/v FCS replaced the standard growth medium and the Genejammer/DNA mixture was added drop wise. Cells were incubated with the Genejammer/DNA mixture for 8 h at 37°C, following which fresh medium was added in replacement. Stably-transfected cell lines were isolated by selection in 600 μg/ml gentamicin (G418).

Prion infection of GFP-proteasome reporter mice

Two lines of transgenic UPS-reporter mice, Ub^{G76V}-GFP1/ and 2 (Lindsten *et al.*, 2003) were used. Mice heterozygous for the transgene were bred to C57BL/6 mice, and the offspring were inoculated intra-cerebrally with 50 μl 1% w/v brain homogenates from 22L

prion-infected or un-inoculated mice. The mice were followed by visual observation and sacrificed at the time when clear signs of clinical disease were manifested (i.e. rocking gait, ruffled fur, and immobility). Mice were sacrificed under deep isoflurane anaesthesia by cardiac perfusion with ice-cold PBS through the left ventricle. The brains removed and processed either for histology or for RNA isolation and real-time PCR (**Section 2.6.1**). Briefly, RNA was isolated using the RNeasy mini kit (Qiagen) and prior to real time PCR, the integrity of RNA was evaluated with an RNA 6000 nano assay kit and Bioanalyser 2100 (Agilent) to visualise and compare 18S and 28S rRNA bands.

Immunohistochemisty on GFP-reporter mice

Following removal, brains were fixed in 3.7% formaldehyde in PBS for 24 h at RT. Sagittal blocks were subjected to processing for dehydration and were embedded in paraffin. Six-micrometer paraffin sagittal sections to be stained for GFP, ubiquitin, and PrP were first subjected to pre-treatment at 120°C for 20 min in citrate buffer (pH 6). Sections for GFAP staining were not pre-treated. Rabbit anti-GFP (Molecular Probes), mouse monoclonal anti-GFP (Roche Applied Science), mouse monoclonal anti-ubiquitin (Stressgen), rabbit anti-GFAP (DAKO) and rabbit anti-mouse PrP residues 89-103 (R30) (Raymond *et al.*, 1997). Staining procedures for all, but GFP, were performed as described (Dimcheff *et al.*, 2003) by using either biotinylated secondary antisera followed by horseradish peroxidise-conjugated streptavidin and amino-ethyl-carbazol as substrate. GFP was detected by using diaminobenzidine as substrate. A total of 20 UbG76V-GFP$^{+/-}$ and 11 UbG76V-GFP$^{-/-}$ scrapie-inoculated mice and ten UbG76V-GFP$^{+/-}$ and two UbG76V-GFP$^{-/-}$ mice inoculated with normal brain homogenate were examined microscopically. Data presented in this thesis are from line 1 mice.

2.5 Cell biology

2.5.1 Lactate dehydrogenase assays for the measurement of cell death

The lactate dehydrogenase (LDH) assay measures cell death by detecting LDH, a stable cytoplasmic enzyme present in most cells. LDH is released in the supernatant upon cell

lysis. All LDH assays were carried out using the LDH assay kit available from Alexis, Nottingham, UK. Briefly, the principle of this method involves two steps: firstly NAD^+ is reduced to $NADH/H^+$ as lactate is converted to pyruvate. Secondly, the catalyst (diaphorase) transfers a proton from $NADH/H^+$ to the tetrazolium salt INT (yellow) which is reduced to formazan (red). Cells were seeded onto 96 microwell plates. They were then centrifuged for 10 min at 250 x *g* at RT. Cell free supernatants were transferred to clear flat bottomed 96 microwell plates. Reaction mixture containing the catalyst was prepared according to manufacturer's instructions and added to each well. Plates were read at 492nm following a 30 min incubation at RT (in the dark).

2.5.2 Immunofluorescence

Preparation of coverslips

For immunofluorescence experiments, 22 mm autoclaved glass coverslips were coated using poly-L-lysine (1 mg/ml) and incubating at RT for 10 min. Coverslips were subsequently washed three times with sterile, double-distilled water and left to dry. Poly-L-lysine enhances electrostatic interaction between negatively-charged ions of the cell membrane and positively-charged surface ions of attachment factors on the culture surface. When adsorbed to the culture surface it enhances the number of positively-charged sites available for cell binding.

Dual-labelling immunofluorescence for the detection of PrP^{Sc} aggresomes

Approximately 100,000 GT-1, ScGT-1, N2aPK-1 and ScN2APK-1 cells plated on poly-L-lysine coated 22 mm glass coverslips were treated for 24 h with 1 μM lactacystin at 37°C. Cells were fixed onto the coverslips with 4 % PFA for 20 min at RT. Coverslips were incubated with 98% formic acid for 5 min to acid-hydrolyse PrP^C and expose PrP^{Sc} and then washed three times with PBS and permeabilised at -20°C with pre-cooled 100 % methanol for 15 min. After washing three times with PBS coverslips were blocked with 10 % normal goat serum (NGS) in PBS for 30 min at 37°C and again washed three times with PBS. Coverslips were incubated for 1 h at 37°C with appropriate primary antibodies that were diluted to

suitable concentrations in 1 % NGS and 1 h at 37°C. After washing, cells were incubated for 45 min at 37°C with secondary antibodies (diluted to suitable concentrations in 1 % NGS). Following washing in PBS, 1 μg/ml DAPI was added to each coverslip; coverslips were mounted on glass slides in 10 μl anti-fade (DAKO). Slides were left to dry and placed at 4°C until analysis.

Confocal image acquisition

Confocal microscopy was used to obtain fluorescence images. The confocal microscope (Zeiss microscope LSM510 META) was equipped with 'plan-Apochromat' 63 x/1.40 Oil DIC objective at RT and was controlled by Zeiss LSM software. Fluorescence was recorded at 488 nm using 30 mW Ar-laser for excitation or at 543 nm using 1 mW HeNE-laser for excitation. Zeiss Imersol™ was used as imaging medium.

2.6 Molecular biology

2.6.1 Quantitative real time polymerase chain reaction (PCR)

Extraction of total RNA

Total RNA was extracted from mock-infected GT-1 and ScGT-1 (that had been treated with or without 1 μM lactacystin for 24 h at 37°C) cells using the TRIZOL™ (Invitrogen) method. Briefly, cells were harvested at a consistent confluency (~80 %) and washed in PBS. 1.5 ml TRIZOL™ reagent was then added directly to a 10 cm plate which was subsequently placed on a shaker for 5 min at RT. TRIZOL™-lysed cells were transferred to 1.5 ml RNase-free tubes (Sarstedt) and were shook for 15 seconds. After being left to stand at RT for 5 min, 200 μl chloroform (VWR) was added to each eppendorf in a fume hood. Following shaking for 15 seconds, samples were left at RT for 5 min. Lysates were centrifuged at 12,000 *x g* at 4°C for 10 min to separate phases; the upper (aqueous) phase was pipetted into a fresh tube and 750 μl of isopropanol (VWR) was added to each reaction tube. After a 15 second shake and a RT incubation of 10 min, samples were centrifuged at 12,000 *x g* at 4°C for 15

min and then immediately placed on ice. Following the addition of 180 µl of 100% ethanol (VWR) samples were centrifuged at 13,000 *x g* at 4°C for 5 min. After discarding the ethanol, the RNA pellet was left to air dry for 10 min before dissolving RNA in DEPC-treated water (AMBION) and storing at -70°C.

Agarose gel electrophoresis RNA

1 % agarose mini-gels were made by heating 1.5 g agarose (AMBION) in 150 ml of 1 X NorthernMAX glyoxyl based gel pre/running buffer (AMBION) in a microwave oven until the agarose was fully dissolved. Gels were then cooled to approximately 50°C by stirring and were poured into a gel tray fitted with the appropriate comb(s) and left to set at RT. RNA samples were adjusted to 50 ng/µl with DEPC-treated water in a final volume of 5 µl. Following this, samples were incubated at 50°C for 30 min with an equal volume of glyoxyl loading dye (containing ethidium bromide; AMBION). 10 µl of sample were loaded into each lane and 5 µl of RNA ladder (AMBION). Gels run for 90 min at 100 mV. RNA was visualized by examining the gel on a BIORAD Gel Doc 1000 imaging system under UV light to evaluate sample integrity. Gels were photographed and analyzed using the Quantity One software (version 4.5.1, BIORAD).

cDNA synthesis

1 µg RNA was combined with 2.5 µl random primers (Invitrogen) and topped to 11 µl with DEPC-treated water in an RNase-free 0.5 ml eppendorf tube (Advanced Biotechnologies) on ice. The RNA was denatured at 70 °C for 10 min and then cooled immediately on ice. After a quick spin the reaction mixture was incubated with 4 µl 5 X First Strand Buffer (Invitrogen), 2 µl DTT (Invitrogen), 1 µl dNTPs (10mM stock; Invitrogen) and 1 µl RNase Out at 25 °C for 10 min. Following this 1 µl of SuperScript® II Reverse Transcriptase (Invitrogen) was added to the mix; the mix was incubated for 10 min at 25 °C, then at 42 °C for 1 h and finally at 70 °C for 10 min. 80 µl of DEPC-treated water were then added to 20 µl cDNA and stored at -70 °C.

Primer design

Primers were designed using the Primer Express™ software (Applied Biosystems) (**Table 2.1**).

Gene	Primer
Beclin 1, *becn1*	Sense 5' CTTCAATGCCACCTTCCACAT 3'
	Anti-sense 5' GCGACCCAGTCTGAAATTATTGAT 3'
Autophagy related 12-like, *Atg12L*	Sense 5' TCAGCCCCACAGCAGTCTTA 3'
	Anti-sense 5' TTTCCACTTCCTCAATGCTAGGA 3'
Autophagy related 16-like, *Atg16L*	Sense 5' TGCCAAATAGGCATGAAATAAGTC 3'
	Anti-sense 5' TGATCCTCAACTGGGCCATT 3'
IkappaB-alpha, *IκB-α*	Sense 5' ACCTGCACACCCCAGCAT 3'
	Anti-sense 5' CGTGTGGCCATTGTAGTTGGT 3'
Actin beta, *Actβ*	Sense 5' CGTGAAAAGATGACCAGATCA 3'
	Anti-sense 5' CACAGCCTGGATGGCTACGT 3'
glyceraldehyde-3-phosphate dehydrogenase, *Gapdh*	Sense 5' AAAATGGTGAAGGTCGGTGTG 3'
	Anti-sense 5' TGACCAGGCGCCCAATAC 3'

Table 2.1 Primer sets

Real time reverse transcriptase PCR

SYBR Green

Reactions took place in 96 well plates. Total RNA samples were reverse transcribed (**See cDNA synthesis**). As a negative control, 1 µg of RNA was processed without addition of reverse transcriptase. Quantitative real-time PCR analysis (Applied Biosystems Sequence Detection System 7500) using SYBR Green (Qiagen) was performed according to the manufacturer's instructions. Briefly, reactions consisted of 12.5 µl of Sybr Green master mix, 1.2 µl of cDNA, sense and anti-sense primers (**Table 2.2**), topped up to 25 µl with DEPC-treated water. Default PCR conditions: a) 40 cycles of 15 min at 95°C, 15 seconds at 95°C, 1 min annealing at 60°C, b) dissociation step of 15 seconds at 95°C, 1 min at 60°C and 15 seconds at 95°C. All primers were assessed for efficiency using SYBR Green conditions prior to being utilized. Gene expression levels were assessed in three biological replicate samples (and three technical replicates of each) from each group using the ΔΔCT method and normalization to *Gapdh* or *Actb*. Standard deviations were calculated using the values of the biological replicates of mock-infected and RML-infected cells.

Gene	Sense/Anti-sense primer (nM)	Volume in reaction (µl)
Gapdh	400/400	1.67/1.67
Actb	300/300	1.5/1.5
Becn1	300/300	1.5/1.5
Atg12	300/300	1.5/1.5
Atg16L	300/300	1.5/1.5

Table 2.2 Primer concentrations in SYBR Green PCR

2.7 Statistical analysis

Data were expressed as mean plus standard error of mean (SEM; sd√n). Data were compared by 2-tailed *t*-tests and considered significantly different when $P<0.05$. Degree of significance was expressed as follows: $P<0.05$*; $P<0.01$**; $P<0.001$***, unless otherwise specified.

3 DISEASE-ASSOCIATED PRION PROTEIN OLIGOMERS INHIBIT THE CATALYTIC β SUBUNITS OF THE 26S PROTEASOME

3.1 Background

Increasing evidence suggests a possible role for the UPS in prion disease (**Section 1.9**). Studies in prion-infected mouse brain have shown a correlation between elevated levels of ubiquitin conjugates and reduced proteasome function (Kang *et al.*, 2004). WT PrP^{C} molecules undergoing ERAD have been shown to accumulate in the cytosol of cells when the proteasome is inhibited (Ma and Lindquist, 2001; Yedidia *et al.*, 2001). Therefore, UPS inhibition may allow for the conversion of PrP^{C} in the cytosol to an abnormal PrP^{Sc}-like form, especially if PrP^{C} accumulation exceeds the degradative capacity of the UPS (Ma and Lindquist, 2002) (**Section 1.9.1**). However, there is conflicting evidence concerning the neurotoxicity of PrP^{C}. Accumulation of cytosolic PrP^{C} in human primary neurones treated with proteasome inhibitors is not toxic, indeed conferring protection against Bax-mediated cell death (Roucou *et al.*, 2003). Importantly, studies in various cell models have challenged the occurrence of retrograde transport of both mutant and WT PrP^{C} prior to proteasome degradation and have suggested that cytosolic PrP^{C} accumulation may be a result of elevated levels of PrP^{C} expression from the CMV promoter used in many of the experiments (Drisaldi *et al.*, 2003; Fioriti *et al.*, 2005).

Large, intracellular peri-centrosomal structures termed 'aggresomes' are thought to be a precise response when cells try to cope with increased levels of misfolded and aggregated proteins, evidenced by the active recruitment of proteasome components and molecular chaperones to these aggregates (Olzmann *et al.*, 2008). Proteasome inhibition has been shown to lead to the formation of both PrP^{C} and PrP^{Sc} aggresomes (Cohen and Taraboulos, 2003; Mishra *et al.*, 2003; Kristiansen *et al.*, 2005; Grenier *et al.*, 2006; Goggin *et al.*, 2008). The formation of cytosolic PrP^{C} aggresomes appears to be toxic in both neuronal and non-neuronal cells (Grenier *et al.*, 2006; Goggin *et al.*, 2008). Kristiansen *et al.* reported that following mild proteasome inhibition, prion-infected cells form PrP^{Sc}-containing cytosolic aggresomes whose formation is temporally associated with caspase 3

and 8 activation and subsequent apoptosis (Kristiansen *et al.*, 2005). They also demonstrated PrP^{Sc}-containing aggresome-like structures in prion-infected mouse brain. Granular deposits of disease-related PrP have been previously reported in neuronal perikarya from post-mortem sporadic CJD cases, suggesting intra-neuronal prion aggregates may play a role in disease pathogenesis (Kovacs *et al.*, 2005).

3.1.1 Aims

The aims of this study were to evaluate the role of the UPS in prion disease pathogenesis and to examine whether there is a direct mechanistic link between aggregated prion protein species and UPS function.

3.1.2 Methods

Western blotting was used for the detection of protein levels (**Section 2.2.1**). A proteasomal β subunit activity probe was used to assay specific β subunit proteolytic activity by Western blotting (**Section 2.4.1**), whereas the three peptidase activities of the 20S proteasome were monitored using fluorogenic substrates (**Section 2.4.2**). Dual-labelling immunofluorescence was undertaken for all co-localisation studies (**Section 2.5.2**). The Ub^{G76V}-GFP proteasome reporter monitored the functional status of the UPS (**Section 2.4.6**) and the experiment was performed by Dr Mark Kristiansen, MRC Prion Unit, UCL Institute of Neurology. NativePAGE™ immunoblotting and substrate overlay methods assayed 26S proteasome dissociation (**Section 2.4.3**). Experiments were performed in collaboration with Dr Mark Kristiansen, MRC Prion Unit, UCL Institute of Neurology. Ub^{G76V}-GFP mouse experiments (**Section 2.4.6**), including an RT-PCR on the mouse brain lysates, were performed by Dr Derek Dimcheff and Dr John Portis, at Rocky Mountain Laboratories, USA.

3.2 Results

3.2.1 Prion infection in cells impairs the proteolytic activity of the 26S proteasome

Mouse hypothalamic neuronal GT-1 (Schatzl *et al.*, 1997) and neuroblastoma N2aPK-1 cells (Klohn *et al.*, 2003) were infected with either 0.1 % RML prion-infected or mock-infected control (CD-1) mouse brain homogenate. Prion infection was demonstrated by immunoblotting with an anti-PrP antibody (ICSM18), which confirmed PK-resistant PrP species in prion-infected cells (ScGT-1 and ScN2aPK-1) (**Figure 3.1**).

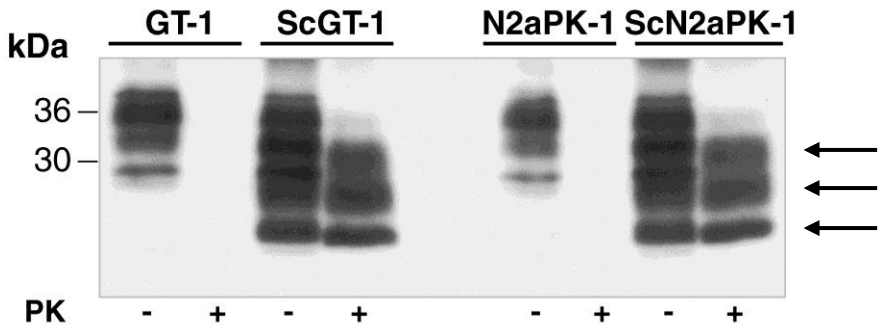

Figure 3.1 Prion infection of N2aPK-1 and GT-1 cells

Cell lysates of uninfected (GT-1 and N2aPK-1) and prion-infected cells (ScGT-1 and ScN2aPK-1) were immunoblotted using an anti-PrP antibody, ICSM18. 25 μg from cell lysates was loaded per lane. PrP^C runs between 50-30 kDa in its three glycosylation states (di-, mono- and unglycosylated). These three bands disappear completely after PK digestion in uninfected cells. In PK-treated ScGT-1 and ScN2aPK-1 cells these bands remain nearly undiminished in intensity, although they shift to lower molecular weight (arrows).

The three peptidase activities of the 20S proteasome are routinely monitored using specific fluorogenic peptides as a measure of proteasomal activity *in vitro*. Chymotrypsin-like, caspase-like and trypsin-like proteolytic activities were measured in prion-infected (ScGT-1), mock infected, and uninfected GT-1 cell lysates. Significant loss of chymotrypsin-like, caspase-like and trypsin-like activities was seen in ScGT-1 cells, but not in mock-infected cells or cells cured of prion infection using anti-PrP (ICSM18) antibody treatment (Enari *et al.*, 2001), as compared to uninfected controls (**Figure 3.2**). Specific proteolytic activity of the ATP-dependent 26S proteasome was confirmed by a near-complete lack of activity in the absence of ATP.

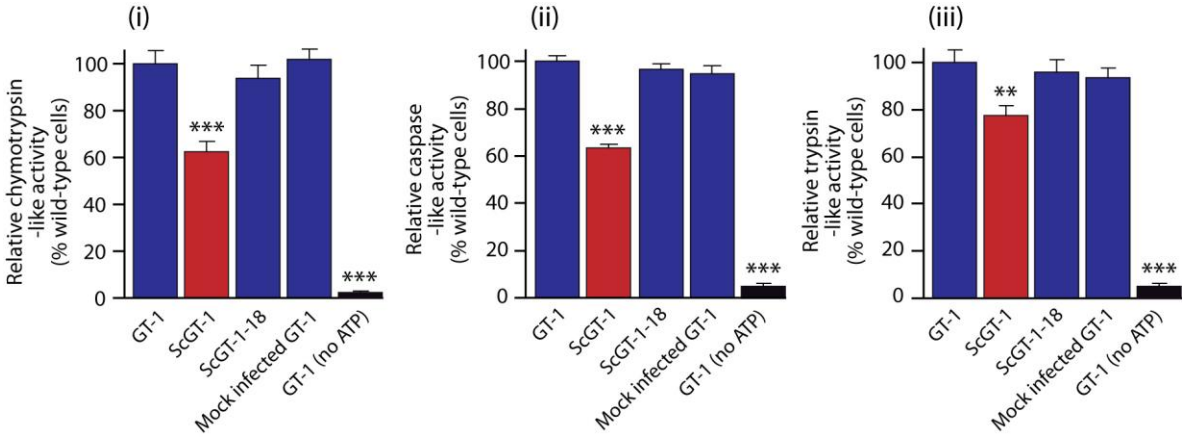

Figure 3.2 Prion infection in cells impairs the proteolytic activity of the 26S

Prion infection of GT-1 cells (ScGT-1) significantly reduces their **(i)** chymotrypsin-like, **(ii)** caspase-like, and **(iii)** trypsin-like proteolytic activities. Peptidase activities of cell lysates (10 μg per reaction) were monitored using fluorogenic substrates specific for each activity: 100 μM Suc-LLVY-AMC (chymotrypsin-like), 100 μM Ac-nLPnLD-AMC (caspase-like) and 100 μM Boc-LLR-AMC (trypsin-like). Lysates were incubated with the fluorogenic substrate for 30 min, following which fluorescence was measured over time at 360 nm excitation and 465 nm emission. Proteolytic activity is nearly abolished in the absence of ATP. Suffix -18 denotes cells cured of prion infection by incubation with the anti-PrP (ICSM18) antibody. Data are from ten independent experiments +SEM. ***p<0.001, **p<0.01 (versus uninfected controls).

3.2.2 Prion infection impairs the 26S proteasome in mouse brain

To see if the loss of proteolytic activity seen in prion-infected cells was mirrored in mouse brain, chymotrypsin-like and caspase-like proteolytic activities were measured in control (CD-1) and RML prion-infected mouse brain homogenates. This demonstrated a significant reduction in chymotrypsin-like and caspase-like activities in RML prion-infected mouse brain compared with control brain (**Figure 3.3**). Of note, assaying proteasomal function in prion-infected brain tissue may be complicated by the presence of marked glial proliferation, which is characteristic of prion neuropathology and may result in an overestimation of proteolytic function.

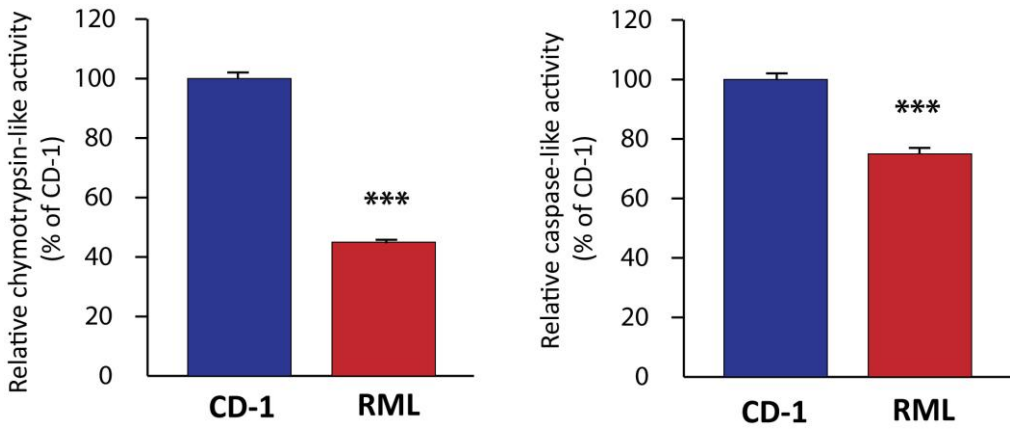

Figure 3.3 Prion infection impairs the 26S in mouse brain

Scrapie infection significantly reduces chymotrypsin-like and caspase-like proteolytic activities in prion-infected mouse brain (RML) compared to control brain (CD-1). Peptidase activities of mouse brain homogenates (10 μg per reaction) were monitored using fluorogenic substrates specific for each activity: 100 μM Suc-LLVY-AMC (chymotrypsin-like), 100 μM and Ac-nLPnLD-AMC (caspase-like). Homogenates were incubated with the fluorogenic substrate for 30 min, following which fluorescence was measured over time at 360 nm excitation and 465 nm emission. Chymotrypsin-like activity data are means of five independent experiments +SEM, whereas caspase-like activity data are means of ten independent experiments +SEM. ***$p<0.001$ (versus uninfected controls).

3.2.3 Prion infection impairs the catalytic β subunits of the 26S proteasome

To further investigate prion-induced loss of proteasome proteolytic activities, a specific proteasome β subunit activity probe was used (Berkers *et al.*, 2005). This is a cell-permeant peptide vinyl sulfone-based competitive inhibitor, which modifies the catalytically active N-terminal threonine residues of the β subunits, forming a covalent β-sulfonyl ether linkage (dansylAhx$_3$L$_3$VS). This probe has a dansyl-sulfonamidohexanoyl hapten tag, which allows accurate monitoring of β subunit activities in live cells and cell lysates.

GT-1 and N2aPK-1 cells were infected with either RML prion-infected or mock-infected (CD-1) mouse brain homogenates. Lysates from prion-infected (ScN2aPK-1), mock infected and uninfected N2aPK1 cells were incubated with the dansylAhx$_3$L$_3$VS activity probe and immunoblotted with an anti-dansyl antibody. Modification of β subunits, indicating a loss of activity, was clearly seen in ScN2aPK-1 cells compared to uninfected, mock-infected and anti-PrP (ICSM18) antibody-cured controls (**Figure 3.4A**). As the β subunit activity probe is cell permeant, it was also used to assay live cells; live ScGT-1 cells demonstrated a significant loss of β subunit activity again as compared to controls (**Figure 3.4B**). Lactacystin, a cell-permeable irreversible proteasome inhibitor (Lee and Goldberg, 1998), completely abrogated β subunit proteolytic activity in N2aPK-1 and GT-1 cells (**Figure 3.4A and B**).

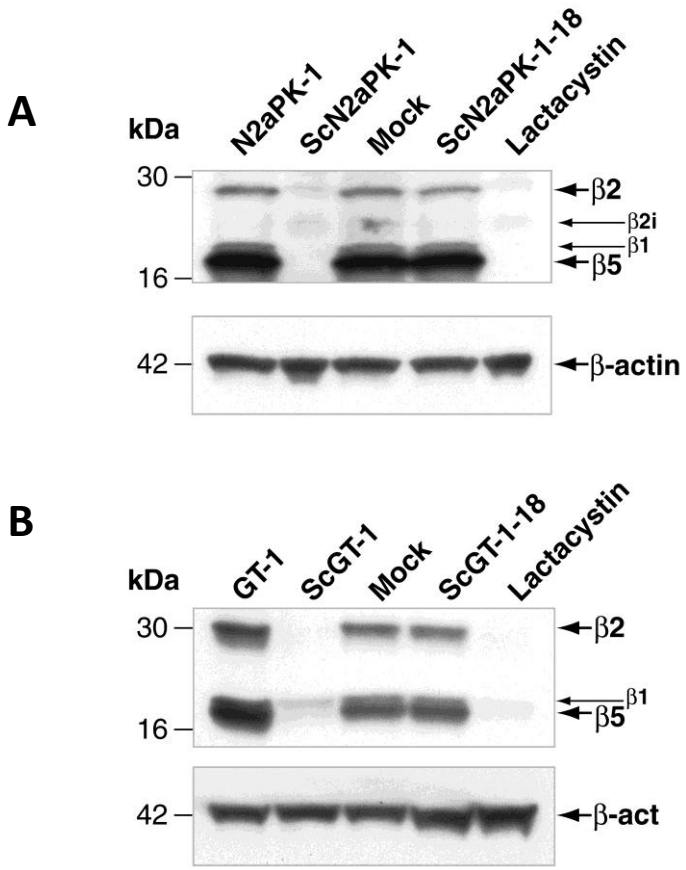

Figure 3.4 Prion infection impairs the proteasome by specifically inhibiting the catalytic β subunit activities

(A) Cell lysates from uninfected (N2aPK-1), prion-infected (ScN2aPK-1), mock-infected and ScN2aPK-1 cells cured of prion infection by treatment with an anti-PrP antibody (ICSM18) (ScN2aPK-1-18) were incubated with the β subunit activity probe (dansylAhx$_3$L$_3$VS; 1 μM) and immunoblotted with a rabbit polyclonal anti-dansyl antibody. Prion infection of N2aPK-1 cells resulted in a loss of proteolytic β subunit activities. No loss of β subunit proteolytic activities was seen in N2aPK-1, mock-infected, or ScN2aPK-1-18 cells. **(B)** Live GT-1 cells were incubated with the cell permeant activity probe in culture, lysed and immunoblotted with an anti-dansyl antibody. A significant reduction in proteolytic β subunit activities was demonstrated in prion-infected GT-1 (ScGT-1) cells but not in mock-infected or ScGT-1 cells cured of prion infection (ScGT-1-18). Lactacystin (50 μM) was used as a positive control for proteasome inhibition. 100 μg of protein from cell lysates was loaded per lane. Levels of an endogenous mouse protein, β-actin (β-act), were assessed by immunoblotting to confirm equal protein loading.

3.2.4 Decreased 26S proteasome β subunit proteolytic activity is not due to decreased β subunit expression

Decreased proteolytic activities in aged cells of different origins have been associated with reductions in levels of proteasome subunits (Ding *et al.*, 2006; Powell, 2006; Hwang *et al.*, 2007). Therefore, it was important to ensure that the decrease in proteolytic activity seen in prion-infected mouse cells and brain was not due to reduced expression of β subunits. Protein levels of α_4, β_2 and β_5 subunits were measured by immunoblotting with antibodies to each of these subunits. This demonstrated no loss of expression in any of the three subunits (**Figure 3.5**), indicating that the reduced proteolytic activity seen in prion-infected mouse cells and brain results from a specific inhibitory effect.

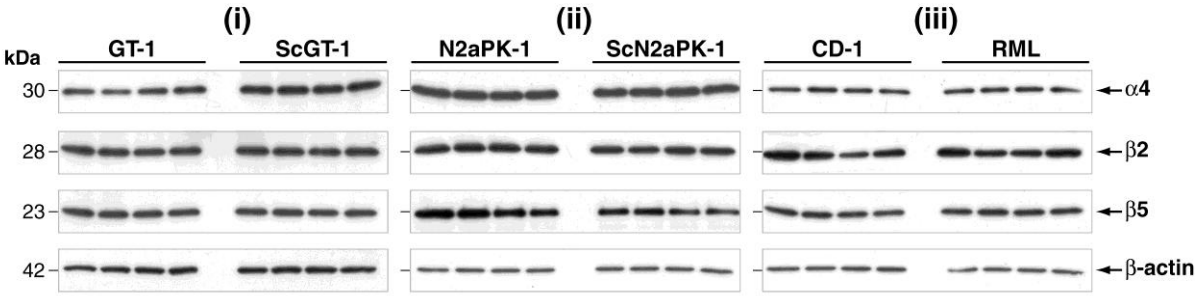

Figure 3.5 Decreased proteolytic activity is not due to decreased β subunit expression

GT-1 and N2aPK-1 cells were infected with RML prions, lysed and immunoblotted for proteasome subunits. **(i)** There was no reduction in α_4, β_2 or β_5 subunit levels in ScGT-1 cell lysates compared to uninfected controls. **(ii)** There was no reduction in α_4, β_2 or β_5 subunit levels in ScN2aPK-1 cell lysates compared to uninfected controls. **(iii)** There was no reduction in α_4, β_2 or β_5 subunit levels in RML-infected mouse brain homogenates compared to uninfected (CD-1). 100 μg protein from cell lysates or mouse brain homogenates was loaded per lane and mouse monoclonal antibodies to α_4, β_2, or β_5 proteasome subunits were used for immunoblotting. Each lane represents an independent experiment. Levels of an endogenous mouse protein, β-actin, were assessed by immunoblotting to confirm equal protein loading.

3.2.5 PrP^{Sc} is localised in the cytosol in prion-infected cells

The 26S proteasome is localised in the cell to both the nucleus and cytosol (Tanaka *et al.*, 1986). It was therefore interesting to investigate whether PrP^{Sc} can gain access to these compartments in prion-infected cells. The sub-cellular distribution of PrP^{Sc} is difficult to assess due to the lack of PrP^{Sc}-specific antibodies. Nonetheless, studies have shown its localisation at the plasma membrane and the endolysosomal compartment (Caughey and Baron, 2006), and it has been recently shown that some PrP can escape macropinosomes and leak into the cytosol (Wadia *et al.*, 2008). Formic acid (FA) was used to pre-treat ScN2aPK-1 cells in order to acid-hydrolyse PrP^{C} and expose PrP^{Sc} (Kristiansen *et al.*, 2005). These ScN2aPK-1 cells were then stained with the anti-PrP (ICSM18) antibody and visualised using confocal fluorescent microscopy. Following FA treatment, PrP^{Sc} was found to be localised on both the cell surface and intracellularly (**Figure 3.6**).

To determine whether PrP^{Sc} is present in the cytosol of ScN2aPK-1 cells, co-immunostaining for endolysosomal and cytosolic markers was undertaken. Confocal microscopy showed that PrP^{Sc} partially co-localised with the endolysosomal marker LAMP-1, but that it also exists outside this compartment (**Figure 3.7A**); a proportion of PrP^{Sc} co-localised with the cytosolic marker Hsc70 as shown in **Figure 3.7B**. Furthermore, true co-localisation between Hsc70 and PrP^{Sc} was revealed by an intensity scatter plot and subtraction of the confocal images (**Figure 3.8**). Indeed this finding suggests that a proportion of PrP^{Sc} is localised in the cytosolic compartment is supported by studies describing neurotoxic PrP^{Sc} aggresomes (Kristiansen *et al.*, 2005). Taken together, these results show that a limited amount of PrP^{Sc} is found in the cytosol of prion-infected cells.

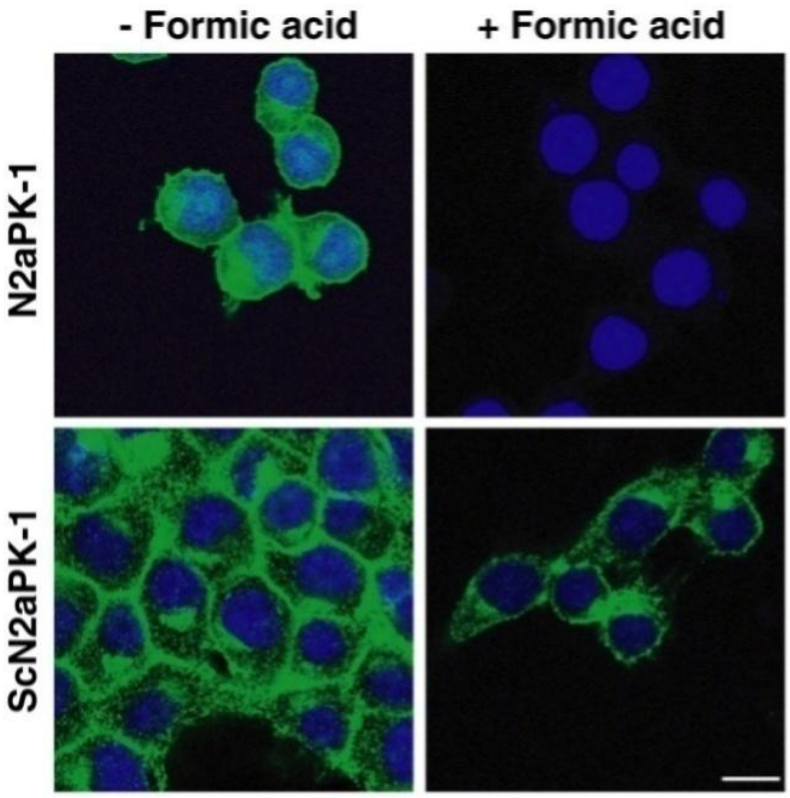

Figure 3.6 Formic acid exposes PrP^{Sc} in ScN2aPK-1 cells

ScN2aPK-1 cells were treated with 98 % formic acid (FA) for 5 min and immunostained with an anti-PrP antibody (green; mouse monoclonal ICSM 18; 10 μg/ml; D-Gen) to reveal PrP^{Sc}. In uninfected N2aPK-1 cells, FA removed all detectable PrP^{C} after 5 min (top right); PrP^{Sc} was localised to the cell surface and intracellularly in ScN2aPK-1 cells (bottom right). DAPI nuclear staining= blue. Scale bar= 20 μm.

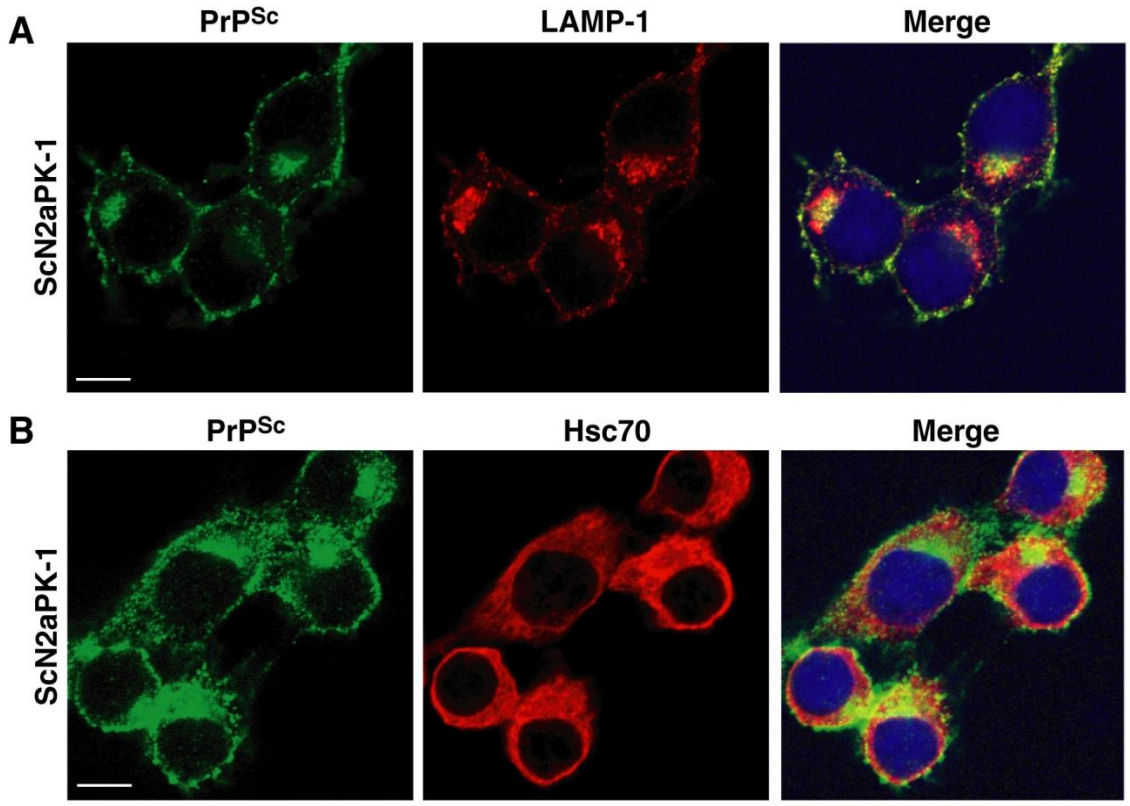

Figure 3.7 PrP^{Sc} is localised in the cytosol in prion-infected cells

ScN2aPK-1 cells were exposed to 98 % formic acid (FA) for 5 min prior to co-immunostaining. **(A)** PrP^{Sc} (green; mouse monoclonal ICSM18; 10 μg/ml; D-Gen) in ScN2aPK1 cells not only partially co-localises with LAMP-1 (red; rat polyclonal; 1:500; Santa-Cruz), but also exists outside this structure. **(B)** A proportion of PrP^{Sc} (green; ICSM18) in ScN2aPK-1 cells co-localises with cytosolic Hsc70 (red; mouse monoclonal IgG_{2a}; 1:500; Santa-Cruz). PrP^{Sc} is also seen abundantly on the cell surface (green). Scale bar= 20 μm; DAPI nuclear staining= blue.

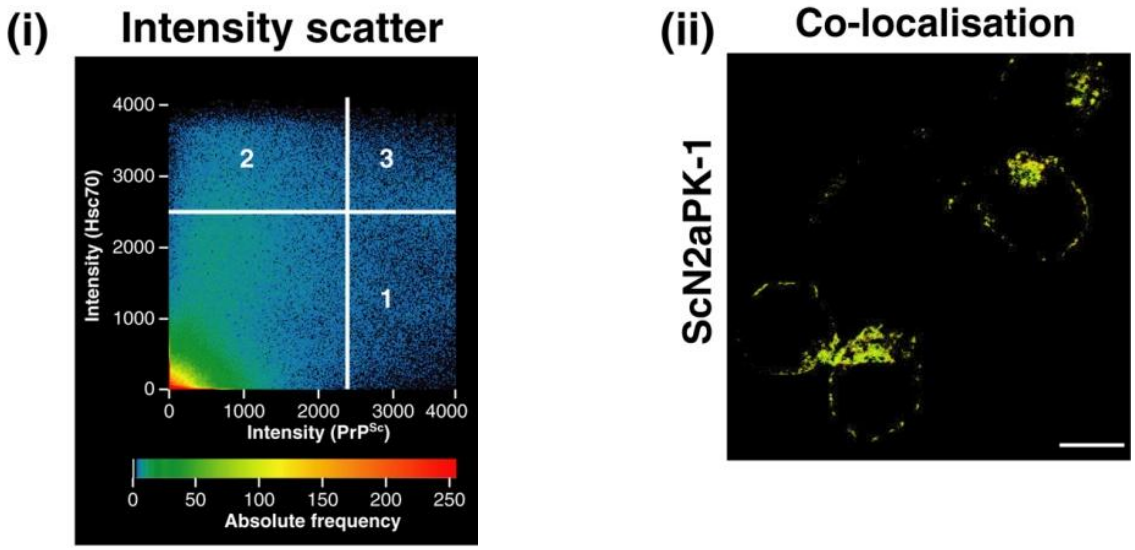

Figure 3.8 A proportion of PrP^{Sc} colocalises with Hsc70

(i) The intensity scatter plots the intensity of the pixels stained either for PrP^{Sc} (x-axis) or Hsc70 (y-axis). Segment 1 reveals pixels with intense PrP^{Sc} staining; segment 2 reveals pixels with intense Hsc70 staining; segment 3 reveals the co-localisation of pixels with both intense PrP^{Sc} and intense Hsc70 staining. **(ii)** Demonstrates a subtraction image revealing true co-localisation (yellow) between Hsc70 and PrP^{Sc} (image corresponds to the intensity scatter segment 3). Scale bar = 20 µm.

3.2.6 Prion infection causes UPS dysfunction in live cells

To test whether the proteolytic dysfunction observed in preparations from prion-infected cells results in real, functionally-significant impairment of the UPS in live cells, N2aPK-1 cells stably expressing the fluorescent proteasome reporter substrate Ub^{G76V}-GFP (Dantuma *et al.*, 2000) were infected with RML prions. Prion infection caused an increase in the steady-state levels of the GFP-tagged reporter indicating functional impairment of the UPS (**Figure 3.9**). Curing prion-infected cells with an anti-PrP antibody (ICSM18) resulted in normal UPS function (**Figure 3.9**). The proteasome inhibitor lactacystin was used as positive control, resulting in an increase in Ub^{G76V}-GFP steady-state levels.

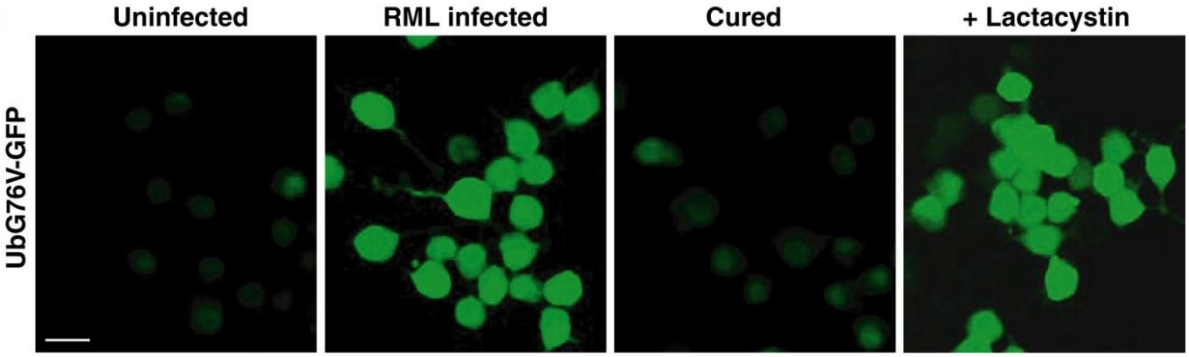

Figure 3.9 Prion infection causes UPS dysfunction in live cells

N2aPK-1 cells expressing the fluorescent UPS reporter (Ub^{G76V}-GFP; green), were infected with RML prions (ScN2aPK-1). Accumulation of the UPS reporter occurred only in prion-infected cells or lactacystin-treated (50μM) N2aPK-1 cells (positive control). Uninfected cells did not accumulate Ub^{G76V}-GFP and cells cured of prion infection by treatment with an anti-PrP antibody (ICSM18) did not stain significantly for the UPS reporter. *This experiment was performed by Dr Mark Kristiansen, MRC Prion Unit, UCL Institute of Neurology.*

3.2.7 Disease-related PrP isoforms directly inhibit the catalytic β subunit activity of the 26S proteasome

To directly assess how prion infection inhibits the catalytic β subunit activity of the 26S proteasome, an *in vitro* assay system was developed to measure the effects of different conformations and aggregation states of PrP on 26S proteasome activity in neuronal cell lysates. Specifically, recombinant mouse PrP (full length; 23-231aa) was used, which had been folded into one of two forms: an α-helical structure, representative of native PrP^{C} (α-PrP) or a predominantly β-sheet species termed β-PrP, which has similar physico-chemical properties to PrP^{Sc} (Jackson *et al.*, 1999). Their effects on 26S proteasome β subunit activity in N2aPK-1 cells and cerebellar granule neurones (CGN) were assayed using the dansylAhx$_3$L$_3$VS activity probe.

Five different PrP species were made: aggregated α-PrP (by heating at 70 °C for 10 min), aggregated β-PrP (by addition of NaCl to a final concentration of 150 mM), which forms small spherical particles 5-10 nm in diameter (Jackson *et al.*, 1999), acidified α-PrP-derived amyloid fibrils (Baskakov *et al.*, 2002), and NaCl-treated α-PrP. Semi-purified PrP^{Sc} was obtained from RML-infected mouse brain and ScGT-1 cells (Kristiansen *et al.*, 2005). Both aggregated β-PrP and PrP^{Sc} (from ScGT-1 cells) inhibited the β subunit activities of N2aPK-1 cells, whereas α-PrP, aggregated α-PrP and amyloid fibrils had no effect (**Figure 3.10A**). Carboxy-methylated α-lactalbumin, a soluble unfolded protein molecule used in protein folding studies as a mimetic of the molten globule state (Kuwajima, 1996), had no inhibitory effect on the β subunit activities (**Figure 3.10A**). A marked inhibition on the β subunit activities of N2aPK-1 cells was also observed by PrP^{Sc} derived from RML prion-infected mouse brain (**Figure 3.10B**). Lactacystin pre-treatment of N2aPK-1 cells completely abrogated their β subunit proteolytic activity (positive control).

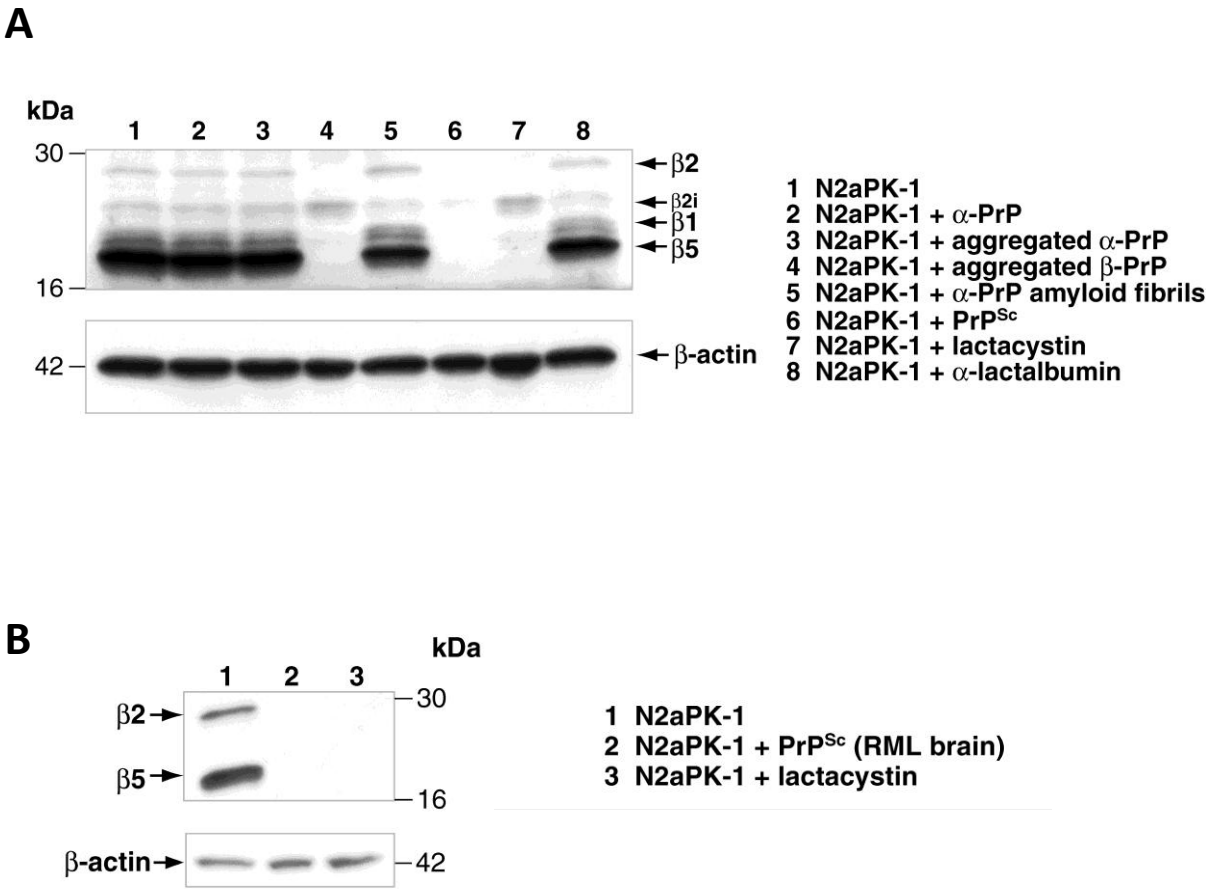

Figure 3.10 PrP^{Sc} and aggregated β-PrP inhibit the catalytic β subunit activity of the 26S

N2aPK-1 cell lysates were incubated with recombinant prion proteins or semi-purified PrP^{Sc} before treatment with the β subunit activity probe (dansylAhx$_3$L$_3$VS; 1 μM) and immunoblotting with an anti-dansyl antibody. **(A)** Only aggregated β-PrP (lane 4), PrP^{Sc} (lane 6; from ScGT-1 cells) or 50 μM lactacystin (lane 7; positive control) resulted in a loss of β subunit activity in N2aPK-1 cell lysates. **(B)** PrP^{Sc} from RML prion-infected mouse brain (lane 2) or 50 μM lactacystin (lane 3; positive control) incubated with N2aPK-1 cell lysates resulted in a loss of β subunit activity. Proteins were assayed at 1 mg/ml (final concentration). 100 μg protein from cell lysates was loaded per lane. Levels of an endogenous mouse protein, β-actin, were assessed by immunoblotting to confirm equal protein loading.

Cytosolic fractions from mouse CGN cultures were also incubated with the various PrP species. **Figure 3.11** shows that only aggregated β-PrP and PrP^{Sc} (from ScGT-1 cells) caused a loss in β subunit, predominantly β_1 and β_5, activities in these cells. Lactacystin (positive control) pre-treatment resulted in complete inhibition of β subunit activities.

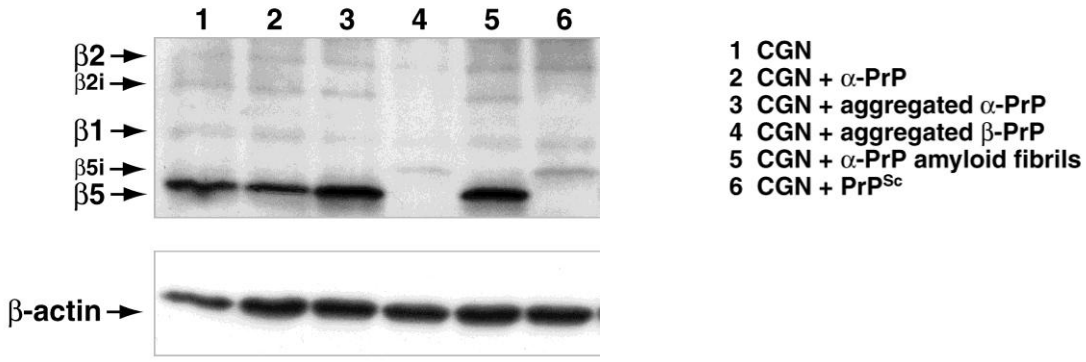

Figure 3.11 Aggregated β-PrP and PrP^{Sc} inhibit the β subunit proteolytic activities of the 26S in primary neurones

CGN cell lysates were incubated with recombinant prion proteins or semi-purified PrP^{Sc} before treatment with the β subunit activity probe (dansylAhx$_3$L$_3$VS; 1 μM) and immunoblotting with an anti-dansyl antibody. Aggregated β-PrP (lane 4), PrP^{Sc} (lane 6; from ScGT-1 cells) or 50 μM lactacystin (lane 9; positive control) resulted in a loss of β_1 and β_5 subunit activity in CGN cell lysates. Proteins were assayed at 1 mg/ml (final concentration). 100 μg of protein from cell lysates was loaded per lane. Levels of an endogenous mouse protein, β-actin, were assessed by immunoblotting to confirm equal protein loading. *Primary cerebellar granule neuronal cultures were prepared by Ms Heike Naumann, MRC Prion Unit, UCL Institute of Neurology.*

3.2.8 Denaturation of β-PrP and PrP^{Sc} abolishes their inhibitory effect on 26S proteasome β subunit activity

To confirm that the inhibitory effect of β-PrP and PrP^{Sc} on the β subunits of the proteasome was dependent on their specific conformation, they were denatured by serial freeze-boiling. Denaturation of aggregated β-PrP and PrP^{Sc} completely removed their inhibitory activity (**Figure 3.12A**). β subunit activities were restored after denaturation of the prion species, indicating that a specific conformation of the inhibitory species in aggregated β-PrP and PrP^{Sc} is necessary for inhibition of the catalytic β subunits. Moreover, an aggregated state was necessary for an inhibitory effect, as non-aggregated β-PrP showed no effect on β subunit proteolytic activities when incubated with N2aPK-1 cells (**Figure 3.12B**). The proteasome inhibitor lactacystin completely abolished β subunit proteolytic activity and was used as a positive control.

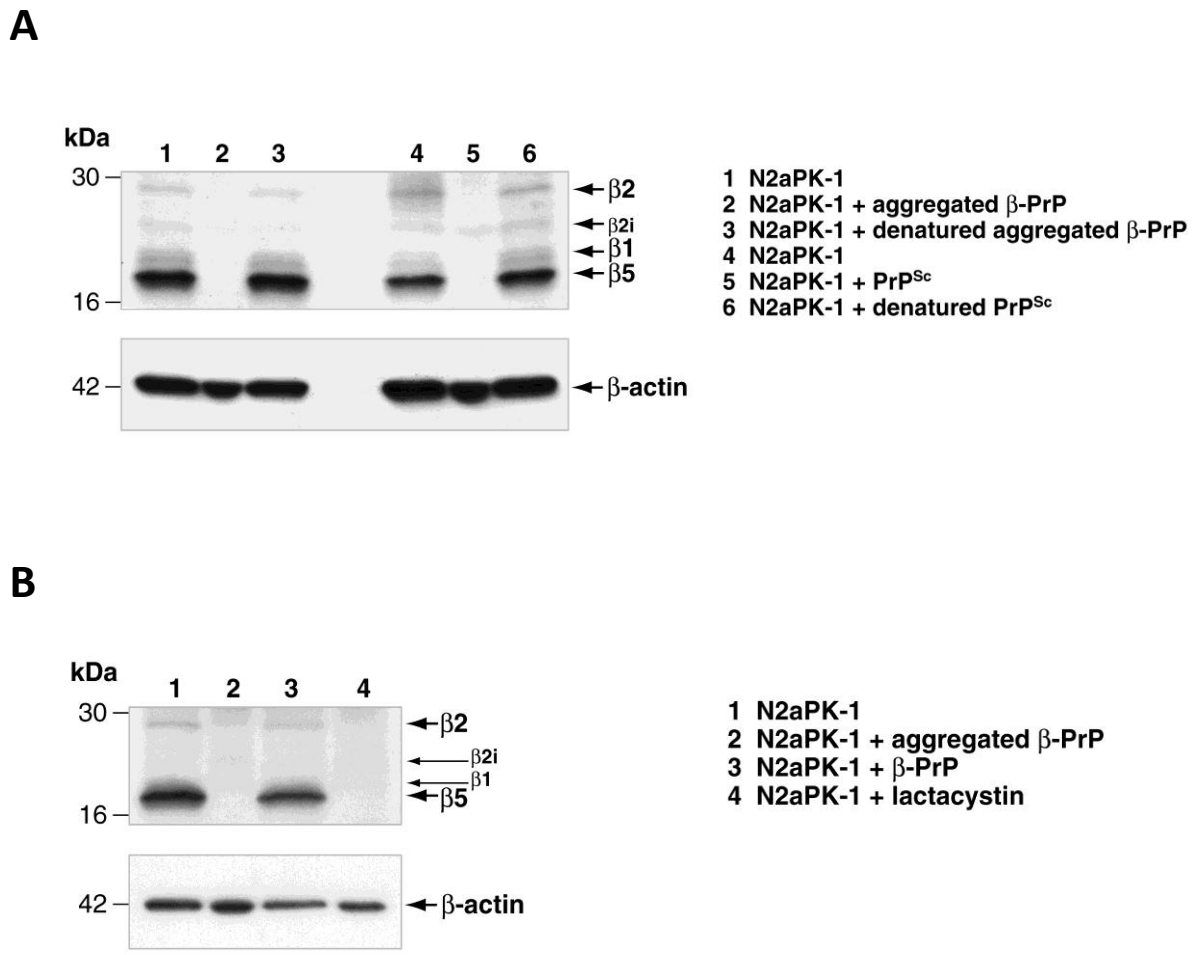

Figure 3.12 The inhibitory effect of PrP^{Sc} and aggregated β-PrP is conformation specific

N2aPK-1 cell lysates were incubated with the prion species in an aggregated or denatured state before treatment with the β subunit activity probe (dansylAhx$_3$L$_3$VS; 1 μM) and immunoblotting with an anti-dansyl antibody. **(A)** Complete denaturation of aggregated β-PrP and PrP^{Sc} (from ScGT-1 cells) by 10 cycles of freeze/boiling restored β subunit catalytic activities (lanes 3 and 6, respectively). **(B)** Only aggregated β-PrP (lane 2) and 50 μM lactacystin (lane 4; positive control) inhibited β subunit activities in N2aPK-1 cell lysates. Proteins were assayed at 1 mg/ml (final concentration). 100 μg protein from cell lysates was loaded per lane. Levels of an endogenous mouse protein, β-actin, were assessed by immunoblotting to confirm equal protein loading.

3.2.9 Other aggregated proteins do not inhibit 26S proteasome β subunit activity

To assess if inhibitory effects on proteolytic activity are specific to PrP^{Sc} and PrP^{Sc}-like species, the effect of other non-prion recombinant aggregated proteins on β subunit activities was investigated. In particular the effects of $A\beta_{1-40}$ amyloid fibrils, WT and mutant SOD1 (G37R) fibrils, as well as lysozyme amyloid fibrils were studied. **Figure 3.13** shows that the inhibitory effect on the 26S β subunits was specific to aggregated conformational isoforms of PrP, as none of the other proteins was inhibitory. The proteasome inhibitor lactacystin was used as positive control.

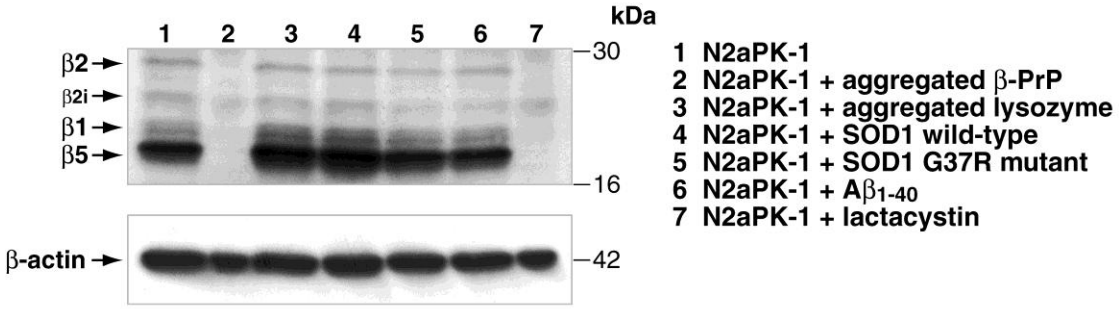

Figure 3.13 Inhibition of the proteasome is specific to conformational isoforms of PrP

N2aPK-1 cell lysates were incubated with recombinant proteins before treatment with the β subunit activity probe (dansylAhx$_3$L$_3$VS; 1 μM) and immunoblotting with an anti-dansyl antibody. Non-prion recombinant aggregated protein species had no effect on 26S proteasome β subunit activities in N2aPK-1 cell lysates. Proteins were assayed at 1 mg/ml (final concentration), with the exception of $A\beta_{1-40}$, which was assayed at 100 μg/ml. For details on recombinant protein preparation see **Section 2.3**. 100 μg protein from cell lysates was loaded per lane. Levels of an endogenous mouse protein, β-actin, were assessed by immunoblotting to confirm equal protein loading.

3.2.10 β-PrP is a potent inhibitor of 26S proteasome β subunit activity

Serial dilutions of aggregated β-PrP were prepared and incubated with cytosolic cell fractions prior to assaying β subunit activity in order to determine the potency of β-PrP in inhibiting the 26S β subunit activities. Concentrations of aggregated β-PrP above 75 ng/ml completely inhibited β subunit proteolytic activity, whereas activity was observed at normal levels using 50 ng/ml aggregated β-PrP (**Figure 3.14**).

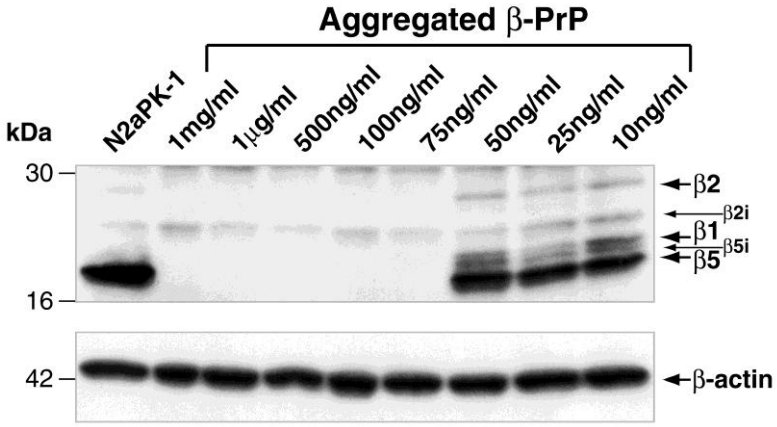

Figure 3.14 Aggregated β-PrP is a potent inhibitor of 26S β subunit activity (cells)

Serial dilutions of aggregated β-PrP (10 ng/ml, 25 ng/ml, 50 ng/ml, 75 ng/ml, 100 ng/ml, 500 ng/ml, 1 μg/ml, or 1 mg/ml) were incubated with 100 μg cytosolic N2aPK-1 cell fractions before incubation with 1 μM activity probe (dansylAhx$_3$L$_3$VS) and immunoblotting with an anti-dansyl antibody. Concentrations of aggregated β-PrP above 75 ng/ml completely inhibited β subunit proteolytic activity, whereas activity was observed at normal levels using 50 ng/ml aggregated β-PrP. Levels of an endogenous mouse protein, β-actin, were assessed by immunoblotting to confirm equal protein loading.

To determine the molar ratio of aggregated β-PrP sufficient to inhibit the proteasome, known concentrations of pure human 26S proteasome were incubated with various molar concentrations of aggregated β-PrP. The concentration of aggregated β-PrP sufficient to inhibit the 26S proteasome was essentially stoichiometric. 1.5 ng β-PrP (2.15 nM) was sufficient to inhibit 100 ng final concentration (fc) 26S (1.39 nM) (**Figure 3.15A**), 3 ng β-PrP (4.3 nM) was sufficient to inhibit 300 ng fc 26S (4.16 nM) (**Figure 3.15B**), and 7.5 ng β-PrP (10.75 nM) was sufficient to inhibit 900 fc ng 26S (12.49 nM) (**Figure 3.15C**). Taken together, these results demonstrated that aggregated β-PrP is a highly potent inhibitor of β subunit proteolytic activity and suggest that it is small aggregated β-sheet-rich PrP isoform(s) that is the inhibitory species.

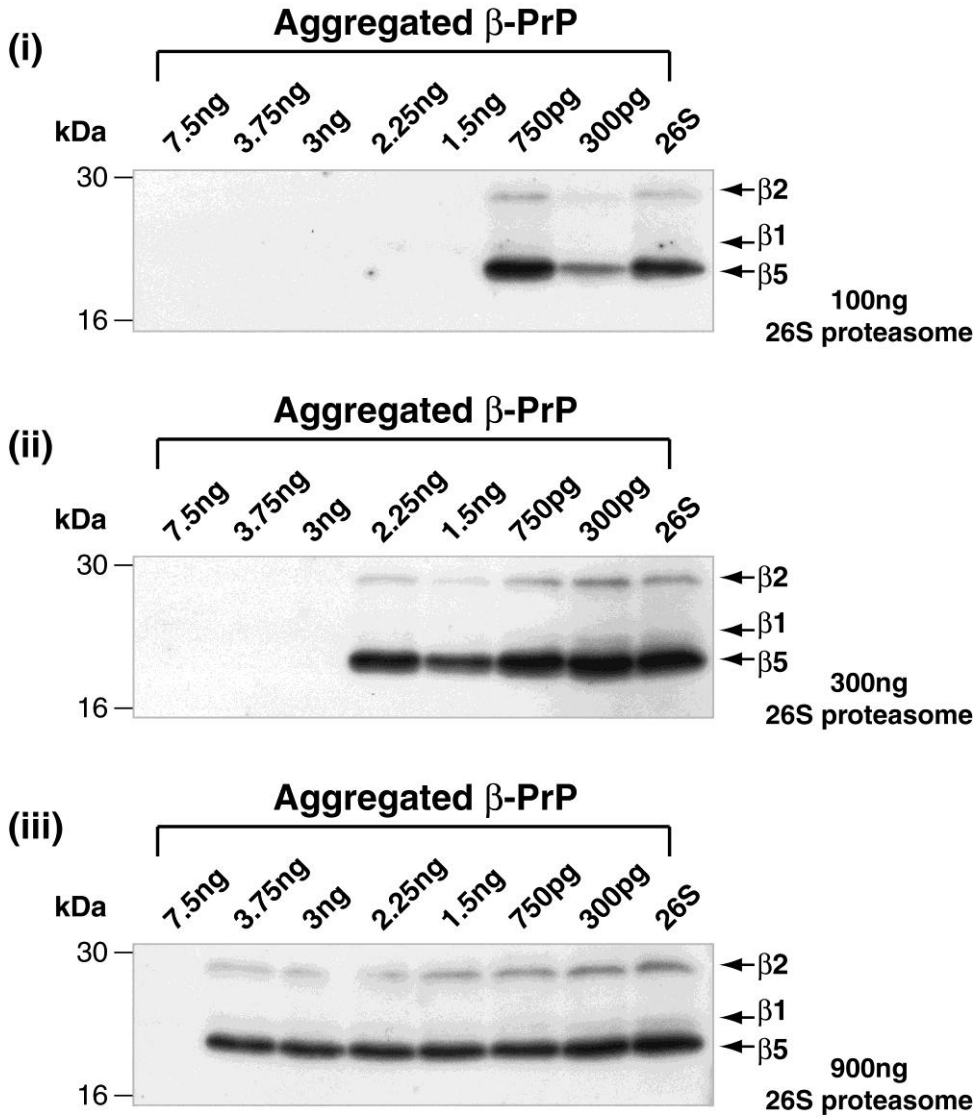

Figure 3.15 Aggregated β-PrP is a potent inhibitor of 26S β subunit activity (pure 26S)

Serial dilutions of aggregated β-PrP were pre-incubated with three different concentrations of pure human 26S proteasome before incubation with the β subunit activity probe (dansylAhx$_3$L$_3$VS; 1 μM) and immunoblotting with an anti-dansyl antibody. **(i)** 1.5 ng β-PrP (2.15 nM) was sufficient to inhibit 100 ng final concentration (fc) 26S (1.39 nM), **(ii)** 3 ng β-PrP (4.3 nM) was sufficient to inhibit 300 ng fc 26S (4.16 nM), and **(iii)** 7.5 ng β-PrP (10.75 nM) was sufficient to inhibit 900 fc ng 26S (12.49 nM). *This experiment was performed by Dr Mark Kristiansen, MRC Prion Unit, UCL Institute of Neurology.*

3.2.11 Pre-incubation with an antibody raised against aggregation intermediates abrogates the inhibition of the 26S proteasome β subunit activity by aggregated β-PrP and PrP^{Sc}

To investigate whether the PrP species responsible for inhibition of β subunit activity was oligomeric, the ability of an antibody raised against aggregation intermediates (Kayed *et al.*, 2003) to prevent inhibition was tested. Pre-incubation of either 0.5 μg/ml aggregated β-PrP or PrP^{Sc} (**Figure 3.16**) with molar excess of anti-oligomer antibody (150 μg/ml) abolished their inhibitory effect on the β subunits. This effect was specific, as pre-incubating both aggregated β-PrP and PrP^{Sc} with a rabbit polyclonal antibody raised against β-actin had no effect.

Moreover, the inhibitory effect of the PrP species was not diminished when aggregated β-PrP and PrP^{Sc} were pre-incubated with the same concentration (150 μg/ml) of three anti-PrP antibodies raised against different regions of the prion protein (**Figure 3.17**), confirming the specificity of the action of the antibody raised against aggregation intermediates. These results are consistent with an oligomeric PrP species in aggregated β-PrP and PrP^{Sc} inhibiting the 26S β subunit activity. The proteasome inhibitor lactacystin completely abolished β subunit proteolytic activity and was used as a positive control.

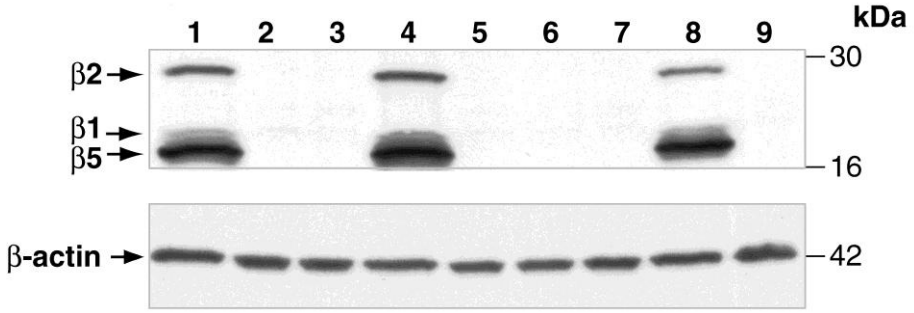

1 N2aPK-1
2 N2aPK-1 + aggregated β-PrP
3 N2aPK-1 + aggregated β-PrP + 5 μg/ml anti-oligomer Ab
4 N2aPK-1 + aggregated β-PrP + 150 μg/ml anti-oligomer Ab
5 N2aPK-1 + aggregated β-PrP + 150 μg/ml polyclonal β-actin
6 N2aPK-1 + PrP^{Sc}
7 N2aPK-1 + PrP^{Sc} + 5 μg/ml anti-oligomer Ab
8 N2aPK-1 + PrP^{Sc} + 150 μg/ml anti-oligomer Ab
9 N2aPK-1 + PrP^{Sc} + 150 μg/ml polyclonal β-actin

Figure 3.16 Inhibition of the β subunit proteolytic activities of the 26S proteasome is abrogated by pre-incubation with an anti-oligomer antibody

Pre-incubating aggregated β-PrP (lane 4) or PrP^{Sc} (lane 8; from ScGT-1 cells) with high concentrations (150 μg/ml) of an antibody raised against aggregation intermediates abolished their inhibitory effect on β subunit activities in N2aPK-1 cell lysates. An unrelated protein (β-actin) had no effect on preventing inhibitory action of β-PrP (lane5) and PrP^{Sc} (lane 9). All proteins were assayed at 500 ng/ml (final concentration). 100 μg of protein from cell lysates was loaded per lane. Levels of an endogenous mouse protein, β-actin, were assessed by immunoblotting to confirm equal protein loading.*This experiment was performed by Dr Mark Kristiansen, MRC Prion Unit, UCL Institute of Neurology.*

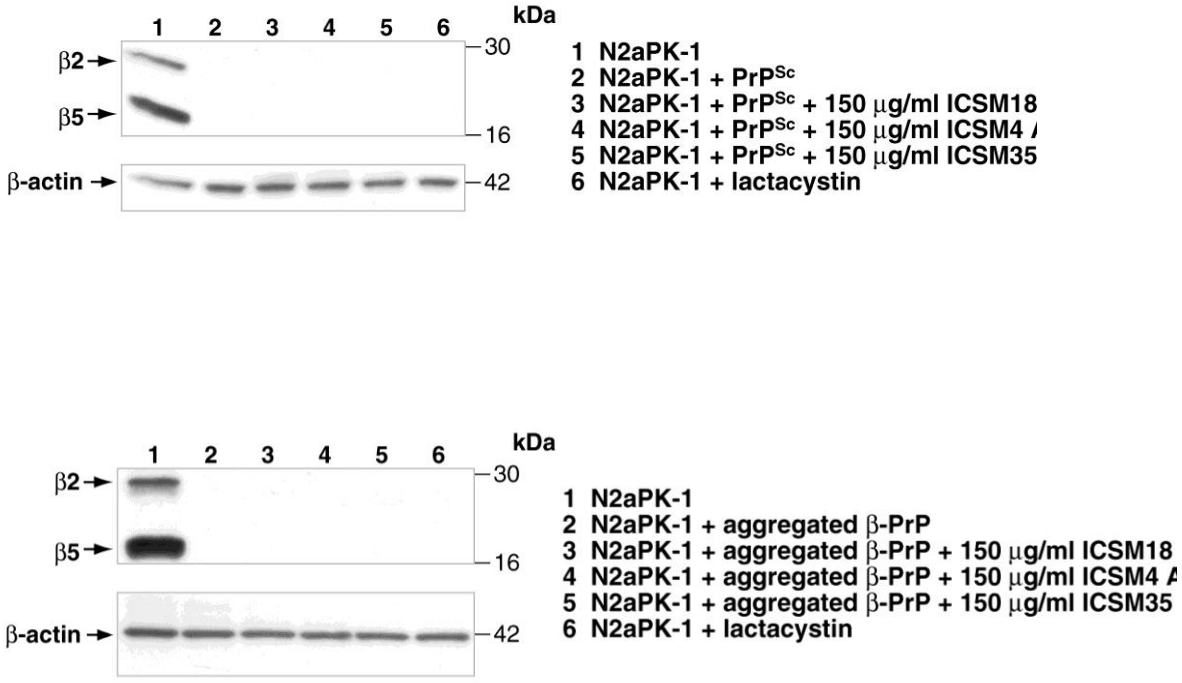

Figure 3.17 Pre-incubation with anti-PrP antibodies does not prevent β subunit inhibition

Pre-incubating PrP^{Sc} (top blot) or aggregated β-PrP (bottom blot) with high concentrations (150 μg/ml) of mouse monoclonal anti-PrP antibodies (ICSM4, 18 or 35) raised against different regions of PrP did not abolish their inhibitory effect on β subunit activities in N2aPK-1 cells. All proteins were assayed at 500 ng/ml (final concentration). 100 μg of protein from cell lysates was loaded per lane. Levels of an endogenous mouse protein, β-actin, were assessed by immunoblotting to confirm equal protein loading.

3.2.12 Aggregated β-sheet-rich prion species inhibit the 20S proteasome catalytic core, but not *via* dissociation of the 26S proteasome

Dissociation of the 26S proteasome into the 20S core particle and 19S regulatory particle causes inhibition of proteolysis (Elsasser *et al.*, 2005). To probe whether the inhibitory effect of aggregated β-PrP and PrP^{Sc} could be explained by dissociation of the 26S proteasome, native gels were used to assess the effect of aggregated β-PrP and PrP^{Sc} on pure human 26S proteasome. NativePAGE™ using 19S and 20S antibodies showed that the prion species did not cause dissociation of the 26S proteasome (**Figure 3.18**).

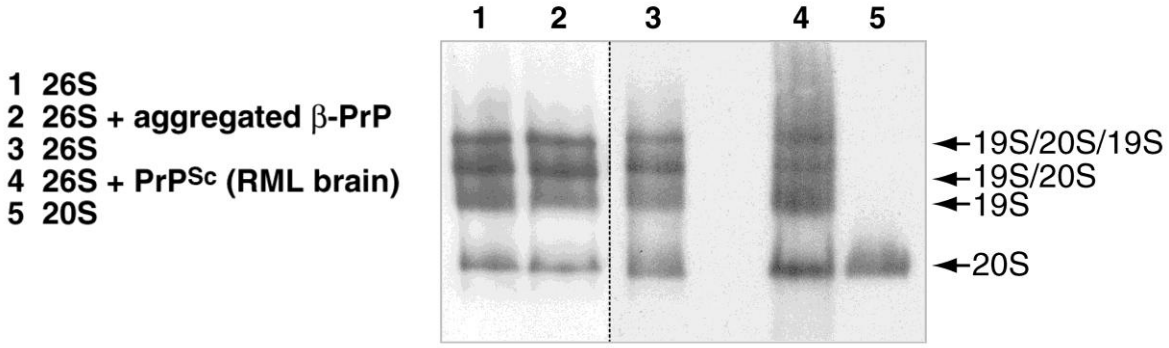

Figure 3.18 Aggregated β-sheet-rich PrP species inhibit the 20S catalytic core, but not *via* dissociation of the 26S (immunoblot)

Native gel immunoblotting using anti-19S and -20S antibodies demonstrated aggregated β-PrP and PrP^{Sc} do not cause dissociation of the 26S proteasome into its 19S and 20S components. Three micrograms of pure human 26S proteasome were incubated with aggregated β-PrP or with PrP^{Sc} (from RML infected mouse brain), run on NativePAGE™ and immunoblotted using an anti-α4 (20S) and an anti-Rpt1 (19S) subunit antibody, both at 1:1000. Proteins were assayed at 30 μg/reaction (final concentration). 19S/20S/19S represents doubly-capped 26S proteasome, whereas 19S/20S represents singly-capped 26S.

That the inhibition of the 20S catalytic core was inhibited, but not by dissociation of the 26S proteasome, was confirmed by native gel activity-staining using the fluorogenic substrate overlay for chymotrypsin-like activity (**Figure 3.19**). Both aggregated β-PrP and PrP^{Sc} inhibited chymotrypsin-like activity in pure human 26S proteasome compared to untreated 26S proteasome alone. To test whether the 26S inhibition in prion-infected mouse cells and brain (**Figure 3.2; 3.3**) was independent of 26S dissociation into 20S and 19S, lysates were run on NativePAGE™. Immunoblotting for 20S and 19S proteasome subunits demonstrated no dissociation of the 26S proteasome in prion-infected GT-1 (ScGT-1) cells and prion-infected CD-1 mouse brain (RML) (**Figure 3.20**).

The effect of oligomeric PrP species on the 20S core particle independent of the 19S regulatory cap was also investigated. The 19S particle was substituted with the PA28 activator (Whitby *et al.*, 2000), which activates the proteasome core particle but does not mediate ubiquitin-dependent proteolysis and many other activities mediated by the 19S regulatory particle (Voges *et al.*, 1999). Assaying PA28-activated 20S showed that aggregated β-PrP and PrP^{Sc} significantly inhibited chymotrypsin-like and caspase like activity, with a lesser effect on trypsin-like activity (**Figure 3.21**). This was the same pattern of inhibition as seen in prion-infected cell lysates (**Figure 3.2**), although with a less profound inhibitory effect. Collectively, these results suggest that the 'oligomeric' inhibitory species exerts its inhibitory effect directly on the 20S core particle, independent of the 19S complex.

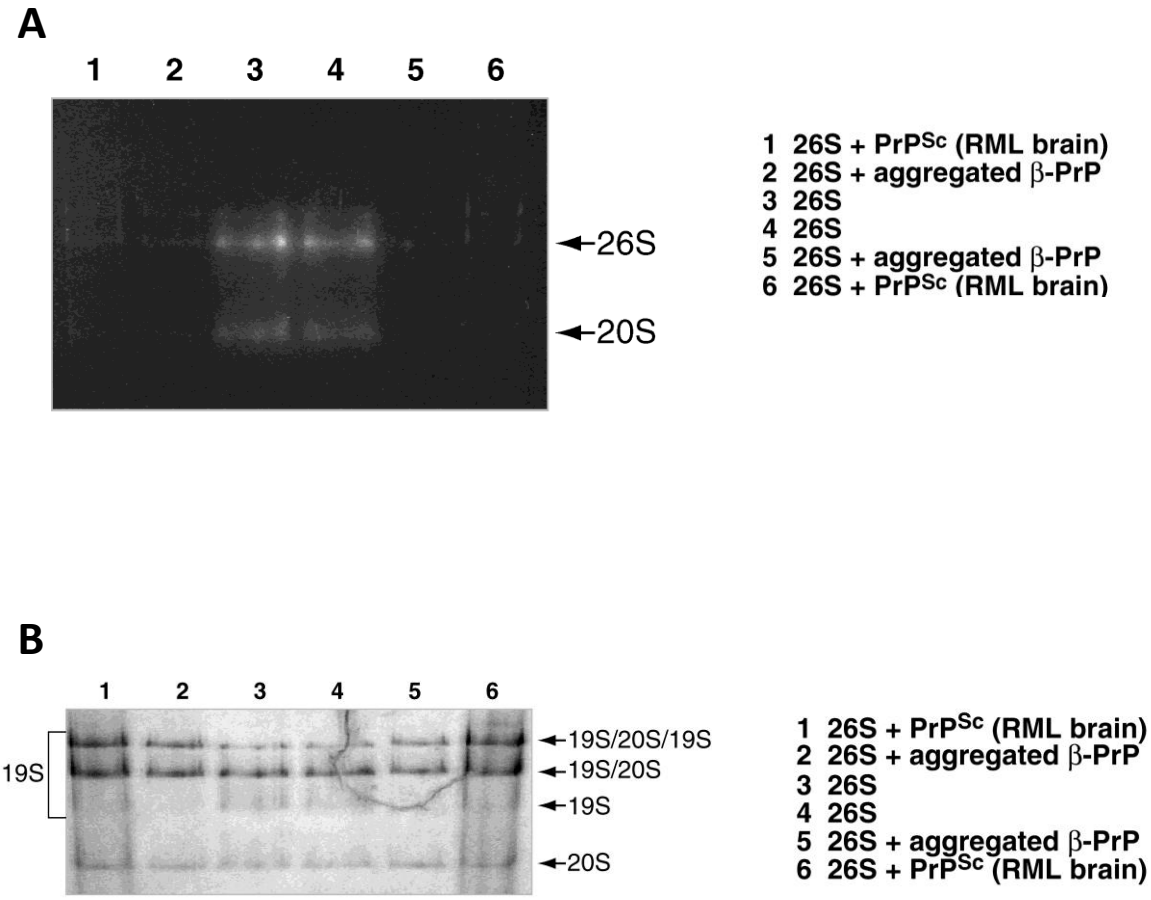

Figure 3.19 Aggregated β-sheet-rich PrP species inhibit the 20S catalytic core, but not *via* dissociation of the 26S (substrate overlay)

(A) Aggregated β-PrP (lanes 2 and 5) and PrP^{Sc} (lanes 1 and 6; from RML-infected mouse brain) significantly inhibited the chymotrypsin-like activity of the 26S proteasome. Three micrograms of pure human 26S proteasome incubated with the prion species were run on a native gel, which was overlaid with 100 μM Suc-LLVY-AMC to detect chymotrypsin-like activity. **(B)** Coomassie-staining on the native gel from **A** confirmed equal protein loading in all lanes. Proteins were assayed at 30 μg/reaction (final concentration). 19S/20S/19S represents doubly-capped 26S proteasome, whereas 19S/20S represents singly-capped 26S.

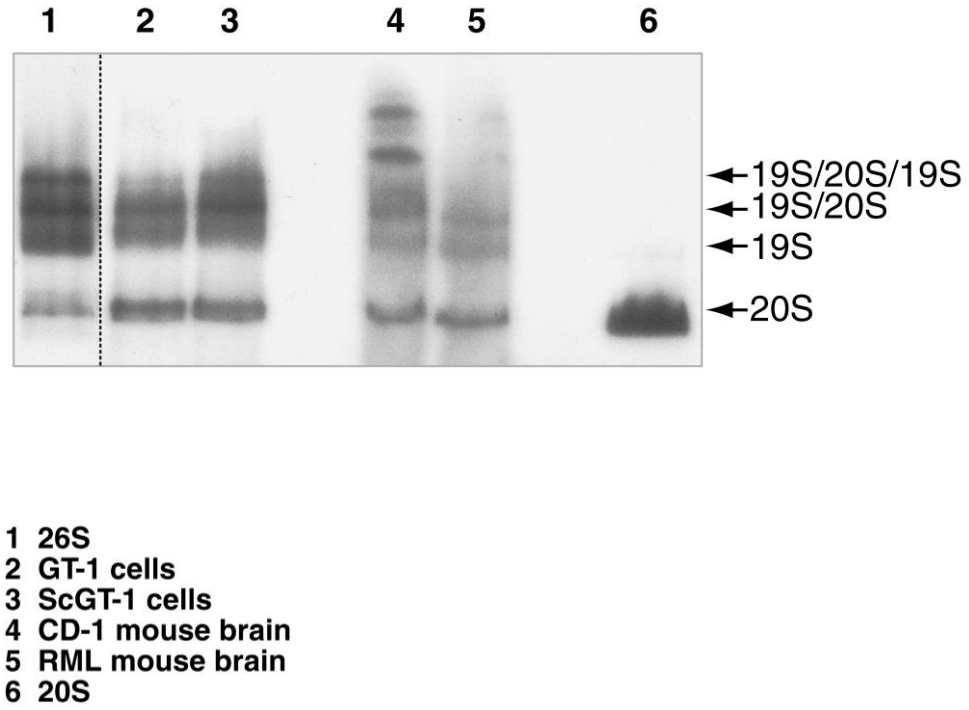

Figure 3.20 Prion infection does not cause dissociation of the 26S

Native gel immunoblotting of prion-infected ScGT-1 cells (lane 3) and prion-infected mouse brain (RML; lane 5) showed no dissociation of 26S proteasome into its 19S and 20S components compared with uninfected GT-1 cell lysates (lane 2) or uninfected CD-1 mouse brain (lane 4). 30 μg of cell lysates and 70 μg of brain homogenate were run on NativePAGE™ and immunoblotted using an anti-α4 (20S) and an anti-Rpt1 (19S) subunit antibody, both at 1:1000. 19S/20S/19S represents doubly-capped 26S proteasome, whereas 19S/20S represents singly-capped 26S.

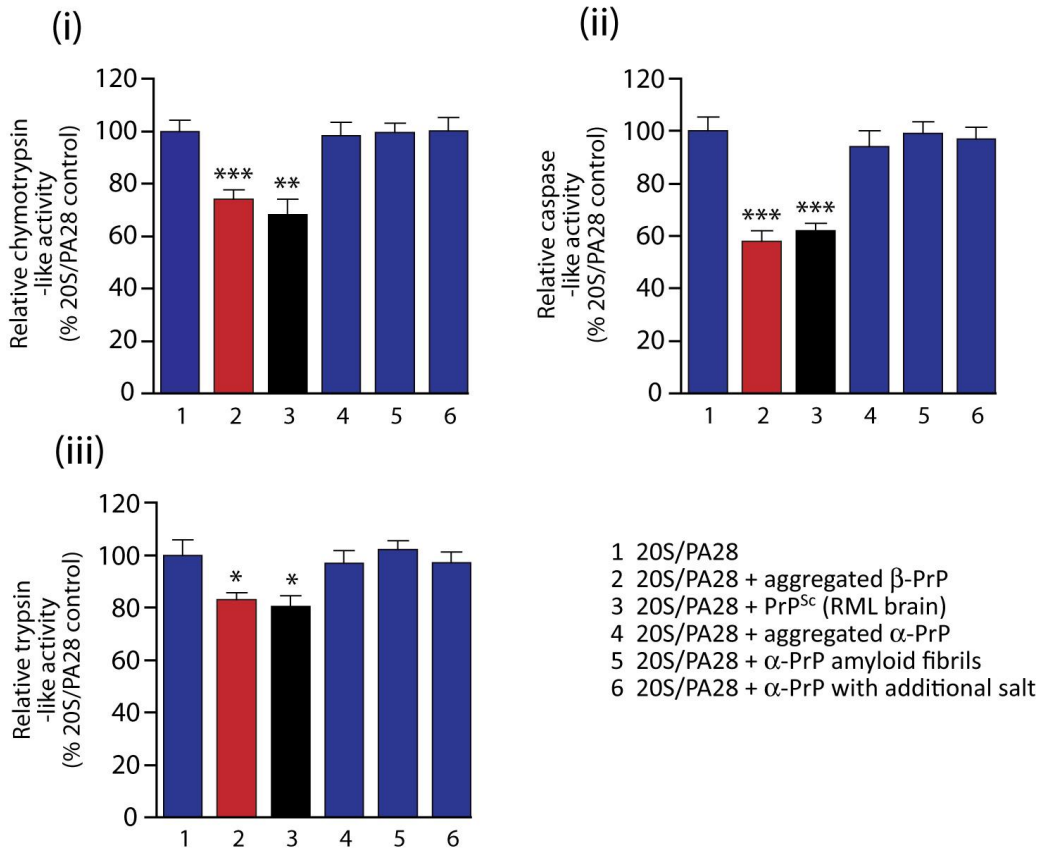

Figure 3.21 Aggregated β-PrP and PrP^{Sc} inhibit the proteolytic activities of PA28-activated 20S

Only aggregated β-PrP and PrP^{Sc}, but not aggregated conformational isoforms of PrP, decrease proteolytic activities of PA28-activated 20S proteasome. Peptidase activities of pure human 20S proteasome (10 ng per reaction) activated by PA28 (32 ng per reaction) were monitored using fluorogenic substrates specific for each activity: 100 μM Suc-LLVY-AMC (chymotrypsin-like), 100 μM Ac-nLPnLD-AMC (caspase-like) and 100 μM Boc-LLR-AMC (trypsin-like). 20S/PA28 preparations were incubated with the recombinant proteins before incubation with the fluorogenic substrate for 30 min. Fluorescence was measured over time at 360 nm excitation and 465 nm emission. Data are from ten independent experiments +SEM. ***p<0.001, **p<0.01, *p<0.05 (versus untreated 20S/PA28 control). *This experiment was performed by Dr Mark Kristiansen, MRC Prion Unit, UCL Insittute of Neurology.*

3.2.13 Prion infection inhibits the UPS *in vivo* in GFP-proteasome reporter transgenic mice

To assess whether UPS impairment also occurs in prion-mediated neurodegeneration *in vivo*, a transgenic mouse model that allows the functional status of the UPS to be monitored was used (Lindsten *et al.*, 2003). These mice express a Ub^{G76V}-GFP reporter, under the control of the CMV-immediate early enhancer and the chicken β-actin promoter, with constitutive and ubiquitous expression throughout the body, including the brain. Accumulation of GFP then indicates dysfunction of UPS activity. Detection of the Ub^{G76V}-GFP reporter was observed only in the 22L (prion strain)-infected transgenic mouse brains, whereas no Ub^{G76V}-GFP accumulation in mice inoculated with normal brain or in 22L prion-infected non-transgenic littermates was seen (**Figure 3.22**). This accumulation was seen in regions of the brain with the most intense neuropathology, consisting of spongiosis, gliosis, and PrP^{Sc} deposition (**Figure 3.22**). Similar results were obtained with the two available reporter mouse strains established from different founders (Lindsten *et al.*, 2003). Quantitative PCR confirmed that the accumulation of Ub^{G76V}-GFP was not due to transcriptional upregulation (**Figure 3.23**).

Furthermore, also observed was accumulation of intraneuronal, granular, ubiquitin deposits in the brains of 22L prion-infected Ub^{G76V}-GFP mice (**Figure 3.24**). These were occasionally observed in the control mice, but with lower frequency and intensity. The expression of the Ub^{G76V}-GFP transgene appeared to have no detectable effect on the deposition of ubiquitinated proteins.

Taken together, these results suggest that UPS dysfunction is associated with prion disease *in vivo* and support the *in vitro* data showing that proteasome function is directly compromised by the presence of PrP^{Sc} or its synthetic mimetic β-PrP.

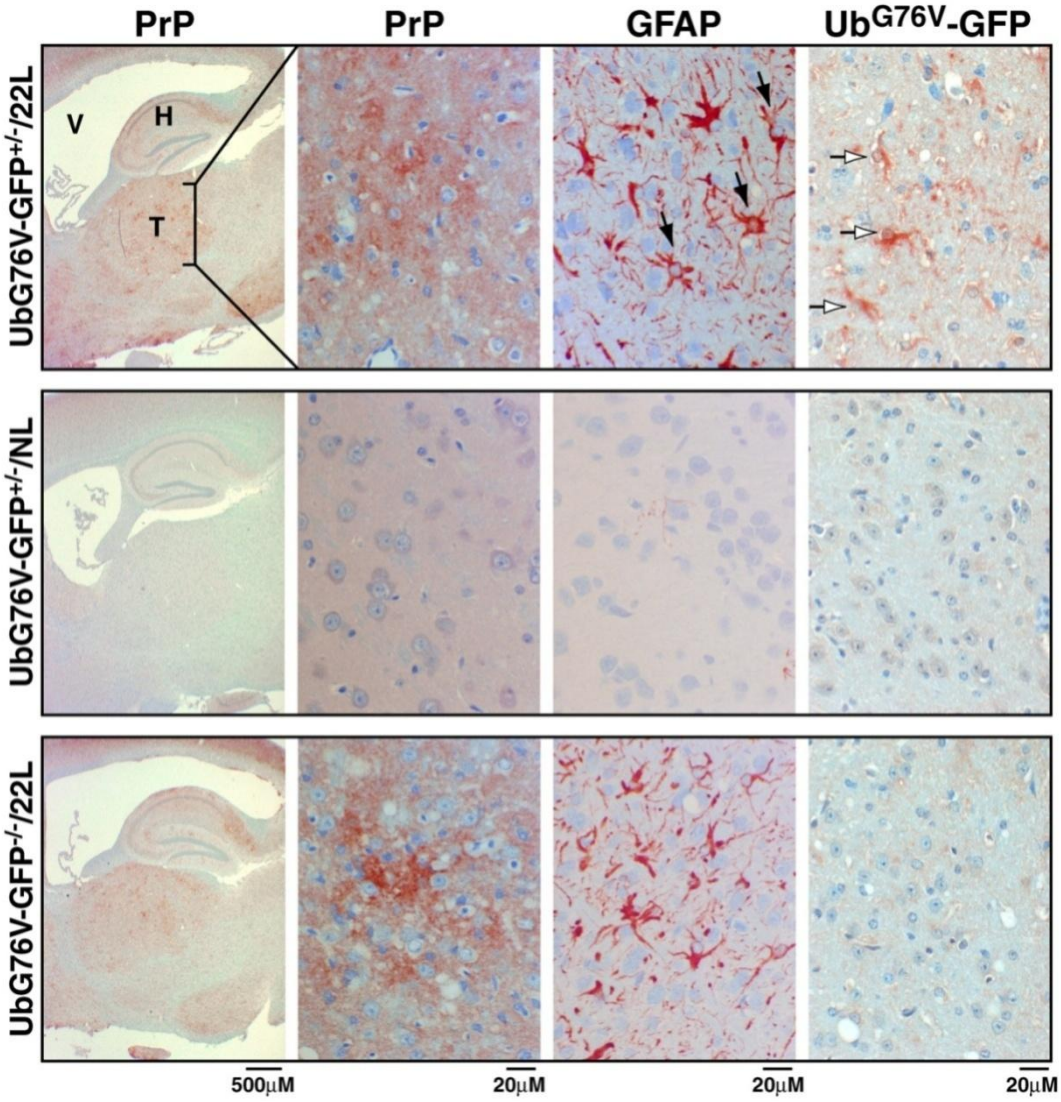

Figure 3.22 Prion infection causes specific inhibition of the UPS in GFP-proteasome reporter transgenic mice

Immunohistochemical studies of UbG76V-GFP$^{+/-}$ transgenic mice inoculated intracerebrally with the 22L strain of mouse scrapie (UbG76V-GFP$^{+/-}$/22L) (top) or normal brain homogenate (UbG76V-GFP$^{+/-}$/NL) (middle) and UbG76V-GFP$^{-/-}$ inoculated with 22L (UbG76V-GFP$^{-/-}$/22L) (bottom). Left panels show low-power views of saggital sections through the hippocampus (H), third ventricle (V), and thalamus (T) stained with anti-PrP antiserum R30. Other panels show high-power views of the thalamus stained for PrP, GFAP, and Ub^{G76V}-GFP. The 22L-inoculated mice exhibited primarily diffuse staining for PrP and extensive astrocytosis (black arrows point to hypertrophic astrocytes). Collections of Ub^{G76V}-GFP positive cells were seen in the 22L-inoculated UbG76V-GFP$^{+/-}$ mice (open arrows). The specificity of the anti-Ub^{G76}V-GFP antiserum is demonstrated by the lack of staining of these cells in the 22L-inoculated UbG76V-GFP$^{-/-}$ mice. *This experiment was performed by Dr Derek Dimcheff and Prof John Portis, Rocky Mountain Laboratories, USA.*

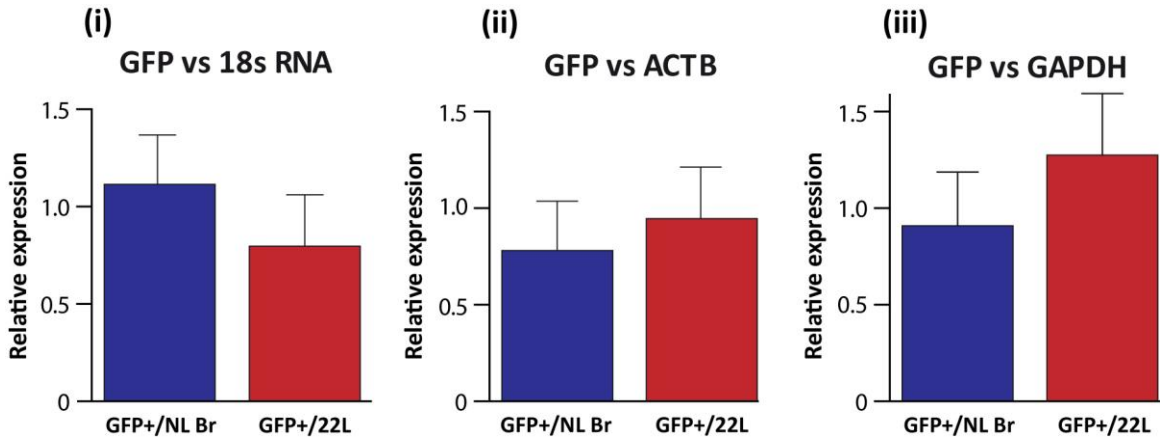

Figure 3.23 Accumulation of the Ub^{G76V}-GFP reporter is not due to transcriptional upregulation

There was no significant difference in expression between prion-infected mice versus mock-infected mice using Real-Time PCR quantified using 3 different house-keeping genes – 18S RNA, β-actin (ACTB) and GAPDH. Data are from five independent experiments + SD. *This experiment was performed by Dr Derek Dimcheff and Prof John Portis, Rocky Mountain Laboratories, USA.*

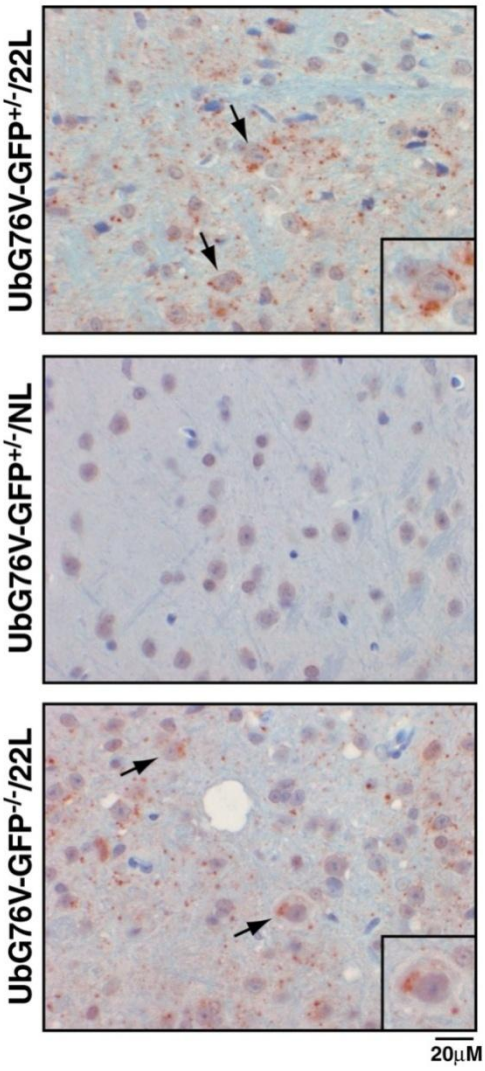

Figure 3.24 Prion infection causes specific inhibition of the UPS in GFP-proteasome reporter transgenic mice with accumulation of ubiquitin deposits

Immunohistochemical staining for ubiquitin in sections of thalamus from UbG76V-GFP$^{+/-}$ inoculated with 22L prion strain or normal brain homogenate. Granular deposits of ubiquitin are seen scattered throughout the sections of the 22L-infected brain but were rarely observed in the control. Arrows point to large neurone-like cells containing ubiquitin deposits that exhibit a perinuclear localisation. The lower panel of a UbG76V-GFP$^{-/-}$ inoculated with 22L demonstrates that the expression of the transgene appeared to have no effect on the deposition of ubiquitinated proteins. The substrate for all antisera was amino-ethyl-carbazol yielding a red product. Sections were counterstained with hematoxylin. *This experiment was performed by Dr Derek Dimcheff and Prof John Portis, Rocky Mountain Laboratories, USA.*

3.3 Discussion

While prion infection causes widespread neuronal loss in the brain, the molecular basis of prion neurotoxicity is unknown. Neurodegeneration cannot be explained by a loss of functional PrP^{C}, as its depletion does not trigger any gross pathology. For example, although PrP^{C} is essential for prion propagation and neurotoxicity (Bueler *et al.*, 1993), PrP^{C} knockout in adult mouse brain has no overt phenotypic effect (Mallucci *et al.*, 2002). In agreement, embryonic PrP^{C} knockout models demonstrate normal development and behaviour (Bueler *et al.*, 1992; Manson *et al.*, 1994). Taken together, PrP^{C} knockout studies effectively exclude loss of PrP^{C} function in neurones as a significant mechanism in prion-mediated neurodegeneration. It is widely hypothesised that an unknown toxic gain of function of PrP^{Sc} is more likely to underlie cell death. Studies have suggested that both full-length PrP^{Sc} (Hetz *et al.*, 2003) and shorter PrP peptides are toxic to cells *in vitro* (Forloni *et al.*, 1993), and their relevance to *in vivo* pathogenesis is under debate. There is strong evidence that PrP^{Sc} itself may not be the toxic entity. For example, PrP^{C}-null tissue can be in close proximity to PrP^{Sc} deposits without suffering deleterious effects (Brandner *et al.*, 1996; Mallucci *et al.*, 2003), and there is no direct correlation between neuronal loss and PrP^{Sc} plaques in CJD brains (Parchi *et al.*, 1996). Furthermore, prion diseases in which PrP^{Sc} is barely detectable have been described (Collinge *et al.*, 1995; Lasmezas *et al.*, 1997), and subclinical infection where high levels of PrP^{Sc} accumulate in the absence of clinical symptoms are also recognized (Hill *et al.*, 2000; Race *et al.*, 2001; Race *et al.*, 2002; Hill and Collinge, 2003a). Prion-infected mice expressing PrP^{C} without a GPI anchor produce infectious prions, accumulate extracellular PrP amyloid plaques, but do not succumb to disease (Chesebro, 2005).

Various mechanisms, all of which are not necessarily mutually exclusive, have been proposed to explain prion-mediated neurotoxicity. It has been suggested that during prion conversion a toxic intermediate (Hill *et al.*, 2000), PrP^{L} , or side products may be produced (Hill and Collinge, 2003a; Collinge and Clarke, 2007). In such models, PrP^{Sc} may represent a moderately inert end-product, whereby the steady-state level of PrP^{L} determines the rate of neurodegeneration (Hill and Collinge, 2003a). PrP^{L} levels would be regulated by natural

clearance mechanisms and would accumulate when the concentration of toxic PrP^{L} overwhelms the clearance capacity, thereby resulting in neurodegeneration. A possible candidate for such a toxic species could be a soluble monomeric or oligomeric conformer of PrP (Hill and Collinge, 2003a). For example, it has been shown that, at acidic pH, recombinant prion protein can fold into soluble β-sheet-rich monomers that are protease resistant and prone to aggregation into fibrils (Jackson *et al.*, 1999), suggesting such a conformer might exist under physiological conditions. This intermediate species may then only elicit neurotoxic effects when present at sufficient concentrations in particular sub-cellular compartments.

Alternatively, studies in which cross-linking PrP^{C} *in vivo* with specific monoclonal antibodies triggered rapid and marked apoptosis in hippocampal and cerebellar neurones *via* aberrant signalling, have suggested that PrP^{Sc} interacts with cell-surface PrP^{C} (Solforosi *et al.*, 2004). Another explanation is that PrP^{Sc}-induced cellular changes may lead to altered trafficking of PrP^{C} with its accumulation in a different cellular compartment resulting in cytotoxicity. For example, as a result of altered trafficking, PrP^{C} can assume two different trans-membrane topologies (^{Ctm}PrP-C trans-membrane PrP with an extracellular C-terminus and ^{Ntm}PrP-N trans-membrane PrP with an extracellular N-terminus), one of which, ^{Ctm}PrP, has been shown to confer severe neurodegeneration in mice with features typical of prion disease (Hegde *et al.*, 1998). Furthermore, extensive PrP^{C} accumulation in the cytoplasm by use of proteasome inhibitors has been associated with neuronal cell death (Ma and Lindquist, 2002). However, the data is conflicting, with evidence both for (Ma *et al.*, 2002; Heller *et al.*, 2003; Rane *et al.*, 2004; Wang *et al.*, 2005; Rambold *et al.*, 2006) and against (Drisaldi *et al.*, 2003; Roucou *et al.*, 2003; Fioriti *et al.*, 2005) this cytoplasmic accumulation of PrP^{C} having neurotoxic sequelae. One of the major drawbacks of many of these studies on cytosolic PrP^{C} is the high levels of proteasome inhibition used, which may limit any physiological relevance to the situation *in vivo* (Ding *et al.*, 2003). Studies in transgenic mice expressing a PrP^{C} mutant lacking the N-terminal targeting signal (cytoPrP) develop normally, but are severely ataxic, with cerebellar degeneration and gliosis; they also accumulate an insoluble PrP^{C} form (Ma *et al.*, 2002).

However, a more recent study showed that accumulation of unglycosylated cytosolic PrP^{C} did not cause any overt phenotype in aged, gene-targeted mice (Cancellotti *et al.*, 2005).

In vitro and *in vivo* experimental evidence presented in this chapter suggest a potential neurotoxic mechanism mediated by specific misfolded forms of PrP. Moreover, *in vivo* functional impairment of the UPS is also demonstrated in a neurodegenerative disease. Furthermore, the data describes that β-sheet-rich, non-native forms of PrP inhibit the activity of the catalytic β subunits of the 26S proteasome, *via* an effect on the 20S proteasome, and that this occurs at stoichiometric concentrations.

Using fluorogenic peptide assays and β subunit activity probes, the data presented here shows that in two prion-infected neuronal cell lines the presence of misfolded PrP significantly inhibits the chymotrypsin-like, caspase-like and trypsin-like activities of the 26S proteasome. This finding was mirrored in RML-prion-infected CD-1 mouse brain. These observations support previous work in mouse brain where impairment of these proteolytic activities was shown when infected with an alternative prion strain (Kang *et al.*, 2004). Inactivation of the chymotrypsin-like sites alone is not enough to halt protein breakdown, and either the trypsin-like or caspase-like activities must also be compromised to achieve this effect (Kisselev *et al.*, 2006); the data presented here are in close agreement with this condition. The results also demonstrate, by way of significant accumulation of a Ub^{G76V}-GFP reporter substrate (Dantuma *et al.*, 2000), that the observed proteasome inhibition results in UPS impairment in live cells. This effect was abrogated by curing the cells of prion infection (Enari *et al.*, 2001), demonstrating a direct link between prion infection and UPS impairment in live cells.

Dose-response analysis showed that inhibition of the catalytic activity of the 26S proteasome by β-PrP occurred at low stoichiometry. However, because the proportion of active 26S proteasome complexes in the preparation is unknown, it is impossible to determine the true molecular stoichiometry for the inhibited proteasome species. Data presented here also supports a cytosolic localisation for a small proportion of PrP^{Sc} in prion-infected neuronal cells, in line with previous studies demonstrating toxic cytosolic PrP^{Sc} aggresomes (Kristiansen *et al.*, 2005). Granular deposits of disease-related PrP have

been reported in the cell body of neurons in CJD brain, suggesting the occurrence of intra-neuronal prion aggregates (Kovacs *et al.*, 2005). The very high-affinity, stoichiometric inhibition of the proteasome means that only a small amount of PrP^{Sc} molecules in the cytosol may be necessary to have a toxic effect. How aggregated β-sheet-rich PrP species traffic inside neurones and enter the cytosol and result in UPS inhibition is poorly understood. Possible sites of entry include retro-translocation from the ER (Ma and Lindquist, 2001; Yedidia *et al.*, 2001) or *via* endolysosomal membrane destabilisation and leakage into the cytosol, as described for diphtheria toxin and other A-B toxins (Sandvig and van Deurs, 2002) and $A\beta_{1-42}$ (Ji *et al.*, 2006). Recently, Wadia *et al.*, reported that some PrP can escape macropinosomes and leak into the cytosol (Wadia *et al.*, 2008). It is also possible that PrP^{Sc} accumulation in the endolysosomal system causes dysfunction of this pathway, resulting indirectly in an increased burden on the UPS. Constant and increased routing of PrP through ERAD during chronic PrP^{Sc} accumulation-induced ER stress has been shown to lead to neurodegeneration (Rane *et al.*, 2008).

To investigate proteasome inhibition by β-sheet-rich PrP species further, an antibody which reacts with aggregation intermediates, but not monomeric or fibrillar forms of amyloidogenic proteins, was used (Kayed *et al.*, 2003). Pre-incubation with this antibody completely abolished any inhibitory effect on the catalytic β-subunits, suggesting that an 'oligomeric' PrP species may be responsible for the inhibition of the 26S proteasome. Observations in subclinical models of prion infection have suggested that prion neurotoxicity may relate not to PrP^{Sc} (or prions) but to critical levels of a toxic oligomeric species produced during prion propagation, PrP^{L} (Hill and Collinge, 2003a; Collinge and Clarke, 2007). This hypothesis explains, amongst other things, why there are prion diseases (Hsiao *et al.*, 1990; Medori *et al.*, 1992; Collinge *et al.*, 1995; Lasmezas *et al.*, 1997) and animal models (Fischer *et al.*, 1996) in which PrP^{Sc} levels are very low at end-stage disease. The implication is that the low PrP^{Sc} signal is not important in terms of prion-mediated neurotoxicity because the amount of an intermediate species or side product during prion conversion, such as PrP^{L}, is high.

Taken together, the data presented here support an inhibitory effect of oligomeric PrP species on the 20S complex, with two possible mechanisms of inhibition (**Figure 3.26**). One possibility is that β-sheet-rich PrP species have a direct inhibitory effect on the β_1 and β_5 proteolytic active sites of the 20S core (**Figure 3.26**). However, the diameter of the gated channel is ~ 2 nm (Pickart and Cohen, 2004), and if the inhibitory PrP species is oligomeric, it would be too large to traverse the gate intact and enter the catalytic chamber. Therefore, direct inhibition would only be possible if the PrP unfolded to thread into the chamber. Alternatively, therefore, prions could inhibit gate-opening of the 20S proteasome (**Figure 3.25**). Entry of substrates into the catalytic chamber of the 20S is regulated by opening of the gated channel, which is normally held closed by the N-terminal tails of the outer α-ring subunits (Whitby *et al.*, 2000; Groll *et al.*, 2000). Studies of gate-opening with addition of hydrophobic peptides, use of the PA28 activator and gate deletion yeast mutants, all of which accelerate substrate entry, stimulate cleavage at the chymotrypsin-like and caspase-like sites by enhancing their V_{max}, but do not stimulate the slower cleavage at the trypsin-like site (Kisselev *et al.*, 2002). Therefore, an inhibitory effect of prions on gate-opening of the 20S proteasome would have a more severe effect on the chymotrypsin-like and caspase-like activities as compared to the trypsin-like site. The levels of proteasome inhibition observed (>50% loss in each caspase-like and chymotrypsin-like activity), if re-capitulated *in vivo*, are likely to have serious consequences for neuronal viability. Moreover, the degradative capacity of the UPS is also known to decline with age (Lee *et al.*, 2000), such that when combined with the effects of disease, levels of UPS dysfunction and resultant neuronal death will be exaggerated (Sherman and Goldberg, 2001).

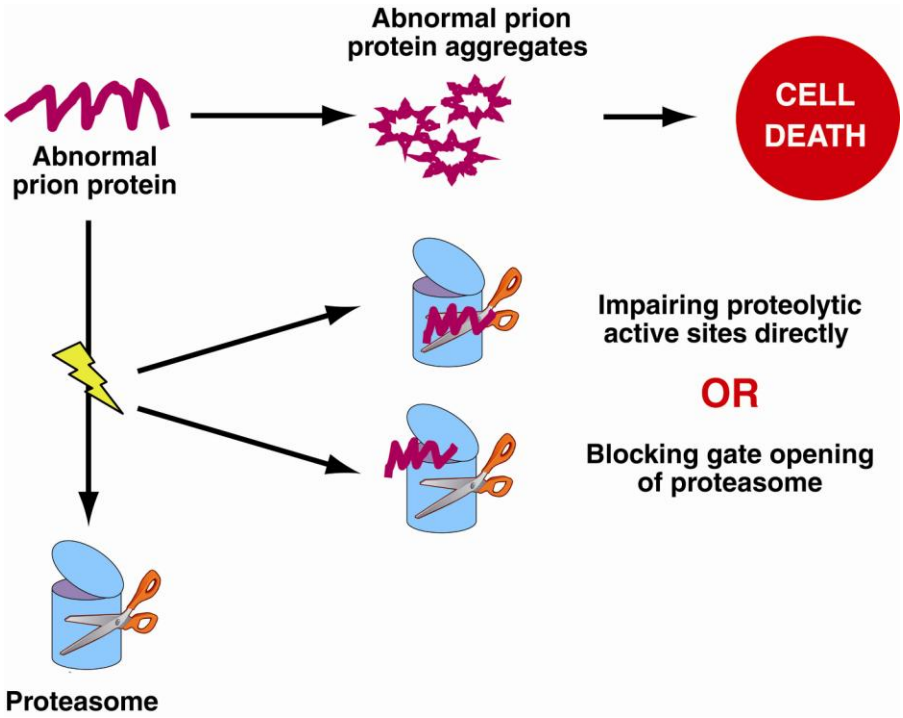

Figure 3.25 Possible mechanisms of proteasome inhibition by misfolded prion protein

Abnormal aggregation-prone prion protein accumulates in cells leading to cell death. Misfolded prion protein inhibits the proteolytic activities of the 26S proteasome. This inhibitory effect can be explained by two possible mechanisms. First, the aberrant prion protein directly inhibits the active sites of the proteasome, which are the catalytically active β subunits. The other possibility is that aggregated β-sheet-rich prion protein species inhibit gate-opening in the 20S particle.

Therefore, to ascertain whether prions exert a similar inhibitory effect on the UPS *in vivo*, Ub^{G76V}-GFP proteasome reporter mice were used (Lindsten *et al.*, 2003). These mice enable *in vivo* testing of the role of the UPS in neurodegeneration and have been used to demonstrate that proteasome impairment does not contribute to pathogenesis in spinocerebellar ataxia 7 mice (Bowman *et al.*, 2005). The GFP-reporter does not accumulate by neuronal apoptosis *per se* and is only seen when there is significant UPS dysfunction. Accumulation of the Ub^{G76V}-GFP reporter occurred only in prion-infected mice brains and was associated with neuronal loss and PrP^{Sc} deposition. Accumulation of intracellular cytosolic granular ubiquitinated deposits was also seen in the brains of prion-infected GFP-reporter mice. These deposits may represent cytosolic ubiquitinated-protein conjugates that accumulate as they are not degraded by the failing proteasome. Interestingly, similar ubiquitin-protein conjugates within neurones have been previously reported in the brains of prion-infected mice whereby intracellular ubiquitinated deposits were seen early and increased with disease progression (Lowe *et al.*, 1992). It was also noted that the pathological accumulation of the intracellular ubiquitin-protein structures corresponded temporally with the earliest detection of PrP^{Sc} (Lowe *et al.*, 1992). These observations may now be explained by the data presented here. Proteasome impairment has been suggested to be important in neurodegenerative diseases from many *in vitro* studies (Ciechanover and Brundin, 2003), but the role of the UPS in disease was unclear due to the lack of *in vivo* evidence. Recently, global changes to the UPS were shown *in vivo* in HD; using a mass spectrometry-based method it was reported that lysine 48-linked poly-ubiquitin chains, typically associated with proteasomal targeting, accumulate early in pathogenesis in both transgenic HD mouse brains and human HD patient brain (Bennett *et al.*, 2007). Moreover, a conditional *Psmc1* (Rpt2) knock-out mouse model with a neurodegenerative phenotype and ubiquitin-positive inclusions displayed 26S proteasomal dysfunction in neurons, providing *in vivo* experimental support for a direct role of the UPS in neurodegenerative disease pathogenesis (Bedford *et al.*, 2008).

Collectively, the data presented here support the view that prion protein neurotoxicity may be mediated through toxic, aggregated β-sheet-rich PrP species. There

is growing evidence in protein misfolding disorders that smaller intermediate protein species may be biologically more active than larger amyloid fibrils (Caughey and Lansbury, 2003). In studies of prion infectivity, non-fibrillar prion particles with masses equivalent to 14-28 PrP molecules are the most efficient initiators of prion disease (Silveira *et al.*, 2005). The present observations could explain how proteasome dysfunction by aggregated β-sheet-rich PrP isoforms, but not PrP amyloid fibrils, may contribute to neurotoxicity (Rane *et al.*, 2008) and are in keeping with proposals suggesting an intermediate toxic species produced during the conversion of PrP^{C} to PrP^{Sc} (Collinge and Clarke, 2007). Furthermore, proteasome inhibition by aggregated β-sheet-rich PrP isoforms may account for altered PrP^{C} trafficking (Ma and Lindquist, 2001; Yedidia *et al.*, 2001), whereby reduced or incomplete proteasomal degradation of PrP^{C} may lead to the accumulation of cytosolic PrP^{C} and lead to neurotoxicity.

3.4 Summary

Work in this chapter describes a significant loss of chymotrypsin-like (β_5) and caspase-like (β_1) proteolytic activity in prion-infected cells and prion-infected mouse brain, with a lesser effect on the trypsin-like (β_2) activity. Moreover, *in vitro* the catalytic β subunits of the human 26S proteasome were found to be inhibited by the prion protein in a non-native β-sheet conformation. This inhibition was shown to occur at near one to one stoichiometry inferring that the inhibitory species is highly potent and binds to the proteasome with high affinity. Challenge with recombinant prion and other amyloidogenic proteins demonstrated that it was only recombinant β-sheet-rich forms of PrP, β-PrP, and semi-purified PrP^{Sc} from either RML prion-infected mouse brain or mouse neuronal cells which mediated this inhibitory effect. Pre-incubation with an antibody raised against aggregation intermediates abrogated the inhibitory effect on the proteolytic activities, suggestive of an oligomeric inhibitory species. Using cell-based GFP-tagged reporters it was shown that they accumulate in prion-infected mouse neuroblastoma cells indicative of functional UPS impairment. Evidence for a direct relationship between prion neuropathology and UPS impairment in UPS-reporter transgenic mice was also presented. Collectively, results in this chapter suggest a possible mechanism for intracellular prion neurotoxicity mediated by oligomers of misfolded prion protein.

4 DISEASE-ASSOCIATED PRION PROTEIN INHIBITS THE UBIQUITIN PROTEASOME SYSTEM BY BLOCKING GATE-OPENING IN THE 20S PARTICLE

4.1 Background

In the UPS, substrates (e.g. misfolded or regulatory proteins) are covalently linked to a chain of ubiquitin molecules, which leads to rapid binding and degradation to small peptides by the 26S proteasome (Glickman and Ciechanover, 2002). There is accumulating evidence that impaired functioning of the UPS contributes to the pathogenesis of neurodegenerative diseases such as HD, PD and AD (Goldberg, 2003; Rubinsztein, 2006). Mutations in the E3 ubiquitin ligase, parkin, cause one of the more common inherited forms of PD (Shimura *et al.*, 2000) and conditional depletion of 26S proteasomes in neurons of the substantia nigra or forebrain in mice results in neurodegeneration with inclusions resembling Lewy bodies (Bedford *et al.*, 2008). Moreover, evidence suggests that in these diseases soluble micro-aggregates of misfolded proteins, rather than larger protein inclusions, are toxic to neurones (Rubinsztein, 2006). One hypothesis of how UPS dysfunction may contribute to neuronal death is that the continuous build-up of such aggregates eventually overwhelms the UPS, causing a functional impairment (Rubinsztein, 2006). Protein aggregates have been reported to impair UPS functional capacity in cell models (Bence *et al.*, 2001). Proteasomes cannot efficiently degrade polyQ-rich aggregates (Verhoef *et al.*, 2002) or polyQ repeat-containing proteins (Verhoef *et al.*, 2002). However, there is conflicting evidence regarding the role of the UPS in polyQ disorders depending on the particular model studied (Davies *et al.*, 2007). Therefore, current experimental evidence suggests that impairment of the UPS may play an important role in neurodegenerative diseases characterised by accumulation of misfolded proteins but to date the biochemical mechanisms underlying the UPS dysfunction are unclear.

Inactivation of any of the three active sites of the 20S slows but does not block protein degradation (Kisselev *et al.*, 2006). The chymotrypsin-like sites as well as either

the caspase-like or the trypsin-like sites need to be inhibited in order to strongly reduce protein degradation (Kisselev *et al.*, 2006). Data showing that aggregated β-sheet-rich PrP oligomers inhibit predominantly the chymotrypsin-like and caspase-like proteolytic activity of the 26S proteasome were presented in chapter 3 of this thesis. There are two possible explanations for these effects. First, the β-sheet-rich PrP species may directly inhibit the active sites of the 20S proteasome (**Figure 3.25**). This seems unlikely as the pore of the 20S does not exceed 2 nm in diameter (Pickart and Cohen, 2004) making it difficult for aggregated proteins to enter (**Figure 3.25**). Alternatively, the β-sheet-rich PrP isoforms may inhibit gate-opening and entry of peptide substrates into the 20S (**Figure 3.25**). Kisselev *et al.*, 2002 showed that agents that promote gate-opening or mutations that disrupt the gate in yeast proteasomes primarily enhance hydrolysis of hydrophobic or acidic peptides whose breakdown is limited by entry into the particle (unlike basic peptides whose hydrolysis is limited by the low turnover rate) (Kisselev *et al.*, 2002). An inhibitory effect of the aggregated PrP on gate-opening would therefore result in a more marked reduction in the chymotrypsin-like and caspase-like activities, as was observed.

4.2 Aims of this study

The aim of the present study was to further investigate the nature of proteasome inhibition by aggregated β-sheet-rich PrP isoforms and to more clearly define the biochemical mechanism of inhibition.

4.3 Methods

Western blotting [used for the detection of IκB-α protein levels (**Section 2.2.1**)] and RT-PCR [used for the detection of IκB-α transcript levels (**Section 2.6.1**)] were performed by Dr Mark Kristiansen, MRC Prion Unit, UCL Institute of Neurology. The three peptidase activities of the 20S proteasome were monitored using fluorogenic substrates (**Section 2.4.2)**. The SensoLyte™ Green Protease Assay Kit was used to monitor the capacity of the 20S proteasome to degrade fluorescent casein (**Section 2.4.5**) and these experiments were performed in collaboration with Dr Kerri Kinghorn, Department of Neurodegenerative disease, UCL Institute of Neurology. Co-immunoprecipitation experiments were performed to confirm a direct interaction between aggregated prion protein and the 20S proteasome (**Section 2.2.2**).

4.4 Results

4.4.1 β-sheet-rich PrP isoforms inhibit WT but not the open-gated 20S yeast mutant

The three peptidase activities of the 20S proteasome are routinely monitored *in vitro* by measuring of the rates of hydrolysis of specific fluorogenic peptides (Kisselev and Goldberg, 2005). To investigate whether aggregated β-sheet-rich PrP isoforms may inhibit gate-opening and substrate entry into the 20S proteasome, the chymotrypsin-like, caspase-like and trypsin-like activities of WT yeast 20S were measured and compared to those of a constitutively 'open-gated' yeast 20S mutant (Groll *et al.*, 2000). Crystallographic analysis of this 'open channel' 20S mutant has shown that deletion of the nine residue tail from the N-terminus of the α3 subunit (α3ΔN strain), opens a channel into the proteolytic chamber, and thus de-represses peptide hydrolysis resulting in strongly enhanced basal peptidase activity levels compared to WT (Groll *et al.*, 2000).

Recombinant full-length mouse PrP in the β-sheet-rich form (β-PrP), which has similar physico-chemical properties to PrP^{Sc}, was used in an aggregated form (Jackson *et al.*, 1999). The effect of semi-purified PrP^{Sc} from RML-prion-infected hypothalamic neuronal (ScGT-1) cells treated with 1μM lactacystin for 24h (Kristiansen *et al.*, 2005) was also studied. Upon incubation with WT 20S, both aggregated β-PrP and PrP^{Sc} caused a large reduction in chymotrypsin-like, caspase-like and trypsin-like activity (**Figure 4.1**). By contrast, no inhibition was observed when the PrP species were incubated with the α3ΔN 20S mutant (**Figure 4.2**).

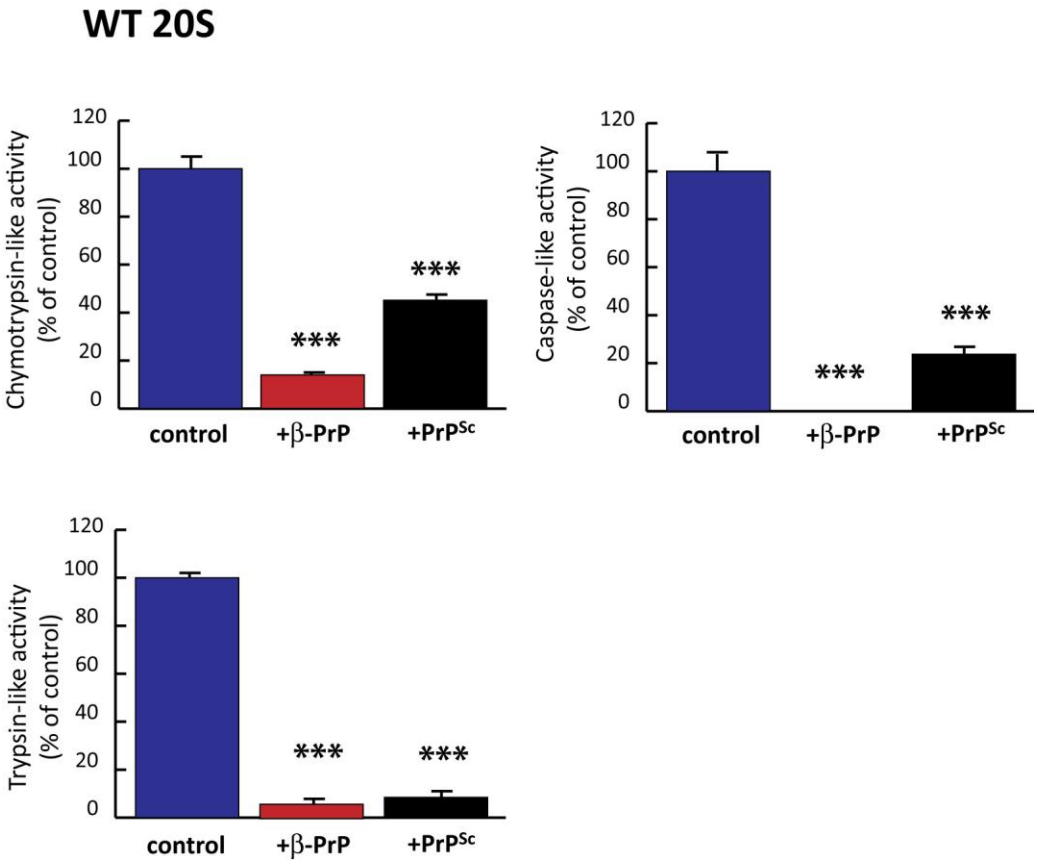

Figure 4.1 Effect of β-sheet-rich PrP on the proteolytic activities of WT yeast 20S

Aggregated mouse β-PrP or PrP^{Sc} purified from RML prion-infected ScGT-1 cells inhibit the chymotrypsin-like, caspase-like and trypsin-like activities of WT yeast 20S proteasome. Peptidase activities of WT yeast 20S (6.25 μg/ml) incubated with or without the PrP species (both at 20 μg/ml) were monitored using fluorogenic substrates specific for each activity: 100 μM Suc-LLVY-AMC (chymotrypsin-like), 100 μM Ac-nLPnLD-AMC (caspase-like) and 100 μM Boc-LLR-AMC (trypsin-like). Following 1 h incubation with the prion species, fluorogenic substrate was added to the reaction and fluorescence was measured over time at 360 nm excitation and 465 nm emission. Data are means of three independent experiments + SEM. ***$p<0.001$ (compared to untreated 20S control).

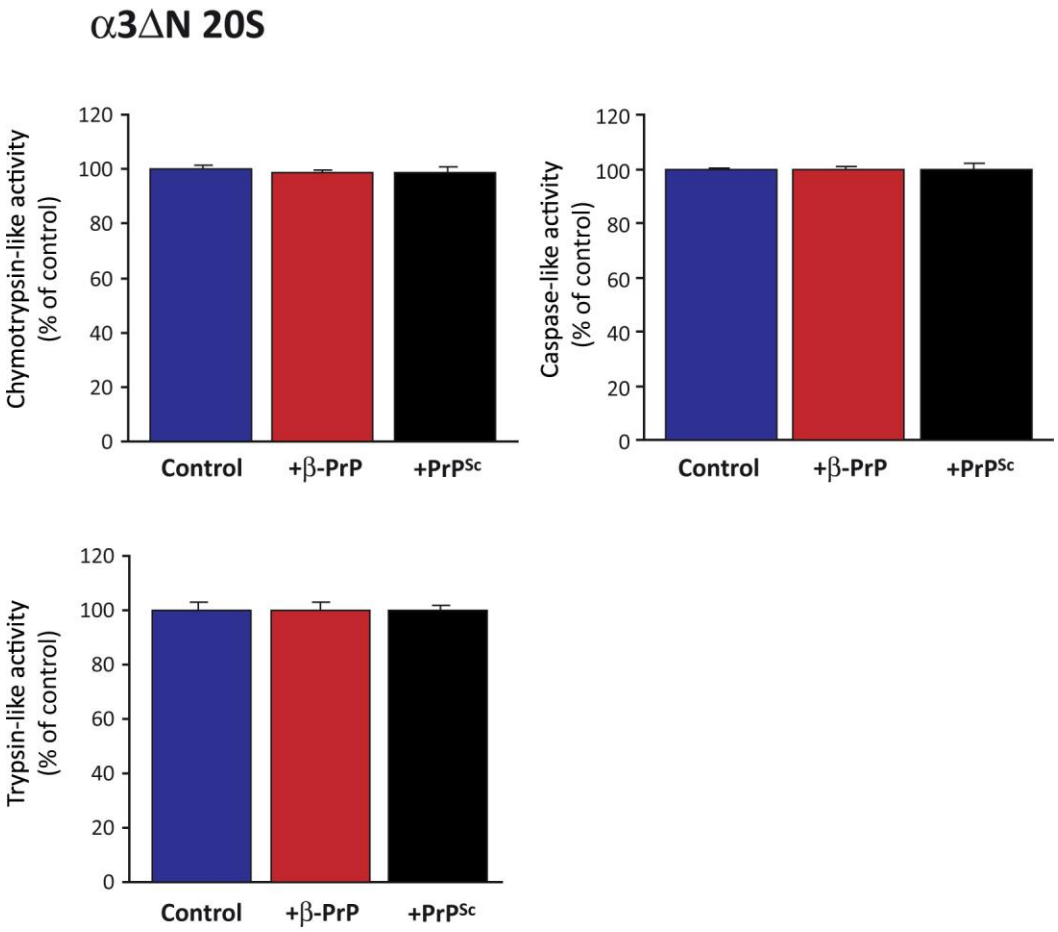

Figure 4.2 Aggregated β-sheet rich PrP species do not inhibit the α3ΔN 20S open-gated mutant

Aggregated mouse β-PrP or PrP^{Sc} purified from RML prion-infected ScGT-1 cells do not have an inhibitory effect on the chymotrypsin-like, caspase-like or trypsin-like activities of the open-gated α3ΔN yeast 20S mutant. Peptidase activities of α3ΔN 20S (6.25 μg/ml) incubated with or without the PrP species (both at 20 μg/ml) were monitored using fluorogenic substrates specific for each activity: 100 μM Suc-LLVY-AMC (chymotrypsin-like), 100 μM Ac-nLPnLD-AMC (caspase-like) and 100 μM Boc-LLR-AMC (trypsin-like). Following 1 h incubation with the prion species, fluorogenic substrate was added to the reaction and fluorescence was measured over time at 360 nm excitation and 465 nm emission. Data are means of three independent experiments + SEM.

An ‘open channel’ proteasome mutant with a double truncation of the N-termini of both α3 and α7 subunits (α3/α7ΔN strain), which makes it more efficient in the proteolysis of model proteins when compared to mutants with either of the two truncations (Bajorek *et al.*, 2003), was also studied. Upon incubation with the α3/α7ΔN 20S, the PrP isoforms caused a reduction in the chymotrypsin-like, caspase-like and trypsin-like activity (**Figure 4.3**). The degree of inhibition by the aggregated β-sheet-rich PrP species on the peptidase activities of the α3/α7ΔN 20S mutant was less when compared to WT 20S.

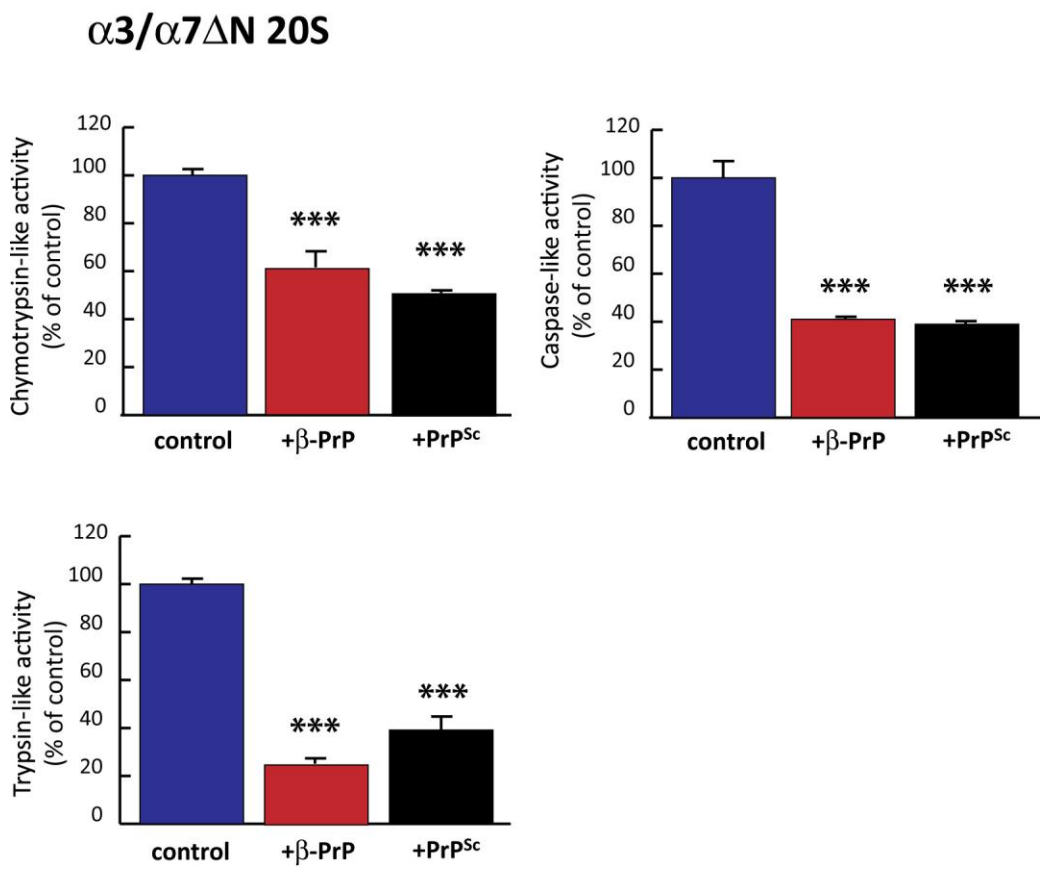

Figure 4.3 Effect of β-sheet-rich PrP on the proteolytic activities of the α3/α7ΔN 20S mutant

Aggregated mouse β-PrP or PrP^{Sc} purified from RML prion-infected ScGT-1 cells moderately inhibit the chymotrypsin-like, caspase-like and trypsin-like activities of the α3/α7ΔN yeast 20S mutant. Peptidase activities of α3/α7ΔN 20S (6.25 μg/ml) incubated with or without the PrP species (both at 20 μg/ml) were monitored using fluorogenic substrates specific for each activity: 100 μM Suc-LLVY-AMC (chymotrypsin-like), 100 μM Ac-nLPnLD-AMC (caspase-like) and 100 μM Boc-LLR-AMC (trypsin-like). Following 1 h incubation with the prion species, fluorogenic substrate was added to the reaction and fluorescence was measured over time at 360 nm excitation and 465 nm emission. Data are means of three independent experiments + SEM. ***$p<0.001$ (compared to untreated α3/α7ΔN 20S control).

As expected, both the α3ΔN and the α3/α7ΔN 20S mutants showed much higher basal chymotrypsin-like activity compared to that of WT 20S (**Figure 4.4**).

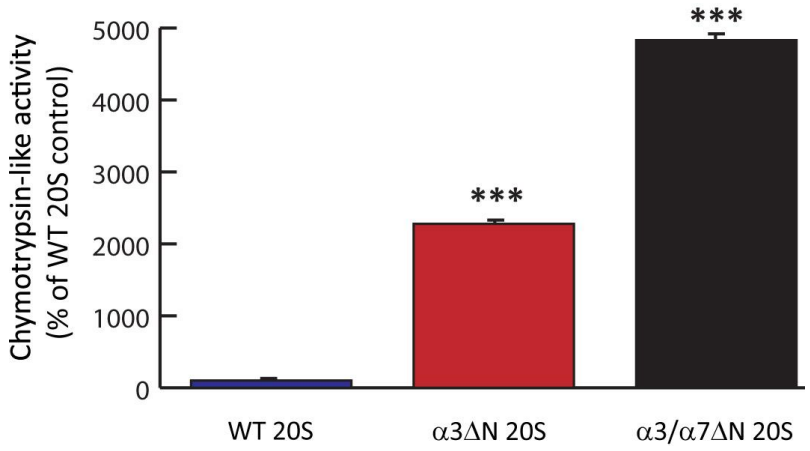

Figure 4.4 The 'open-gated' 20S mutants have much higher basal activity than WT 20S

The basal chymotrypsin-like activity of either the α3ΔN or the α3/α7ΔN 20S yeast mutant is much higher than that of the WT 20S. The chymotrypsin-like activities of WT, α3ΔN or α3/α7ΔN 20S (all at 6.25 μg/ml) were monitored using 100 μM Suc-LLVY-AMC. Fluorescence was measured over time at 360 nm excitation and 465 nm emission. Data are means of three independent experiments + SEM. ***p<0.001 (compared to WT 20S control).

Epoxomicin, a natural product isolated from an *Actinomycetes* species is an α, β-epoxy-ketone tetrapeptide proteasome inhibitor, which covalently binds to the β subunits of the proteasome (Meng *et al.*, 1999). To confirm that proteasome activity and not a contaminating activity was being measured, WT, α3ΔN and α3/α7ΔN 20S were treated with epoxomicin, which completely abrogated the chymotrypsin-like activity of all preparations (**Figure 4.5**).

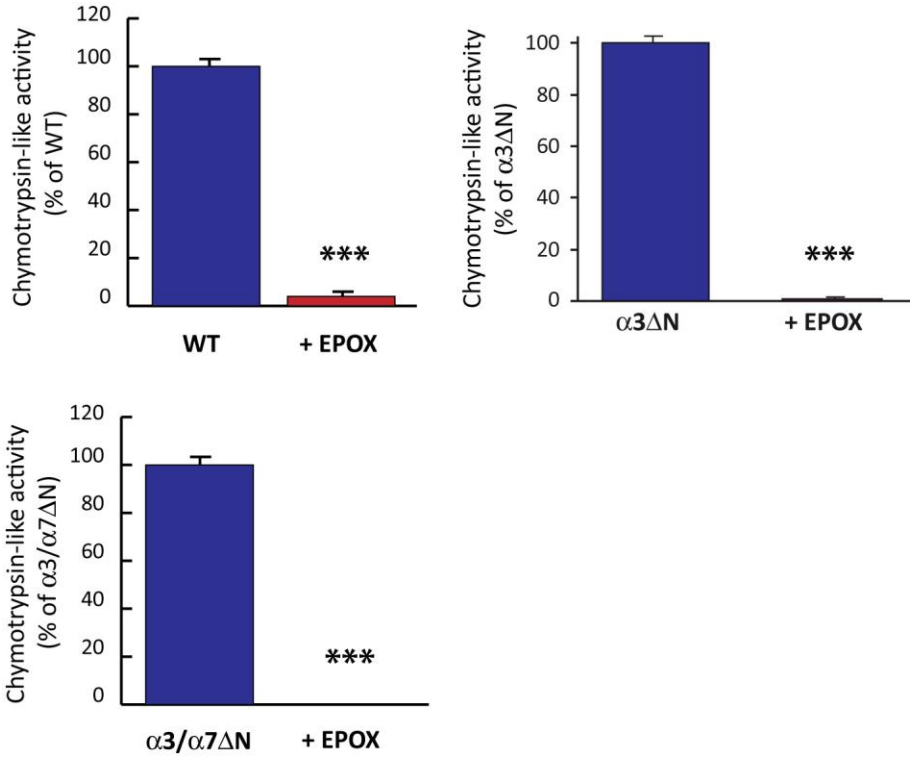

Figure 4.5 Epoxomicin abolishes proteolytic activity in both the α3ΔN and α3/α7ΔN 20S mutants

Chymotrypsin-like activity is completely abrogated in both WT yeast 20S, α3ΔN 20S and α3/α7ΔN 20S proteasome after pre-treatment with 50 μM epoxomicin (EPOX). Chymotrypsin-like activity of WT, α3ΔN 20S, or α3/α7ΔN 20S (6.25 μg/ml) was monitored using 100 μM Suc-LLVY-AMC fluorogenic substrate following 30 min incubation with 50 μM epoxomicin. Fluorescence was measured over time at 360 nm excitation and 465 nm emission. Data are means from five independent experiments +SEM. ***p<0.001 (compared to untreated control).

4.4.2 Aggregated β-sheet-rich PrP isoforms inhibit peptide hydrolysis by the 20S at low concentrations

Dose-response experiments presented in chapter 3 of this thesis (**Section 3.2.10**) showed that aggregated β-PrP is a highly potent inhibitor of 26S proteasome β subunit proteolysis. Upon incubation of cytosolic cell fractions with 50 ng/ml aggregated β-PrP the proteolytic β subunit activity, as monitored by a proteasome activity probe (Berkers *et al.*, 2005), was restored to normal levels (**Figure 3.14**). Furthermore, the molar ratio of β-PrP that inhibits the 26S proteasome was shown to be essentially stoichiometric from assays with pure 26S proteasome with known concentrations (**Figure 3.15**).

The above mentioned experiments were undertaken using a covalent probe of proteasome activity (Berkers *et al.*, 2005), which is less sensitive than direct fluorogenic enzyme assays for proteasomal activities. These previous data suggested that the inhibitory species are small aggregates of oligomeric β-sheet-rich PrP. To define the inhibitory species, the chymotrypsin-like activity of WT yeast 20S was monitored with fluorogenic peptides after incubation with increasing concentrations of aggregated β-PrP. Half-maximal inhibition of the 20S (9 nM) was observed between 90 and 180 nM aggregated β-PrP, where concentrations are based upon the free monomeric protein (**Figure 4.6**). However, the number of β-PrP molecules in the inhibitory species is unclear.

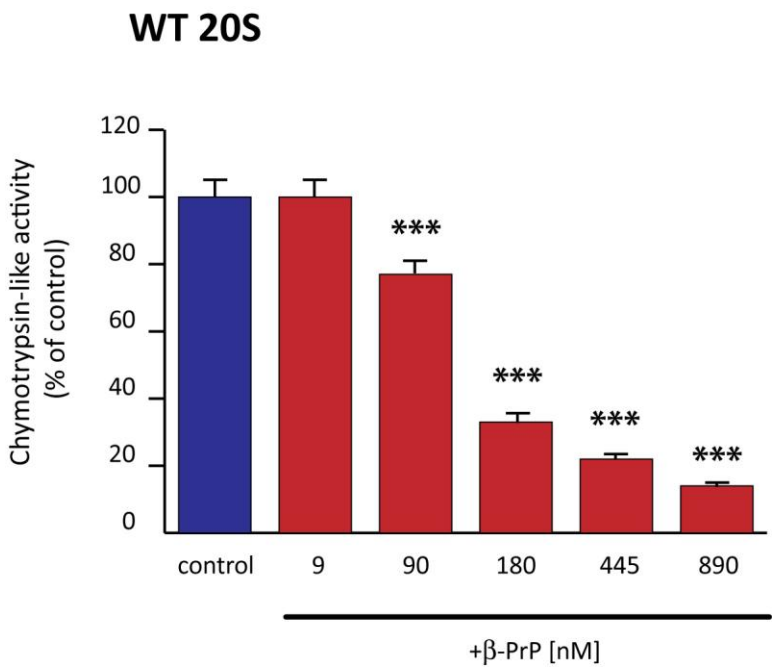

Figure 4.6 Aggregated β-PrP inhibits the proteolytic activity of the 20S proteasome at low molar concentrations

Half-maximal inhibition of WT yeast 20S is observed between 90 and 180 nM aggregated β-PrP. Following incubation of WT 20S (6.25 μg/ml; 9 nM) with increasing concentrations of aggregated β-PrP (9-890 nM), the rate of hydrolysis of 100 μM Suc-LLVY-AMC fluorogenic substrate by the chymotrypsin-like sites was measured. Fluorescence was measured over time at 360 nm excitation and 465 nm emission. Data are means of five independent experiments + SEM. ***$p<0.001$ (compared to untreated WT 20S control).

4.4.3 Malate dehydrogenase does not inhibit WT 20S

To test whether a similar inhibition of the WT yeast 20S by β-sheet-rich PrP species is seen with other misfolded proteins, WT 20S was incubated with either folded or unfolded malate dehydrogenase (MDH). Unfolded MDH has been shown to bind tightly to the mobile outer domains of the molecular chaperonin complex of GroEL (Chen *et al.*, 1994; Ranson *et al.*, 1997), which has a heptameric structure similar to that of the 20S. Neither folded nor unfolded MDH reduced peptide hydrolysis by the WT 20S (**Figure 4.7**) and is consistent with a mode of inhibition that is specific to the conformation and aggregation state of the β-sheet-rich PrP species.

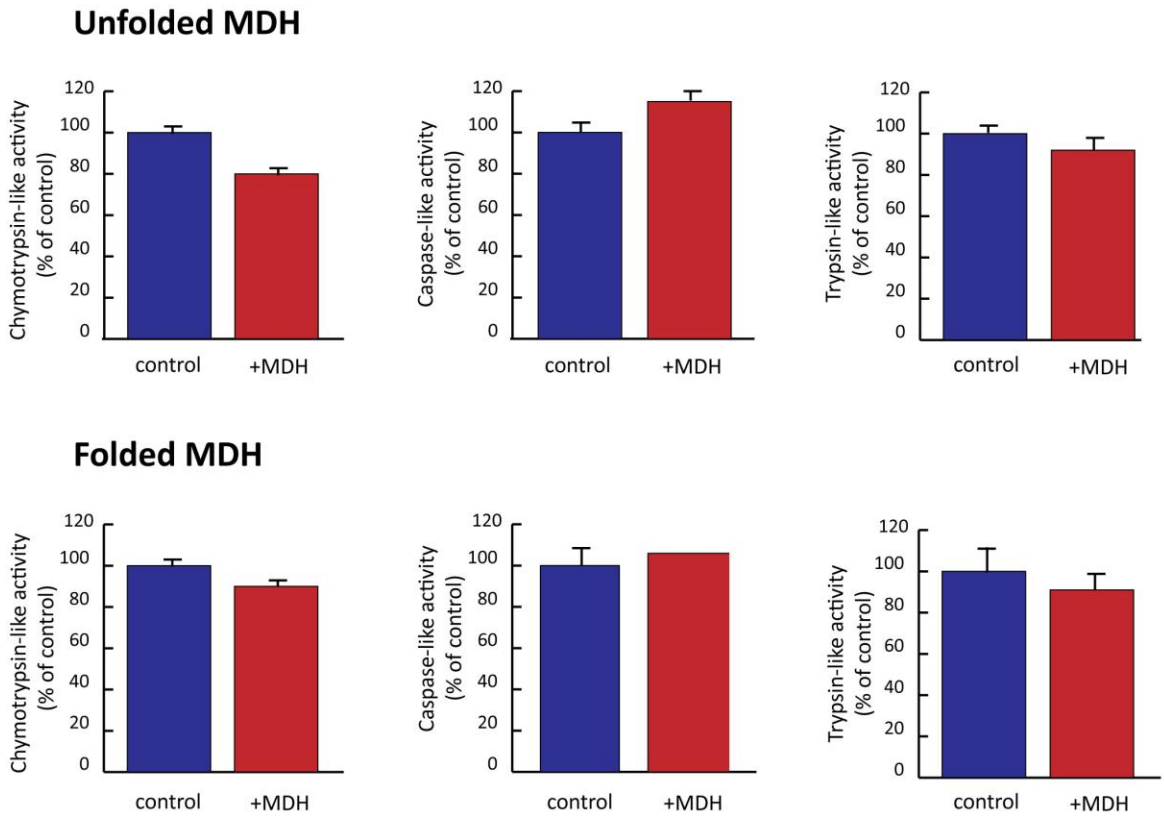

Figure 4.7 Unfolded malate dehydrogenase does not inhibit WT 20S

A hydrophobic protein, malate dehydrogenase (MDH), has no inhibitory effect on the proteolytic activities of the WT yeast 20S proteasome. Peptidase activities of WT 20S (0.1 μg/ml) incubated with unfolded or folded MDH (both at 3.3 μg/ml) were monitored using fluorogenic substrates specific for each activity: 100 μM Suc-LLVY-AMC (chymotrypsin-like), 100 μM Ac-nLPnLD-AMC (caspase-like) and 100 μM Boc-LLR-AMC (trypsin-like). Following 1 h incubation with either of the two proteins, fluorogenic substrate was added to the reaction and fluorescence was measured over time at 360 nm excitation and 465 nm emission. Folded malate dehydrogenase (MDH) was incubated at room temperature (RT) for 30 min in the presence of 4M GdHCl and 10mM DTT to unfold it. Data are means of five independent experiments +SEM.

4.4.4 β-sheet-rich PrP isoforms inhibit the WT, but partially affect the open-gated 26S yeast mutant

To test whether the inhibitory trend seen in WT versus 'open-gated' 20S proteasomes was also seen in the 26S proteasomes, WT or open-gated α3/α7ΔN 26S (Bajorek *et al.*, 2003) were incubated with aggregated β-PrP or PrP^{Sc} and the rates of hydrolysis of substrates by the chymotrypsin-like and caspase-like sites were monitored. Incubation of WT 26S with aggregated β-PrP or PrP^{Sc} resulted in a significant loss of chymotrypsin-like activity and caspase-like activity (**Figure 4.8**). Incubation of the α3/α7ΔN open-gated 26S mutant with the prion species resulted in a moderate inhibition of its chymotrypsin-like activity, whereas the caspase-like activity of the mutant was not affected (**Figure 4.9**). This pattern of inhibition seen with the α3/α7ΔN 26S mutant is different to the one observed with the α3/a7ΔN 20S, as there was a smaller inhibitory effect (**Figure 4.3**).

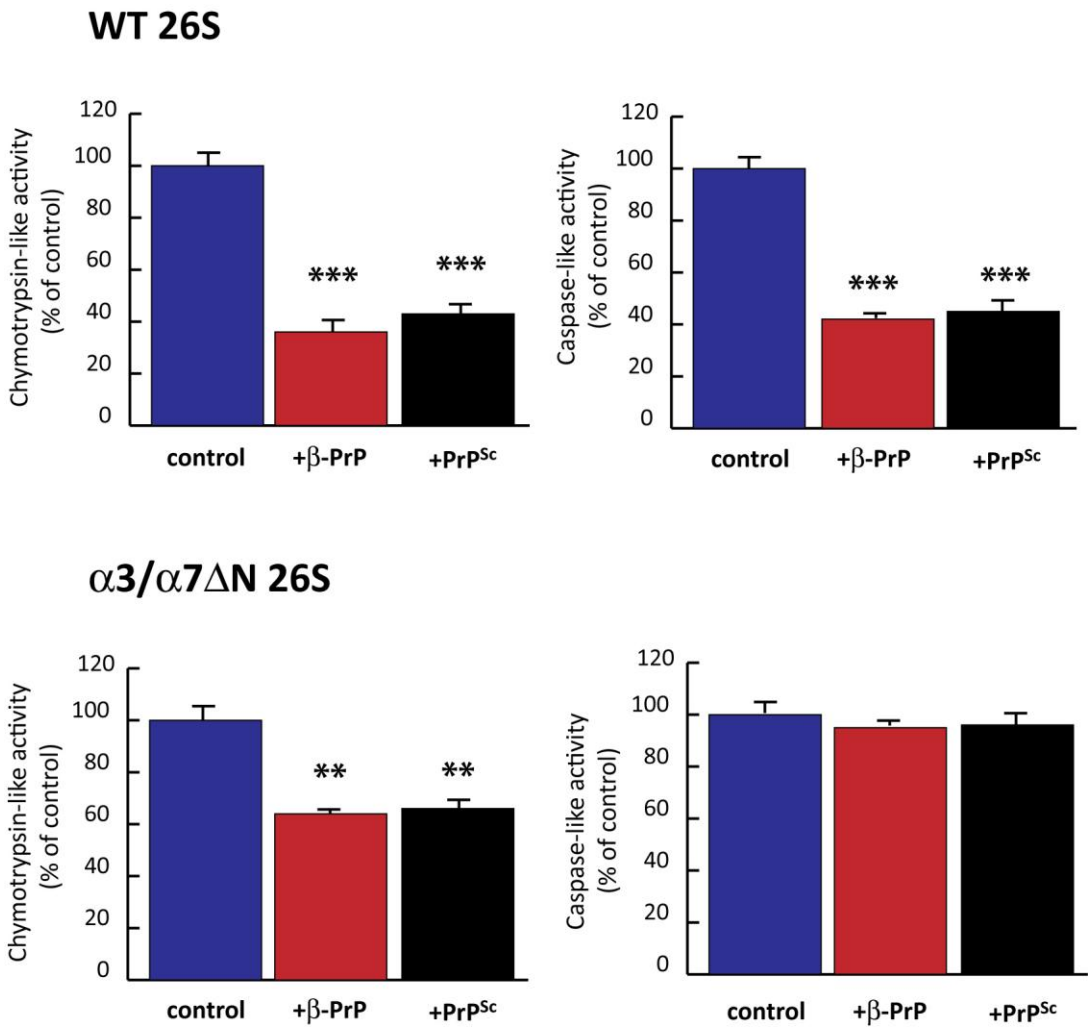

Figure 4.8 Effect of aggregated β-sheet-rich PrP on WT and α3/α7ΔN 26S

Aggregated mouse β-PrP or PrP^{Sc} purified from RML prion-infected ScGT-1 cells inhibit the chymotrypsin-like and caspase-like activities of the WT 26S but have a partial inhibitory effect on the α3/α7ΔN 26S mutant. Peptidase activities of both WT and α3/α7ΔN 20S (1 μg/ml) incubated with or without the PrP species (10 μg/ml) were monitored using fluorogenic substrates specific for each activity: 100 μM Suc-LLVY-AMC (chymotrypsin-like) and 100 μM Ac-nLPnLD-AMC (caspase-like). Following 1h incubation with the prion species, fluorogenic substrate was added to the reaction and fluorescence was measured over time at 360 nm excitation and 465 nm emission. Data are means of three independent experiments + SEM. ***$p<0.001$, **$p<0.01$ (compared to untreated control).

4.4.5 The inhibitory effect of aggregated β-PrP on the trypsin-like activity of the 26S is competitive with respect to substrate concentration

Cleavage of substrates by the proteasome's chymotrypsin-like or caspase-like sites is more sensitive to gate-opening than substrates of the trypsin-like sites because gate-opening of latent 20S will only stimulate substrate hydrolysis if the entry rate of diffusion of the substrate into the 20S is slower than its cleavage rate and the trypsin-like site has low turnover numbers. However, the entry of such peptides can be made rate-limiting by lowering the concentration of a substrate (Kisselev *et al.*, 2002), and with low concentrations of substrates, gate-opening also becomes limiting for the trypsin-like activity.

To test whether the β-sheet-rich PrP species were having an inhibitory effect on proteasome gating, human 26S was incubated with aggregated β-PrP, following which a range of concentrations (20-100 μM) of the fluorogenic substrate Boc-LRR-AMC was used to monitor the trypsin-like activity. If the β-sheet-rich PrP isoforms are affecting the cleavage of this substrate by blocking gate-opening, the aggregated β-PrP should reduce Boc-LRR-AMC cleavage at low substrate concentrations. Aggregated β-PrP was more inhibitory at lower Boc-LRR-AMC concentrations (**Figure 4.10**) where entry into the particle becomes rate-limiting (Kisselev *et al.*, 2002). These findings would therefore further support the conclusion that the PrP species are inhibiting the proteasome *via* an inhibition on gate-opening.

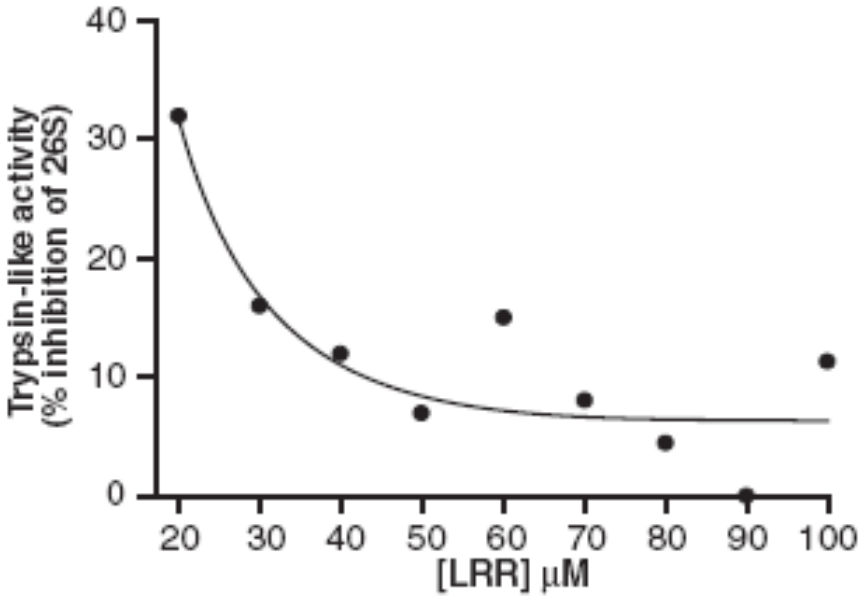

Figure 4.9 Boc-LRR-AMC concentration gradient in 26S incubated with β-PrP

Trend-line representing the relative % inhibition of the trypsin-like activity of human 26S by aggregated β-PrP. Inhibition of the trypsin-like activity of the 26S increases as the Boc-LRR-AMC fluorogenic substrate concentration decreases. Human 26S proteasome (1 μg/ml) was incubated with 10 μg/ml aggregated β-PrP before the addition of 20, 30, 40, 50, 60, 70, 80, 90, or 100 μM Boc-LRR-AMC substrate in order to monitor the trypsin-like activity. Fluorescence was measured over time at 360 nm excitation and 465 nm emission. This experiment was repeated three times and each time similar results were obtained.

4.4.6 Aggregated β-sheet-rich PrP isoforms inhibit Rpt5-mediated gate-opening in 20S

When they bind ATP, C-termini of certain 19S ATPase subunits dock into inter-subunit pockets in the 20S α-ring, induce gate-opening and allow substrate entry (Smith *et al.*, 2007; Rabl *et al.*, 2008; Gillette *et al.*, 2008) and this effect requires the presence of an essential HbYX amino acid motif in the C-terminus. Synthetic eight-residue peptides from the C-terminus of the mammalian Rpt2 and Rpt5 19S ATPase subunits have been shown to induce gate-opening in 20S from rabbit muscle (Smith *et al.*, 2007) as well as bovine erythrocyte 20S (Gillette *et al.*, 2008). To investigate whether aggregated β-sheet-rich PrP isoforms can influence peptide-mediated activation of the 20S, an 8-mer synthetic peptide corresponding to the C-terminus of the Rpt5 subunit of the 19S (KANLQYYA) was used. The Rpt5 C-terminal peptide (CtRpt5) strongly induced gate-opening in human 20S proteasome, since substrate cleavage by all three proteolytic sites were markedly enhanced (**Figure 4.10**).

Following the pre-incubation of 20S proteasomes with the aggregated β-sheet-rich PrP species, their effect on CtRpt5-mediated activation 20S was tested. Although CtRpt5 was added to the 20S/PrP sample in a fifty fold molar excess over both aggregated β-PrP and PrP^{Sc}, which must represent a much higher excess over the number of aggregates, these β-sheet-rich PrP isoforms abrogated the ability of the CtRpt5 peptide to induce gate-opening (**Figure 4.11**). They also seemed to reduce basal opening seen in the absence of CtRpt5 when the CtRpt5 activator was added *before* the aggregated β-PrP or PrP^{Sc}. Under these conditions, the aggregated β-sheet-rich PrP species still inhibited CtRpt5-mediated 20S activation (**Figure 4.12**).

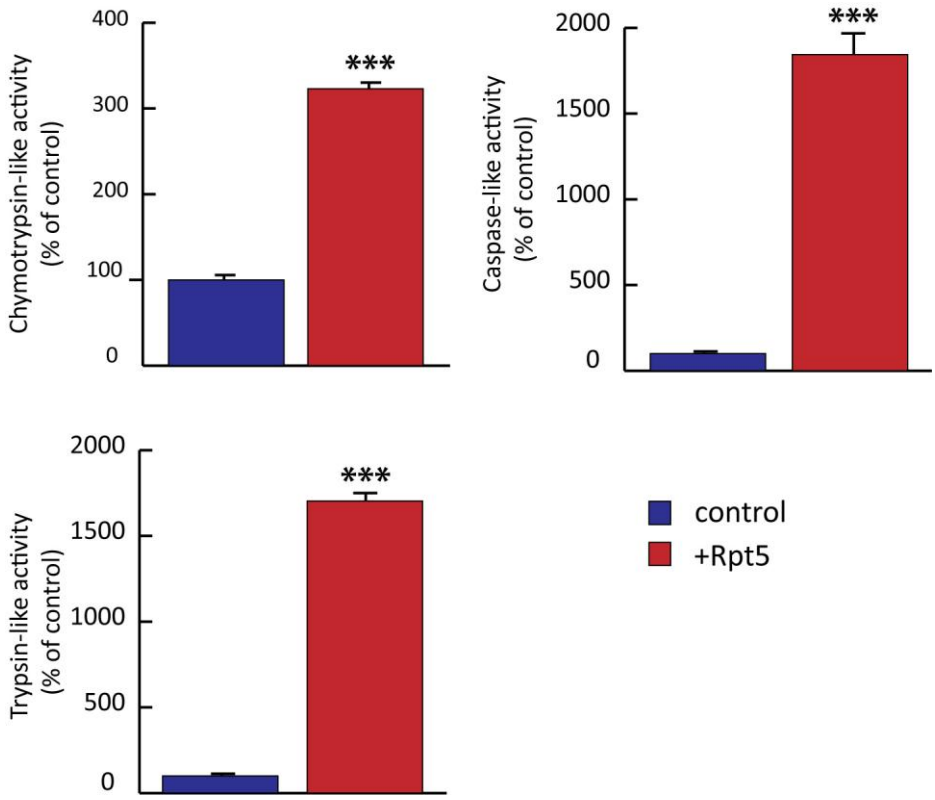

Figure 4.10 Rpt5 peptide activates human 20S

CtRpt5 strongly enhances the chymotrypsin-like, caspase-like and trypsin-like activities of human 20S proteasome. Peptidase activities of pure human 20S proteasome (1 μg/ml) were monitored using fluorogenic substrates specific for each activity: 100 μM Suc-LLVY-AMC (chymotrypsin-like) and 100 μM Ac-nLPnLD-AMC (caspase-like). CtRpt5 (Rpt5; 250μM) was added to 20S. Fluorescence was measured over time at 360 nm excitation and 465 nm emission. Data are means of three independent experiments + SEM. ***p<0.001 (versus untreated control).

20S pre-incubation with prion protein species before addition of Rpt5 peptide

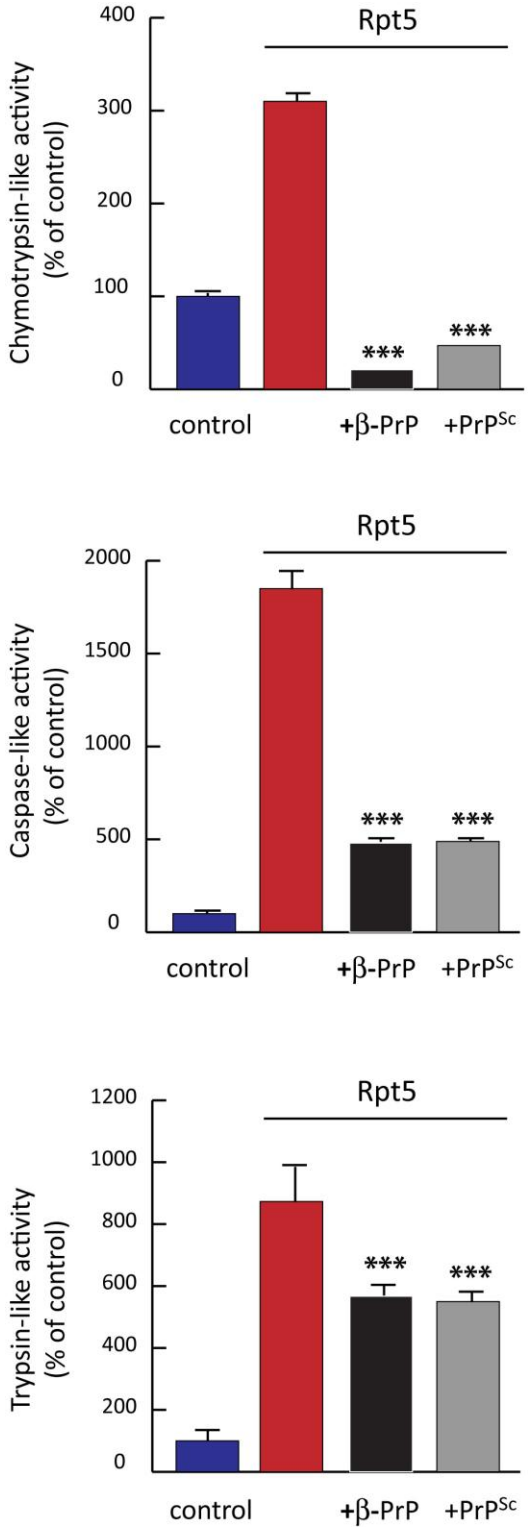

Figure 4.11 Rpt5-mediated human 20S proteasome activation is inhibited by β-sheet-rich PrP species-I

Pre-incubating human 20S proteasome with the prion species before the addition of CtRpt5 prevents CtRpt5-mediated 20S activation. Pure human 20S proteasome (1 μg/ml) was incubated with the prion species (100 μg/ml) for 1 h before addition of the CtRpt5 peptide (Rpt5; 250 μM). Peptidase activities were monitored using fluorogenic substrates specific for each activity: 100 μM Suc-LLVY-AMC (chymotrypsin-like) and 100 μM Ac-nLPnLD-AMC (caspase-like). Reaction buffer (**Section 2.4.2**) was the vehicle for the prion species and was added to 20S/Rpt5. Fluorescence was measured over time at 360 nm excitation and 465 nm emission. Data are means of three independent experiments + SEM. ***p<0.001 (versus untreated 20S/Rpt5 control).

20S pre-activation with Rpt5 peptide before addition of prion protein species

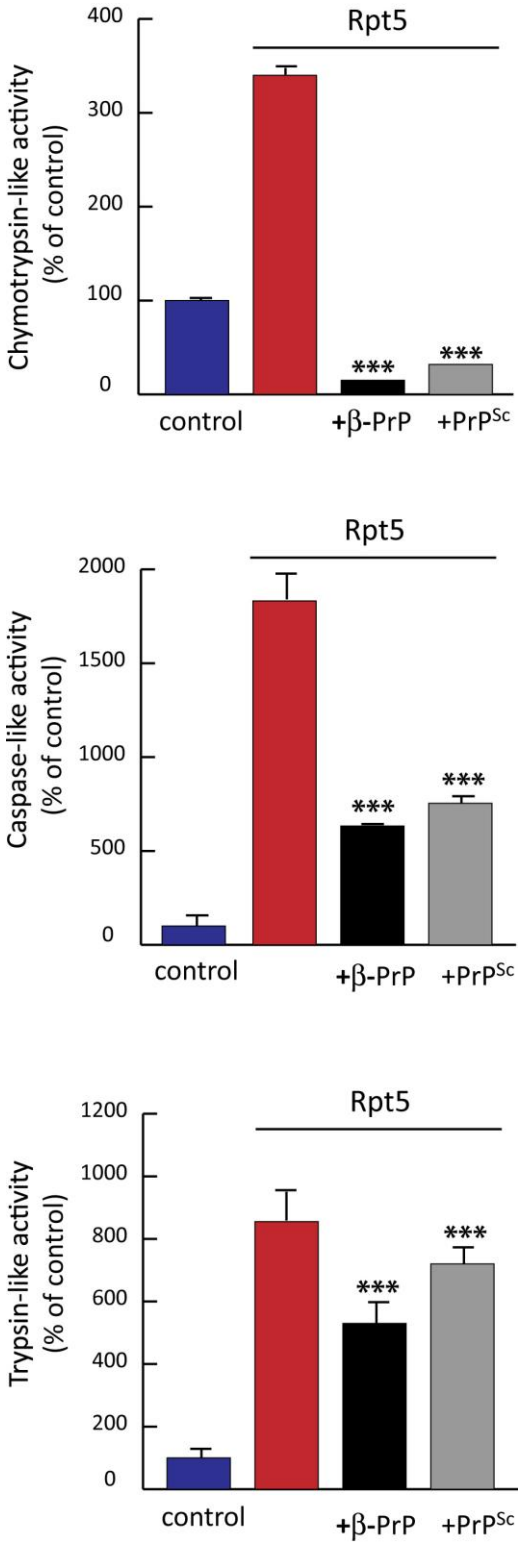

Figure 4.12 Rpt5-mediated human 20S proteasome activation is inhibited by β-sheet-rich PrP species-II

Pre-activating human 20S proteasome with CtRpt5 before the addition of the prion species prevents CtRpt5-mediated 20S activation. CtRpt5 (Rpt5; 250 μM) was added to pure human 20S proteasome (1 μg/ml) before incubation with the prion species (100 μg/ml) for 1 h. Peptidase activities were monitored using fluorogenic substrates specific for each activity: 100 μM Suc-LLVY-AMC (chymotrypsin-like) and 100 μM Ac-nLPnLD-AMC (caspase-like). Reaction buffer (**Section 2.4.2**) was the vehicle for the prion species and was added to 20S/Rpt5. Fluorescence was measured over time at 360 nm excitation and 465 nm emission. Data are means of three independent experiments + SEM. ***p<0.001 (versus untreated 20S/Rpt5 control).

4.4.7 Saturating the 20S inter-subunit pockets with CtRpt5 does not prevent the inhibitory effect of aggregated β-sheet-rich PrP isoforms on proteolytic activities

To investigate whether aggregated β-PrP and PrP^{Sc} were competing with the CtRpt5 peptide for the same inter-subunit pockets, 20S proteasome was saturated with high concentrations of CtRpt5 before incubating with PrP species. Both aggregated β-PrP and PrP^{Sc} inhibited the ability of CtRpt5 to activate the 20S proteasome, as evidenced by a lack of enhancement of its chymotrypsin-like activity, when the CtRpt5 peptide was present at a hundred fold molar excess over the prion species (**Figure 4.13**).

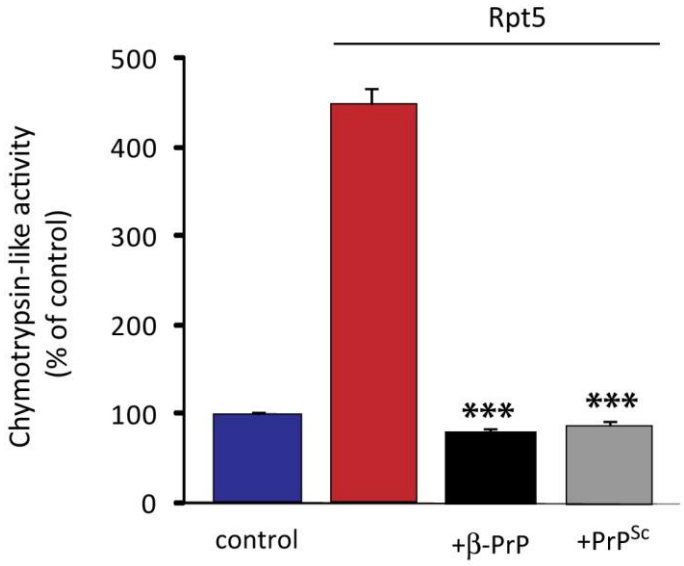

Figure 4.13 Saturating the inter-subunit pockets of the 20S α-ring does not prevent inhibition of CtRpt5-mediated 20S proteasome activation by the prion species

High concentrations of the CtRpt5 peptide do not abrogate the inhibitory effect of β-sheet-rich PrP isoforms on 20S activation. CtRpt5 (Rpt5; 500 μM) was added to pure human 20S proteasome (1 μg/ml) before incubation with the prion species (100 μg/ml) for 1 h. Chymotrypsin-like activity was monitored using 100 μM Suc-LLVY-AMC. Reaction buffer (**Section 2.4.2**) was the vehicle for the prion species and was added to 20S/Rpt5. Fluorescence was measured over time at 360 nm excitation and 465 nm emission. Data are means of three independent experiments + SEM. ***p<0.001 (versus untreated 20S/Rpt5 control).

4.4.8 The inhibitory effect on CtRpt5-mediated 20S activation is conformation specific

In order to confirm that the concentration of NaCl in the aggregated β-PrP preparation (15 mM in final reaction volume) was not inhibiting CtRp5-mediated 20S activation, NaCl was incubated with human 20S proteasome and the effect on the chymotrypsin-like activity of 20S/CtRpt5 was assessed. The addition of NaCl in the reaction mixture did not inhibit the ability of CtRpt5-mediated 20S activation, as evidenced by an increase in 20S chymotrypsin-like activity (**Figure 4.14**). Furthermore, in agreement with previous findings (**chapter 3**), proteasomes were only inhibited by a specific conformation of β-PrP and PrP^{Sc}, as neither heat-denatured β-PrP, denatured PrP^{Sc} nor thermally-aggregated α-PrP (a recombinant PrP mimetic of PrP^{C}) were inhibitory (**Figure 4.15**). Taken together, the CtRpt5 series of experiments suggest that the aggregated β-sheet-rich PrP isoforms may interact with the gate directly or bind to the same inter-subunit 'docking' pockets in the α-ring of the 20S and inactivate or block this action (Smith *et al.*, 2007; Rabl *et al.*, 2008; Gillette *et al.*, 2008).

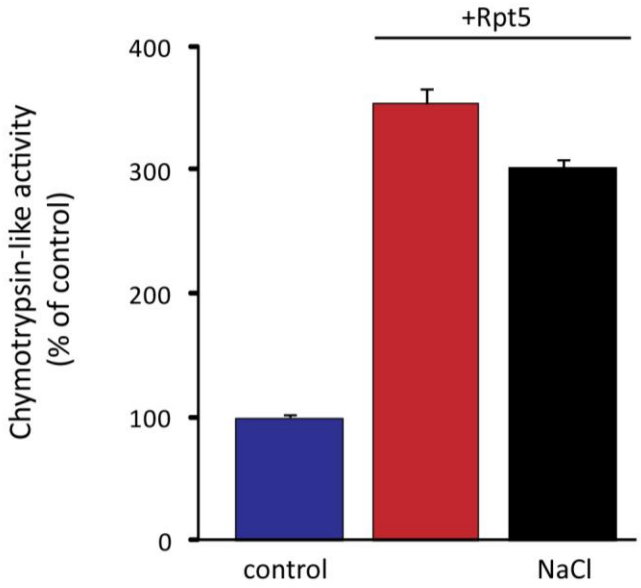

Figure 4.14 Effect of NaCl on CtRpt5-mediated 20S activation

CtRpt5-mediated 20S proteasome activation is not inhibited by treatment with NaCl. Pure human 20S proteasome (1 μg/ml) was incubated with CtRpt5 (Rpt5; 250 μM) and with 15 mM NaCl for 1h. Chymotrypsin-like activity was monitored using 100 μM Suc-LLVY-AMC. Reaction buffer (**Section 2.4.2**) was the vehicle for the proteins and was added to 20S/Rpt5. Fluorescence was measured over time at 360 nm excitation and 465 nm emission. Data are means of three independent experiments + SEM.

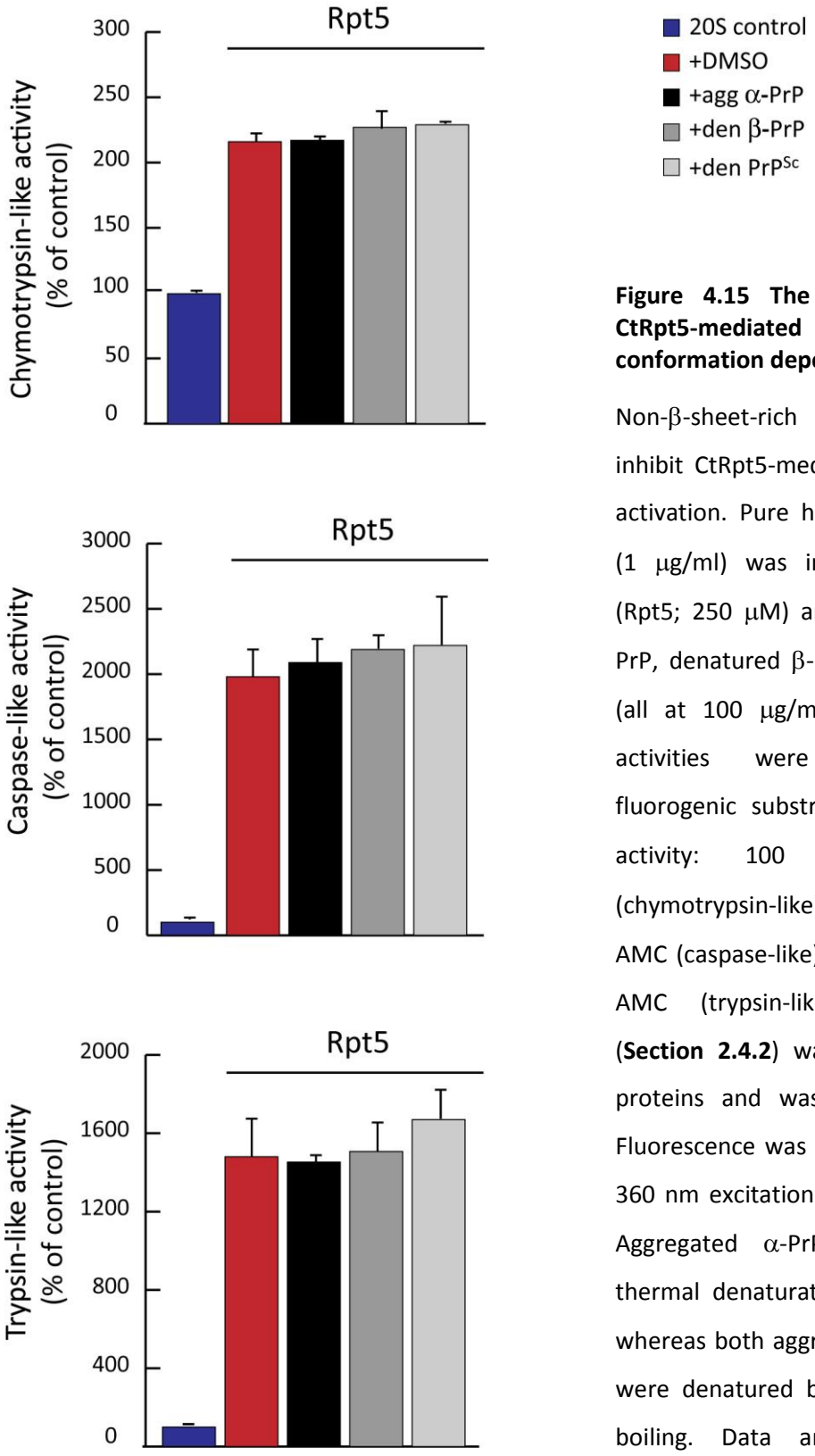

Figure 4.15 The inhibitory effect on CtRpt5-mediated 20S activation is conformation dependent

Non-β-sheet-rich PrP isoforms do not inhibit CtRpt5-mediated 20S proteasome activation. Pure human 20S proteasome (1 μg/ml) was incubated with CtRpt5 (Rpt5; 250 μM) and with aggregated α-PrP, denatured β-PrP or denatured PrP^{Sc} (all at 100 μg/ml) for 1 h. Peptidase activities were monitored using fluorogenic substrates specific for each activity: 100 μM Suc-LLVY-AMC (chymotrypsin-like), 100 μM Ac-nLPnLD-AMC (caspase-like) and 100 μM Boc-LRR-AMC (trypsin-like). Reaction buffer (**Section 2.4.2**) was the vehicle for the proteins and was added to 20S/Rpt5. Fluorescence was measured over time at 360 nm excitation and 465 nm emission. Aggregated α-PrP was obtained *via* thermal denaturation (10 min at 70 °C) whereas both aggregated β-PrP and PrP^{Sc} were denatured by 10 cycles of freeze-boiling. Data are means of three independent experiments + SEM.

4.4.9 UPS substrate protein accumulates in prion-infected mouse brain

Evidence for impairment of proteasomes and the UPS in prion-infected brains of transgenic mice expressing a short-lived reporter protein was presented in chapter 3 of this thesis (**Section 3.2.13**). In order to further document functional impairment of the UPS, IκB levels were assayed in prion-infected mouse brain. IκBα is an important substrate, which inhibits the activation of the transcription factor NF-κB, the transcription factor involved in many pathological and inflammatory responses, and potent inhibitor of apoptosis (Perkins and Gilmore, 2006).

IκBα levels are controlled *via* ubiquitination and degradation by the 26S (Palombella *et al.*, 1994). As IκB is rapidly degraded and accumulates with all known proteasome inhibitors, IκBα levels were therefore assayed in RML prion-infected mouse brain. The results shown in **Figure 4.16** reveal a significant accumulation of IκBα in RML prion-infected mouse brain compared to matched controls.

4.4.10 β-sheet-rich PrP isoforms inhibit the degradation of casein

To determine whether the proteolytic activity of the proteasome by aggregated β-sheet-rich PrP resulted in real functional impairment, the degradation of a model protein was studied. Casein is degraded in an ATP-dependent manner in the absence of ubiquitination (Kisselev *et al.*, 1999; Tarcsa *et al.*, 2000; Cascio *et al.*, 2001). Following the modification of casein by the fluorescent FIT2 group, it was used as a substrate in assays where WT yeast 20S had been pre-incubated with varying concentrations of aggregated β-PrP. Aggregated β-PrP significantly reduced the degradation of this fluorescently-labelled casein conjugate (**Figure 4.17**) and this inhibitory effect depended on the concentration of β-PrP. For reasons that are not clear, aggregated α-PrP, the recombinant mimetic of PrP^{C}, had a small effect on the FITC-casein degradation (**Figure 4.18**).

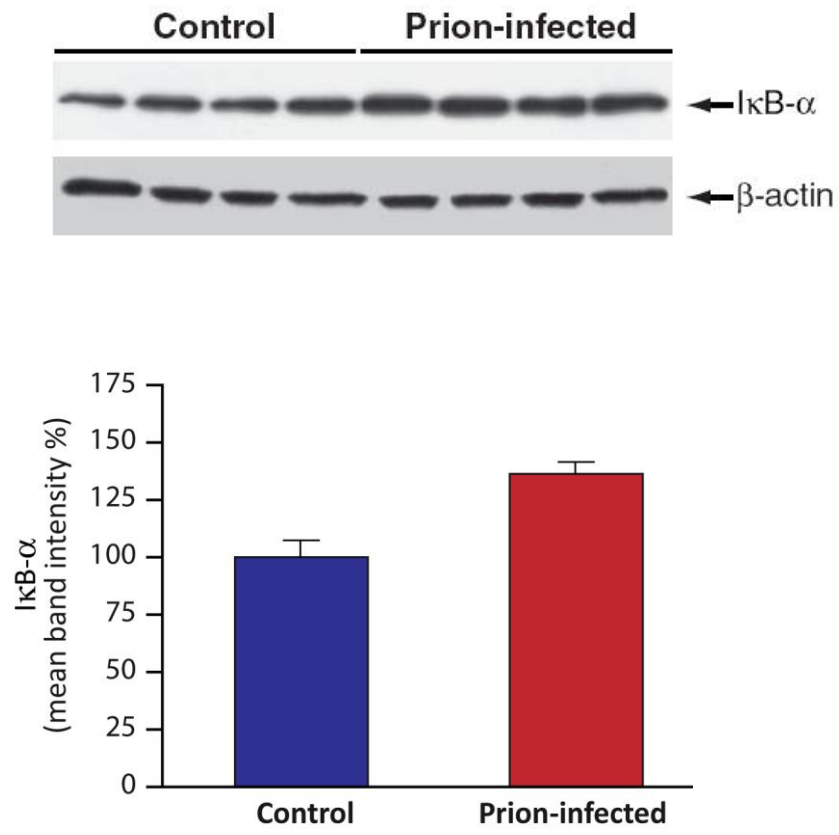

Figure 4.16 Accumulation of cellular UPS substrates occurs in prion disease *in vivo*

IκB-α levels are significantly increased in prion-infected mouse brain (RML) compared to control (CD-1). Four different CD-1 or RML mouse brains were homogenised and immunoblotted with an anti-IκB-α antibody. The graph represents the relative mean IκB-α band intensity relative to β-actin expression (p=0.0081). *This experiment was performed by Dr Mark Kristiansen, MRC Prion Unit, UCL Insitute of Neurology.*

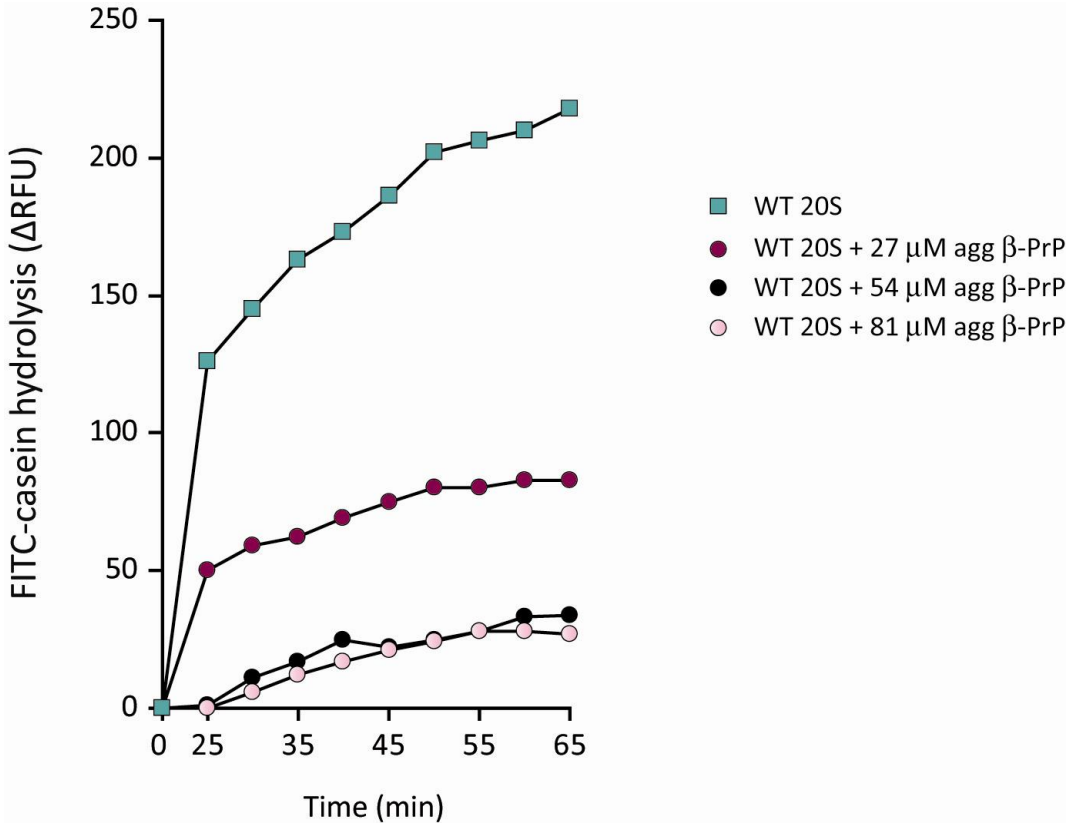

Figure 4.17 FITC-casein degradation by WT 20S is inhibited by aggregated β-PrP

The degradation rate of FITC-labelled casein by WT yeast 20S is significantly reduced in the presence of β-PrP. 20 μg of WT 20S was pre-incubated with 27, 54 or 81 μM aggregated β-PrP (agg β-PrP) for 1 h before addition of FITC-labelled casein as per manufacturer's instructions (**Section 2.4.5**). FITC-casein hydrolysis was measured by fluorimetry. Fluorescence was measured over time at 492 nm excitation and 535 nm emission. This experiment was performed at least three times with similar results. *This experiment was designed and analysed by myself, but was performed by Dr Kerri Kinghorn, MRC Prion Unit, UCL Insitute of Neurology.*

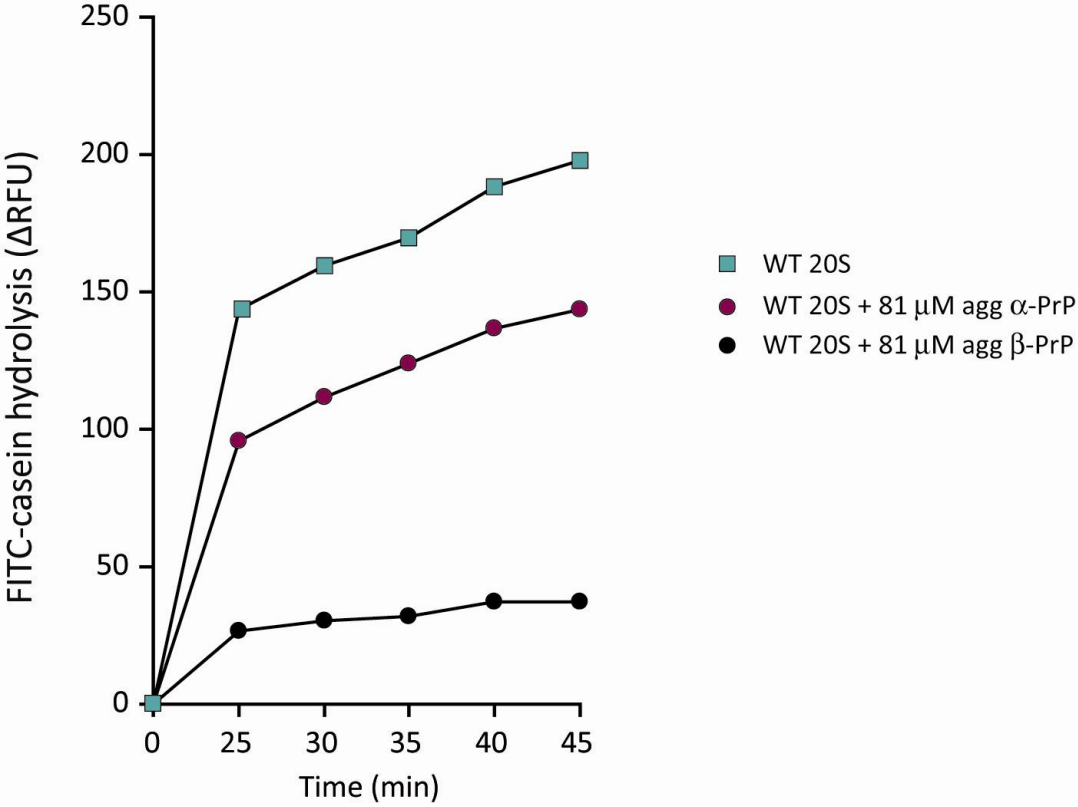

Figure 4.18 Aggregated α-PrP has a small inhibitory effect on FITC-casein degradation by WT 20S

The degradation rate of FITC-labelled casein by WT yeast 20S is significantly reduced in the presence of β-PrP, but not in the presence of α-PrP. 20 μg of WT 20S was pre-incubated with 81 μM aggregated α-PrP (agg α-PrP) or 81 μM aggregated β-PrP (agg β-PrP) for 1 h before addition of FITC-labelled casein as per manufacturer's instructions (**Section 2.4.5**). FITC-casein hydrolysis was measured by fluorimetry. Fluorescence was measured over time at 492 nm excitation and 535 nm emission. This experiment was performed at least three times with similar results. *This experiment was designed and analysed by myself, but was performed by Dr Kerri Kinghorn, MRC Prion Unit, UCL Insitute of Neurology.*

4.4.11 Aggregated β-PrP binds directly to human 20S

To ascertain whether aggregated β-PrP was directly interacting with the 20S particle, anti-PrP antibody-coated magnetic beads were used to co-immunoprecipitate the proteasome. Human 20S was incubated with either aggregated β-PrP, or heat-aggregated α-PrP or with reaction buffer (control), before incubation with anti-PrP coated beads. 20S subunits were precipitated in the presence of aggregated β-PrP (**Figure 4.18** lane 4). The nonpathogenic species protein, aggregated α-PrP, was not co-immunoprecipated with the 20S (lane 9). A small amount of 20S bound to the beads alone (lane 5), considerably less than with anti-PrP coated beads (lane 4). This result demonstrates a direct interaction between the β-sheet-rich PrP species and the 20S proteasome.

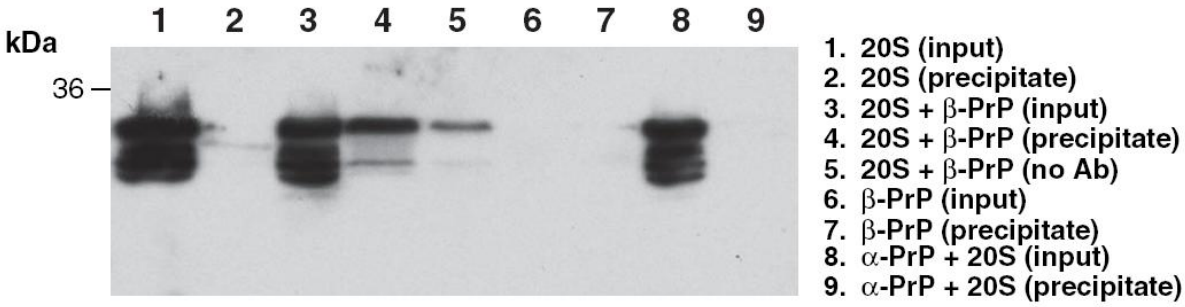

Figure 4.19 Aggregated β-PrP binds directly to 20S

Aggregated β-PrP and the 20S proteasome can be co-immunoprecipitated. Human 20S (5 μg) was incubated with aggregated β-PrP (3 μg) for 1 h at 37^{o}C and then co-immunoprecipitated using anti-PrP antibody-coated magnetic beads (ICSM18; 24 μg per reaction). The complex was visualized on SDS-PAGE by immunoblotting with an anti-20S antibody (1:1000). Aggregated β-PrP co-immunoprecipitates with the 20S (lane 4). The control protein, heat-aggregated α-helical PrP (3 μg), did not co-immunoprecipitate with the 20S (lane 9). 20S alone and aggregated β-PrP alone were used to demonstrate the specificities of the antibodies (lanes 2 and 7). The starting mixtures prior to incubation with the anti-PrP antibody-coated magnetic beads are also shown (input). The anti-20S antibody recognises the α_5/α_7, β_1, β_5, β_{5i} and β_7 proteasomal subunits, which run between 22 kDa (β_5) and ~30 kDa (all others). Ab= antibody.

4.5 Discussion

Oligomeric β-sheet-rich PrP isoforms have been shown to cause an impairment of protein degradation by the UPS in mouse brain and cultured neurones by inhibiting the function of the 26S proteasome (**chapter 3**). These prion protein species block cleavage of small peptides by the proteasome, but the exact mechanism by which these species block its activity was unclear. The aim of this study was to investigate the mechanism of inhibition of the UPS by prion species at the biochemical and molecular level. The present study has demonstrated that this inhibition by prion species occurs by a novel biochemical mechanism, in which the β-sheet-rich PrP isoforms impair the function of the 20S and 26S proteasomes by blocking gate-opening and substrate entry into the 20S core particle.

β-sheet-rich PrP species were shown to inhibit the hydrolysis of fluorogenic peptides by yeast and mammalian 20S, which can account for previous findings that oligomeric non-native PrP reduces their hydrolysis by human 26S (**chapter 3**). However, PrP species did not have an inhibitory effect on the peptidase activities of the open-gated yeast 20S mutant (Groll *et al.*, 2000), where peptides can freely enter the particle and are rapidly hydrolysed. In the 26S particle, the opening of this gated entry channel into the 20S is regulated by the 19S ATPases. In addition, several other regulatory factors (PA28, P200) are known to activate the proteasome by causing gate-opening. In the latent (non-activated) state, this gate is formed by the interactions of N-terminal tails of the seven α subunits (Groll *et al.*, 2000; Groll and Huber, 2003). Transient gate-opening occurs *in vivo* when the ATPases' C-termini cause a destabilization of these interactions or when other proteasome activators (PA28) maintain these N-termini in the open-conformation (Smith *et al.*, 2007; Rabl *et al.*, 2008). The N-terminus of the α3 subunit comprises the structural support for the gate (Groll *et al.*, 2000) and its deletion in the α3ΔN mutant proteasomes studied here prevents the formation of the closed-gate conformation and leaves the proteasome in a continually activated form. The inability of the aggregated β-sheet-rich PrP species to inhibit the open-gated α3ΔN mutant provides strong evidence that they act directly or indirectly to block gate-opening and to stabilize the closed conformation. By contrast, if the PrP species were able to traverse the 20S pore and to directly inhibit the

active sites, which are located in the central chamber of the 20S, the magnitude of the inhibition of peptide hydrolysis should be greater in the α3ΔN mutant 20S than in WT particles, exactly opposite to the present findings. The aggregated β-sheet-rich PrP species moderately inhibited the proteolytic activities of the α3/α7ΔN open-channel yeast 20S and 26S proteasome mutants (Bajorek *et al.*, 2003), but did so to a much lesser extent when compared to their WT counterparts. The deletion of the N-termini from two opposing α-subunits may act synergistically to relieve hindrance of protein entry into the 20S core and thus result in a wide-open pore (Bajorek *et al.*, 2003; Bajorek and Glickman, 2004), which may allow for the entry of some PrP molecules. Another observation consistent with an effect on gating was that the PrP aggregates, like treatments that cause gate-opening [e.g. the α3ΔN deletion (open-gated 20S) or treatment with SDS] or that favour the closed state (incubation with intracellular levels of KCl) caused larger changes in the hydrolysis of substrates of the chymotrypsin-like and caspase-like sites than of trypsin-like site (whose destruction is slower and not dependent on rate of entry). Together, these experiments indicate that pathogenic PrP aggregates inhibit proteasomes at the level of gate-opening rather than by affecting the active sites. This novel mechanism of inhibition thus contrasts sharply with that of the proteasome inhibitors widely used as research tools and in the clinic for treatment of hematological malignancies, all of which bind to the active sites in the central chamber, primarily the chymotrypsin-like site (Kisselev and Goldberg, 2001; Kisselev *et al.*, 2006).

There is growing evidence in several other protein-misfolding disorders that soluble protein aggregates, rather than large insoluble aggregates, are the toxic species causing neurodegenerative disease (Caughey and Lansbury, 2003; Haass and Selkoe, 2007). Models of subclinical prion disease (Hill and Collinge, 2003a) suggest that prion neurotoxicity may not be due to PrP^{Sc} *per se* but to the accumulation of a toxic oligomeric intermediate produced during prion conversion or breakdown of PrP^{Sc} (Collinge and Clarke, 2007). Accordingly, prion particles with very small masses (14-28 PrP molecules) appear to be the most efficient initiators of prion disease (Silveira *et al.*, 2005; Simoneau *et al.*, 2007). In the present experiments, incubation of WT yeast 20S with increasing

concentrations of aggregated β-PrP indicated that 90 to 180 nM of the β-sheet-rich PrP monomers was sufficient to maximally inhibit the chymotrypsin-like activity. This concentration corresponds to a molar ratio of between 10 and 20 PrP per 20S, and if the aggregates contain on the average 2-5 molecules of prion protein, then the marked inhibition of gating occurs with only a small molar excess of aggregates over 20S.

Structural studies of recombinant PrP have shown that its protease-resistant core can fold not only into amyloid fibrils, but also into β-sheet-rich oligomers (Baskakov *et al.*, 2002; Sokolowski *et al.*, 2003; Govaerts *et al.*, 2004). The size of such β-oligomers remains poorly defined, despite attempts to characterise their structure (Baskakov *et al.*, 2002; Martins *et al.*, 2006; Gerber *et al.*, 2007; Gerber *et al.*, 2008). It has been previously demonstrated that unlike aggregated β-sheet-rich PrP species, PrP amyloid fibrils did not inhibit the 26S proteasome (**chapter 3**). Moreover, pre-incubation of the β-sheet-rich PrP isoforms with an antibody raised against aggregation intermediates (Kayed *et al.*, 2003) abrogated their inhibitory effect on the 26S (**chapter 3**). The current observations also support the notion that the inhibitory species is small, although structural characterization at this stage is not possible due to the insoluble heterogeneous nature of PrP aggregates.

The inhibitory effect on the proteasomal peptidase activities was not merely due to the hydrophobic nature of the β-sheet-rich PrP species, *per se*, as no effect was seen with a hydrophobic unfolded protein, malate dehydrogenase (MDH). Unfolded MDH binds tightly to the mobile outer domains of the molecular chaperone complex of GroEL and GroES (Chen *et al.*, 1994; Ranson *et al.*, 1997). GroEL has two stacked heptameric subunit rings analogous to the 20S subunit rings (Hartl and Hayer-Hartl, 2002). Although hydrophobic and able to bind to GroEL with high affinity, unfolded MDH did not inhibit the peptidase activities of the proteasome.

To define further how PrP inhibits gate-opening, the effect of these aggregates on the capacity of the C-terminus of the 19S ATPase Rpt5 to cause 20S activation was investigated. The present findings demonstrate that PrP isoforms inhibit Rpt5-mediated 20S gating. In an ATP-driven reaction the 19S binds substrates, unfolds them, removes the poly-ubiquitin chain, and translocates the polypeptide into the 20S for degradation

(Pickart and Cohen, 2004). The C-termini of the 19S ATPases contain a conserved HbYX motif, which docks into the pockets between the adjacent α subunits of the 20S. Peptides seven residues or longer that correspond to these ATPases C-termini and also contain the HbYX motif, such as CtRpt5, dock into the same pockets and induce gate-opening (Smith *et al.*, 2007; Gillette *et al.*, 2008). When the ATPases bind a nucleotide, these C-termini function like a 'key in a lock' to open the gate. Cryo-electron microscopy of the PAN/20S complex indicates that the HbYX residues in PAN's C-termini interact with conserved residues in the 20S, triggering slight rotations of the α subunits that cause gate-opening (Rabl *et al.*, 2008). In the present experiments, inhibition of gate-opening was observed irrespective of whether the PrP species were added before or after 20S activation with CtRpt5. These peptides have relatively low affinities for the 20S inter-subunit pockets and thus under these *in vitro* conditions must be continually binding and dissociating leading to continual opening and closing of the gate. Three possible modes of action could account for these results: 1) the binding of the β-sheet-rich PrP species to the α-ring may block binding of the Rpt5 C-terminus to the inter-subunit pockets; 2) the prion aggregates may alter the structure of the α-ring, such that Rtp5 binding no longer leads to subunit rotation and gate-opening; 3) it may directly interact with the gating residues to favor the closed-gate conformation. Unfortunately, it is unclear whether the CtRpt5 peptide binds to a specific inter-subunit pocket in the α-ring. Some insight into possible binding sites for the ATPases' C-termini comes from archaebacterial 20S-PAN gate-opening studies (Rabl *et al.*, 2008). However, the eukaryotic 26S proteasome differs from the 20S-PAN complex in having seven different inter-subunit pockets and six different ATPases. Only three of the six 19S ATPases contain the HbYX motif (Smith *et al.*, 2007) and out of the seven inter-subunit pockets in the 20S α-ring (Groll *et al.*, 1997; Whitby *et al.*, 2000) only six contain the conserved Lys66, which is essential for gate-opening. Moreover, all inter-subunit pockets contain a hydrophobic residue in place of Leu81, one more residue essential for gate-opening. In the 26S, the C-termini of the different ATPase subunits probably bind into specific inter-subunit pockets and most likely occupancy of only one or a two key pockets is sufficient to cause gate-opening (Smith *et al.*, 2007; Rabl *et al.*, 2008; Gillette *et al.*,

2008). In agreement, cross-linking studies of CtRpt2 and CtRpt5 peptides to the 20S proteasome have revealed different binding locations for the two different ATPases (Gillette *et al.*, 2008).

Complete unfolding of polypeptides is a pre-requisite for entry through the pore of the proteasome (Wenzel and Baumeister, 1995). For example, EM studies have shown that when the insulin B-chain, which is otherwise easily degraded by the proteasome, is attached to a 2 nm wide Nanogold™ particle it cannot pass through the 20S opening and sits at the center of the α-ring (Wenzel and Baumeister, 1995). Also, when a substrate of the archaebacterial 20S-PAN ATPase complex is linked to a very large avidin molecule, so that it can't be translocated through the narrow pores in the ATPase and the 20S, it becomes a dominant inhibitor preventing the degradation of other substrates (Navon and Goldberg, 2001). Similarly, the aggregated β-sheet-rich PrP species could be acting like a 'plug'; i.e. a dominant inhibitor that prevents peptide entry into the 20S. Such PrP aggregates by associating with the outer ring of the 20S may also block the association of the 19S ATPase C-termini with the inter-subunit pockets on the α-ring, thereby inhibiting 26S assembly and protein degradation. Interestingly, it was recently reported that a conditional *Psmc1* (Rpt2) knock-out mouse shows not only 26S proteasomal dysfunction but also ubiquitin-positive inclusions and neurodegeneration (Bedford *et al.*, 2008). As all six ATPases are functionally non-redundant, deletion of Rpt2 prevents formation of the hexameric ring in the base of the 19S thereby disrupting 26S assembly, gate-opening and protein degradation (Bedford *et al.*, 2008). Presumably the PrP aggregates by inhibiting Rpt5-mediated 20S activation could be neurotoxic *via* similar mechanisms (Bedford *et al.*, 2008).

Data presented in chapter 3 indicate a large impairment of protein degradation by the UPS in prion-infected cells and mouse brain, such as the accumulation of ubiquitinated proteins and of the model substrate, Ub^{G76V}-GFP (Dantuma *et al.*, 2000; Lindsten *et al.*, 2003), which is rapidly degraded by the proteasome after ubiquitination by the UFD pathway. To define this further at the biochemical level the degradation of casein, a model UPS substrate protein, which is a useful measure of protease activity was studied.

By directly monitoring the degradation of fluorescently labeled casein conjugate, the present data demonstrate that aggregated β-PrP functionally impairs 20S-mediated degradation of FITC-linked casein.

One critical consequence of proteasome inhibition in cells is a failure to degrade the key inhibitor of the inflammatory response, IκBα. In many disease states, it is rapidly degraded by the proteasome following its phosphorylation and ubiquitination (Palombella *et al.*, 1994; Alkalay *et al.*, 1995). The increased levels of IκB in prion-infected mouse brain shown here provide further evidence for a general inhibition of proteasomal function. Normally, IκB prevents the activation of the transcription factor NF-κB (Alkalay *et al.*, 1995), and its level falls due to rapid proteolysis in many different pathophysiological processes including neurodegeneration (Mattson and Camandola, 2001). If gating in the 20S particle is inhibited, a vast number of critical short-lived proteins that regulate fundamental cellular processes are likely to accumulate and this accumulation of key proteins destined for degradation by the UPS would impair neuronal function and may contribute to prion neurotoxicity *in vivo*. In this regard, the accumulation of IκB by preventing activation of NF-κB should be particularly important, since NF-κB is critical in prolonging viability (i.e. inhibiting apoptosis) and inducing host (immune) defence mechanisms. These data also support the biochemical evidence of functional impairment of degradation of a model protein *in vitro* (i.e. FITC-casein). The UPS is involved in the turnover of a vast number of critical proteins participating in fundamental biological processes such as cell growth, cell differentiation, apoptosis and inflammation (Goldberg, 2003). Consequently, accumulation of ubiquitinated substrates destined for degradation by the UPS would impair cellular function and contribute to prion neurotoxicity *in vivo*.

Inhibition of proteasomal function has often been proposed as a mechanism contributing to neurodegenerative disease (Goldberg, 2003). However, direct evidence for such an inhibition or a specific mechanism has been generally lacking. The various observations presented here together demonstrate that prions can act at the level of the 20S gate, leading to functional impairment of its degradative capacity. The co-immunoprecipitation studies demonstrate that there is a direct and stable interaction

between aggregated β-PrP and the 20S proteasome. The inhibitory species binding to this site is likely to be small, in view of the relatively low stoichiometry, and the previous finding that an antibody raised against aggregation intermediates can abrogate the inhibitory effect of prions on the 26S (**chapter 3**). These findings serve as a model for understanding the more general unanswered question in the field of neurodegenerative diseases as to how misfolded β-sheet-rich proteins impair UPS function. The present findings may therefore have relevance for understanding the pathogenesis of other neurodegenerative diseases that are also characterized by the accumulation of β-sheet-rich proteins. Such aggregates may act similarly to aggregated prion protein to prevent gate-opening and function as a dominant inhibitors of protein degradation, which is essential for cellular homeostasis and viability.

4.6 Summary

Pathogenesis in prion disease is associated with the conversion of mainly α-helical PrP^{C} to a β-sheet dominant isoform (PrP^{Sc}) and previous studies suggest a role for the UPS in prion disease pathogenesis. Data presented here demonstrate a novel mechanism of proteasome inhibition by aggregated β-sheet-rich prion protein (PrP) *via* an effect on gate-opening in the 20S particle. Direct binding of low concentrations of PrP is sufficient to inhibit the proteasome. Incubation with other hydrophobic proteins or PrP in other conformational states had little effect, demonstrating that inhibition is specific and depends on sequence, conformation and aggregation state. Moreover, β-sheet-rich PrP isoforms cause functional impairment of proteasome-mediated protein degradation and lead to accumulation of a key UPS substrate in prion-infected mouse brain. Findings presented here suggest a mechanism for proteasome inhibition that may be relevant to other diseases characterized by accumulation of misfolded β-sheet-rich proteins.

5 AUTOPHAGY AND CLEARANCE OF DISEASE-ASSOCIATED PRION PROTEIN

5.1 Background

Dysfunction of either of the two principal intracellular protein-degradation pathways, UPS and autophagy, may contribute to the pathology of various neurodegenerative disorders (Rubinsztein, 2006; Kundu and Thompson, 2008). Recent studies have suggested a clear role for UPS dysfunction in the pathogenesis of prion disease, whereby mild proteasome impairment invokes a neurotoxic mechanism involving the intracellular formation of cytosolic PrP^{Sc} aggresomes that trigger caspase-dependent neuronal apoptosis (Kristiansen *et al.*, 2005). Furthermore, data presented in chapters 3 and 4 of this thesis demonstrate that aggregated β-sheet-rich PrP isoforms inhibit the 26S proteasome by blocking gate-opening in the 20S particle, and thereby interfere with substrate accessibility to the proteolytic chamber.

In contrast to the UPS, which predominantly degrades short-lived cytosolic and nuclear proteins, autophagy can degrade much larger substrates, including protein aggregates and whole organelles (Kundu and Thompson, 2008). Although autophagy occurs at basal levels during growth and development, it can be induced under physiological stress conditions; increased numbers of autophagosomes have been observed in a range of neurological diseases as well as after neuronal injury (Rubinsztein *et al.*, 2005; Kundu and Thompson, 2008; Mizushima *et al.*, 2008). However, it is not always clear whether this accumulation is due to increased autophagy or reduced autophagosome-lysosome fusion, and the precise relationship between autophagy and neuronal cell death remains unclear. All published studies to date have demonstrated autophagy to have a neuroprotective role in the context of disease (Kundu and Thompson, 2008; McCray and Taylor, 2008). Furthermore, two studies published in Nature showed that the KO of two Atg genes, *Atg5* and *Atg7*, which are essential for autophagy, causes early postnatal lethality in mice (Komatsu *et al.*, 2006; Hara *et al.*, 2006). Even in the absence of the expression of aggregate-prone proteins, autophagy defects, specifically in

the neurones of these mice, resulted in the formation of intracellular inclusions in the brain and development of neurodegenerative symptoms (Komatsu *et al.*, 2006; Hara *et al.*, 2006).

Ultra-structural studies demonstrating the presence of autophagic vacuoles in the cortical neurones of scrapie and CJD rodent experimental models (Boellaard *et al.*, 1989; Boellaard *et al.*, 1991; Liberski *et al.*, 1992a), as well as in naturally-occurring BSE (Liberski *et al.*, 1992b), have suggested a role for autophagy in prion disease. These autophagic vacuoles have been shown to be accompanied by increased membrane proliferation and sequestering of neuronal cytoplasm (Liberski *et al.*, 2002). Human prion diseases (Sikorska *et al.*, 2004) and experimental models of BSE (Jeffrey *et al.*, 1992b) and scrapie (Sikorska *et al.*, 2007) have demonstrated such vacuoles throughout the neuronal cell, but especially at synaptic endings. This suggests a possible link between autophagosome formation and synaptic dysregulation in prion disease and *in vivo* evidence has shown that autophagic vacuoles are closely associated with the protein product encoded by scrapie-responsive gene (Scrg)1 (Dron *et al.*, 2005). This gene's transcript is markedly increased in a variety of prion diseases (Dandoy-Dron *et al.*, 1998; Dron *et al.*, 1998; Dandoy-Dron *et al.*, 2000). Whether increases in autophagosome numbers by PrP^{Sc} formation correlates with enhanced autophagy or delayed autophagosome clearance, and how this relates to prion disease pathogenesis, remains unclear. However, autophagy may have an important role in the normal degradation of PrP^{Sc} in prion-infected cells, as suggested by reports of the use of the tyrosine kinase inhibitor, immatinib mesylate (also known as ST1571 or Gleevec), to induce lysosomal degradation of cellular PrP^{Sc} (Ertmer *et al.*, 2004). Ertmer *et al.*, have recently suggested that this probably occurs *via* autophagy as lysosomal inhibition increases basal levels of PrP^{Sc} (Ertmer *et al.*, 2007).

5.1.1 Aims

The aims of this study were to correlate markers of autophagosome formation with prion infection and to evaluate the role of autophagy in prion disease pathogenesis, both *in vitro* and *in vivo*.

5.1.2 Methods

Western blotting was used for the detection of LC3I and LC3II protein levels in cell lysates and brain homogenates (**Section 2.2.1**). Following RNA extraction and cDNA synthesis, SYBR Green reverse transcriptase real-time PCR was undertaken to assess *beclin1*, *Atg12L* and *Atg16L* mRNA levels in uninfected and prion-infected mouse GT-1 cells (**Section 2.6**). The scrapie cell assay (SCA) was used to monitor PrP^{Sc} clearance after treatment with an autophagy inducer (**Section 2.1.3**). The LDH assay was used to monitor amelioration or exacerbation of cell death following treatment with proteasome inhibitors and autophagy inducers/inhibitors (**Section 2.5.1**). Experiments were performed in collaboration with Mrs Christine Butler-Cole, MRC Prion Unit, UCL Institute of Neurology.

5.2 Results

5.2.1 Enhanced LC3II levels in prion-infected GT-1 cells

It has been difficult to differentiate autophagosomes from other vesicles in the absence of specific markers. The identification of LC3II, which is associated with mammalian autophagosomes simplified this problem (Kabeya *et al.*, 2000). LC3 lipidation is measured on a Western blot, and may reflect either enhanced autophagosome formation due to increases in autophagic activity, or to a reduced autophagosome turnover (Klionsky *et al.*, 2008). Autophagic flux can be measured by inferring LC3II turnover by Western blot in the presence and absence of lysosomal degradation, which can be achieved by using drugs such as bafilomycin A_1 that alter the lysosomal pH (Fass *et al.*, 2006).

In order to investigate whether prion infection affects autophagy flux, LC3II levels were assessed in uninfected and prion-infected GT-1 cells, in the presence or absence of bafilomycin. Mouse hypothalamic neuronal GT-1 were infected with 0.1 % RML prion-infected mouse brain homogenate. Uninfected or RML-infected GT-1 cells (ScGT-1) were treated with bafilomycin. Furthermore, to investigate autophagy flux following proteasome inhibition, lactacystin, a proteasome inhibitor, was used in the presence or absence of bafilomycin in prion-infected GT-1 (ScGT-1) and uninfected GT-1 cells. LC3I and LC3II levels were measured by Western blot (**Figure 5.1**).

The use of bafilomycin demonstrates that LC3II levels, which correlate with autophagosome numbers, were significantly enhanced in the prion-infected GT-1 (ScGT-1) cells compared to uninfected controls (**Figure 5.1; lanes 8 and 4 respectively**). ScGT-1 cells treated with lactacystin and bafilomycin showed increased LC3II levels compared to uninfected GT-1 cells (**Figure 5.1; lanes 7 and 3 respectively**). Conversely, prion-infected (ScGT-1) cells that were not bafilomycin-treated showed lower LC3II levels compared to controls (**Figure 5.1; lanes 5 and 1 respectively).** This was mirrored in the lactacystin-treated prion-infected cells compared to uninfected GT-1 cells (**Figure 5.1; lanes 6 and 2 respectively**).

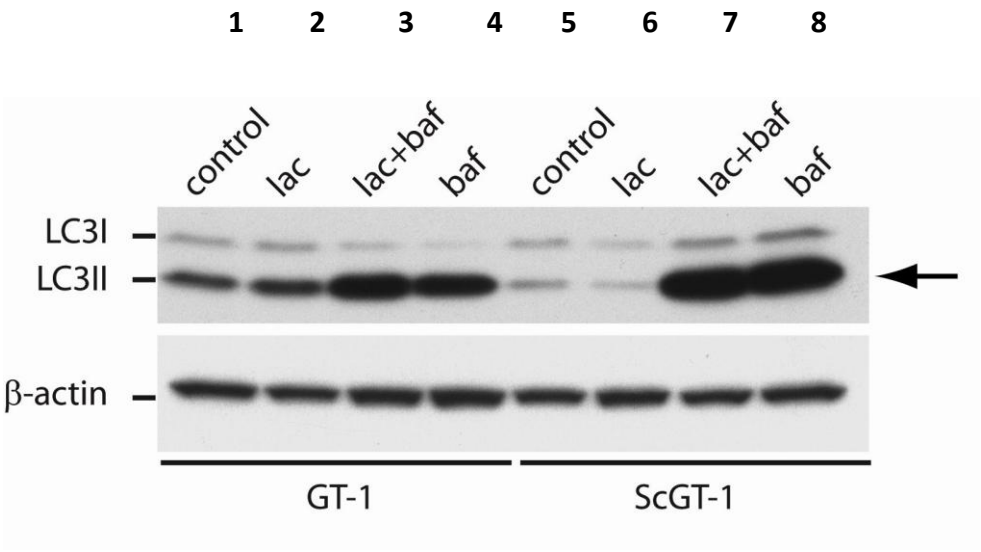

Figure 5.1 Up-regulation of the autophagosome marker LC3II in prion-infected GT1 cells

RML-infected ScGT-1 and control uninfected GT-1 cells were treated with 1 μM lactacystin (LAC) and/or 100 nM bafilomycin (BAF) for 24 h. Levels of LC3II and LC3I were assessed by Western blotting using an anti-LC3 antibody (1:1000; Novus Biologicals). The use of bafilomycin clearly demonstrates that levels of LC3II, correlating to autophagosome numbers, are significantly increased in prion-infected cells. 30 μg of total protein from cell lysates were loaded per lane. Levels of an endogenous mouse protein, β-actin, were assessed by immunoblotting to confirm equal protein loading. Image is representative of two independent experiments.

5.2.2 Up-regulation of *Atg* gene transcript markers in prion-infected cells when the proteasome is inhibited

Mild proteasome inhibition in prion-infected neuronal cells has been shown to result in the formation of large, cytosolic PrP^{Sc}-containing aggresomes (Kristiansen *et al.*, 2005). The autophagy-lysosomal system relies on the expression of over twenty essential autophagy-related genes (*Atg*), which are responsible for the formation of the autophagosomal membrane in eukaryotes (Reggiori, 2006). In order to investigate a putative induction of autophagy as a response to proteasome inhibition and aggresome formation in prion-disease, mRNA transcript levels of three *Atg* genes essential for autophagosome formation were measured.

GT-1 cells were either mock-infected with CD-1 mouse brain homogenate, or infected with RML prions. Both mock-infected (GT-1) and RML prion-infected (ScGT-1) cells were treated with the proteasome inhibitor lactacystin for 24 h. Following RNA isolation, cDNA was synthesised in the presence of reverse transcriptase and mRNA transcript levels were detected using the SYBR Green PCR system. **Figure 5.2** shows that *beclin1*, *Atg12L* and *Atg16L* mRNA transcripts are significantly enhanced in prion-infected (ScGT-1) cells compared to controls (GT-1), suggesting that autophagy is up-regulated in response to proteasome inhibition and aggresome formation.

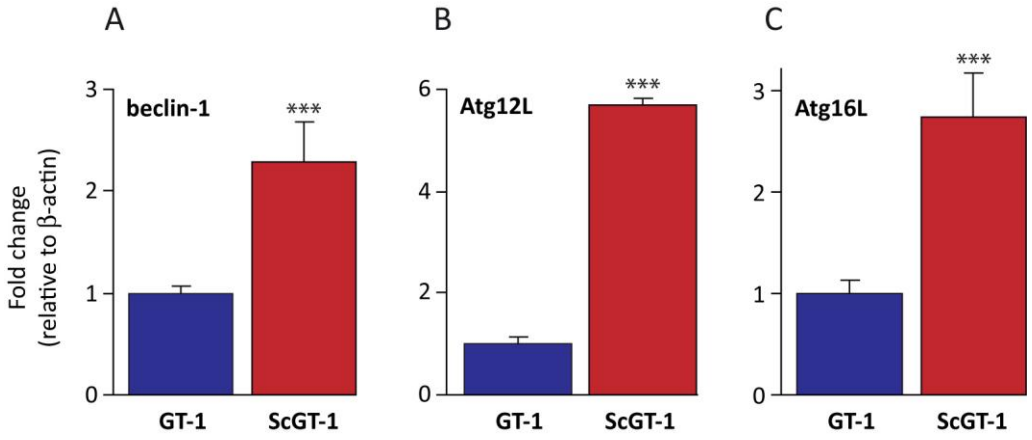

Figure 5.2 Up-regulation of *Atg* genes in prion-infected cells

Mock-infected and RML prion-infected GT-1 cells (ScGT-1) were treated with 1 μM lactacystin for 24 h, following which levels of the mRNA transcripts for (**A**) *beclin1*, (**B**) *Atg12L* and (**C**) *Atg16L* were assessed by real-time SYBR-green quantitative RT-PCR. Each gene is significantly up-regulated in prion-infected cells compared to uninfected controls. Values expressed relative to the expression of β-actin. Data are the mean + SEM of five independent samples. ***p <0.001 (versus uninfected controls).

5.2.3 Induction of autophagy partially rescues prion-infected cells from cell death when the proteasome is inhibited

Following proteasome inhibition prion-infected cells have been shown to form PrP^{Sc}-containing aggresomes, which in turn trigger caspase 3 and 8 activation leading to cell death (Kristiansen *et al.*, 2005). Rapamycin, a lipophilic antibiotic has been demonstrated to induce autophagy by inactivating the mammalian target of rapamycin (mTOR), and as such serves as an autophagy enhancer (Berger *et al.*, 2006). Several studies have shown that rapamycin has protective effects in cell and animal models of neurodegenerative diseases such as polyQ and AD (Sarkar *et al.*, 2009). Therefore, it was interesting to test *in vitro* if induction of autophagy, by means of rapamycin treatment, ameliorates the cell death observed in prion-infected cells when the proteasome is challenged by the proteasome inhibitor lactacystin.

Both uninfected (GT-1 and N2aPK-1) and prion-infected (ScGT-1 and ScN2aPK-1) cells were treated with a low concentration of lactacystin for 24 h, in the presence or absence of rapamycin. LDH assays, which are used to measure cell death, showed that prion-infected cells (ScGT-1 and ScN2aPK-1) displayed significant levels of cell death following lactacystin treatment compared to uninfected controls (**Figures 5.3 and 5.4**), in agreement with previous findings (Kristiansen *et al.*, 2005). However, in the concomitant presence of rapamycin, ScGT-1 (**Figure 5.3**) and ScN2aPK-1 (**Figure 5.4**) cells were partially rescued from the deleterious effects of the proteasome inhibitor, suggesting that, in part, autophagy could be conferring a compensatory degradative mechanism in these cells.

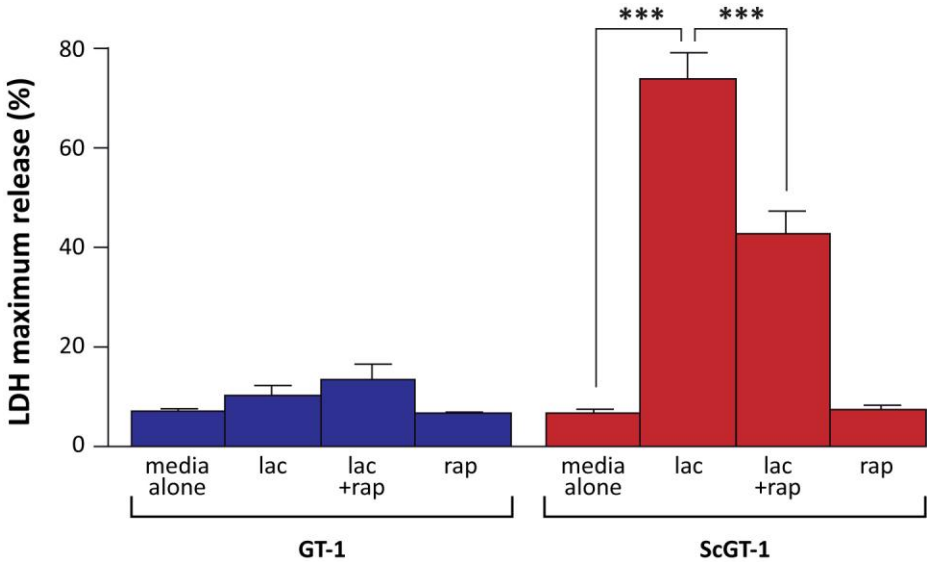

Figure 5.3 Induction of autophagy partially rescues prion-infected GT-1 cells from cell death

RML-infected ScGT-1 and control uninfected GT-1 cells were treated with 1 µM lactacystin and/or 0.2 µM rapamycin to induce autophagy for 24 h. Rapamycin significantly reduces prion-induced cytotoxicity in cells in which the proteasome is mildly impaired. Values are expressed as percentage LDH release relative to maximal cell death obtained from lysing untreated cells with 1 % (v/v) Triton X-100. Data are the mean + SEM of eight independent samples. ****P* <0.001.

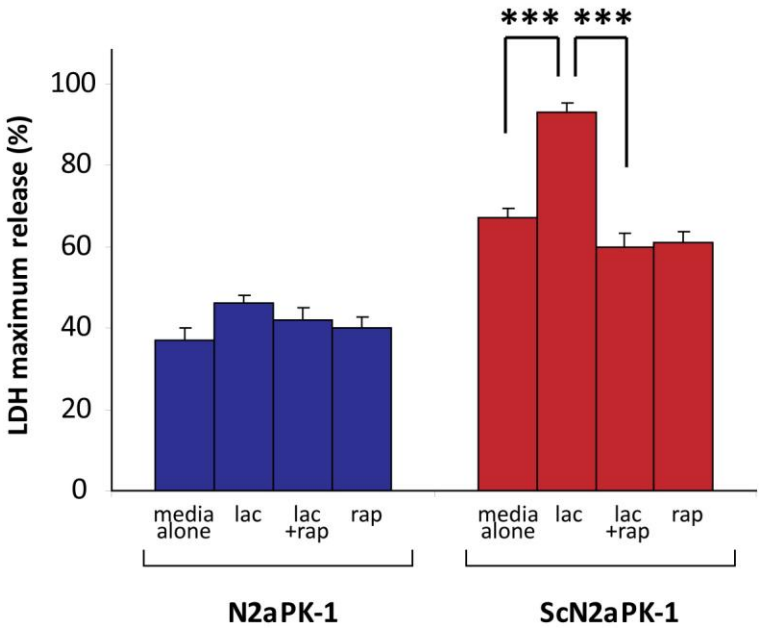

Figure 5.4 Induction of autophagy partially rescues prion-infected N2aPK-1 cells from cell death

RML prion-infected N2aPK-1 and control uninfected N2aPK-1 cells were treated with 1 µM lactacystin and/or 0.2 µM rapamycin to induce autophagy for 24 h. Rapamycin significantly reduces prion-induced cytotoxicity in cells in which the proteasome is mildly impaired. Values are expressed as percentage LDH release relative to maximal cell death obtained from lysing untreated cells with 1 % (v/v) Triton X-100. Data are the mean + SEM of eight independent samples. ****P* <0.001.

5.2.4 Inhibition of autophagy exacerbates cell death in prion-infected cells

3-methyladenine (3-MA) inhibits the sequestration stage of autophagy, where a double membraned structure, the autophagosome, forms around a portion of the cytosol (Klionsky and Ohsumi, 1999). 3-MA was used to further investigate a role for autophagy in prion disease.

Both uninfected (GT-1 and N2aPK-1) and prion-infected (ScGT-1 and ScN2aPK-1) cells were treated with 3-MA for 24 h. LDH assays, which are used to measure cell death, showed that both uninfected (GT-1 and N2APK-1) and prion-infected (ScGT-1 and ScN2aPK-1) cells displayed significant levels of cell death following 3-MA treatment (**Figures 5.5 and 5.6**). However, ScGT-1 (**Figure 5.5**) and ScN2aPK-1 (**Figure 5.6**) were less able to tolerate the 3-MA treatment compared to uninfected controls (GT-1 and N2aPK-1). Cell death in cells cured of prion-infection, by means of treatment with an anti-PrP antibody (ICSM18; ScGT-18 and ScN2aPK-1-18), was similar to that of uninfected controls. Together these results suggest that autophagy could have some importance in PrP^{Sc} clearance and thereby cell viability.

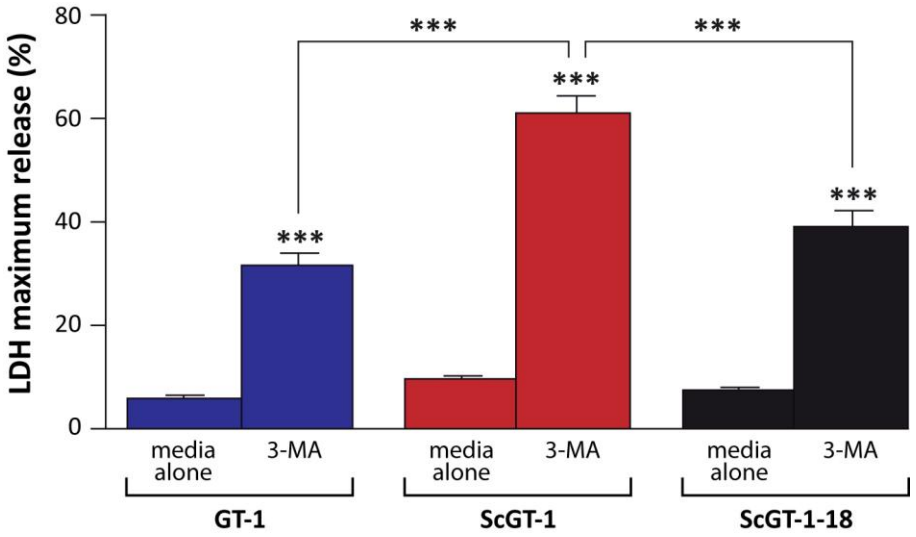

Figure 5.5 Autophagy inhibition exacerbates cell death in prion-infected GT-1 cells

RML-infected ScGT-1 and control uninfected GT-1 cells were treated with or without 10 mM 3-MA to inhibit autophagy. 3-MA significantly induces cell death in both uninfected (GT-1) and prion-infected (ScGT-1) cells, however there is significantly more cell death observed in ScGT-1 cells compared to controls. In cells cured of prion infection (ScGT-1-18), by treatment with an anti-PrP antibody (ICSM18), cell death is restored to levels seen in uninfected (GT-1) cells. Values are expressed as percentage LDH release relative to maximal cell death obtained from lysing untreated cells with 1 % (v/v) Triton X-100. Data are the mean + SEM of eight independent samples. ***P <0.001. *This experiment was designed by myself, but was performed and analysed by Mrs Christine Butler-Cole, MRC Prion Unit, UCL Institute of Neurology.*

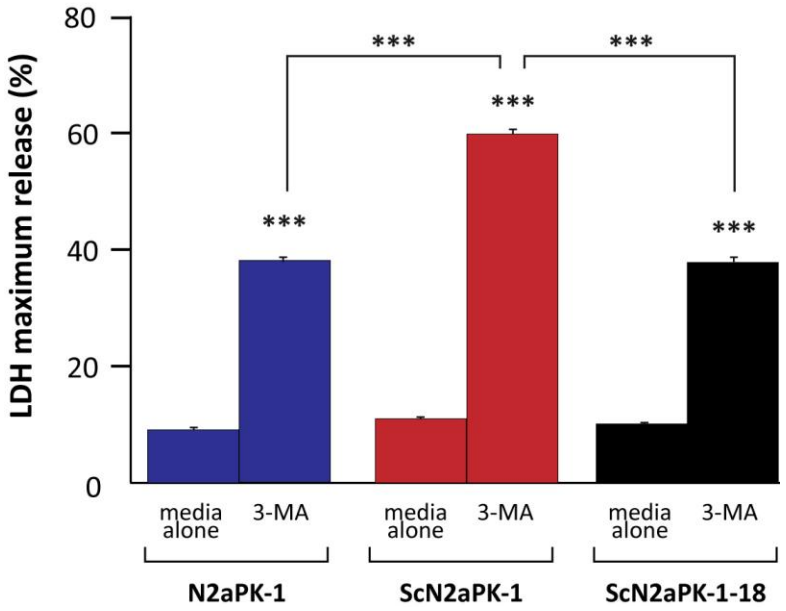

Figure 5.6 Autophagy inhibition exacerbates cell death in prion-infected N2aPK-1 cells

RML-infected ScN2aPK-1 and control uninfected N2aPK-1 cells were treated with or without 10 mM 3-MA to inhibit autophagy. 3-MA significantly induces cell death in both uninfected (N2aPK-1) and prion-infected (ScN2aPK-1) cells, however there is significantly more cell death observed in ScN2aPK-1 cells compared to controls. In cells cured of prion infection (N2aPK-1-18), by treatment with an anti-PrP antibody (ICSM18), cell death is restored to levels seen in uninfected (N2aPK-1) cells. Values are expressed as percentage LDH release relative to maximal cell death obtained from lysing untreated cells with 1 % (v/v) Triton X-100. Data are the mean + SEM of >eight independent samples. ***P <0.001. *This experiment was designed by myself, but was performed and analysed by Mrs Christine Butler-Cole, MRC Prion Unit, UCL Institute of Neurology.*

5.2.5 Induction of autophagy clears PrP^{Sc} from prion-infected cells

In vitro studies, by use of pharmacological means to induce or inhibit autophagy, have demonstrated that certain neurodegenerative disease-causing proteins are degraded by autophagy (Ravikumar *et al.*, 2002; Webb *et al.*, 2003). Furthermore, the tyrosine kinase inhibitor immatinib has been shown to induce the cellular clearance of prion-infected cells from PrP^{Sc} by activating its lysosomal degradation (Ertmer *et al.*, 2004; Ertmer *et al.*, 2007).

To test the role of autophagy on PrP^{Sc} clearance in prion-infected neuronal cells (ScGT-1 and ScN2aPK-1), they were induced for 24 h, by means of 0.2 μM rapamycin treatment. Following this, the scrapie cell assay (SCA) was used to calculate the percentage of PrP^{Sc}-positive spots in the prion-infected (ScGT-1 and ScN2aPK-1) and in uninfected cells (GT-1 and N2aPK-1), which were used as negative controls. All cell lines were plated at 5000 cells per well in a 96 well plate.

Rapamycin increased clearance of PrP^{Sc} in both ScN2aPK-1 and ScGT-1 cells (**Figure 5.7 A and B**). Rapamycin-treated ScN2aPK-1 cells had 50% less PrP^{Sc}-positive spots compared to untreated ScN2aPK-1 cells (**Figure 5.7 A**). ScGT-1 cells treated with rapamycin also showed a decrease in PrP^{Sc}-positive spot number (30% less than untreated ScGT-1) (**Figure 5.7 B**). These results suggest that inducing autophagy allows for some PrP^{Sc} clearance in prion-infected cells.

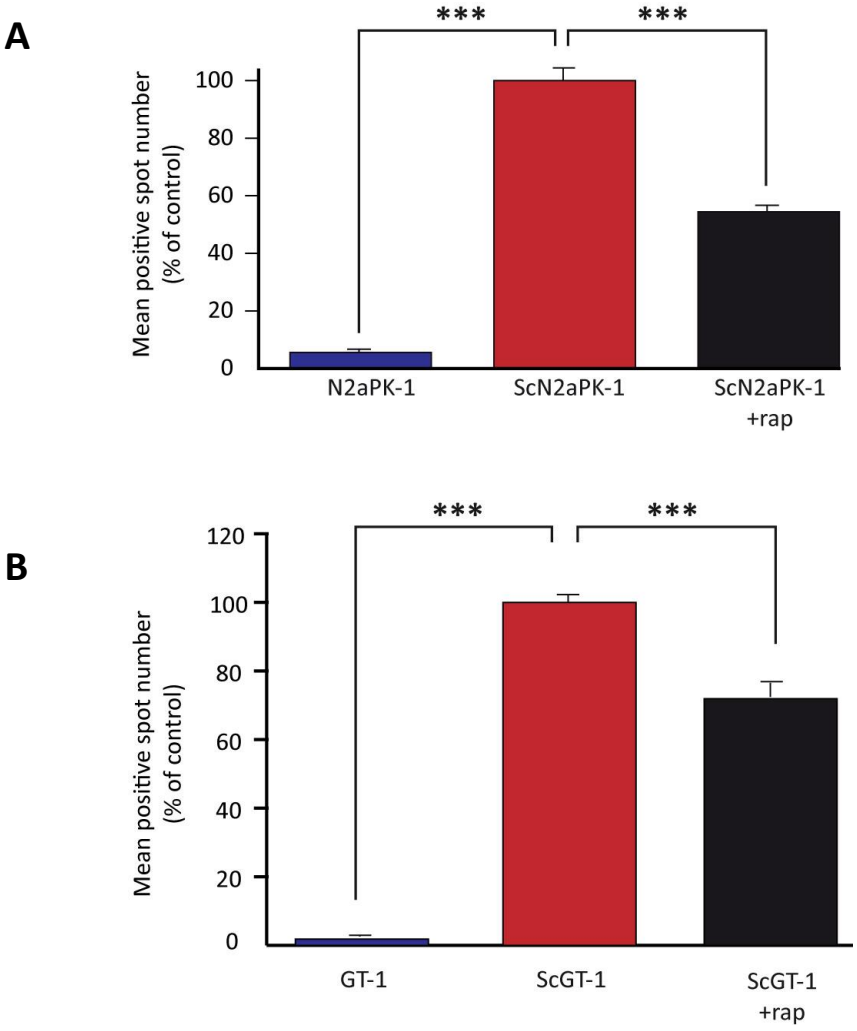

Figure 5.7 Induction of autophagy clears PrP^{Sc} from prion-infected cells

RML prion-infected ScN2aPK-1 (**A**) or ScGT-1 (**B**) and were treated with 0.2 µM rapamycin for 24 h. PrP^{Sc} levels were measured by the SCA assay. 5000 cells were plated in individual wells of 96 well plates. Values are expressed as the number of PrP^{Sc}-positive cells compared to control (**A**-N2aPK-1 and **B**-GT-1). Data are the mean + SEM of 8 independent samples. ****P* <0.001 as compared to controls. *These experiments were designed, performed and analysed by myself, apart from **B** which was performed and analysed by Mrs Christine Butler-Cole, MRC Prion Unit, UCL Institute of Neurology.*

5.2.6 Up-regulation of LC3II *in vivo* in prion-infected mouse brain

Levels of LC3II on a Western blot correspond to autophagosome numbers and can be used to assess autophagy flux (Tanida *et al.*, 2005). **Figure 5.1** shows that bafilomycin-treated prion-infected cells have higher levels of LC3II compared to bafilomycin-treated uninfected controls, suggesting that prion infection results in an increased autophagy flux. In order to investigate whether this also occurred *in vivo*, LC3II levels were measured by Western blotting using an anti-LC3 antibody. Four FVB and four RML-infected FVB mouse brains (both groups at end-stage disease) were homogenised and run on SDS-PAGE. LC3II levels, which correlate with autophagosome numbers, were higher in RML-infected FVB mice compared to uninfected control mouse brains (**Figure 5.8; arrow**).

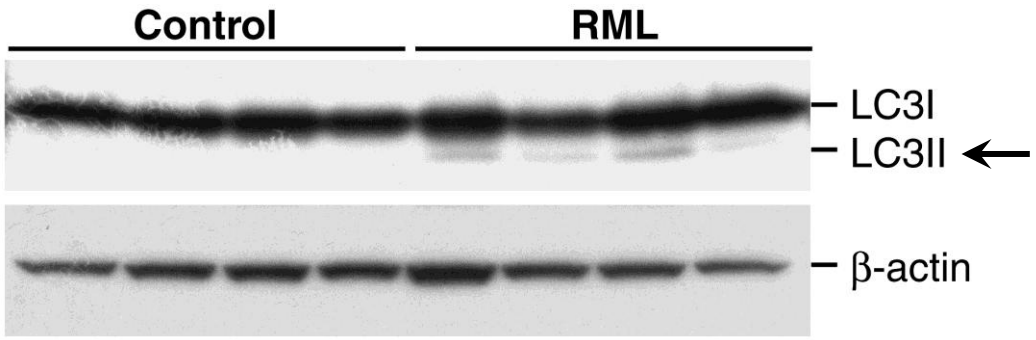

Figure 5.8 Up-regulation of LC3II *in vivo* in prion-infected FVB mouse brain

FVB mice were inoculated with RML or control-infected CD-1 mouse homogenate and culled at end-stage clinical disease. Brain tissue was then homogenised and analysed for the presence of LC3II by immunoblotting using an anti-LC3 antibody (1:1000; Novus Biologicals). Image shows results for four individual mice in each group and demonstrates that LC3II levels are increased in the brains of RML-prion-infected FVB mice (arrow). Levels of an endogenous mouse protein, β-actin, were assessed by immunoblotting to confirm equal protein loading.

5.3 Discussion

Accumulation of misfolded protein deposits in affected brain regions is a characteristic feature of many neurodegenerative diseases, suggesting a failure in the cell's degradative capacity. Experimental evidence suggests that neuronal death may be associated with UPS impairment, although whether this is a cause or consequence of neurodegeneration is still unclear. UPS impairment is thought to be important in prion disease (Ma and Lindquist, 2002; Ma *et al.*, 2002; Kang *et al.*, 2004; Kristiansen *et al.*, 2005), also evidenced by data presented in chapters 3 and 4 of this thesis. In contrast, the role, if any, of the alternative major protein degradation pathway, autophagy, in prion disease is still unclear as data to date are confined to a few electron-microscopy papers (Liberski *et al.*, 1989; Liberski *et al.*, 1992a; Liberski *et al.*, 2005). Autophagosome-like structures have been described using EM (Kopnika *et al.*, 2008), however biochemical evidence for a role in prion pathogenesis is lacking. The aim of this study was to investigate the role of autophagy in prion-mediated neurodegeneration by biochemical analysis. Results presented in this chapter indicate that autophagy, by measurement of LC3II levels, is up-regulated in prion-infected cells and *in vivo* at end-stage disease. Furthermore, data presented here show that interference with autophagy by pharmacological induction or inhibition, alters levels of PrP^{Sc} and cell viability patterns in prion-infected cells where the UPS is inhibited. An up-regulation of three key *Atg* genes, which are required for autophagosome formation, was also demonstrated.

Autophagy involves the delivery of cytoplasmic cargo randomly sequestered inside double-membraned vesicles, or autophagosomes, to the lysosome (**Figure 5.9**). Under normal conditions, autophagy occurs at low basal levels to perform homeostatic functions. Autophagy can be readily enhanced during stress, such as during birth or nutrient starvation, or when pharmacologically manipulated (**Figure 5.9**). There are various methods for monitoring autophagy (Klionsky *et al.*, 2008), however as the molecular mechanisms regulating this process are not fully understood at present, there are a number of limitations in interpreting results (Klionsky *et al.*, 2008).

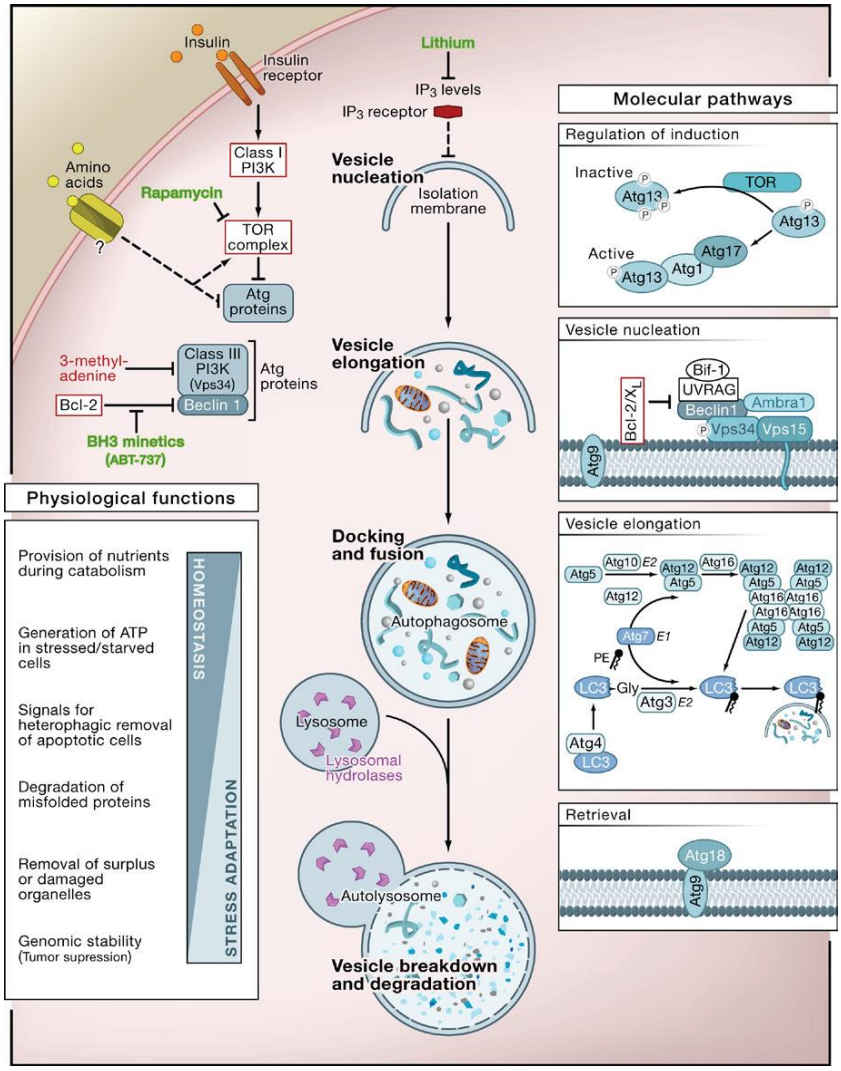

Figure 5.9 The cellular, molecular and physiological aspects of autophagy[15]

The cellular events during autophagy follow distinct stages: vesicle nucleation (formation of the isolation membrane/phagofore), vesicle elongation and completion (growth and closure), fusion of the double-membraned autophagosome with the lysosome to form an autolysosome, and lysis of the autophagosome inner membrane and breakdown of its contents inside the autolysosome. This process occurs at a basal level and is regulated by numerous different signalling pathways. Shown here are only the regulatory pathways that have been targeted pharmacologically for experimental or clinical purposes. Inhibitors and activators of autophagy are shown in red and green, respectively. At the molecular level, Atg proteins form different complexes that function in distinct stages of autophagy. Shown here are the complexes that have been identified in mammalian cells, with the exception of Atg13 and Atg17 that have only identified in yeast. Shown here are functions revealed by in vivo studies of mice that cannot undergo autophagy.

[15] Reprinted from Cell, Vol 132, Levine, B., and Kroemer, G., Autophagy in the pathogenesis of disease, pp 27-42, © 2008, with permission from Elsevier.

For example, increased levels of the autophagosomal marker LC3II may reflect enhanced autophagosome formation due to a) increases in autophagic activity, or b) to reduced turnover of autophagosomes by fusion with lysosomes. In particular, enhanced LC3II levels are not a measure of autophagic flux *per se*, which includes the final step of cargo delivery to lysosomes. Autophagic flux is measured by analysing LC3II levels by Western blot (Tanida *et al.*, 2005) in the absence of lysosomal fusion and degradation. The use of bafilomycin, which prevents lysosomal degradation, and which resulted in enhanced LC3II levels in prion-infected cells, suggests that prion infection leads to increased autophagic flux. In sharp contrast, steady-state measurement of autophagosome formation, by inferring LC3II levels in the absence of bafilomycin, showed less LC3II in prion-infected cells compared to uninfected controls. This infers that increased LC3II levels as a marker of increased autophagic flux are matched by increased degradation *via* rapid lysosomal turnover. Therefore, LC3II turnover in the presence of bafilomycin is more relevant when investigating the role of autophagy in any system (Klionsky *et al.*, 2008).

At present there are no ideal methods to monitor autophagic flux *in vivo* or in organs. Some of the most useful methods include GFP-LC3 analysis, morphological detection of autophagosomes using fluorescence or electron microscopy, and immunohistochemical staining, however *in vivo* analyses have proven relatively complex (Klionsky *et al.*, 2008). Data here shows that there are enhanced LC3II levels in prion-infected, end-stage mouse brains, indicating increased autophagosome numbers. To obtain autophagy flux data *in vivo* it would be necessary to include a bafilomycin treatment regime. However, the ability of bafilomycin to cross the blood-brain barrier is still unknown. Furthermore, in order to obtain flux data a time course would also need to be included to follow changes in substrate accumulation (including LC3II). Such a time course would also test whether induction of autophagy is an early or late phenomenon in prion disease.

Mild proteasome inhibition in prion-infected neuronal cells leads to PrP^{Sc}-aggresome formation, caspase 3 and 8 activation and subsequent apoptosis (Kristiansen *et al.*, 2005). Experiments were carried out to determine whether inducing autophagy conferred neuroprotection in prion-infected cells when the proteasome is inhibited. Co-

treatment with rapamycin and the proteasome inhibitor lactacystin resulted in a partial rescue of cell death in prion-infected cells. Conversely, inhibition of autophagy by 3-MA exacerbated cell death. These results suggest that autophagy could be acting as a compensatory degradative mechanism when the UPS is impaired in prion-infected cells. Indeed, proteasome inhibition has been demonstrated to lead to the accumulation of various critical molecules that need to be tightly regulated, such as p53, and is toxic (Chen *et al.*, 2005). In addition, global proteasome inhibition may lead to intra-cellular aggregate formation (Rideout *et al.*, 2001). More recently it was shown that proteasome inhibition is toxic to *Drosophila* eyes, as illustrated by retinal degeneration, and that this can be rescued by induction of autophagy, by means of rapamycin treatment or *HDAC6* over-expression (Pandey *et al.*, 2007). HDAC6 is a microtubule- and dynein-associated protein; microtubules and dynein are both involved in autophagosome transport for lysosomal delivery (Rubinsztein, 2006). Pandey *et al.* suggested that HDAC6 is an essential link between the two degradation pathways, rescuing toxicity caused by UPS inhibition by providing an alternative route for substrate clearance (autophagy). Further work is needed in the prion cell model used here to elucidate whether HDAC6 also functions as a mechanistic link between prion-induced proteasome inhibition and an up-regulation of autophagy, leading to the partial rescue of the deleterious phenotype. Data presented in this chapter are also in agreement with studies in other neurodegenerative diseases characterised by the accumulation of aggregation-prone proteins, in which rapamycin treatment has been shown to attenuate toxicity (Ravikumar *et al.*, 2002; Webb *et al.*, 2003; Ravikumar *et al.*, 2004; Berger *et al.*, 2006). Rapamycin may therefore be beneficial in prion disease and could be used as a potential therapeutic. Indeed, a rapamycin analogue, CCI-779, has been shown to improve performance in various behavioural tasks and decrease aggregate formation in a mouse model of HD (Ravikumar *et al.*, 2004).

Stimulation of autophagy resulted in some clearance of PrP^{Sc} in prion-infected neuronal cell lines. This result suggests that PrP^{Sc}, is at least in part, degraded by autophagy. This is in agreement with previously published studies, where the use of the tyrosine kinase inhibitor immatinib, which was subsequently shown to be an inducer of autophagy, activated the lysosomal degradation of PrP^{Sc} in prion-infected cells in a time-

and dose-dependent manner (Ertmer *et al.*, 2004). Prion-infected GT-1 (ScGT-1) and N2a (ScN2a) cells were both almost equally sensitive to the autophagy inducer, with PrP^{Sc} levels undetectable following 3 days of immatinib treatment (Ertmer *et al.*, 2004). The current data confirm these observations in that an inducer of autophagy results in PrP^{Sc} clearance. However, the data presented here indicate that prion-infected N2aPK-1 (ScN2aPK-1) and GT-1 (ScGT-1) cells display slightly different sensitivities to the autophagy inducer rapamycin in terms of the amount of PrP^{Sc} cleared. This could be due to signalling differences between the two cell lines, as well as due to differences in protein composition in either cell line. However, there are several other possible explanations for this. First, this study used a different autophagy inducer, namely rapamycin instead of immatinib. Rapamycin acts by inactivating the mTOR (Noda and Ohsumi, 1998), which normally inhibits autophagy, and although the details of this regulatory mechanism are still unclear, the mode of autophagy induction is different to that of immatinib (Ertmer *et al.*, 2007). Second, the method of quantification of PrP^{Sc} levels in the previous study depended on Western blot analysis for PK-resistant PrP, whereas in this study the much more sensitive SCA was used (Klohn *et al.*, 2003). This may be the reason why the present data shows clearance of PrP^{Sc} in cells in as little as 24 h post-autophagy induction, as compared to day 2 of drug treatment. Finally, the differences can also be attributed to the cell lines used, for example Ertmer *et al.* used N2a cells, whereas this study used N2aPK-1 cells, which propagate prions more readily.

Autophagy induction is sometimes accompanied by enhanced mRNA levels of some autophagy genes, such as *Atg12L* (Kouroku *et al.*, 2007). The present study showed that three key *Atg* genes, *beclin1*, *Atg12L* and *Atg16L*, were significantly up-regulated in prion-infected cells when the proteasome was inhibited. This finding supports the experiments described above, and further suggests that autophagy could be induced as a compensatory mechanism when the proteasome is inhibited. However, it is not clear whether changes in mRNA transcripts are sufficient to induce autophagy, and therefore such measurements alone are not sufficient. Additional follow-up of protein levels would be necessary, as that is the definitive readout with respect to initiation and completion of autophagy (Klionsky *et al.*, 2008).

Autophagy probably acts to clear monomeric and oligomeric precursors of aggregates, rather than the aggregates themselves. In support of this, no study has yet reported inclusions that are membrane-bound and the size of inclusions is often much larger than mammalian autophagosomes (Rubinsztein *et al.*, 2005). Chapters 3 and 4 suggest that small, oligomeric β-sheet-rich PrP isoforms inhibit the proteolytic activities of the 26S proteasome by blocking gate-opening in the 20S particle and subsequent substrate accessibility. Furthermore, the most infectious PrP molecules has been shown to have very small masses (14-28) (Silveira *et al.*, 2005; Simoneau *et al.*, 2007). Therefore, further work is required to elucidate whether induction of autophagy in prion disease allows for the partial rescue of the deleterious phenotype (conferred by proteasome inhibition) (Kristiansen *et al.*, 2005) by clearing PrP^{Sc}-aggresomes themselves, or by clearing small oligomeric precursors of PrP^{Sc}. This could be achieved by treating cells with rapamycin or 3-MA, after treatment with proteasome inhibitors, and conducting immunofluorescence studies to check for alterations in the presence of PrP^{Sc}-aggresomes. If autophagy is neuroprotective by clearing PrP^{Sc}-aggresomes themselves, then rapamycin treatment should reduce their number. On the other hand, if inhibition of autophagy results in increased numbers of PrP^{Sc}-aggresomes, then this would suggest that normally autophagy could be clearing some of the small PrP precursors that are sequestered into PrP^{Sc}-aggresomes. Under normal circumstances autophagy could be reducing the amount of PrP precursors available for the formation of PrP^{Sc}-aggresomes and thereby conferring some level of neuroprotection.

The key questions concerning autophagy in neurodegenerative disease remain unanswered. It remains unclear as to whether autophagosome numbers increase due to enhanced autophagy or decreased autophagosome clearance, and of course whether autophagy is beneficial or not. These questions will most probably be answered when the molecular aspects of mammalian autophagy are better understood, which would provide valuable tools in answering these questions in prion disease and other clinical conditions characterised by protein misfolding.

5.4 Summary

Results presented in this chapter show that autophagosome numbers appear to increase in prion-infected cells. Furthermore, induction of autophagy by use of rapamycin is able to rescue cells from the deleterious effects of proteasome inhibition, implying a degree of compensation between the two protein degradation pathways. Moreover, transcripts of markers of early autophagosome formation, including the tumour-suppressor gene *beclin1* and components of the Atg12-Atg5-Atg16L ubiquitin-like conjugation system are rapidly up-regulated in prion-infected neuronal cells, and levels of LC3II, a membrane marker of mature autophagosomes, are similarly elevated. Induction of autophagy is able to clear cellular PrP^{Sc} from infected cells. Finally, it was also shown that autophagosome formation is elevated *in vivo* at end-stage prion disease. Taken together, these data demonstrate that autophagy is up-regulated in prion disease and suggest a mechanistic insight into interactions between the major protein degradation pathways during prion-mediated cellular neurotoxicity.

6 CONCLUSIONS AND FUTURE WORK

6.1 Thesis summary and conclusions

The work presented in this thesis aimed to investigate the cellular mechanisms involved in prion-mediated neurodegeneration. Specifically, it aimed to define the role of the two major degradation systems, namely the UPS and autophagy, in prion disease pathogenesis. Studies have previously suggested a role for the UPS in prion disease (Ma *et al.*, 2002; Kang *et al.*, 2004; Kristiansen *et al.*, 2005), whereas the role of autophagy in prion disease pathogenesis is not well characterised.

Work presented here indicates that β-sheet-rich PrP molecules specifically inhibit the proteolytic β subunits of the 26S proteasome *via* a novel inhibitory effect on gate-opening and subsequent substrate entry into the 20S proteolytic core. This effect was demonstrated in purified proteasome incubated with recombinant β-sheet-rich PrP and with semi-purified PrP^{Sc} (from prion-infected cells and/or mouse brain), as well as in scrapie-infected cell lines. The inhibitory effect was only seen when PrP was in a non-native, β-sheet conformation, as other amyloidogenic proteins and recombinant α-helix-dominant PrP were not inhibitory. Only aggregated β-sheet-rich PrP directly binds to the 20S proteasome, but not aggregated α-helix-dominant PrP, further suggesting the inhibitory effect depends on conformation. Pre-incubation with an antibody raised against aggregation intermediates abrogated the inhibitory effect, consistent with an oligomeric species mediating this effect. Indeed, assaying various molar concentrations of aggregated, recombinant β-sheet-rich PrP, where calculations are based on the monomeric protein, show that half-maximal inhibition of the proteasome occurs when there are 10 to 20 PrP molecules present. Inhibition of the proteasome so that it can no longer degrade proteins, such as casein and IκB shown here, indicates functional impairment of the UPS. Therefore, considering the wide range of physiological functions the UPS is involved in, UPS inhibition can be deleterious. A direct relationship between prion neuropathology and UPS impairment was demonstrated in scrapie-infected proteasome-reporter mice. Autophagy was also shown to be induced in prion disease,

both *in vitro* and *in vivo*, and to ameliorate cell death associated with proteasome inhibition by clearing some PrP^{Sc}, suggesting it acts as a compensatory mechanism following UPS inhibition.

The pathogenesis of prion disease is likely to be multifactorial, but the potent inhibition of the proteasome by pathogenic PrP, by blocking gate-opening in the 20S particle, is likely to result in neuronal perturbation and contribute to the widespread neuronal loss. Data presented here also help explain how cytosolic PrP^{c} may accumulate in the cytosol, with UPS inhibition leading to cytosolic accumulation of PrP^{C} destined for ERAD (Ma and Lindquist, 2002). Impairment of the UPS leads to cellular dysfunction and apoptosis through various mechanisms (Goldberg, 2003). Induction of autophagy may help clear some disease-related PrP, and by doing so will slightly decrease UPS burden and ameliorate the deleterious phenotype linked to proteasome inhibition. However, the key feature of prion disease, the autocatalytic conversion of PrP^{C} to PrP^{Sc}, will form a positive feedback loop by inhibiting the UPS, thereby further reducing the rate of clearance of PrP^{Sc} and thus stimulating the formation of more PrP^{Sc}, until the levels of proteasome function are too low for cell survival. A key question that arises is whether the findings described here are relevant to other neurodegenerative diseases where protein misfolding occurs, or a unique property to prion diseases.

6.2 Suggestions for future work

6.2.1 Development of model cell system to study PrP^{Sc} trafficking

At present, cellular PrP^{Sc} trafficking is poorly understood, as studies are hindered by the lack of PrP^{Sc}-specific antibodies. Research suggests PrP^{Sc} localisation at the plasma membrane and in the endolysosomal compartment (Caughey and Raymond, 1991; Arnold *et al.*, 1995), whereas the site of conversion of PrP^{C} to PrP^{Sc} remains controversial (Campana *et al.*, 2005). Once PrP^{Sc} is formed, it has been shown to accumulate on the cell surface, lysosomes and autophagosomes (Caughey and Baron, 2006). The work presented in this thesis indicates that aggregated, β-sheet-rich PrP molecules inhibit the UPS. However, it is unclear how PrP^{Sc} may travel to the cytoplasm and interact with the UPS.

Studies with WT and mutant PrP^C forms have suggested that it is retro-translocated from the ER (Ma and Lindquist, 2001; Yedidia *et al.*, 2001). Another possibility comprises destabilisation of endolysosomal membranes and leakage into the cytosol, as shown for $A\beta_{1-42}$ (Ji *et al.*, 2006). The accumulation of PrP^{Sc} in the endolysosomal system could be causing UPS dysfunction and imposing an increased burden on the degradative pathway. To answer many of these questions and try to establish the exact details of PrP^{Sc} trafficking, PrP^C could be tagged with a GFP construct. Although this method would, in principle, allow for tracking the formation of newly-converted PrP^{Sc} and its cellular trafficking, the major drawback however, is the size of the GFP tag. It is quite possible that the attachment of such a big protein, approximately 28 kDa, to PrP^C will probably block the conversion of PrP^C to PrP^{Sc}. Indeed, several groups have failed to demonstrate successful prion propagation using GFP-PrP^C constructs (Negro *et al.*, 2001; Ivanova *et al.*, 2001; Lee *et al.*, 2001b; Lorenz *et al.*, 2002; Hachiya *et al.*, 2004). Conversely, Bian *et al.* have been able to show compromised prion replication in transgenic mice using GFP-tagged PrP, but with the mice manifesting atypical neuropathology and increased disease onset, and the tagged PrP lacking the full spectrum of PrP^{Sc}-associated biochemical properties (Bian *et al.*, 2006). Therefore, alternative detection methods, such as by use of c-myc or FLAG tags, would be the preferential means by which to study prion protein trafficking. In fact, FLAG-tagged PrP constructs have been successfully used in transgenic mice in the past, without loss of prion propagation (Telling *et al.*, 1997). Accordingly, the expression of a c-myc- or FLAG-tagged PrP construct in KO neuroblastoma cells, alongside the use of anti c-myc or anti-FLAG antibodies, can track *de novo* PrP^{Sc} production. Once this system is established, antibodies to various cellular compartments can be used to define PrP^{Sc} localisation and trafficking. Furthermore, a time-course study may also be undertaken to track intracellular PrP^{Sc} at serial time-points following UPS inhibition (by low dose of proteasome inhibitor) to assess its route into the cytosol to form PrP^{Sc} aggresomes (Kristiansen *et al.*, 2005).

6.2.2 Development of a human cell model to study the UPS in the context of human prion disease

Cell models of prion disease are in principle good systems in which to study and analyse prion propagation as well as potential therapeutic targets. Such models are now as sensitive as bioassays and can replace the latter in some instances (Bosque and Prusiner, 2000; Klohn *et al.*, 2003). Nonetheless, research into PrP^{Sc} cell biology is hindered by the sparse number of cell lines able to propagate PrP^{Sc}. Prion-propagating cell lines to date include rat PC12 cells (Rubenstein *et al.*, 1984), murine N2a cells (Butler *et al.*, 1988) and murine GT-1 cells (Schatzl *et al.*, 1997) and these are susceptible to mouse-adapted, hamster-adapted, or sheep scrapie strains. However, at present there is no known cell line documented to propagate human prions. The development of such a cell line, particularly of neuronal origin, is critical to facilitate studies on the pathophysiology of human prion diseases, which currently rely on the use of transgenic mice. The use of animal models is both time-consuming (incubation time of prion disease) and costly. Furthermore, mouse models do not always represent the optimal system, for example when studying mechanisms at the molecular and cellular level. One possible way to propagate human prions into cells would be to use a human neural stem cell line. Stem cells from human foetal ventral mesencephalon are available from ReNeuron, and following growth factor removal, they can be differentiated into mature human neurones. These cells express high levels of PrP^{C} and are 129MM, which is the *PRNP* genotype associated with vCJD. Therefore, vCJD infection of these cells at various stages of their differentiation could lead to the propagation of human prions *in vitro*. Such a human neuronal model can be used to study the pathobiology of human prion disease, including PrP^{Sc} accumulation, and also to screen prion therapeutics. Furthermore, these cells could be stably transfected with the Ub^{G76V}-GFP UPS reporter substrate (**chapter 3**) at the stem cell stage. Following their differentiation and subsequent prion-infection, levels of the UPS reporter could be directly assessed to ascertain its accumulation and whether there is progressive UPS dysfunction. This could potentially allow for understanding the temporal relationship between prion infection, neuronal dysfunction and UPS impairment.

This human cell system could also be used to define the temporal relationship between UPS function and ER stress in human prion disease. ER stress has been implicated in prion disease pathogenesis, but it is not yet know whether it is primary or secondary to UPS dysfunction (Hetz *et al.*, 2003; Hetz *et al.*, 2007). Studies have linked UPS impairment with ER stress, showing it has a general inhibitory effect on UPS function (Menendez-Benito *et al.*, 2005). Alternatively, work presented here suggests that UPS impairment, as a result of prion infection, may result in the accumulation of misfolded proteins in the ER, which would otherwise be degraded by ERAD, and result in ER stress. Constant and increased routing of PrP through ERAD may thus contribute to neurodegeneration in prion disease. This raises two hypotheses: 1) accumulation of PrP^{Sc} may lead to ER stress and reduced translocation of nascent PrP into the ER lumen; 2) at least a subset of the neurodegenerative sequelae of prion infection may be directly inducible, even when PrP^{Sc} or misfolded PrP aggregates are absent, just by changing the PrP^{C} metabolism to that occurring during chronic ER stress. Interestingly, evidence of ER stress and decreased translocation of native PrP to the ER during prion infection was recently presented (Rane *et al.*, 2008). Furthermore, the authors showed that the expression of a mutant PrP (with reduced translocation at levels expected during ER stress) in transgenic mice was sufficient to cause various mild, age-dependent manifestations of PrP-mediated neurodegeneration, and thereby provided a link between PrP^{Sc}-induced ER stress with neuronal cell death.

6.2.3 *In vivo* time-course pathogenesis study in UPS reporter transgenic mice

Results presented in this thesis show that the proteolytic activities of the 26S proteasome are significantly inhibited in prion-infected cells and prion-infected mouse brain. However, the mice used to study UPS inhibition were culled at the end-stage of prion disease. Therefore, from these experiments alone it is unclear whether *in vivo* UPS inhibition is an early or late phenomenon. Hence, in addition to the human cell model described above, an *in vivo* pathogenesis study using the Ub^{G76V}-GFP UPS reporter construct would also help clarifying the temporal and spatial relationship between UPS dysfunction and prion disease pathogenesis. Such an experiment, where Ub^{G76V}-GFP-

expressing transgenic mice are culled at different time points following prion infection, would provide information as to how critical UPS dysfunction is to the neuronal loss associated with prion disease. Various experimental techniques, such as immunohistochemistry, Western blotting, RT-PCR and co-immunoprecipitation, could be used to assess different aspects of prion neurobiology and the role of degradation systems (UPS and autophagy) in prion pathogenesis.

The ubiquitosome, a marker of early proteasome dysfunction, should also be investigated by looking at the accumulation of lys 48-linked ubiquitinated peptides in the UPS reporter mice and in WT mice, again by culling at serial time points. Most poly-ubiquitinated substrates targeted for proteasomal degradation are lys 48-linked (Pickart and Fushman, 2004), and thus their steady-state cellular levels should reflect proteasome function. Recently, Bennett *et al.* exploited a mass-spectrometry method to quantify poly-ubiquitin chains (Kirkpatrick *et al.*, 2006) and demonstrated that the abundance of these chains is a faithful endogenous biomarker of UPS function (Bennett *et al.*, 2007). The authors found that lys 48-linked poly-ubiquitin chains accumulate early in pathogenesis in brains from transgenic mouse models of HD and from human HD patients, establishing UPS dysfunction as a consistent feature of HD pathology. Therefore, this method, both in prion-infected WT and UPS reporter transgenic mice, should allow for an evaluation of the function of the UPS in prion disease.

Recently Wang *et al.* used adenoviral fluorescent reporters to measure synaptic UPS activity *in vitro* and *in vivo* and observed a significant decrease in synaptic UPS activity in HD mice (Wang *et al.*, 2008). Therefore, these reporters can serve as a tool for measuring the function of the synaptic UPS and its regulation under physiological or pathological conditions. Synaptic dysfunction is well documented in other neurodegenerative diseases such as AD and PD (Klyubin *et al.*, 2005), where UPS impairment is also thought to be involved (Ross and Pickart, 2004). Earlier studies and work presented in this thesis suggest that UPS impairment may be involved in prion disease pathogenesis. Specifically, total lysates from prion-infected mouse brain showed reduced proteolytic activities compared to uninfected controls. Considering the localisation of PrP^{C} as a GPI-anchored protein and its putative role in cellular signalling, as

well as the possibility that the site of conversion of PrP^{C} to PrP^{Sc} is at the plasma membrane (Caughey and Baron, 2006), it would be interesting to investigate whether misfolded PrP can affect synaptic UPS function in prion disease. This could be done by comparing UPS proteolytic activities of synapses with those in total lysates.

6.2.4 Defining cross-talk between UPS and autophagy in prion disease

The UPS and autophagy have been viewed as independent, parallel degradation systems with no point of intersection. However, increasing evidence now suggests that these two pathways are functionally interrelated (Rideout *et al.*, 2001; Iwata *et al.*, 2005b; Pandey *et al.*, 2007) and demonstrate co-ordinated, occasionally compensatory, function. Furthermore, in contrast to the notion that the UPS degrades short-lived proteins whereas autophagy degrades long-lived polypepides, studies have demonstrated that some proteins may be degraded by either pathway (Webb *et al.*, 2003; Fuertes *et al.*, 2003a; Fuertes *et al.*, 2003b; Li, 2006). Links between the two systems have also been illustrated in studies of the *Atg5* and *Atg7* KO mice, as they display neurodegeneration with ubiquitin-positive pathology (Komatsu *et al.*, 2006; Hara *et al.*, 2006).

Following UPS inhibition, either by accumulation of misfolded proteins or use of pharmacological inhibitors, ubiquitinated, misfolded proteins are actively transported to aggresomes (Johnston *et al.*, 1998). At present, evidence indicates that clearance of misfolded proteins from aggresomes is mediated at least in part by autophagy, suggesting that autophagy may act as a compensatory mechanism for degrading misfolded proteins when the proteasome is impaired (Taylor *et al.*, 2003; Iwata *et al.*, 2005a; Iwata *et al.*, 2005b; Yamamoto *et al.*, 2006). Work presented here shows that in prion-infected mouse cells, induction of autophagy ameliorates the deleterious effects caused by the proteasome inhibitor lactacystin. Indeed, induction of autophagy following UPS impairment appears to be cytoprotective since degenerative phenotypes associated with proteasome impairment in *Drosophila* are enhanced in an autophagy-deficient background, but suppressed when autophagy is induced by means of rapamycin treatment (Pandey *et al.*, 2007). Recently, pre-treatment of PC12 cells with rapamycin showed that it attenuates lactacystin-induced apoptosis and reduces lactacystin-induced

ubiquitinated protein aggregation (Pan *et al.*, 2008). Therefore, induction of autophagy may be a compensatory mechanism for PrP^{Sc} clearance when the proteasome is impaired. In agreement with other studies (Ertmer *et al.*, 2004), induction of autophagy resulted in some PrP^{Sc} clearance in prion-infected neuronal cells, suggesting this pathway is involved in PrP^{Sc} degradation.

However, at present there are difficulties in the use and interpretation of assays to monitor autophagy (Klionsky *et al.*, 2008) making it hard to define whether induction of autophagy has a role in prion pathogenesis, and whether it is associated with enhanced autophagic flux or delayed autophagosome clearance. Furthermore, the mechanism by which autophagy and UPS are co-ordinated is unclear, but there are several regulators that are thought to be key players in mediating this cross-talk and include: HDAC6 (Iwata *et al.*, 2005b; Pandey *et al.*, 2007), p62 (Bjorkoy *et al.*, 2005) and the FYVE-domain containing protein Alfy (Simonsen *et al.*, 2004). Future experiments to establish whether there is an increase in autophagy flux in prion disease should include: monitoring the turnover of long-lived proteins and use of a GFP-LC3 construct to assess lysosomal delivery and proteolysis (to generate free GFP). Furthermore, cross-talk between the UPS and autophagy in prion disease should also be investigated. One possibility would be to assess p62 levels, as it has been shown to serve as a link between LC3 and ubiquitinated substrates (Bjorkoy *et al.*, 2005) when it becomes incorporated into the completed autophagosome and degraded in autolysosomes (Mizushima and Yoshimori, 2007). Recently, it was demonstrated that inhibition of autophagy correlates with increased levels of p62, implying that steady state levels of this protein reflect the autophagic status (Wang *et al.*, 2006; Komatsu *et al.*, 2007). Additional evidence for UPS/autophagy cross-talk in prion disease could be obtained by assessing the role of HDAC6. HDAC6 activity is thought to be important for trafficking ubiquitinated proteins and lysosomes, proposing that it co-ordinates substrate delivery to the autophagic machinery (Iwata *et al.*, 2005b; Pandey *et al.*, 2007). Specifically, HDAC6 over-expression in *Drosophila* has been shown to suppress degeneration associated with UPS dysfunction and caused by toxic polyQ expression (Pandey *et al.*, 2007). Investigating the role of autophagy in the pathogenesis

of human prion disease may have therapeutic implications as modulators of autophagy are already in clinical trials for human cancers.

6.2.5 Site of PrP binding on the 20S core particle

As evidenced here (**chapter 4**), aggregated β-sheet-rich PrP co-immunoprecipitates with the 20S proteasome, indicating a direct binding interaction between the two. The disease-related PrP isoform inhibits the UPS by blocking gate-opening and substrate accessibility in the 20S proteasome (**chapter 4**). The aggregated β-sheet-rich PrP species inhibited the WT yeast 20S proteasome, but not the open-gated 20S mutant (α3ΔN), and abrogated the ability of a synthetic octamer from the C-terminus of the 19S ATPase Rpt5 to mediate 20S activation. Taken together, these results suggest that these PrP species inhibit the 20S at the level of the gate. However, the exact binding location of the C-termini of the 19S ATPases is unknown, and therefore it is not clear if the aggregated β-sheet-rich PrP species bind to the same inter-subunit pocket as the ATPases or to a different location on the 20S particle to exert their inhibitory effect. This could be further investigated using an EM approach and/or chemical cross-linking. Specifically, single-particle cryo-EM would be very useful in elucidating the exact binding location, and could also provide some structural information on the inhibitory species itself, studies on which are currently hindered due to its highly aggregated nature. The other possible way to investigate where β-sheet-rich PrP binds on the 20S is to use a cross-linker to bind the PrP and the 20S. Recently, a study using gluteraldehyde to cross-link various 20S subunits demonstrated the existence of a previously poorly described unit within the 20S, comprising non-ATPases Rpn1 and Rpn2 (Rosenzweig *et al.*, 2008). The authors used mass spectroscopy, amino acid sequencing, and AFM to elucidate the binding locations of their cross-linked subunits on the 20S proteasome and established that both Rpn1-Rpn2 and the ATPases of the 19S appear to be required for substrate translocation and gating of the proteolytic channel. Such methods should also be used to define the precise location of the β-sheet-rich PrP species on the 20S.

6.2.6 Effect of other oligomeric proteins on the activity of the proteasome

The ability of aggregated, oligomeric β-sheet-rich PrP isoforms to block gate-opening and substrate entry into the proteasome (**chapter 4**) may have relevance to other neurodegenerative diseases where there is an accumulation of misfolded β-sheet-rich proteins and impairment of protein degradation by the UPS. Therefore, it will be interesting to investigate whether such β-sheet-rich proteins associated with other neurodegenerative diseases, such as AD and PD, can also inhibit the UPS. The species used here (**chapter 3**) did not inhibit the proteasome, most probably because they were in a fibrillar form. There is growing evidence in several protein-misfolding disorders that soluble protein aggregates, rather than large insoluble aggregates, are the toxic species causing neurodegenerative disease (Caughey and Lansbury, 2003; Haass and Selkoe, 2007). For example, in AD, $A\beta_{40}$ and $A\beta_{42}$ are particularly toxic to cells when they are in the form of small oligomers at the early stage of peptide aggregation before they form Aβ fibrils (Hardy and Selkoe, 2002). Given that oligomeric, β-sheet-rich PrP isoforms are potent inhibitors of the proteolytic activity of the 20S proteasome, the effect of other aggregate-prone proteins in an oligomeric state on the function of the UPS should also be assessed. This would help understand whether the effects seen here are unique to prion disease.

7 REFERENCE LIST

Aguzzi,A., Glatzel,M., Montrasio,F., Prinz,M., and Heppner,F.L. (2001). Interventional strategies against prion diseases. Nat. Rev. Neurosci. *2*, 745-749.

Aguzzi,A. and Polymenidou,M. (2004). Mammalian prion biology. One century of evolving concepts. Cell *116*, 313-327.

Ahlberg,J., Marzella,L., and Glaumann,H. (1982). Uptake and degradation of proteins by isolated rat liver lysosomes. Suggestion of a microautophagic pathway of proteolysis. Lab Invest *47*, 523-532.

Alkalay,I., Yaron,A., Hatzubai,A., Orian,A., Ciechanover,A., and Benneriah,Y. (1995). Stimulation-Dependent I-Kappa-B-Alpha Phosphorylation Marks the Nf-Kappa-B Inhibitor for Degradation Via the Ubiquitin-Proteasome Pathway. Proc. Natl. Acad. Sci. USA *92*, 10599-10603.

Almer,G., Hainfellner,H.A., Jellinger,K., Kleinert,R., Bayer,G., Windl,O., Kretzschmar,H., Hill AF, Sidle,K.C., Collinge J, and Budka,H. (1999). Fatal familial insomnia: a new Austrian family. Brain *122*, 5-16.

Alper,T., Cramp,W.A., Haig,D.A., and Clarke,M.C. (1967). Does the agent of scrapie replicate without nucleic acid? Nature *214*, 764-766.

Alper,T., Haig,D.A., and Clarke,M.C. (1978). The scrapie agent: evidence against its dependence for replication on intrinsic nucleic acid. J. Gen. Virol. *41*, 503-516.

Alpers M (1987). Epidemiology and Clinical Aspects of Kuru. In Prions: Novel infectious pathogens causing scrapie and Creutzfeldt-Jakob disease., S.B.Prusiner and M.P.McKinley, eds. (San Diego: Academic Press), pp. 451-465.

Anderson,R.M., Donnelly,C.A., Ferguson,N.M., Woolhouse,M.E.J., Watt,C.J., Udy,H.J., MaWhinney,S., Dunstan,S.P., Southwood,T.R.E., Wilesmith,J.W., Ryan,J.B.M., Hoinville,L.J., Hillerton,J.E., Austin,A.R., and Wells,G.A.H. (1996). Transmission dynamics and epidemiology of BSE in British cattle. Nature *382*, 779-788.

Anglade,P., Vyas,S., Javoy-Agid,F., Herrero,M.T., Michel,P.P., Marquez,J., Mouatt-Prigent,A., Ruberg,M., Hirsch,E.C., and Agid,Y. (1997). Apoptosis and autophagy in nigral neurons of patients with Parkinson's disease. Histol. Histopathol. *12*, 25-31.

Ardley,H.C. and Robinson,P.A. (2005). E3 ubiquitin ligases. Essays Biochem. *41*, 15-30.

Arnold,J.E., Tipler,C., Laszlo,L., Hope,J., Landon,M., and Mayer,R.J. (1995). The abnormal isoform of the prion protein accumulates in late-endosome-like organelles in scrapie-infected mouse brain. J. Pathol. *176*, 403-411.

Asante,E.A., Linehan,J.M., Desbruslais,M., Joiner,S., Gowland,I., Wood,A.L., Welch,J., Hill,A.F., Lloyd,S.E., Wadsworth,J.D., and Collinge,J. (2002). BSE prions propagate as either variant CJD-like or sporadic CJD-like prion strains in transgenic mice expressing human prion protein. EMBO J. *21*, 6358-6366.

Bajorek,M., Finley,D., and Glickman,M.H. (2003). Proteasome disassembly and downregulation is correlated with viability during stationary phase. Curr. Biol. *13*, 1140-1144.

Bajorek,M. and Glickman,M.H. (2004). Keepers at the final gates: regulatory complexes and gating of the proteasome channel. Cell Mol. Life Sci. *61*, 1579-1588.

Barbanti,P., Fabbrini,G., Salvatore,M., Petraroli,R., Cardone,F., Maras,B., Equestre,M., Macchi,G., Lenzi,G.L., and Pocchiari,M. (1996). Polymorphism at codon 129 or codon 219 of *PRNP* and clinical heterogeneity in a previously unreported family with Gerstmann-Straussler-Scheinker disease (PrP-P102L mutation). Neurology *47*, 734-741.

Baron,G.S. and Caughey,B. (2003). Effect of glycosylphosphatidylinositol anchor-dependent and -independent prion protein association with model raft membranes on conversion to the protease-resistant isoform. J. Biol. Chem. *278*, 14883-14892.

Baron,G.S., Wehrly,K., Dorward,D.W., Chesebro,B., and Caughey,B. (2002). Conversion of raft associated prion protein to the protease-resistant state requires insertion of PrP-res (PrP(Sc)) into contiguous membranes. EMBO J. *21*, 1031-1040.

Baron,T., Bencsik,A., Biacabe,A.G., Morignat,E., and Bessen,R.A. (2007). Phenotypic Similarity of Transmissible Mink Encephalopathy in Cattle and L-type Bovine Spongiform Encephalopathy in a Mouse Model. Emerg. Infect. Dis. *13*, 1887-1894.

Barry,R.A., Kent,S.B., McKinley,M.P., Meyer,R.K., DeArmond,S.J., Hood,L.E., and Prusiner,S.B. (1986). Scrapie and cellular prion proteins share polypeptide epitopes. J. Infect. Dis. *153*, 848-854.

Bartz,J.C., Bessen,R.A., McKenzie,D., Marsh,R.F., and Aiken,J.M. (2000). Adaptation and selection of prion protein strain conformations following interspecies transmission of transmissible mink encephalopathy. J. Virol. *74*, 5542-5547.

Baskakov,I.V., Legname,G., Baldwin,M.A., Prusiner,S.B., and Cohen,F.E. (2002). Pathway complexity of prion protein assembly into amyloid. J. Biol. Chem. *277*, 21140-21148.

Basler,K., Oesch,B., Scott,M., Westaway,D., Walchli,M., Groth,D.F., McKinley,M.P., Prusiner,S.B., and Weissmann,C. (1986). Scrapie and cellular PrP isoforms are encoded by the same chromosomal gene. Cell *46*, 417-428.

Baumann,F., Tolnay,M., Brabeck,C., Pahnke,J., Kloz,U., Niemann,H.H., Heikenwalder,M., Rulicke,T., Burkle,A., and Aguzzi,A. (2007). Lethal recessive myelin toxicity of prion protein lacking its central domain. EMBO J. *26*, 538-547.

Bedford,L., Hay,D., Devoy,A., Paine,S., Powe,D.G., Seth,R., Gray,T., Topham,I., Fone,K., Rezvani,N., Mee,M., Soane,T., Layfield,R., Sheppard,P.W., Ebendal,T., Usoskin,D., Lowe,J., and Mayer,R.J. (2008). Depletion of 26S proteasomes in mouse brain neurons causes neurodegeneration and Lewy-like inclusions resembling human pale bodies. J. Neurosci. *28*, 8189-8198.

Belin,A.C. and Westerlund,M. (2008). Parkinson's disease: a genetic perspective. FEBS J. *275*, 1377-1383.

Bence,N.F., Sampat,R.M., and Kopito,R.R. (2001). Impairment of the ubiquitin-proteasome system by protein aggregation. Science *292*, 1552-1555.

Bendheim,P.E., Barry,R.A., DeArmond,S.J., Stites,D.P., and Prusiner,S.B. (1984). Antibodies to a scrapie prion protein. Nature *310*, 418-421.

Bennett,E.J., Shaler,T.A., Woodman,B., Ryu,K.Y., Zaitseva,T.S., Becker,C.H., Bates,G.P., Schulman,H., and Kopito,R.R. (2007). Global changes to the ubiquitin system in Huntington's disease. Nature *448*, 704-708.

Beranger,F., Mange,A., Goud,B., and Lehmann,S. (2002). Stimulation of PrPC retrograde transport towards the endoplasmic reticulum increases accumulation of PrPSc in prion-infected cells. J. Biol. Chem. *277*, 38972-38977.

Berg,T.O., Fengsrud,M., Stromhaug,P.E., Berg,T., and Seglen,P.O. (1998). Isolation and characterization of rat liver amphisomes. Evidence for fusion of autophagosomes with both early and late endosomes. J. Biol. Chem. *273*, 21883-21892.

Berger,Z., Ravikumar,B., Menzies,F.M., Oroz,L.G., Underwood,B.R., Pangalos,M.N., Schmitt,I., Wullner,U., Evert,B.O., O'Kane,C.J., and Rubinsztein,D.C. (2006). Rapamycin alleviates toxicity of different aggregate-prone proteins. Hum. Mol. Genet. *15*, 433-442.

Berkers,C.R., Verdoes,M., Lichtman,E., Fiebiger,E., Kessler,B.M., Anderson,K.C., Ploegh,H.L., Ovaa,H., and Galardy,P.J. (2005). Activity probe for in vivo profiling of the specificity of proteasome inhibitor bortezomib. Nat. Methods *2*, 357-362.

Bessen,R.A., Kocisko,D.A., Raymond,G.J., Nandan,S., Lansbury,P.T., and Caughey,B. (1995). Non-genetic propagation of strain-specific properties of scrapie prion protein. Nature *375*, 698-700.

Bessen,R.A. and Marsh,R.F. (1992). Biochemical and physical properties of the prion protein from two strains of the transmissible mink encephalopathy agent. J. Virol. *66*, 2096-2101.

Bessen,R.A. and Marsh,R.F. (1994). Distinct PrP properties suggest the molecular basis of strain variation in transmissible mink encephalopathy. J. Virol. *68*, 7859-7868.

Bett,J.S., Goellner,G.M., Woodman,B., Pratt,G., Rechsteiner,M., and Bates,G.P. (2006). Proteasome impairment does not contribute to pathogenesis in R6/2 Huntington's disease mice: exclusion of proteasome activator REGgamma as a therapeutic target. Hum. Mol. Genet. *15*, 33-44.

Bhutani,N., Venkatraman,P., and Goldberg,A.L. (2007). Puromycin-sensitive aminopeptidase is the major peptidase responsible for digesting polyglutamine sequences released by proteasomes during protein degradation. EMBO J. *26*, 1385-1396.

Bian,J., Nazor,K.E., Angers,R., Jernigan,M., Seward,T., Centers,A., Green,M., and Telling,G.C. (2006). GFP-tagged PrP supports compromised prion replication in transgenic mice. Biochem. Biophys. Res. Commun. *340*, 894-900.

Bjorkoy,G., Lamark,T., Brech,A., Outzen,H., Perander,M., Overvatn,A., Stenmark,H., and Johansen,T. (2005). p62/SQSTM1 forms protein aggregates degraded by autophagy and has a protective effect on huntingtin-induced cell death. J. Cell Biol. *171*, 603-614.

Blommaart,E.F., Luiken,J.J., Blommaart,P.J., van Woerkom,G.M., and Meijer,A.J. (1995). Phosphorylation of ribosomal protein S6 is inhibitory for autophagy in isolated rat hepatocytes. J. Biol. Chem. *270*, 2320-2326.

Boellaard,J.W., Kao,M., Schlote,W., and Diringer,H. (1991). Neuronal autophagy in experimental scrapie. Acta Neuropathol. *82*, 225-228.

Boellaard,J.W., Schlote,W., and Tateishi,J. (1989). Neuronal autophagy in experimental Creutzfeldt-Jakob's disease. Acta Neuropathol. *78*, 410-418.

Bolton,D.C., McKinley,M.P., and Prusiner,S.B. (1982). Identification of a protein that purifies with the scrapie prion. Science *218*, 1309-1311.

Borchelt,D.R., Rogers,M., Stahl,N., Telling,G., and Prusiner,S.B. (1993). Release of the cellular prion protein from cultured cells after loss of its glycoinositol phospholipid anchor. Glycobiology. *3*, 319-329.

Borchelt,D.R., Taraboulos,A., and Prusiner,S.B. (1992). Evidence for synthesis of scrapie prion proteins in the endocytic pathway. J. Biol. Chem. *267*, 16188-16199.

Bosque,P.J. and Prusiner,S.B. (2000). Cultured cell sublines highly susceptible to prion infection. J. Virol. *74*, 4377-4386.

Botto,L., Masserini,M., Cassetti,A., and Palestini,P. (2004). Immunoseparation of Prion protein-enriched domains from other detergent-resistant membrane fractions, isolated from neuronal cells. FEBS Lett. *557*, 143-147.

Bounhar,Y., Zhang,Y., Goodyer,C.G., and LeBlanc,A. (2001). Prion protein protects human neurons against Bax-mediated apoptosis. J. Biol. Chem. *276*, 39145-39149.

Bowman,A.B., Yoo,S.Y., Dantuma,N.P., and Zoghbi,H.Y. (2005). Neuronal dysfunction in a polyglutamine disease model occurs in the absence of ubiquitin-proteasome system impairment and inversely correlates with the degree of nuclear inclusion formation. Hum. Mol. Genet. *14*, 679-691.

Brandner,S., Raeber,A., Sailer,A., Blattler,T., Fischer,M., Weissmann,C., and Aguzzi,A. (1996). Normal host prion protein (PrPC) is required for scrapie spread within the central nervous system. Proc. Natl. Acad. Sci. U. S. A *93*, 13148-13151.

Brown,D.R., Herms,J., and Kretzschmar,H.A. (1994a). Mouse cortical cells lacking cellular PrP survive in culture with a neurotoxic PrP fragment. Neuroreport *5*, 2057-2060.

Brown,D.R., Schmidt,B., and Kretzschmar,H.A. (1996). Role of microglia and host prion protein in neurotoxicity of a prion protein fragment. Nature *380*, 345-347.

Brown,D.R., Schulz-Schaeffer,W.J., Schmidt,B., and Kretzschmar,H.A. (1997). Prion protein-deficient cells show altered response to oxidative stress due to decreased SOD-1 activity. Exp. Neurol. *146*, 104-112.

Brown,P. and Bradley,R. (1998). 1755 and all that: a historical primer of transmissible spongiform encephalopathy. BMJ. *317*, 1688-1692.

Brown,P., Cathala,F., Raubertas,R.F., Gajdusek,D.C., and Castaigne,P. (1987). The epidemiology of Creutzfeldt-Jakob disease: conclusion of a 15-year investigation in France and review of the world literature. Neurology *37*, 895-904.

Brown,P., Gibbs,C.J., Jr., Rodgers-Johnson,P., Asher,D.M., Sulima,M.P., Bacote,A., Goldfarb,L.G., and Gajdusek,D.C. (1994b). Human spongiform encephalopathy: the National Institutes of Health series of 300 cases of experimentally transmitted disease. Ann. Neurol. *35*, 513-529.

Brown,P., Green,E.M., and Gajdusek,D.C. (1978). Effect of different gradient solutions on the buoyant density of scrapie infectivity. Proc. Soc. Exp. Biol. Med. *158*, 513-516.

Brown,P., Preece,M., Brandel,J.P., Sato,T., McShane,L., Zerr,I., Fletcher,A., Will,R.G., Pocchiari,M., Cashman,N.R., D'Aignaux,J.H., Cervenáková,L., Fradkin,J., Schonberger,L.B., and Collins,S.J. (2000). Iatrogenic Creutzfeldt-Jakob disease at the millennium. Neurology *55*, 1075-1081.

Brown,P., Preece,M.A., and Will,R.G. (1992). "Friendly fire" in medicine: hormones, homografts, and Creutzfeldt-Jakob disease. Lancet *340*, 24-27.

Brown,P., Rodgers-Johnson,P., Cathala,F., Gibbs,C.J., Jr., and Gajdusek,D.C. (1984). Creutzfeldt-Jakob disease of long duration: clinicopathological characteristics, transmissibility, and differential diagnosis. Ann. Neurol. *16*, 295-304.

Browning,S.R., Mason,G.L., Seward,T., Green,M., Eliason,G.A., Mathiason,C., Miller,M.W., Williams,E.S., Hoover,E., and Telling,G.C. (2004). Transmission of prions from mule deer and elk with chronic wasting disease to transgenic mice expressing cervid PrP. J. Virol. *78*, 13345-13350.

Bruce,M., Chree,A., McConnell,I., Foster,J., Pearson,G., and Fraser,H. (1994). Transmission of bovine spongiform encephalopathy and scrapie to mice: Strain variation and the species barrier. Philos. Trans. R. Soc. Lond. [Biol.] *343*, 405-411.

Bruce,M.E., Will,R.G., Ironside,J.W., McConnell,I., Drummond,D., Suttie,A., McCardle,L., Chree,A., Hope,J., Birkett,C., Cousens,S., Fraser,H., and Bostock,C.J. (1997). Transmissions to mice indicate that 'new variant' CJD is caused by the BSE agent. Nature *389*, 498-501.

Brugger,B., Graham,C., Leibrecht,I., Mombelli,E., Jen,A., Wieland,F., and Morris,R. (2004). The membrane domains occupied by glycosylphosphatidylinositol-anchored prion protein and Thy-1 differ in lipid composition. J. Biol. Chem. *279*, 7530-7536.

Budka,H. (2003). Neuropathology of prion diseases. Br. Med. Bull. *66*, 121-130.

Budka,H., Aguzzi,A., Brown,P., Brucher,J.M., Bugiani,O., Gullotta,F., Haltia,M., Hauw,J.J., Ironside,J.W., Jellinger,K., Kretzschmar,H.A., Lantos,P.L., Masullo,C., Schlote,W., Tateishi,J., and Weller,R.O. (1995). Neuropathological diagnostic criteria for Creutzfeldt-Jakob disease (CJD) and other human spongiform encephalopathies (Prion diseases). Brain Pathol. *5*, 459-466.

Bueler,H., Aguzzi,A., Sailer,A., Greiner,R.A., Autenried,P., Aguet,M., and Weissmann,C. (1993). Mice devoid of PrP are resistant to scrapie. Cell *73*, 1339-1347.

Bueler,H., Fischer,M., Lang,Y., Bluethmann,H., Lipp,H.-P., DeArmond,S.J., Prusiner,S.B., Aguet,M., and Weissmann,C. (1992). Normal development and behaviour of mice lacking the neuronal cell-surface PrP protein. Nature *356*, 577-582.

Butler,D.A., Scott,M.R., Bockman,J.M., Borchelt,D.R., Taraboulos,A., Hsiao,K.K., Kingsbury,D.T., and Prusiner,S.B. (1988). Scrapie-infected murine neuroblastoma cells produce protease-resistant prion proteins. J. Virol. *62*, 1558-1564.

Calzolai,L., Lysek,D.A., Perez,D.R., Guntert,P., and Wuthrich,K. (2005). Prion protein NMR structures of chickens, turtles, and frogs. Proc. Natl. Acad. Sci. U. S. A *102*, 651-655.

Campana,V., Sarnataro,D., Fasano,C., Casanova,P., Paladino,S., and Zurzolo,C. (2006). Detergent-resistant membrane domains but not the proteasome are involved in the misfolding of a PrP mutant retained in the endoplasmic reticulum. J. Cell Sci. *119*, 433-442.

Campana,V., Sarnataro,D., and Zurzolo,C. (2005). The highways and byways of prion protein trafficking. Trends Cell Biol. *15*, 102-111.

Cancellotti,E., Wiseman,F., Tuzi,N.L., Baybutt,H., Monaghan,P., Aitchison,L., Simpson,J., and Manson,J.C. (2005). Altered glycosylated PrP proteins can have different neuronal trafficking in brain but do not acquire scrapie-like properties. J. Biol. Chem. *280*, 42909-42918.

Caramelli,M., Ru,G., Acutis,P., and Forloni,G. (2006). Prion diseases : current understanding of epidemiology and pathogenesis, and therapeutic advances. CNS Drugs *20*, 15-28.

Carimalo,J., Cronier,S., Petit,G., Peyrin,J.M., Boukhtouche,F., Arbez,N., Lemaigre-Dubreuil,Y., Brugg,B., and Miquel,M.C. (2005). Activation of the JNK-c-Jun pathway during the early phase of neuronal apoptosis induced by PrP106-126 and prion infection. Eur. J. Neurosci. *21*, 2311-2319.

Cascio,P., Hilton,C., Kisselev,A.F., Rock,K.L., and Goldberg,A.L. (2001). 26S proteasomes and immunoproteasomes produce mainly N-extended versions of an antigenic peptide. EMBO J. *20*, 2357-2366.

Castilla,J., Saa,P., Hetz,C., and Soto,C. (2005). In vitro generation of infectious scrapie prions. Cell *121*, 195-206.

Caughey,B. and Baron,G.S. (2006). Prions and their partners in crime. Nature *443*, 803-810.

Caughey,B. and Lansbury,P.T. (2003). Protofibrils, pores, fibrils, and neurodegeneration: separating the responsible protein aggregates from the innocent bystanders. Annu. Rev. Neurosci. *26*, 267-298.

Caughey,B., Neary,K., Buller,R., Ernst,D., Perry,L.L., Chesebro,B., and Race,R.E. (1990). Normal and scrapie-associated forms of prion protein differ in their sensitivities to phospholipase and proteases in intact neuroblastoma cells. J. Virol. *64*, 1093-1101.

Caughey,B. and Raymond,G.J. (1991). The scrapie-associated form of PrP is made from a cell surface precursor that is both protease- and phospholipase-sensitive. J. Biol. Chem. *266*, 18217-18223.

Chandler,R.L. (1961). Encephalopathy in mice produced by inoculation with scrapie brain material. Lancet *1*, 1378-1379.

Chapman,J., Brown,P., Goldfarb,L.G., Arlazoroff,A., Gajdusek,D.C., and Korczyn,A.D. (1993). Clinical heterogeneity and unusual presentations of Creutzfeldt-Jakob disease in Jewish patients with the PRNP codon 200 mutation. J. Neurol. Neurosurg. Psychiatry *56*, 1109-1112.

Chen,Q., Ding,Q., Thorpe,J., Dohmen,R.J., and Keller,J.N. (2005). RNA interference toward UMP1 induces proteasome inhibition in Saccharomyces cerevisiae: evidence for protein oxidation and autophagic cell death. Free Radic. Biol. Med. *38*, 226-234.

Chen,S., Roseman,A.M., Hunter,A.S., Wood,S.P., Burston,S.G., Ranson,N.A., Clarke,A.R., and Saibil,H.R. (1994). Location of a folding protein and shape changes in GroEL-ûGroES complexes imaged by cryo-electron microscopy. Nature *371*, 261-264.

Chesebro,B. (1998). Prion diseases - BSE and prions: Uncertainties about the agent. Science *279*, 42-43.

Chesebro,B., Trifilo,M., Race,R., Meade-White,K., Teng,C., LaCasse,R., Raymond,L., Favara,C., Baron,G., Priola,S., Caughey,B., Masliah,E., and Oldstone,M. (2005). Anchorless prion protein results in infectious amyloid disease without clinical scrapie. Science *308*, 1435-1439.

Cho,H.J. (1976). Is the scrapie agent a virus? Nature *262*, 411-412.

Chu-Ping,M., Vu,J.H., Proske,R.J., Slaughter,C.A., and DeMartino,G.N. (1994). Identification, purification, and characterization of a high molecular weight, ATP-dependent activator (PA700) of the 20 S proteasome. J. Biol. Chem. *269*, 3539-3547.

Ciechanover,A. and Brundin,P. (2003). The ubiquitin proteasome system in neurodegenerative diseases. Sometimes the chicken, sometimes the egg. Neuron *40*, 427-446.

Ciechanover,A., Orian,A., and Schwartz,A.L. (2000). Ubiquitin-mediated proteolysis: biological regulation via destruction. Bioessays *22*, 442-451.

Cohen,E. and Taraboulos,A. (2003). Scrapie-like prion protein accumulates in aggresomes of cyclosporin A-treated cells. EMBO J. *22*, 404-417.

Cohen,F.E., Pan,K.-M., Huang,Z., Baldwin,M., Fletterick,R.J., and Prusiner,S.B. (1994). Structural clues to prion replication. Science *264*, 530-531.

Collinge J, Palmer,M.S., Sidle,K.C.L., Gowland,I., Medori,R., Ironside,J., and Lantos,P.L. (1995). Transmission of fatal familial insomnia to laboratory animals. Lancet *346*, 569-570.

Collinge J., Palmer,M.S., Gowland,I., Sidle,K.C.L., Hill AF, and Meads,J. (1995). Transmission of human prion disease to transgenic mice expressing human prion protein. Quarterly Journal of Medicine *88*, 839-840.

Collinge,J. (1997). Human prion diseases and bovine spongiform encephalopathy (BSE). Hum. Mol. Genet. *6*, 1699-1705.

Collinge,J. (1999). Variant Creutzfeldt-Jakob disease. Lancet *354*, 317-323.

Collinge,J. (2001). Prion diseases of humans and animals: their causes and molecular basis. Annu. Rev. Neurosci. *24*, 519-550.

Collinge,J. (2005). Molecular neurology of prion disease. J. Neurol. Neurosurg. Psychiatry *76*, 906-919.

Collinge,J., Beck,J., Campbell,T., Estibeiro,K., and Will,R.G. (1996a). Prion protein gene analysis in new variant cases of Creutzfeldt-Jakob disease. Lancet *348*, 56.

Collinge,J. and Clarke,A.R. (2007). A general model of prion strains and their pathogenicity. Science *318*, 930-936.

Collinge,J., Palmer,M.S., Sidle,K.C., Gowland,I., Medori,R., Ironside,J., and Lantos,P. (1995). Transmission of fatal familial insomnia to laboratory animals. Lancet *346*, 569-570.

Collinge,J. and Rossor,M. (1996). A new variant of prion disease. Lancet *347*, 916-917.

Collinge,J., Sidle,K.C., Meads,J., Ironside,J., and Hill,A.F. (1996b). Molecular analysis of prion strain variation and the aetiology of 'new variant' CJD. Nature *383*, 685-690.

Collinge,J., Whitfield,J., McKintosh,E., Beck,J., Mead,S., Thomas,D.J., and Alpers,M.P. (2006). Kuru in the 21st century--an acquired human prion disease with very long incubation periods. Lancet *367*, 2068-2074.

Collinge,J., Whittington,M.A., Sidle,K.C., Smith,C.J., Palmer,M.S., Clarke,A.R., and Jefferys,J.G. (1994). Prion protein is necessary for normal synaptic function. Nature *370*, 295-297.

Collins,S., Law,MG., Fletcher,A., Boyd,A., Kaldor,J., and Masters,C.L. (1999). Surgical treatment and risk of sporadic Creutzfeldt-jakob disease: a case-control study. Lancet *353*, 693-697.

Collins,S.J., Sanchez-Juan,P., Masters,C.L., Klug,G.M., van Duijn,C., Poleggi,A., Pocchiari,M., Almonti,S., Cuadrado-Corrales,N., Pedro-Cuesta,J., Budka,H., Gelpi,E., Glatzel,M., Tolnay,M., Hewer,E., Zerr,I., Heinemann,U., Kretszchmar,H.A., Jansen,G.H., Olsen,E., Mitrova,E., Alperovitch,A., Brandel,J.P., Mackenzie,J., Murray,K., and Will,R.G. (2006). Determinants of diagnostic investigation sensitivities across the clinical spectrum of sporadic Creutzfeldt-Jakob disease. Brain *129*, 2278-2287.

Combs,C.K., Johnson,D.E., Cannady,S.B., Lehman,T.M., and Landreth,G.E. (1999). Identification of microglial signal transduction pathways mediating a neurotoxic response to amyloidogenic fragments of β-amyloid and prion proteins. J. Neurosci. *19*, 928-939.

Coux,O., Tanaka,K., and Goldberg,A.L. (1996). Structure and functions of the 20S and 26S proteasomes. Annu. Rev. Biochem. *65*, 801-847.

Cronier,S., Laude,H., and Peyrin,J.M. (2004). Prions can infect primary cultured neurons and astrocytes and promote neuronal cell death. Proc. Natl. Acad. Sci. U. S. A *101*, 12271-12276.

Cuillé,J. and Chelle,P.L. (1936). La maladie dite tremblante du mouton est-elle inocuable? C. R. Acad. Sci. *203*, 1552-1554.

Dahlmann,B., Kuehn,L., Grziwa,A., Zwickl,P., and Baumeister,W. (1992). Biochemical properties of the proteasome from Thermoplasma acidophilum. Eur. J. Biochem. *208*, 789-797.

Dandoy-Dron,F., Benboudjema,L., Guillo,F., Jaegly,A., Jasmin,C., Dormont,D., Tovey,M.G., and Dron,M. (2000). Enhanced levels of scrapie responsive gene mRNA in BSE-infected mouse brain. Mol. Brain Res. *76*, 173-179.

Dandoy-Dron,F., Guillo,F., Benboudjema,L., Deslys,J.P., Lasmézas,C., Dormont,D., Tovey,M.G., and Dron,M. (1998). Gene expression in scrapie - Cloning a new scrapie-responsive gene and the identification of increased levels of seven other mRNA transcripts. J. Biol. Chem. *273*, 7691-7697.

Dantuma,N.P., Lindsten,K., Glas,R., Jellne,M., and Masucci,M.G. (2000). Short-lived green fluorescent proteins for quantifying ubiquitin/proteasome-dependent proteolysis in living cells. Nat. Biotechnol. *18*, 538-543.

Daude,N., Marella,M., and Chabry,J. (2003). Specific inhibition of pathological prion protein accumulation by small interfering RNAs. J. Cell Sci. *116*, 2775-2779.

Davies,J.E., Sarkar,S., and Rubinsztein,D.C. (2006). Trehalose reduces aggregate formation and delays pathology in a transgenic mouse model of oculopharyngeal muscular dystrophy. Hum. Mol. Genet. *15*, 23-31.

Davies,J.E., Sarkar,S., and Rubinsztein,D.C. (2007). The ubiquitin proteasome system in Huntington's disease and the spinocerebellar ataxias. BMC. Biochem. *8 Suppl 1*, S2.

Dice,J.F. (1990). Peptide sequences that target cytosolic proteins for lysosomal proteolysis. Trends Biochem. Sci. *15*, 305-309.

Dick,T.P., Nussbaum,A.K., Deeg,M., Heinemeyer,W., Groll,M., Schirle,M., Keilholz,W., Stevanovic,S., Wolf,D.H., Huber,R., Rammensee,H.G., and Schild,H. (1998). Contribution of

proteasomal beta-subunits to the cleavage of peptide substrates analyzed with yeast mutants. J. Biol. Chem. *273*, 25637-25646.

Dimcheff,D.E., Askovic,S., Baker,A.H., Johnson-Fowler,C., and Portis,J.L. (2003). Endoplasmic reticulum stress is a determinant of retrovirus-induced spongiform neurodegeneration. J. Virol. *77*, 12617-12629.

Ding,Q., Dimayuga,E., and Keller,J.N. (2006). Proteasome regulation of oxidative stress in aging and age-related diseases of the CNS. Antioxid. Redox. Signal. *8*, 163-172.

Ding,Q., Dimayuga,E., Martin,S., Bruce-Keller,A.J., Nukala,V., Cuervo,A.M., and Keller,J.N. (2003). Characterization of chronic low-level proteasome inhibition on neural homeostasis. J. Neurochem. *86*, 489-497.

Dodelet,V.C. and Cashman,N.R. (1998). Prion protein expression in human leukocyte differentiation. Blood *91*, 1556-1561.

Donnelly,C.A., Ferguson,N.M., Ghani,A.C., and Anderson,R.M. (2002). Implications of BSE infection screening data for the scale of the British BSE epidemic and current European infection levels. Proc. R. Soc. Lond B Biol. Sci. *269*, 2179-2190.

Dorandeu,A., Wingertsmann,L., Chretien,F., Delisle,M.B., Vital,C., Parchi,P., Montagna,P., Lugaresi,E., Ironside,J.W., Budka,H., Gambetti,P., and Gray,F. (1998). Neuronal apoptosis in fatal familial insomnia. Brain Pathol. *8*, 531-537.

Drisaldi,B., Stewart,R.S., Adles,C., Stewart,L.R., Quaglio,E., Biasini,E., Fioriti,L., Chiesa,R., and Harris,D.A. (2003). Mutant PrP is delayed in its exit from the endoplasmic reticulum, but neither wild-type nor mutant PrP undergoes retrotranslocation prior to proteasomal degradation. J. Biol. Chem. *278*, 21732-21743.

Dron,M., Bailly,Y., Beringue,V., Haeberle,A.M., Griffond,B., Risold,P.Y., Tovey,M.G., Laude,H., and Dandoy-Dron,F. (2005). Scrg1 is induced in TSE and brain injuries, and associated with autophagy. Eur. J. Neurosci. *22*, 133-146.

Dron,M., Dandoy-Dron,F., Guillo,F., Benboudjema,L., Hauw,J.J., Lebon,P., Dormont,D., and Tovey,M.G. (1998). Characterization of the human analogue of a Scrapie-responsive gene. J. Biol. Chem. *273*, 18015-18018.

Eghiaian,F., Grosclaude,J., Lesceu,S., Debey,P., Doublet,B., Treguer,E., Rezaei,H., and Knossow,M. (2004). Insight into the PrPC -> PrPSc conversion from the structures of antibody-bound ovine prion scrapie-susceptibility variants. Proc. Natl. Acad Sci U. S. A *101*, 10254-10259.

Elsasser,S., Schmidt,M., and Finley,D. (2005). Characterization of the proteasome using native gel electrophoresis. In Methods in Enzymology, Elsevier Academic Press), pp. 353-363.

Enari,M., Flechsig,E., and Weissmann,C. (2001). Scrapie prion protein accumulation by scrapie-infected neuroblastoma cells abrogated by exposure to a prion protein antibody. Proc. Natl. Acad. Sci. USA *98*, 9295-9299.

Endo,T., Groth,D., Prusiner,S.B., and Kobata,A. (1989). Diversity of oligosaccharide structures linked to asparagines of the scrapie prion protein. Biochemistry *28*, 8380-8388.

Ertmer,A., Gilch,S., Yun,S.W., Flechsig,E., Klebl,B., Stein-Gerlach,M., Klein,M.A., and Schatzl,H.M. (2004). The tyrosine kinase inhibitor STI571 induces cellular clearance of PrPSc in prion-infected cells. J. Biol. Chem. *279*, 41918-41927.

Ertmer,A., Huber,V., Gilch,S., Yoshimori,T., Erfle,V., Duyster,J., Elsasser,H.P., and Schatzl,H.M. (2007). The anticancer drug imatinib induces cellular autophagy. Leukemia *21*, 936-942.

Ettaiche,M., Pichot,R., Vincent,J.P., and Chabry,J. (2000). In vivo cytotoxicity of the prion protein fragment 106-126. J. Biol. Chem. *275*, 36487-36490.

Fass,E., Shvets,E., Degani,I., Hirschberg,K., and Elazar,Z. (2006). Microtubules support production of starvation-induced autophagosomes but not their targeting and fusion with lysosomes. J. Biol. Chem. *281*, 36303-36316.

Fenteany,G., Standaert,R.F., Lane,W.S., Choi,S., Corey,E.J., and Schreiber,S.L. (1995). Inhibition of proteasome activities and subunit-specific amino-terminal threonine modification by lactacystin. Science *268*, 726-731.

Fevrier,B., Vilette,D., Archer,F., Loew,D., Faigle,W., Vidal,M., Laude,H., and Raposo,G. (2004). Cells release prions in association with exosomes. Proc. Natl. Acad. Sci. U. S. A *101*, 9683-9688.

Fioriti,L., Dossena,S., Stewart,L.R., Stewart,R.S., Harris,D.A., Forloni,G., and Chiesa,R. (2005). Cytosolic prion protein (PrP) is not toxic in N2a cells and primary neurons expressing pathogenic PrP mutations. J. Biol. Chem. *280*, 11320-11328.

Fischer,M., Rulicke,T., Raeber,A., Sailer,A., Moser,M., Oesch,B., Brandner S, Aguzzi,A., and Weissmann,C. (1996). Prion protein (PrP) with amino-proximal deletions restoring susceptibility of PrP knockout mice to scrapie. EMBO J. *15*, 1255-1264.

Flechsig,E., Hegyi,I., Enari,M., Schwarz,P., Collinge,J., and Weissmann,C. (2001). Transmission of scrapie by steel-surface-bound prions. Mol. Med. *7*, 679-684.

Forloni,G., Angeretti,N., Chiesa,R., Monzani,E., Salmona,M., Bugiani,O., and Tagliavini,F. (1993). Neurotoxicity of a prion protein fragment. Nature *362*, 543-546.

Forster,A. and Hill,C.P. (2003). Proteasome degradation: enter the substrate. Trends Cell Biol. *13*, 550-553.

Fuertes,G., Martin De Llano,J.J., Villarroya,A., Rivett,A.J., and Knecht,E. (2003a). Changes in the proteolytic activities of proteasomes and lysosomes in human fibroblasts produced by serum withdrawal, amino-acid deprivation and confluent conditions. Biochem. J. *375*, 75-86.

Fuertes,G., Villarroya,A., and Knecht,E. (2003b). Role of proteasomes in the degradation of short-lived proteins in human fibroblasts under various growth conditions. Int. J. Biochem. Cell Biol. *35*, 651-664.

Gajdusek,D.C., Gibbs,C.J.Jr., and Alpers M (1966). Experimental transmission of a kuru-like syndrome to chimpanzees. Nature *209*, 794-796.

Gasset,M., Baldwin,M.A., Fletterick,R.J., and Prusiner,S.B. (1993). Perturbation of the secondary structure of the scrapie prion protein under conditions that alter infectivity. Proc. Natl. Acad. Sci. U. S A. *90*, 1-5.

Gasset,M., Baldwin,M.A., Lloyd,D.H., Gabriel,J.M., Holtzman,D.M., Cohen,F., Fletterick,R., and Prusiner,S.B. (1992). Predicted alpha-helical regions of the prion protein when synthesized as peptides form amyloid. Proc. Natl. Acad. Sci. U. S A. *89*, 10940-10944.

Gauczynski,S., Peyrin,J.M., Haïk,S., Leucht,C., Hundt,C., Rieger,R., Krasemann,S., Deslys,J.P., Dormont,D., Lasmézas,C.I., and Weiss,S. (2001). The 37-kDa/67-kDa laminin receptor acts as the cell-surface receptor for the cellular prion protein. EMBO J. *20*, 5863-5875.

Gerber,R., Tahiri-Alaoui,A., Hore,P.J., and James,W. (2007). Oligomerization of the human prion protein proceeds via a molten globule intermediate. J. Biol. Chem. *282*, 6300-6307.

Gerber,R., Tahiri-Alaoui,A., Hore,P.J., and James,W. (2008). Conformational pH dependence of intermediate states during oligomerization of the human prion protein. Protein Sci. *17*, 537-544.

Ghani,A.C., Ferguson,N.M., Donnelly,C.A., Hagenaars,T.J., and Anderson,R.M. (1998). Epidemiological determinants of the pattern and magnitude of the vCJD epidemic in Great Britain. Proc. Biol. Sci. *265*, 2443-2452.

Gibbs,C.J.Jr., Gajdusek,D.C., Asher,D.M., Alpers M, Beck,E., Daniel,P.M., and Matthews,W.B. (1968). Creutzfeldt-Jakob Disease (Spongiform Encephalopathy): Transmission to the Chimpanzee. Science *161*, 388-389.

Gillette,T.G., Kumar,B., Thompson,D., Slaughter,C.A., and DeMartino,G.N. (2008). Differential roles of the COOH termini of AAA subunits of PA700 (19 S regulator) in asymmetric assembly and activation of the 26 S proteasome. J. Biol. Chem. *283*, 31813-31822.

Glickman,M.H. and Ciechanover,A. (2002). The ubiquitin-proteasome proteolytic pathway: destruction for the sake of construction. Physiol Rev. *82*, 373-428.

Glover,K.J., Whiles,J.A., Wood,M.J., Melacini,G., Komives,E.A., and Vold,R.R. (2001). Conformational dimorphism and transmembrane orientation of prion protein residues 110-136 in bicelles. Biochemistry *40*, 13137-13142.

Goggin,K., Beaudoin,S., Grenier,C., Brown,A.A., and Roucou,X. (2008). Prion protein aggresomes are poly(A)+ ribonucleoprotein complexes that induce a PKR-mediated deficient cell stress response. Biochim. Biophys. Acta *1783*, 479-491.

Goldberg,A.L. (2003). Protein degradation and protection against misfolded or damaged proteins. Nature *426*, 895-899.

Goldfarb,L.G., Brown,P., Haltia,M., Ghiso,J., Frangione,B., and Gajdusek,D.C. (1993). Synthetic peptides corresponding to different mutated regions of the amyloid gene in familial Creutzfeldt-Jakob disease show enhanced in vitro formation of morphologically different amyloid fibrils. Proc. Natl. Acad. Sci. U. S. A *90*, 4451-4454.

Gordon W.S. (1946). Advances in veterinary research. Louping-ill, tick-borne fever and scrapie. Veterinary Record *58*, 516-520.

Govaerts,C., Wille,H., Prusiner,S.B., and Cohen,F.E. (2004). Evidence for assembly of prions with left-handed beta-helices into trimers. Proc. Natl. Acad. Sci U. S. A *101*, 8342-8347.

Graner,E., Mercadante,A.F., Zanata,S.M., Forlenza,O.V., Cabral,A.L.B., Veiga,S.S., Juliano,M.A., Roesler,R., Walz,R., Minetti,A., Izquierdo,I., Martins,V.R., and Brentani,R.R. (2000). Cellular prion protein binds laminin and mediates neuritogenesis. Mol. Brain Res. *76*, 85-92.

Grenier,C., Bissonnette,C., Volkov,L., and Roucou,X. (2006). Molecular morphology and toxicity of cytoplasmic prion protein aggregates in neuronal and non-neuronal cells. J. Neurochem. *97*, 1456-1466.

Griffith,J.S. (1967). Self Replication and Scrapie. Nature *215*, 1043-1044.

Groll,M., Bajorek,M., Kohler,A., Moroder,L., Rubin,D.M., Huber,R., Glickman,M.H., and Finley,D. (2000). A gated channel into the proteasome core particle. Nat Struct. Biol. *7*, 1062-1067.

Groll,M., Ditzel,L., Lowe,J., Stock,D., Bochtler,M., Bartunik,H.D., and Huber,R. (1997). Structure of 20S proteasome from yeast at 2.4 angstrom resolution. Nature *386*, 463-471.

Groll,M., Heinemeyer,W., Jager,S., Ullrich,T., Bochtler,M., Wolf,D.H., and Huber,R. (1999). The catalytic sites of 20S proteasomes and their role in subunit maturation: a mutational and crystallographic study. Proc. Natl. Acad. Sci. U. S. A *96*, 10976-10983.

Groll,M. and Huber,R. (2003). Substrate access and processing by the 20S proteasome core particle. Int. J. Biochem. Cell Biol. *35*, 606-616.

Haass,C. and Selkoe,D.J. (2007). Soluble protein oligomers in neurodegeneration: lessons from the Alzheimer's amyloid beta-peptide. Nat. Rev. Mol. Cell Biol. *8*, 101-112.

Hachiya,N.S., Watanabe,K., Yamada,M., Sakasegawa,Y., and Kaneko,K. (2004). Anterograde and retrograde intracellular trafficking of fluorescent cellular prion protein. Biochem. Biophys. Res. Commun. *315*, 802-807.

Haire,L.F., Whyte,S.M., Vasisht,N., Gill,A.C., Verma,C., Dodson,E.J., Dodson,G.G., and Bayley,P.M. (2004). The crystal structure of the globular domain of sheep prion protein. J. Mol. Biol. *336*, 1175-1183.

Hara,T., Nakamura,K., Matsui,M., Yamamoto,A., Nakahara,Y., Suzuki-Migishima,R., Yokoyama,M., Mishima,K., Saito,I., Okano,H., and Mizushima,N. (2006). Suppression of basal autophagy in neural cells causes neurodegenerative disease in mice. Nature *441*, 885-889.

Haraguchi,T., Fisher,S., Olofsson,S., Endo,T., Groth,D., Tarentino,A., Borchelt,D.R., Teplow,D., Hood,L., Burlingame,A., and . (1989). Asparagine-linked glycosylation of the scrapie and cellular prion proteins. Arch. Biochem. Biophys. *274*, 1-13.

Hardy,J. and Selkoe,D.J. (2002). The amyloid hypothesis of Alzheimer's disease: progress and problems on the road to therapeutics. Science *297*, 353-356.

Hartl,F.U. and Hayer-Hartl,M. (2002). Molecular chaperones in the cytosol: from nascent chain to folded protein. Science *295*, 1852-1858.

Hay,B., Barry,R.A., Lieberburg,I., Prusiner,S.B., and Lingappa,V.R. (1987). Biogenesis and transmembrane orientation of the cellular isoform of the scrapie prion protein. Mol. Cell Biol. *7*, 914-920.

Heath,C.A., Barker,R.A., Esmonde,T.F., Harvey,P., Roberts,R., Trend,P., Head,M.W., Smith,C., Bell,J.E., Ironside,J.W., Will,R.G., and Knight,R.S. (2006). Dura mater-associated Creutzfeldt-Jakob disease: experience from surveillance in the UK. J. Neurol. Neurosurg. Psychiatry *77*, 880-882.

Hegde,R.S., Mastrianni,J.A., Scott,M.R., DeFea,K.A., Tremblay,P., Torchia,M., DeArmond,S.J., Prusiner,S.B., and Lingappa,V.R. (1998). A transmembrane from of the prion protein in neurodegenerative disease. Science *279*, 827-834.

Hegde,R.S., Tremblay,P., Groth,D., DeArmond,S., Prusiner,S.B., and Lingappa,V.R. (1999). Transmissible and genetic prion diseases share a common pathway of neurodegeneration. Nature *402*, 822-826.

Heller,U., Winklhofer,K.F., Heske,J., Reintjes,A., and Tatzelt,J. (2003). Post-translational import of the prion protein into the endoplasmic reticulum interferes with cell viability: a critical role for the putative transmembrane domain. J. Biol. Chem. *278*, 36139-36147.

Heppner,F.L., Musahl,C., Arrighi,I., Klein,M.A., Rülicke,T., Oesch,B., Zinkernagel,R.M., Kalinke,U., and Aguzzi,A. (2001). Prevention of scrapie pathogenesis by transgenic expression of anti-prion protein antibodies. Science *294*, 178-182.

Hershko,A. and Ciechanover,A. (1998). The ubiquitin system. Annu. Rev. Biochem. *67*, 425-479.

Hetz,C., Castilla,J., and Soto,C. (2007). Perturbation of endoplasmic reticulum homeostasis facilitates prion replication. J. Biol. Chem. *282*, 12725-12733.

Hetz,C., Russelakis-Carneiro,M., Maundrell,K., Castilla,J., and Soto,C. (2003). Caspase-12 and endoplasmic reticulum stress mediate neurotoxicity of pathological prion protein. EMBO J. *22*, 5435-5445.

Hill AF, Joiner S, Wadsworth J, Sidle,K.C., Bell,J.E., Budka,H., Ironside,J.W., and Collinge J (2003). Molecular classification of sporadic Creutzfeldt-Jakob disease. Brain *126*, 1333-1346.

Hill,A.F., Butterworth,R.J., Joiner,S., Jackson,G., Rossor,M.N., Thomas,D.J., Frosh,A., Tolley,N., Bell,J.E., Spencer,M., King,A., Al Sarraj,S., Ironside,J.W., Lantos,P.L., and Collinge,J. (1999). Investigation of variant Creutzfeldt-Jakob disease and other human prion diseases with tonsil biopsy samples. Lancet *353*, 183-189.

Hill,A.F. and Collinge,J. (2003a). Subclinical prion infection. Trends Microbiol. *11*, 578-584.

Hill,A.F. and Collinge,J. (2003b). Subclinical prion infection in humans and animals. Br. Med. Bull. *66*, 161-170.

Hill,A.F., Desbruslais,M., Joiner,S., Sidle,K.C., Gowland,I., Collinge,J., Doey,L.J., and Lantos,P. (1997). The same prion strain causes vCJD and BSE. Nature *389*, 448-50, 526.

Hill,A.F., Joiner,S., Beck,J.A., Campbell,T.A., Dickinson,A., Poulter,M., Wadsworth,J.D., and Collinge,J. (2006). Distinct glycoform ratios of protease resistant prion protein associated with PRNP point mutations. Brain *129*, 676-685.

Hill,A.F., Joiner,S., Linehan,J., Desbruslais,M., Lantos,P.L., and Collinge,J. (2000). Species-barrier-independent prion replication in apparently resistant species. Proc. Natl. Acad. Sci. U. S. A *97*, 10248-10253.

Hill,A.F., Joiner,S., Wadsworth,J.D., Sidle,K.C., Bell,J.E., Budka,H., Ironside,J.W., and Collinge,J. (2003). Molecular classification of sporadic Creutzfeldt-Jakob disease. Brain *126*, 1333-1346.

Hilton,D.A., Ghani,A.C., Conyers,L., Edwards,P., McCardle,L., Penney,M., Ritchie,D., and Ironside,J.W. (2002). Accumulation of prion protein in tonsil and appendix: review of tissue samples. BMJ *325*, 633-634.

Hilton,D.A., Ghani,A.C., Conyers,L., Edwards,P., McCardle,L., Ritchie,D., Penney,M., Hegazy,D., and Ironside,J.W. (2004). Prevalence of lymphoreticular prion protein accumulation in UK tissue samples. J. Pathol. *203*, 733-739.

Hoffman,L. and Rechsteiner,M. (1994). Activation of the multicatalytic protease. The 11 S regulator and 20 S ATPase complexes contain distinct 30-kilodalton subunits. J. Biol. Chem. *269*, 16890-16895.

Hope,J., Morton,L.J., Farquhar,C.F., Multhaup,G., Beyreuther,K., and Kimberlin,R.H. (1986). The major polypeptide of scrapie-associated fibrils (SAF) has the same size, charge distribution and N-terminal protein sequence as predicted for the normal brain protein (PrP). EMBO J. *5*, 2591-2597.

Horn,I.R., van den Berg,B.M., Moestrup,S.K., Pannekoek,H., and van Zonneveld,A.J. (1998). Plasminogen activator inhibitor 1 contains a cryptic high affinity receptor binding site that is exposed upon complex formation with tissue-type plasminogen activator. Thromb. Haemost. *80*, 822-828.

Hosszu,L.L.P., Baxter,N.J., Jackson GS, Power,A., Clarke A, Waltho,J.P., Craven,C.J., and Collinge J (1999). Structural mobility of the human prion protein probed by backbone hydrogen exchange. Nature Struct. Biol. *6*, 740-743.

Hsiao,K., Baker,H.F., Crow,T.J., Poulter,M., Owen,F., Terwilliger,J.D., Westaway,D., Ott,J., and Prusiner,S.B. (1989). Linkage of a prion protein missense variant to Gerstmann-Straussler syndrome. Nature *338*, 342-345.

Hsiao,K.K., Scott,M., Foster,D., Groth,D.F., DeArmond,S.J., and Prusiner,S.B. (1990). Spontaneous neurodegeneration in transgenic mice with mutant prion protein. Science *250*, 1587-1590.

Hundt,C., Peyrin,J.M., Haïk,S., Gauczynski,S., Leucht,C., Rieger,R., Riley,M.L., Deslys,J.P., Dormont,D., Lasmézas,C.I., and Weiss,S. (2001). Identification of interaction domains of the prion protein with its 37-kDa/67-kDa laminin receptor. EMBO J. *20*, 5876-5886.

Hunter,G.D. and Millson,G.C. (1967). Attempts to release the scrapie agent from tissue debris. J. Comp Pathol. *77*, 301-307.

Hwang,J.S., Hwang,J.S., Chang,I., and Kim,S. (2007). Age-associated decrease in proteasome content and activities in human dermal fibroblasts: restoration of normal level of proteasome subunits reduces aging markers in fibroblasts from elderly persons. J. Gerontol. A Biol. Sci. Med. Sci. *62*, 490-499.

Ivanova,L., Barmada,S., Kummer,T., and Harris,D.A. (2001). Mutant prion proteins are partially retained in the endoplasmic reticulum. J. Biol. Chem. *276*, 42409-42421.

Iwata,A., Christianson,J.C., Bucci,M., Ellerby,L.M., Nukina,N., Forno,L.S., and Kopito,R.R. (2005a). Increased susceptibility of cytoplasmic over nuclear polyglutamine aggregates to autophagic degradation. Proc. Natl. Acad. Sci. U. S. A *102*, 13135-13140.

Iwata,A., Riley,B.E., Johnston,J.A., and Kopito,R.R. (2005b). HDAC6 and microtubules are required for autophagic degradation of aggregated huntingtin. J. Biol. Chem. *280*, 40282-40292.

Jackson,G.S., Hosszu,L.L., Power,A., Hill,A.F., Kenney,J., Saibil,H., Craven,C.J., Waltho,J.P., Clarke,A.R., and Collinge,J. (1999). Reversible conversion of monomeric human prion protein between native and fibrilogenic conformations. Science *283*, 1935-1937.

Jackson,G.S., Murray,I., Hosszu,L.L., Gibbs,N., Waltho,J.P., Clarke,A.R., and Collinge,J. (2001). Location and properties of metal-binding sites on the human prion protein. Proc. Natl. Acad. Sci. U. S. A *98*, 8531-8535.

Jeffrey,M., Goodsir,C.M., Bruce,M.E., McBride,P.A., Scott,J.R., and Halliday,W.G. (1992a). Infection specific prion protein (PrP) accumulates on neuronal plasmalemma in scrapie infected mice. Neurosci. Lett. *147*, 106-109.

Jeffrey,M., Scott,J.R., Williams,A., and Fraser,H. (1992b). Ultrastructural features of spongiform encephalopathy transmitted to mice from three species of bovidae. Acta Neuropathol (Berl) *84*, 559-569.

Ji,Z.S., Mullendorff,K., Cheng,I.H., Miranda,R.D., Huang,Y., and Mahley,R.W. (2006). Reactivity of apolipoprotein E4 and amyloid beta peptide: lysosomal stability and neurodegeneration. J. Biol. Chem. *281*, 2683-2692.

Jin,T., Gu,Y., Zanusso,G., Sy,M., Kumar,A., Cohen,M., Gambetti,P., and Singh,N. (2000). The chaperone protein BiP binds to a mutant prion protein and mediates its degradation by the proteasome. J. Biol. Chem. *275*, 38699-38704.

Jobling,M.F., Stewart,L.R., White,A.R., McLean,C., Friedhuber,A., Maher,F., Beyreuther,K., Masters,C.L., Barrow,C.J., Collins,S.J., and Cappai,R. (1999). The hydrophobic core sequence modulates the neurotoxic and secondary structure properties of the prion peptide 106-126. J. Neurochem. *73*, 1557-1565.

Johnston,J.A., Ward,C.L., and Kopito,R.R. (1998). Aggresomes: a cellular response to misfolded proteins. J. Cell Biol. *143*, 1883-1898.

Kabeya,Y., Mizushima,N., Ueno,T., Yamamoto,A., Kirisako,T., Noda,T., Kominami,E., Ohsumi,Y., and Yoshimori,T. (2000). LC3, a mammalian homologue of yeast Apg8p, is localized in autophagosome membranes after processing. EMBO J. *19*, 5720-5728.

Kanaani,J., Prusiner,S.B., Diacovo,J., Baekkeskov,S., and Legname,G. (2005). Recombinant prion protein induces rapid polarization and development of synapses in embryonic rat hippocampal neurons in vitro. J. Neurochem. *95*, 1373-1386.

Kaneko,K., Vey,M., Scott,M., Pilkuhn,S., Cohen,F.E., and Prusiner,S.B. (1997). COOH-terminal sequence of the cellular prion protein directs subcellular trafficking and controls conversion into the scrapie isoform. Proc. Natl. Acad Sci U. S. A *94*, 2333-2338.

Kang,S.C., Brown,D.R., Whiteman,M., Li,R., Pan,T., Perry,G., Wisniewski,T., Sy,M.S., and Wong,B.S. (2004). Prion protein is ubiquitinated after developing protease resistance in the brains of scrapie-infected mice. J. Pathol. *203*, 603-608.

Kanu,N., Imokawa,Y., Drechsel,D.N., Williamson,R.A., Birkett,C.R., Bostock,C.J., and Brockes,J.P. (2002). Transfer of scrapie prion infectivity by cell contact in culture
246. Curr. Biol. *12*, 523-530.

Kayed,R., Head,E., Thompson,J.L., McIntire,T.M., Milton,S.C., Cotman,C.W., and Glabe,C.G. (2003). Common structure of soluble amyloid oligomers implies common mechanism of pathogenesis. Science *300*, 486-489.

Kegel,K.B., Kim,M., Sapp,E., McIntyre,C., Castano,J.G., Aronin,N., and DiFiglia,M. (2000). Huntingtin Expression Stimulates Endosomal-Lysosomal Activity, Endosome Tubulation, and Autophagy. J. Neurosci. *20*, 7268-7278.

Keller,J.N., Gee,J., and Ding,Q. (2002). The proteasome in brain aging. Ageing Res. Rev. *1*, 279-293.

Khalili-Shirazi,A., Summers,L., Linehan J, Mallinson,G., Anstee,D., Hawke,S., Jackson GS, and Collinge J (2005). PrP glycoforms are associated in a strain-specific ratio in native PrPSc. J. Gen. Virol. *86*, 2635-2644.

Khosravani,H., Zhang,Y., Tsutsui,S., Hameed,S., Altier,C., Hamid,J., Chen,L., Villemaire,M., Ali,Z., Jirik,F.R., and Zamponi,G.W. (2008). Prion protein attenuates excitotoxicity by inhibiting NMDA receptors. J. Gen. Physiol *131*, i5.

Kimberlin,R.H. and Marsh,R.F. (1975). Comparison of scrapie and transmissible mink encephalopathy in hamsters. I. Biochemical studies of brain during development of disease. J. Infect. Dis. *131*, 97-103.

Kirkpatrick,D.S., Hathaway,N.A., Hanna,J., Elsasser,S., Rush,J., Finley,D., King,R.W., and Gygi,S.P. (2006). Quantitative analysis of in vitro ubiquitinated cyclin B1 reveals complex chain topology. Nat. Cell Biol. *8*, 700-710.

Kisselev,A.F., Akopian,T.N., and Goldberg,A.L. (1998). Range of sizes of peptide products generated during degradation of different proteins by archaeal proteasomes. J. Biol. Chem. *273*, 1982-1989.

Kisselev,A.F., Akopian,T.N., Woo,K.M., and Goldberg,A.L. (1999). The sizes of peptides generated from protein by mammalian 26 and 20 S proteasomes. Implications for understanding the degradative mechanism and antigen presentation. J. Biol. Chem. *274*, 3363-3371.

Kisselev,A.F., Callard,A., and Goldberg,A.L. (2006). Importance of the different proteolytic sites of the proteasome and the efficacy of inhibitors varies with the protein substrate. J. Biol. Chem. *281*, 8582-8590.

Kisselev,A.F. and Goldberg,A.L. (2001). Proteasome inhibitors: from research tools to drug candidates. Chem. Biol. *8*, 739-758.

Kisselev,A.F. and Goldberg,A.L. (2005). Monitoring activity and inhibition of 26S proteasomes with fluorogenic peptide substrates. Methods Enzymol. *398*, 364-378.

Kisselev,A.F., Kaganovich,D., and Goldberg,A.L. (2002). Binding of hydrophobic peptides to several non-catalytic sites promotes peptide hydrolysis by all active sites of 20 S proteasomes. Evidence for peptide-induced channel opening in the alpha-rings. J. Biol. Chem. *277*, 22260-22270.

Klionsky,D.J., Abeliovich,H., Agostinis,P., Agrawal,D.K., Aliev,G., Askew,D.S., Baba,M., Baehrecke,E.H., Bahr,B.A., Ballabio,A., Bamber,B.A., Bassham,D.C., Bergamini,E., Bi,X., Biard-Piechaczyk,M., Blum,J.S., Bredesen,D.E., Brodsky,J.L., Brumell,J.H., Brunk,U.T., Bursch,W., Camougrand,N., Cebollero,E., Cecconi,F., Chen,Y., Chin,L.S., Choi,A., Chu,C.T., Chung,J., Clarke,P.G., Clark,R.S., Clarke,S.G., Clave,C., Cleveland,J.L., Codogno,P., Colombo,M.I., Coto-Montes,A., Cregg,J.M., Cuervo,A.M., Debnath,J., Demarchi,F., Dennis,P.B., Dennis,P.A., Deretic,V., Devenish,R.J., Di Sano,F., Dice,J.F., DiFiglia,M., Dinesh-Kumar,S., Distelhorst,C.W., Djavaheri-Mergny,M., Dorsey,F.C., Droge,W., Dron,M., Dunn,W.A., Jr., Duszenko,M., Eissa,N.T., Elazar,Z., Esclatine,A., Eskelinen,E.L., Fesus,L., Finley,K.D., Fuentes,J.M., Fueyo,J., Fujisaki,K., Galliot,B., Gao,F.B., Gewirtz,D.A., Gibson,S.B., Gohla,A., Goldberg,A.L., Gonzalez,R., Gonzalez-Estevez,C., Gorski,S., Gottlieb,R.A., Haussinger,D., He,Y.W., Heidenreich,K., Hill,J.A., Hoyer-Hansen,M., Hu,X., Huang,W.P., Iwasaki,A., Jaattela,M., Jackson,W.T., Jiang,X., Jin,S., Johansen,T., Jung,J.U., Kadowaki,M., Kang,C., Kelekar,A., Kessel,D.H., Kiel,J.A., Kim,H.P., Kimchi,A., Kinsella,T.J., Kiselyov,K., Kitamoto,K., Knecht,E., Komatsu,M., Kominami,E., Kondo,S., Kovacs,A.L., Kroemer,G., Kuan,C.Y., Kumar,R., Kundu,M., Landry,J., Laporte,M., Le,W., Lei,H.Y., Lenardo,M.J., Levine,B., Lieberman,A., Lim,K.L., Lin,F.C., Liou,W., Liu,L.F., Lopez-Berestein,G., Lopez-Otin,C., Lu,B., Macleod,K.F., Malorni,W., Martinet,W., Matsuoka,K., Mautner,J., Meijer,A.J., Melendez,A., Michels,P., Miotto,G., Mistiaen,W.P., Mizushima,N., Mograbi,B., Monastyrska,I., Moore,M.N., Moreira,P.I., Moriyasu,Y., Motyl,T., Munz,C., Murphy,L.O., Naqvi,N.I., Neufeld,T.P., Nishino,I., Nixon,R.A., Noda,T., Nurnberg,B., Ogawa,M., Oleinick,N.L., Olsen,L.J., Ozpolat,B., Paglin,S., Palmer,G.E., Papassideri,I., Parkes,M., Perlmutter,D.H., Perry,G., Piacentini,M., Pinkas-Kramarski,R., Prescott,M., Proikas-Cezanne,T., Raben,N., Rami,A., Reggiori,F., Rohrer,B., Rubinsztein,D.C., Ryan,K.M., Sadoshima,J., Sakagami,H., Sakai,Y., Sandri,M., Sasakawa,C., Sass,M., Schneider,C.,

Seglen,P.O., Seleverstov,O., Settleman,J., Shacka,J.J., Shapiro,I.M., Sibirny,A., Silva-Zacarin,E.C., Simon,H.U., Simone,C., Simonsen,A., Smith,M.A., Spanel-Borowski,K., Srinivas,V., Steeves,M., Stenmark,H., Stromhaug,P.E., Subauste,C.S., Sugimoto,S., Sulzer,D., Suzuki,T., Swanson,M.S., Tabas,I., Takeshita,F., Talbot,N.J., Talloczy,Z., Tanaka,K., Tanaka,K., Tanida,I., Taylor,G.S., Taylor,J.P., Terman,A., Tettamanti,G., Thompson,C.B., Thumm,M., Tolkovsky,A.M., Tooze,S.A., Truant,R., Tumanovska,L.V., Uchiyama,Y., Ueno,T., Uzcategui,N.L., van,d.K., I, Vaquero,E.C., Vellai,T., Vogel,M.W., Wang,H.G., Webster,P., Wiley,J.W., Xi,Z., Xiao,G., Yahalom,J., Yang,J.M., Yap,G., Yin,X.M., Yoshimori,T., Yu,L., Yue,Z., Yuzaki,M., Zabirnyk,O., Zheng,X., Zhu,X., and Deter,R.L. (2008). Guidelines for the use and interpretation of assays for monitoring autophagy in higher eukaryotes. Autophagy. *4*, 151-175.

Klionsky,D.J. and Ohsumi,Y. (1999). Vacuolar import of proteins and organelles from the cytoplasm. Annu. Rev. Cell Dev. Biol. *15*, 1-32.

Klohn,P.C., Stoltze,L., Flechsig,E., Enari,M., and Weissmann,C. (2003). A quantitative, highly sensitive cell-based infectivity assay for mouse scrapie prions. Proc. Natl. Acad. Sci. U. S. A *100*, 11666-11671.

Klyubin,I., Walsh,D.M., Lemere,C.A., Cullen,W.K., Shankar,G.M., Betts,V., Spooner,E.T., Jiang,L., Anwyl,R., Selkoe,D.J., and Rowan,M.J. (2005). Amyloid beta protein immunotherapy neutralizes Abeta oligomers that disrupt synaptic plasticity in vivo. Nat. Med. *11*, 556-561.

Knaus,K.J., Morillas,M., Swietnicki,W., Malone,M., Surewicz,W.K., and Yee,V.C. (2001). Crystal structure of the human prion protein reveals a mechanism for oligomerization. Nat. Struct. Biol. *8*, 770-774.

Knight,R. (2006). Creutzfeldt-Jakob disease: a rare cause of dementia in elderly persons. Clin. Infect. Dis. *43*, 340-346.

Kocisko,D.A., Come,J.H., Priola,S.A., Chesebro,B., Raymond,G.J., Lansbury,P.T., and Caughey,B. (1994). Cell-free formation of protease-resistant prion protein. Nature *370*, 471-474.

Kohler,A., Cascio,P., Leggett,D.S., Woo,K.M., Goldberg,A.L., and Finley,D. (2001). The axial channel of the proteasome core particle is gated by the Rpt2 ATPase and controls both substrate entry and product release. Mol. Cell *7*, 1143-1152.

Koike,M., Nakanishi,H., Saftig,P., Ezaki,J., Isahara,K., Ohsawa,Y., Schulz-Schaeffer,W., Watanabe,T., Waguri,S., Kametaka,S., Shibata,M., Yamamoto,K., Kominami,E., Peters,C., von Figura,K., and Uchiyama,Y. (2000). Cathepsin D deficiency induces lysosomal storage with ceroid lipofuscin in mouse CNS neurons. J. Neurosci. *20*, 6898-6906.

Koike,M., Shibata,M., Waguri,S., Yoshimura,K., Tanida,I., Kominami,E., Gotow,T., Peters,C., von Figura,K., Mizushima,N., Saftig,P., and Uchiyama,Y. (2005). Participation of autophagy

in storage of lysosomes in neurons from mouse models of neuronal ceroid-lipofuscinoses (Batten disease). Am. J. Pathol. *167*, 1713-1728.

Komatsu,M., Waguri,S., Chiba,T., Murata,S., Iwata,J., Tanida,I., Ueno,T., Koike,M., Uchiyama,Y., Kominami,E., and Tanaka,K. (2006). Loss of autophagy in the central nervous system causes neurodegeneration in mice. Nature *441*, 880-884.

Komatsu,M., Wang,Q.J., Holstein,G.R., Friedrich,V.L., Jr., Iwata,J., Kominami,E., Chait,B.T., Tanaka,K., and Yue,Z. (2007). Essential role for autophagy protein Atg7 in the maintenance of axonal homeostasis and the prevention of axonal degeneration. Proc. Natl. Acad. Sci. U. S. A *104*, 14489-14494.

Kouroku,Y., Fujita,E., Tanida,I., Ueno,T., Isoai,A., Kumagai,H., Ogawa,S., Kaufman,R.J., Kominami,E., and Momoi,T. (2007). ER stress (PERK/eIF2alpha phosphorylation) mediates the polyglutamine-induced LC3 conversion, an essential step for autophagy formation. Cell Death. Differ. *14*, 230-239.

Kovacs,G.G., Preusser,M., Strohschneider,M., and Budka,H. (2005). Subcellular localization of disease-associated prion protein in the human brain. Am. J. Pathol. *166*, 287-294.

Kristiansen,M., Messenger,M.J., Klohn,P.C., Brandner,S., Wadsworth,J.D., Collinge,J., and Tabrizi,S.J. (2005). Disease-related prion protein forms aggresomes in neuronal cells leading to caspase activation and apoptosis. J. Biol. Chem. *280*, 38851-38861.

Kubler,E., Oesch,B., and Raeber,A.J. (2003). Diagnosis of prion diseases. Br. Med. Bull. *66*, 267-279.

Kuhlbrodt,K., Mouysset,J., and Hoppe,T. (2005). Orchestra for assembly and fate of polyubiquitin chains. Essays Biochem. *41*, 1-14.

Kundu,B., Maiti,N.R., Jones,E.M., Surewicz,K.A., Vanik,D.L., and Surewicz,W.K. (2003). Nucleation-dependent conformational conversion of the Y145Stop variant of human prion protein: structural clues for prion propagation. Proc. Natl. Acad. Sci. U. S. A *100*, 12069-12074.

Kundu,M. and Thompson,C.B. (2008). Autophagy: basic principles and relevance to disease. Annu. Rev. Pathol. *3*, 427-455.

Kuwahara,C., Takeuchi,A.M., Nishimura,T., Haraguchi,K., Kubosaki,A., Matsumoto,Y., Saeki,K., Yokoyama,T., Itohara,S., and Onodera,T. (1999). Prions prevent neuronal cell-line death. Nature *400*, 225-226.

Kuwajima,K. (1996). The molten globule state of alpha-lactalbumin. FASEB J. *10*, 102-109.

Lasmezas,C.I., Deslys,J.P., Robain,O., Jaegly,A., Beringue,V., Peyrin,J.M., Fournier,J.G., Hauw,J.J., Rossier,J., and Dormont,D. (1997). Transmission of the BSE agent to mice in the absence of detectable abnormal prion protein. Science *275*, 402-405.

Lee,C.K., Weindruch,R., and Prolla,T.A. (2000). Gene-expression profile of the ageing brain in mice. Nat. Genet. *25*, 294-297.

Lee,D.H. and Goldberg,A.L. (1998). Proteasome inhibitors: valuable new tools for cell biologists. Trends Cell Biol. *8*, 397-403.

Lee,H.S., Brown,P., Cervenakova,L., Garruto,R.M., Alpers,M.P., Gajdusek,D.C., and Goldfarb,L.G. (2001a). Increased susceptibility to Kuru of carriers of the PRNP 129 methionine/methionine genotype. J. Infect. Dis. *183*, 192-196.

Lee,K.S., Magalhaes,A.C., Zanata,S.M., Brentani,R.R., Martins,V.R., and Prado,M.A.M. (2001b). Internalization of mammalian fluorescent cellular prion protein and N-terminal deletion mutants in living cells. J. Neurochem. *79*, 79-87.

Leggett,M.M., Dukes,J., and Pirie,H.M. (1990). A spongiform encephalopathy in a cat. Vet. Rec. *127*, 586-588.

Legname,G., Baskakov,I.V., Nguyen,H.O., Riesner,D., Cohen,F.E., DeArmond,S.J., and Prusiner,S.B. (2004). Synthetic mammalian prions. Science *305*, 673-676.

Levine,B. and Kroemer,G. (2008). Autophagy in the pathogenesis of disease. Cell *132*, 27-42.

Lewis,P.A., Properzi,F., Prodromidou,K., Clarke,A.R., Collinge,J., and Jackson,G.S. (2006). Removal of the glycosylphosphatidylinositol anchor from PrP(Sc) by cathepsin D does not reduce prion infectivity. Biochem. J. *395*, 443-448.

Li,A., Barmada,S.J., Roth,K.A., and Harris,D.A. (2007a). N-terminally deleted forms of the prion protein activate both Bax-dependent and Bax-independent neurotoxic pathways. J. Neurosci. *27*, 852-859.

Li,A., Christensen,H.M., Stewart,L.R., Roth,K.A., Chiesa,R., and Harris,D.A. (2007b). Neonatal lethality in transgenic mice expressing prion protein with a deletion of residues 105-125. EMBO J. *26*, 548-558.

Li,D. (2006). Selective degradation of the IkappaB kinase (IKK) by autophagy. Cell Res. *16*, 855-856.

Liberski,P.P., Asher,D.M., Yanagihara,R., Gibbs,C.J.Jr., and Gajdusek,D.C. (1989). Serial ultrastructural studies of scrapie in hamsters. J. Comp. Pathol. *101*, 429-442.

Liberski,P.P., Brown,D.R., Sikorska,B., Caughey,B., and Brown,P. (2008). Cell death and autophagy in prion diseases (transmissible spongiform encephalopathies). Folia Neuropathol. *46*, 1-25.

Liberski,P.P., Gajdusek,D.C., and Brown,P. (2002). How do neurons degenerate in prion diseases or transmissible spongiform encephalopathies (TSEs): neuronal autophagy revisited. Acta Neurobiol. Exp. (Warsz.) *62*, 141-147.

Liberski,P.P., Streichenberger,N., Giraud,P., Soutrenon,M., Meyronnet,D., Sikorska,B., and Kopp,N. (2005). Ultrastructural pathology of prion diseases revisited: brain biopsy studies. Neuropathol. Appl. Neurobiol. *31*, 88-96.

Liberski,P.P., Yanagihara,R., Gibbs,C.J., Jr., and Gajdusek,D.C. (1992a). Neuronal autophagic vacuoles in experimental scrapie and Creutzfeldt-Jakob disease. Acta Neuropathol. *83*, 134-139.

Liberski,P.P., Yanagihara,R., Wells,G.A., Gibbs,C.J., Jr., and Gajdusek,D.C. (1992b). Comparative ultrastructural neuropathology of naturally occurring bovine spongiform encephalopathy and experimentally induced scrapie and Creutzfeldt-Jakob disease. J. Comp Pathol. *106*, 361-381.

Linden,R., Martins,V.R., Prado,M.A., Cammarota,M., Izquierdo,I., and Brentani,R.R. (2008). Physiology of the prion protein. Physiol. Rev. *88*, 673-728.

Lindenbaum,S. (1979). Kuru Sorcery: Disease and Danger in the New Guinea Highlands. Palo Alto: Mayfield).

Lindsten,K., Menendez-Benito,V., Masucci,M.G., and Dantuma,N.P. (2003). A transgenic mouse model of the ubiquitin/proteasome system. Nat. Biotechnol. *21*, 897-902.

Llewelyn,C.A., Hewitt,P.E., Knight,R.S.G., Amar,K., Cousens,S., Mackenzie,J., and Will,R.G. (2004). Possible transmission of variant Creutzfeldt-Jakob disease by blood transfusion. Lancet *363*, 417-421.

Lloyd,S.E., Onwuazor,O.N., Beck,J.A., Mallinson,G., Farrall,M., Targonski,P., Collinge,J., and Fisher,E.M. (2001). Identification of multiple quantitative trait loci linked to prion disease incubation period in mice. Proc. Natl. Acad. Sci. U. S. A *98*, 6279-6283.

Lloyd,S.E., Uphill,J.B., Targonski,P.V., Fisher,E.M., and Collinge,J. (2002). Identification of genetic loci affecting mouse-adapted bovine spongiform encephalopathy incubation time in mice. Neurogenetics. *4*, 77-81.

Lorenz,H., Windl,O., and Kretzschmar,H.A. (2002). Cellular phenotyping of secretory and nuclear prion proteins associated with inherited prion diseases. J. Biol. Chem. *277*, 8508-8516.

Lowe,J., Fergusson,J., Kenward,N., Laszlo,L., Landon,M., Farquhar,C., Brown,J., Hope,J., and Mayer,R.J. (1992). Immunoreactivity to ubiquitin-protein conjugates is present early in the disease process in the brains of scrapie-infected mice. J Pathol. *168*, 169-177.

Lowe,J., Stock,D., Jap,B., Zwickl,P., Baumeister,W., and Huber,R. (1995). Crystal structure of the 20S proteasome from the archaeon T. acidophilum at 3.4 A resolution. Science *268*, 533-539.

Ma,J. and Lindquist,S. (2002). Conversion of PrP to a self-perpetuating PrPSc-like conformation in the cytosol. Science *298*, 1785-1788.

Ma,J., Wollmann,R., and Lindquist,S. (2002). Neurotoxicity and neurodegeneration when PrP accumulates in the cytosol. Science *298*, 1781-1785.

Ma,J.Y. and Lindquist,S. (2001). Wild-type PrP and a mutant associated with prion disease are subject to retrograde transport and proteasome degradation. Proc. Natl. Acad. Sci. USA *98*, 14955-14960.

Madore,N., Smith,K.L., Graham,C.H., Jen,A., Brady,K., Hall,S., and Morris,R. (1999). Functionally different GPI proteins are organized in different domains on the neuronal surface. EMBO J. *18*, 6917-6926.

Magalhaes,A.C., Silva,J.A., Lee,K.S., Martins,V.R., Prado,V.F., Ferguson,S.S., Gomez,M.V., Brentani,R.R., and Prado,M.A. (2002). Endocytic intermediates involved with the intracellular trafficking of a fluorescent cellular prion protein. J. Biol. Chem. *277*, 33311-33318.

Mallucci,G. and Collinge,J. (2005). Rational targeting for prion therapeutics. Nat. Rev. Neurosci. *6*, 23-34.

Mallucci,G., Dickinson,A., Linehan,J., Klohn,P.C., Brandner,S., and Collinge,J. (2003). Depleting neuronal PrP in prion infection prevents disease and reverses spongiosis. Science *302*, 871-874.

Mallucci,G.R., Ratte,S., Asante,E.A., Linehan,J., Gowland,I., Jefferys,J.G., and Collinge,J. (2002). Post-natal knockout of prion protein alters hippocampal CA1 properties, but does not result in neurodegeneration. EMBO J. *21*, 202-210.

Mallucci,G.R., White,M.D., Farmer,M., Dickinson,A., Khatun,H., Powell,A.D., Brandner,S., Jefferys,J.G., and Collinge,J. (2007). Targeting cellular prion protein reverses early cognitive deficits and neurophysiological dysfunction in prion-infected mice. Neuron *53*, 325-335.

Malone,T.G., Marsh,R.F., Hanson,R.P., and Semancik,J.S. (1978). Membrane-free scrapie activity. J. Virol. *25*, 933-935.

Mange,A., Crozet,C., Lehmann,S., and Beranger,F. (2004). Scrapie-like prion protein is translocated to the nuclei of infected cells independently of proteasome inhibition and interacts with chromatin. J. Cell Sci. *117*, 2411-2416.

Manson,J.C., Clarke A, Hooper,M.L., Aitchison,L., McConnell,I., and Hope,J. (1994). 129/Ola mice carrying a null mutation in PrP that abolishes mRNA production are developmentally normal. Mol. Neurobiol. *8*, 121-127.

Marsh,R.F. (1992). Transmissible Mink Encephalopathy. In Prion Diseases of Humans and Animals, S.B.Prusiner, Collinge J, J.Powell, and B.Anderton, eds. (London: Ellis Horwood).

Marsh,R.F., Bessen,R.A., Lehmann,S., and Hartsough,G.R. (1991). Epidemiological and experimental studies on a new incident of transmissible mink encephalopathy. J. Gen. Virol. *72*, 589-594.

Martins,S.M., Frosoni,D.J., Martinez,A.M., De Felice,F.G., and Ferreira,S.T. (2006). Formation of soluble oligomers and amyloid fibrils with physical properties of the scrapie isoform of the prion protein from the C-terminal domain of recombinant murine prion protein mPrP-(121-231). J. Biol. Chem. *281*, 26121-26128.

Masters,C.L., Gajdusek,D.C., and Gibbs,C.J.Jr. (1981a). Creutzfeldt-Jakob disease virus isolations from the Gerstmann- Straussler syndrome with an analysis of the various forms of amyloid plaque deposition in the virus-induced spongiform encephalopathies. Brain *104*, 559-588.

Masters,C.L., Gajdusek,D.C., and Gibbs,C.J.Jr. (1981b). The familial occurrence of Creutzfeldt-Jakob disease and Alzheimer's disease. Brain *104*, 535-558.

Mathiason,C.K., Powers,J.G., Dahmes,S.J., Osborn,D.A., Miller,K.V., Warren,R.J., Mason,G.L., Hays,S.A., Hayes-Klug,J., Seelig,D.M., Wild,M.A., Wolfe,L.L., Spraker,T.R., Miller,M.W., Sigurdson,C.J., Telling,G.C., and Hoover,E.A. (2006). Infectious prions in the saliva and blood of deer with chronic wasting disease. Science *314*, 133-136.

Mattson,M.P. and Camandola,S. (2001). NF-kappaB in neuronal plasticity and neurodegenerative disorders. J. Clin. Invest. *107*, 247-254.

McCray,B.A. and Taylor,J.P. (2008). The role of autophagy in age-related neurodegeneration. Neurosignals. *16*, 75-84.

McKinley,M.P., Taraboulos,A., Kenaga,L., Serban,D., Stieber,A., DeArmond,S.J., Prusiner,S.B., and Gonatas,N. (1991). Ultrastructural localization of scrapie prion proteins in cytoplasmic vesicles of infected cultured cells. Lab Invest. *65*, 622-630.

McNaught,K.S., Belizaire,R., Isacson,O., Jenner,P., and Olanow,C.W. (2003). Altered proteasomal function in sporadic Parkinson's disease. Exp. Neurol. *179*, 38-46.

Mead,S. (2006). Prion disease genetics. Eur. J. Hum. Genet. *14*, 273-281.

Mead,S., Mahal,S.P., Beck,J., Campbell,T., Farrall,M., Fisher,E., and Collinge,J. (2001). Sporadic--but not variant--Creutzfeldt-Jakob disease is associated with polymorphisms upstream of PRNP exon 1. Am. J. Hum. Genet. *69*, 1225-1235.

Mead,S., Poulter,M., Beck,J., Webb,T.E., Campbell,T.A., Linehan,J.M., Desbruslais,M., Joiner,S., Wadsworth,J.D., King,A., Lantos,P., and Collinge,J. (2006). Inherited prion disease with six octapeptide repeat insertional mutation--molecular analysis of phenotypic heterogeneity. Brain *129*, 2297-2317.

Mead,S., Poulter,M., Uphill,J., Beck,J., Whitfield,J., Webb,T.E., Campbell,T., Adamson,G., Deriziotis,P., Tabrizi,S.J., Hummerich,H., Verzilli,C., Alpers,M.P., Whittaker,J.C., and Collinge,J. (2009). Genetic risk factors for variant Creutzfeldt-Jakob disease: a genome-wide association study. Lancet Neurol. *8*, 57-66.

Mead,S., Stumpf,M.P., Whitfield,J., Beck,J.A., Poulter,M., Campbell,T., Uphill,J.B., Goldstein,D., Alpers,M., Fisher,E.M., and Collinge,J. (2003). Balancing selection at the prion protein gene consistent with prehistoric kurulike epidemics. Science *300*, 640-643.

Medori,R., Montagna,P., Tritschler,H.J., LeBlanc,A., Cortelli,P., Tinuper,P., Lugaresi,E., and Gambetti,P. (1992). Fatal familial insomnia: A second kindred with mutation of prion protein gene at codon 178. Neurology *42*, 669-670.

Mehlhorn,I., Groth,D., Stöckel,J., Moffat,B., Reilly,D., Yansura,D., Willett,W.S., Baldwin,M., Fletterick,R., Cohen,F.E., Vandlen,R., Henner,D., and Prusiner,S.B. (1996). High-level expression and characterization of a purified 142-residue polypeptide of the prion protein. Biochemistry *35*, 5528-5537.

Menendez-Benito,V., Verhoef,L.G., Masucci,M.G., and Dantuma,N.P. (2005). Endoplasmic reticulum stress compromises the ubiquitin-proteasome system. Hum. Mol. Genet. *14*, 2787-2799.

Meng,L., Mohan,R., Kwok,B.H., Elofsson,M., Sin,N., and Crews,C.M. (1999). Epoxomicin, a potent and selective proteasome inhibitor, exhibits in vivo antiinflammatory activity. Proc. Natl. Acad. Sci. U. S. A *96*, 10403-10408.

Merz,P.A., Somerville,R.A., Wisniewski,H.M., and Iqbal,K. (1981). Abnormal fibrils from scrapie-infected brain. Acta Neuropathol. *54*, 63-74.

Meusser,B., Hirsch,C., Jarosch,E., and Sommer,T. (2005). ERAD: the long road to destruction. Nat. Cell Biol. *7*, 766-772.

Miller,M.W. and Williams,E.S. (2003). Prion disease: horizontal prion transmission in mule deer. Nature *425*, 35-36.

Mironov,A., Jr., Latawiec,D., Wille,H., Bouzamondo-Bernstein,E., Legname,G., Williamson,R.A., Burton,D., DeArmond,S.J., Prusiner,S.B., and Peters,P.J. (2003). Cytosolic prion protein in neurons. J. Neurosci. *23*, 7183-7193.

Mishra,R.S., Bose,S., Gu,Y., Li,R., and Singh,N. (2003). Aggresome formation by mutant prion proteins: the unfolding role of proteasomes in familial prion disorders. J. Alzheimers. Dis. *5*, 15-23.

Mizushima,N. (2005). The pleiotropic role of autophagy: from protein metabolism to bactericide. Cell Death Differ. *12*, 1535-1541.

Mizushima,N., Levine,B., Cuervo,A.M., and Klionsky,D.J. (2008). Autophagy fights disease through cellular self-digestion. Nature *451*, 1069-1075.

Mizushima,N. and Yoshimori,T. (2007). How to interpret LC3 immunoblotting. Autophagy. *3*, 542-545.

Moore,R.A., Vorberg,I., and Priola,S.A. (2005). Species barriers in prion diseases--brief review. Arch. Virol. Suppl 187-202.

Morales,R., Abid,K., and Soto,C. (2007). The prion strain phenomenon: molecular basis and unprecedented features. Biochim. Biophys. Acta *1772*, 681-691.

Morris,R.J., Parkyn,C.J., and Jen,A. (2006). Traffic of prion protein between different compartments on the neuronal surface, and the propagation of prion disease. FEBS Lett. *580*, 5565-5571.

Mouillet-Richard,S., Ermonval,M., Chebassier,C., Laplanche,J.L., Lehmann,S., Launay,J.M., and Kellermann,O. (2000). Signal transduction through prion protein. Science *289*, 1925-1928.

Mould,D.L., Smith,W., and Dawson,A.M. (1965). Centrifugation studies on the infectivities of cellular fractions derived from mouse brain infected with scrapie (Suffolk strain). J. Gen. Microbiol. *40*, 71-79.

Muramoto,T., DeArmond,S., Scott,M., Telling,G.C., Cohen,F.E., and Prusiner,S.B. (1997). Heritable disorder reseming neuronal storage disease in mice expressing prion protein with deletion of an alpha-helix. Nature Med. *3*, 750-755.

Myllykangas,L., Tyynela,J., Page-McCaw,A., Rubin,G.M., Haltia,M.J., and Feany,M.B. (2005). Cathepsin D-deficient Drosophila recapitulate the key features of neuronal ceroid lipofuscinoses. Neurobiol. Dis. *19*, 194-199.

Naslavsky,N., Shmeeda,H., Friedlander,G., Yanai,A., Futerman,A.H., Barenholz,Y., and Taraboulos,A. (1999). Sphingolipid depletion increases formation of the scrapie prion protein in neuroblastoma cells infected with prions. J. Biol. Chem. *274*, 20763-20771.

Naslavsky,N., Stein,R., Yanai,A., Friedlander,G., and Taraboulos,A. (1997). Characterization of detergent-insoluble complexes containing the cellular prion protein and its scrapie isoform. J. Biol. Chem. *272*, 6324-6331.

Navon,A. and Goldberg,A.L. (2001). Proteins are unfolded on the surface of the ATPase ring before transport into the proteasome. Mol. Cell *8*, 1339-1349.

Nedelsky,N.B., Todd,P.K., and Taylor,J.P. (2008). Autophagy and the ubiquitin-proteasome system: collaborators in neuroprotection. Biochim. Biophys. Acta *1782*, 691-699.

Negro,A., Ballarin,C., Bertoli,A., Massimino,M.L., and Sorgato,M.C. (2001). The metabolism and imaging in live cells of the bovine prion protein in its native form or carrying single amino acid substitutions. Mol. Cell. Neurosci. *17*, 521-538.

Nixon,R.A., Wegiel,J., Kumar,A., Yu,W.H., Peterhoff,C., Cataldo,A., and Cuervo,A.M. (2005). Extensive involvement of autophagy in Alzheimer disease: an immuno-electron microscopy study. J. Neuropathol. Exp. Neurol. *64*, 113-122.

Noda,T. and Ohsumi,Y. (1998). Tor, a phosphatidylinositol kinase homologue, controls autophagy in yeast. J. Biol. Chem. *273*, 3963-3966.

Nussbaum,A.K., Dick,T.P., Keilholz,W., Schirle,M., Stevanovic,S., Dietz,K., Heinemeyer,W., Groll,M., Wolf,D.H., Huber,R., Rammensee,H.G., and Schild,H. (1998). Cleavage motifs of the yeast 20S proteasome beta subunits deduced from digests of enolase 1. Proc. Natl. Acad. Sci. U. S. A *95*, 12504-12509.

O'Donovan,C.N., Tobin,D., and Cotter,T.G. (2001). Prion protein fragment PrP-(106-126) induces apoptosis via mitochondrial disruption in human neuronal SH-SY5Y cells. J. Biol. Chem. *276*, 43516-43523.

Oesch,B., Westaway,D., Walchli,M., McKinley,M.P., Kent,S.B.H., Aebersold,R., Barry,R.A., Tempst,P., Teplow,D.B., Hood,L.E., Prusiner,S.B., and Weissmann,C. (1985). A Cellular Gene Encodes Scrapie Prp 27-30 Protein. Cell *40*, 735-746.

Olzmann,J.A., Li,L., and Chin,L.S. (2008). Aggresome formation and neurodegenerative diseases: therapeutic implications. Curr. Med. Chem. *15*, 47-60.

Orlowski,M. (1990). The multicatalytic proteinase complex, a major extralysosomal proteolytic system. Biochemistry *29*, 10289-10297.

Orlowski,M. and Wilk,S. (2003). Ubiquitin-independent proteolytic functions of the proteasome. Arch. Biochem. Biophys. *415*, 1-5.

Owen,F., Poulter,M., Lofthouse,R., Collinge J, Crow,T.J., Risby,D., Baker,H.F., Ridley,R.M., Hsiao,K., and Prusiner,S.B. (1989). Insertion in prion protein gene in familial Creutzfeldt-Jakob disease. Lancet *1*, 51-52.

Palmer,M.S., Dryden,A.J., Hughes,J.T., and Collinge J (1991). Homozygous prion protein genotype predisposes to sporadic Creutzfeldt-Jakob disease. Nature *352*, 340-342.

Palombella,V.J., Rando,O.J., Goldberg,A.L., and Maniatis,T. (1994). The ubiquitin-proteasome pathway is required for processing the NF-kappa B1 precursor protein and the activation of NF-kappa B. Cell *78*, 773-785.

Pan,K.M., Baldwin,M., Nguyen,J., Gasset,M., Serban,A., Groth,D., Mehlhorn,I., Huang,Z., Fletterick,R.J., Cohen,F.E., and . (1993). Conversion of alpha-helices into beta-sheets features in the formation of the scrapie prion proteins. Proc. Natl. Acad. Sci. U. S. A *90*, 10962-10966.

Pan,T., Kondo,S., Zhu,W., Xie,W., Jankovic,J., and Le,W. (2008). Neuroprotection of rapamycin in lactacystin-induced neurodegeneration via autophagy enhancement. Neurobiol. Dis. *32*, 16-25.

Pan,T., Wong,B.S., Liu,T., Li,R., Petersen,R.B., and Sy,M.S. (2002). Cell-surface prion protein interacts with glycosaminoglycans. Biochem. J. *368*, 81-90.

Pandey,U.B., Nie,Z., Batlevi,Y., McCray,B.A., Ritson,G.P., Nedelsky,N.B., Schwartz,S.L., DiProspero,N.A., Knight,M.A., Schuldiner,O., Padmanabhan,R., Hild,M., Berry,D.L., Garza,D., Hubbert,C.C., Yao,T.P., Baehrecke,E.H., and Taylor,J.P. (2007). HDAC6 rescues neurodegeneration and provides an essential link between autophagy and the UPS. Nature *447*, 859-863.

Parchi,P., Castellani,R., Capellari,S., Ghetti,B., Young,K., Chen,S.G., Farlow,M., Dickson,D.W., Sima,A.A., Trojanowski,J.Q., Petersen,R.B., and Gambetti,P. (1996). Molecular basis of phenotypic variability in sporadic Creutzfeldt-Jakob disease. Ann. Neurol. *39*, 767-778.

Parchi,P., Giese,A., Capellari,S., Brown,P., Schulz-Schaeffer,W., Windl,O., Zerr,I., Budka,H., Kopp,N., Piccardo,P., Poser,S., Rojiani,A., Streichemberger,N., Julien,J., Vital,C., Ghetti,B., Gambetti,P., and Kretzschmar,H. (1999). Classification of sporadic Creutzfeldt-Jakob disease based on molecular and phenotypic analysis of 300 subjects. Ann. Neurol. *46*, 224-233.

Park,T.S., Kleinman,G.M., and Richardson,E.P. (1980). Creutzfeldt-Jakob disease with extensive degeneration of white matter. Acta Neuropathol. *52*, 239-242.

Parkin,E.T., Watt,N.T., Hussain,I., Eckman,E.A., Eckman,C.B., Manson,J.C., Baybutt,H.N., Turner,A.J., and Hooper,N.M. (2007). Cellular prion protein regulates beta-secretase cleavage of the Alzheimer's amyloid precursor protein. Proc. Natl. Acad. Sci. U. S. A *104*, 11062-11067.

Parkyn,C.J., Vermeulen,E.G., Mootoosamy,R.C., Sunyach,C., Jacobsen,C., Oxvig,C., Moestrup,S., Liu,Q., Bu,G., Jen,A., and Morris,R.J. (2008). LRP1 controls biosynthetic and endocytic trafficking of neuronal prion protein. J. Cell Sci. *121*, 773-783.

Parry,H.B. (1979). Elimination of natural scrapie in sheep by sire genotype selection. Nature *277*, 127-129.

Peden,A.H., Head,M.W., Ritchie,D.L., Bell,J.E., and Ironside,J.W. (2004). Preclinical vCJD after blood transfusion in a PRNP codon 129 heterozygous patient. Lancet *364*, 527-529.

Peden,A.H., Ritchie,D.L., Head,M.W., and Ironside,J.W. (2006). Detection and localization of PrPSc in the skeletal muscle of patients with variant, iatrogenic, and sporadic forms of Creutzfeldt-Jakob disease. Am. J. Pathol. *168*, 927-935.

Peden,A.H., Ritchie,D.L., and Ironside,J.W. (2005). Risks of transmission of variant Creutzfeldt-Jakob disease by blood transfusion. Folia Neuropathol. *43*, 271-278.

Peng,J., Schwartz,D., Elias,J.E., Thoreen,C.C., Cheng,D., Marsischky,G., Roelofs,J., Finley,D., and Gygi,S.P. (2003). A proteomics approach to understanding protein ubiquitination. Nat. Biotechnol. *21*, 921-926.

Peretz,D., Scott,M.R., Groth,D., Williamson,R.A., Burton,D.R., Cohen,F.E., and Prusiner,S.B. (2001a). Strain-specified relative conformational stability of the scrapie prion protein. Prot. Sci. *10*, 854-863.

Peretz,D., Williamson,R.A., Kaneko,K., Vergara,J., Leclerc,E., Schmitt-Ulms,G., Mehlhorn,I.R., Legname,G., Wormald,M.R., Rudd,P.M., Dwek,R.A., Burton,D.R., and Prusiner,S.B. (2001b). Antibodies inhibit prion propagation and clear cell cultures of prion infectivity. Nature *412*, 739-743.

Perkins,N.D. and Gilmore,T.D. (2006). Good cop, bad cop: the different faces of NF-kappaB. Cell Death. Differ. *13*, 759-772.

Peters,P.J., Mironov,A., Jr., Peretz,D., van Donselaar,E., Leclerc,E., Erpel,S., DeArmond,S.J., Burton,D.R., Williamson,R.A., Vey,M., and Prusiner,S.B. (2003). Trafficking of prion proteins through a caveolae-mediated endosomal pathway. J. Cell Biol. *162*, 703-717.

Petersen,A., Larsen,K.E., Behr,G.G., Romero,N., Przedborski,S., Brundin,P., and Sulzer,D. (2001). Expanded CAG repeats in exon 1 of the Huntington's disease gene stimulate dopamine-mediated striatal neuron autophagy and degeneration. Hum. Mol. Genet. *10*, 1243-1254.

Piccardo,P., Manson,J.C., King,D., Ghetti,B., and Barron,R.M. (2007). Accumulation of prion protein in the brain that is not associated with transmissible disease. Proc. Natl. Acad. Sci U. S A *104*, 4712-4717.

Pickart,C.M. and Cohen,R.E. (2004). Proteasomes and their kin: proteases in the machine age. Nat. Rev. Mol. Cell Biol. *5*, 177-187.

Pickart,C.M. and Fushman,D. (2004). Polyubiquitin chains: polymeric protein signals. Curr. Opin. Chem. Biol. *8*, 610-616.

Powell,S.R. (2006). The ubiquitin-proteasome system in cardiac physiology and pathology. Am. J. Physiol Heart Circ. Physiol *291*, H1-H19.

Prusiner,S.B. (1982). Novel proteinaceous infectious particles cause scrapie. Science *216*, 136-144.

Prusiner,S.B. (1998). Prions. Proc. Natl. Acad. Sci. U. S. A *95*, 13363-13383.

Prusiner,S.B., Bolton,D.C., Groth,D.F., Bowman,K., Cochran,S.P., and Mc Kinley,M.P. (1982a). Further purification and characterization of scrapie prions. Biochemistry *21*, 6942-6950.

Prusiner,S.B., Cochran,S.P., Groth,D.F., Downey,D.E., Bowman,K.A., and Martinez,H.M. (1982b). Measurement of the scrapie agent using an incubation time interval assay. Ann. Neurol. *11*, 353-358.

Prusiner,S.B., Garfin,D.E., Cochran,S.P., McKinley,M.P., Groth,D.F., Hadlow,W.J., Race,R.E., and Eklund,C.M. (1980a). Experimental scrapie in the mouse: electrophoretic and sedimentation properties of the partially purified agent. J. Neurochem. *35*, 574-582.

Prusiner,S.B., Groth,D.F., Cochran,S.P., Masiarz,F.R., McKinley,M.P., and Martinez,H.M. (1980b). Molecular properties, partial purification, and assay by incubation period measurements of the hamster scrapie agent. Biochemistry *19*, 4883-4891.

Prusiner,S.B., Groth,D.F., Cochran,S.P., McKinley,M.P., and Masiarz,F.R. (1980c). Gel electrophoresis and glass permeation chromatography of the hamster scrapie agent after enzymatic digestion and detergent extraction. Biochemistry *19*, 4892-4898.

Prusiner,S.B., Hadlow,W.J., Eklund,C.M., and Race,R.E. (1977). Sedimentation properties of the scrapie agent. Proc. Natl. Acad. Sci. U. S. A *74*, 4656-4660.

Prusiner,S.B., Hadlow,W.J., Eklund,C.M., Race,R.E., and Cochran,S.P. (1978). Sedimentation characteristics of the scrapie agent from murine spleen and brain. Biochemistry *17*, 4987-4992.

Prusiner,S.B., McKinley,M.P., Bowman,K., Bolton,D.C., Bendheim,P.E., Groth,D.F., and Glenner,G.G. (1983). Scrapie prions aggregate to form amyloid-like birefringent rods. Cell *35*, 349-358.

Prusiner,S.B., McKinley,M.P., Groth,D.F., Bowman,K., Mock,N.I., Cochran,S.P., and Masiarz,F.R. (1981). Scrapie agent contains a hydrophobic protein. Proc. Natl. Acad. Sci. U. S. A. *78*, 6675-6679.

Puhler,G., Weinkauf,S., Bachmann,L., Muller,S., Engel,A., Hegerl,R., and Baumeister,W. (1992). Subunit stoichiometry and three-dimensional arrangement in proteasomes from Thermoplasma acidophilum. EMBO J. *11*, 1607-1616.

Rabl,J., Smith,D.M., Yu,Y., Chang,S.C., Goldberg,A.L., and Cheng,Y. (2008). Mechanism of gate opening in the 20S proteasome by the proteasomal ATPases. Mol. Cell *30*, 360-368.

Race,R., Meade-White,K., Raines,A., Raymond,G.J., Caughey,B., and Chesebro,B. (2002). Subclinical Scrapie Infection in a Resistant Species: Persistence, Replication, and Adaptation of Infectivity during Four Passages. J. Infect. Dis. *186*, S166-S170.

Race,R., Raines,A., Raymond,G.J., Caughey,B., and Chesebro,B. (2001). Long-term subclinical carrier state precedes scrapie replication and adaptation in a resistant species: analogies to bovine spongiform encephalopathy and variant Creutzfeldt-Jakob disease in humans. J. Virol. *75*, 10106-10112.

Rambold,A.S., Miesbauer,M., Rapaport,D., Bartke,T., Baier,M., Winklhofer,K.F., and Tatzelt,J. (2006). Association of Bcl-2 with misfolded prion protein is linked to the toxic potential of cytosolic PrP. Mol. Biol. Cell *17*, 3356-3368.

Rambold,A.S., Muller,V., Ron,U., Ben Tal,N., Winklhofer,K.F., and Tatzelt,J. (2008). Stress-protective signalling of prion protein is corrupted by scrapie prions. EMBO J. *27*, 1974-1984.

Rane,N.S., Kang,S.W., Chakrabarti,O., Feigenbaum,L., and Hegde,R.S. (2008). Reduced translocation of nascent prion protein during ER stress contributes to neurodegeneration. Dev. Cell *15*, 359-370.

Rane,N.S., Yonkovich,J.L., and Hegde,R.S. (2004). Protection from cytosolic prion protein toxicity by modulation of protein translocation. EMBO J. *23*, 4550-4559.

Ranson,N.A., Burston,S.G., and Clarke,A.R. (1997). Binding, encapsulation and ejection: substrate dynamics during a chaperonin-assisted folding reaction. J. Mol. Biol. *266*, 656-664.

Ravikumar,B., Duden,R., and Rubinsztein,D.C. (2002). Aggregate-prone proteins with polyglutamine and polyalanine expansions are degraded by autophagy. Hum. Mol. Genet. *11*, 1107-1117.

Ravikumar,B., Vacher,C., Berger,Z., Davies,J.E., Luo,S., Oroz,L.G., Scaravilli,F., Easton,D.F., Duden,R., O'Kane,C.J., and Rubinsztein,D.C. (2004). Inhibition of mTOR induces autophagy

and reduces toxicity of polyglutamine expansions in fly and mouse models of Huntington disease. Nat. Genet. *36*, 585-595.

Raymond,G.J., Hope,J., Kocisko,D.A., Priola,S.A., Raymond,L.D., Bossers,A., Ironside,J., Will,R.G., Chen,S.G., Petersen,R.B., Gambetti,P., Rubenstein,R., Smits,M.A., Lansbury,P.T., and Caughey,B. (1997). Molecular assessment of the potential transmissibilities of BSE and scrapie to humans. Nature *388*, 285-288.

Reggiori,F. (2006). 1. Membrane origin for autophagy. Curr. Top. Dev. Biol. *74*, 1-30.

Rideout,H.J., Larsen,K.E., Sulzer,D., and Stefanis,L. (2001). Proteasomal inhibition leads to formation of ubiquitin/alpha-synuclein-immunoreactive inclusions in PC12 cells. J. Neurochem. *78*, 899-908.

Rieger,R., Edenhofer,F., Lasmézas,C.I., and Weiss,S. (1997). The human 37-kDa laminin receptor precursor interacts with the prion protein in eukaryotic cells. Nat. Med. *3*, 1383-1388.

Riek,R., Hornemann,S., Wider,G., Billeter,M., Glockshuber,R., and Wuthrich,K. (1996). NMR structure of the mouse prion protein domain PrP (121-231). Nature *382*, 180-182.

Riek,R., Wider,G., Billeter,M., Hornemann,S., Glockshuber,R., and Wuthrich,K. (1998). Prion protein NMR structure and familial human spongiform encephalopathies. Proc. Natl. Acad. Sci. U. S. A *95*, 11667-11672.

Riesner,D. (2003). Biochemistry and structure of PrP(C) and PrP(Sc). Br. Med. Bull. *66*, 21-33.

Rosenzweig,R., Osmulski,P.A., Gaczynska,M., and Glickman,M.H. (2008). The central unit within the 19S regulatory particle of the proteasome. Nat. Struct. Mol. Biol. *15*, 573-580.

Ross,C.A. and Pickart,C.M. (2004). The ubiquitin-proteasome pathway in Parkinson's disease and other neurodegenerative diseases. Trends Cell Biol. *14*, 703-711.

Ross,C.A. and Poirier,M.A. (2004). Protein aggregation and neurodegenerative disease. Nat. Med. *10*, S10-S17.

Ross,C.A. and Poirier,M.A. (2005). Opinion: What is the role of protein aggregation in neurodegeneration? Nat. Rev. Mol. Cell Biol. *6*, 891-898.

Roucou,X., Guo,Q., Zhang,Y., Goodyer,C.G., and LeBlanc,A.C. (2003). Cytosolic prion protein is not toxic and protects against Bax-mediated cell death in human primary neurons. J. Biol. Chem. *278*, 40877-40881.

Rubenstein,R., Carp,R.I., and Callahan,S.M. (1984). In vitro replication of scrapie agent in a neuronal model: infection of PC12 cells. J Gen. Virol. *65*, 2191-2198.

Rubinsztein,D.C. (2006). The roles of intracellular protein-degradation pathways in neurodegeneration. Nature *443*, 780-786.

Rubinsztein,D.C., DiFiglia,M., Heintz,N., Nixon,R.A., Qin,Z.H., Ravikumar,B., Stefanis,L., and Tolkovsky,A. (2005). Autophagy and its possible roles in nervous system diseases, damage and repair. Autophagy. *1*, 11-22.

Rudd,P.M., Endo,T., Colominas,C., Groth,D., Wheeler,S.F., Harvey,D.J., Wormald,M.R., Serban,H., Prusiner,S.B., Kobata,A., and Dwek,R.A. (1999). Glycosylation differences between the normal and pathogenic prion protein isoforms. Proc. Natl. Acad. Sci. USA *96*, 13044-13049.

Rudd,P.M., Wormald,M.R., Wing,D.R., Prusiner,S.B., and Dwek,R.A. (2001). Prion glycoprotein: Structure, dynamics, and roles for the sugars. Biochemistry *40*, 3759-3766.

Safar,J., Wang,W., Padgett,M.P., Ceroni,M., Piccardo,P., Zopf,D., Gajdusek,D.C., and Gibbs,C.J.Jr. (1990). Molecular mass, biochemical composition, and physicochemical behavior of the infectious form of the scrapie precursor protein monomer. Proc. Natl. Acad. Sci. U. S. A. *87*, 6373-6377.

Sandvig,K. and van Deurs,B. (2002). Membrane traffic exploited by protein toxins. Annu. Rev. Cell Dev. Biol. *18*, 1-24.

Santuccione,A., Sytnyk,V., Leshchyns'ka,I., and Schachner,M. (2005). Prion protein recruits its neuronal receptor NCAM to lipid rafts to activate p59fyn and to enhance neurite outgrowth. J. Cell Biol. *169*, 341-354.

Sapp,E., Schwarz,C., Chase,K., Bhide,P.G., Young,A.B., Penney,J., Vonsattel,J.P., Aronin,N., and DiFiglia,M. (1997). Huntingtin localization in brains of normal and Huntington's disease patients. Ann. Neurol. *42*, 604-612.

Sarkar,S., Davies,J.E., Huang,Z., Tunnacliffe,A., and Rubinsztein,D.C. (2007). Trehalose, a novel mTOR-independent autophagy enhancer, accelerates the clearance of mutant huntingtin and alpha-synuclein. J. Biol. Chem. *282*, 5641-5652.

Sarkar,S., Krishna,G., Imarisio,S., Saiki,S., O'Kane,C.J., and Rubinsztein,D.C. (2008). A rational mechanism for combination treatment of Huntington's disease using lithium and rapamycin. Hum. Mol. Genet. *17*, 170-178.

Sarkar,S., Ravikumar,B., Floto,R.A., and Rubinsztein,D.C. (2009). Rapamycin and mTOR-independent autophagy inducers ameliorate toxicity of polyglutamine-expanded huntingtin and related proteinopathies. Cell Death. Differ. *16*, 46-56.

Sarnataro,D., Campana,V., Paladino,S., Stornaiuolo,M., Nitsch,L., and Zurzolo,C. (2004). PrP(C) association with lipid rafts in the early secretory pathway stabilizes its cellular conformation. Mol. Biol. Cell *15*, 4031-4042.

Sarnataro,D., Paladino,S., Campana,V., Grassi,J., Nitsch,L., and Zurzolo,C. (2002). PrPC Is Sorted to the Basolateral Membrane of Epithelial Cells Independently of its Association with Rafts. Traffic. *3*, 810-821.

Schatzl,H.M., Laszlo,L., Holtzman,D.M., Tatzelt,J., DeArmond,S.J., Weiner,R.I., Mobley,W.C., and Prusiner,S.B. (1997). A hypothalamic neuronal cell line persistently infected with scrapie prions exhibits apoptosis. J. Virol. *71*, 8821-8831.

Schmitt-Ulms,G., Legname,G., Baldwin,M.A., Ball,H.L., Bradon,N., Bosque,P.J., Crossin,K.L., Edelman,G.M., DeArmond,S.J., Cohen,F.E., and Prusiner,S.B. (2001). Binding of neural cell adhesion molecules (N-CAMs) to the cellular prion protein. J. Mol. Biol. *314*, 1209-1225.

Schousboe,A. and Pasantes-Morales,H. (1989). Potassium-stimulated release of [3H]taurine from cultured GABAergic and glutamatergic neurons. J. Neurochem. *53*, 1309-1315.

Scott,M.R., Groth,D., Tatzelt,J., Torchia,M., Tremblay,P., DeArmond,S.J., and Prusiner,S.B. (1997). Propagation of prion strains through specific conformers of the prion protein. J. Virol. *71*, 9032-9044.

Seemuller,E., Lupas,A., Stock,D., Lowe,J., Huber,R., and Baumeister,W. (1995). Proteasome from Thermoplasma-Acidophilum - A Threonine Protease. Science *268*, 579-582.

Semancik,J.S., Marsh,R.F., Geelen,J.L., and Hanson,R.P. (1976). Properties of the scrapie agent-endomembrane complex from hamster brain. J. Virol. *18*, 693-700.

Semple,C.A. (2003). The comparative proteomics of ubiquitination in mouse. Genome Res. *13*, 1389-1394.

Seo,H., Sonntag,K.C., and Isacson,O. (2004). Generalized brain and skin proteasome inhibition in Huntington's disease. Ann. Neurol. *56*, 319-328.

Serio,T.R. and Lindquist,S.L. (2000). Protein-only inheritance in yeast: something to get [PSI+]-ched about. Trends Cell Biol. *10*, 98-105.

Shacka,J.J., Klocke,B.J., Young,C., Shibata,M., Olney,J.W., Uchiyama,Y., Saftig,P., and Roth,K.A. (2007). Cathepsin D deficiency induces persistent neurodegeneration in the absence of Bax-dependent apoptosis. J. Neurosci. *27*, 2081-2090.

Sherman,M.Y. and Goldberg,A.L. (2001). Cellular defenses against unfolded proteins: a cell biologist thinks about neurodegenerative diseases. Neuron *29*, 15-32.

Shimura,H., Hattori,N., Kubo,S., Mizuno,Y., Asakawa,S., Minoshima,S., Shimizu,N., Iwai,K., Chiba,T., Tanaka,K., and Suzuki,T. (2000). Familial Parkinson disease gene product, parkin, is a ubiquitin-protein ligase. Nat. Genet. *25*, 302-305.

Shmerling,D., Hegyi,I., Fischer,M., Blättler,T., Brandner S, Götz,J., Rülicke,T., Flechsig,E., Cozzio,A., von Mering,C., Hangartner,C., Aguzzi,A., and Weissmann,C. (1998). Expression of amino-terminally truncated PrP in the mouse leading to ataxia and specific cerebellar lesions. Cell *93*, 203-214.

Shyng,S.L., Huber,M.T., and Harris,D.A. (1993). A prion protein cycles between the cell surface and an endocytic compartment in cultured neuroblastoma cells. J. Biol. Chem. *268*, 15922-15928.

Shyng,S.-L., Heuser,J.E., and Harris,D.A. (1994). A glycolipid-anchored prion protein is endocytosed via clathrin- coated pits. J. Cell Biol. *125*, 1239-1250.

Siakotos,A.N., Gajdusek,D.C., Gibbs,C.J.Jr., Traub,R.D., and Bucana,C. (1976). Partial purification of the scrapie agent from mouse brain by pressure disruption and zonal centrifugation in sucrose-sodium chloride gradients. Virology *70*, 230-237.

Sigurdson,C.J. and Aguzzi,A. (2007). Chronic wasting disease. Biochim. Biophys. Acta *1772*, 610-618.

Sikorska,B., Liberski,P.P., and Brown,P. (2007). Neuronal autophagy and aggresomes constitute a consistent part of neurodegeneration in experimental scrapie. Folia Neuropathol. *45*, 170-178.

Sikorska,B., Liberski,P.P., Giraud,P., Kopp,N., and Brown,P. (2004). Autophagy is a part of ultrastructural synaptic pathology in Creutzfeldt-Jakob disease: a brain biopsy study. Int. J. Biochem. Cell Biol. *36*, 2563-2573.

Silveira,J.R., Raymond,G.J., Hughson,A.G., Race,R.E., Sim,V.L., Hayes,S.F., and Caughey,B. (2005). The most infectious prion protein particles. Nature *437*, 257-261.

Simoneau,S., Rezaei,H., Sales,N., Kaiser-Schulz,G., Lefebvre-Roque,M., Vidal,C., Fournier,J.G., Comte,J., Wopfner,F., Grosclaude,J., Schatzl,H., and Lasmezas,C.I. (2007). In vitro and in vivo neurotoxicity of prion protein oligomers. PLoS Pathog. *3*, e125.

Simons,K. and Ikonen,E. (1997). Functional rafts in cell membranes. Nature *387*, 569-572.

Simonsen,A., Birkeland,H.C., Gillooly,D.J., Mizushima,N., Kuma,A., Yoshimori,T., Slagsvold,T., Brech,A., and Stenmark,H. (2004). Alfy, a novel FYVE-domain-containing protein associated with protein granules and autophagic membranes. J. Cell Sci. *117*, 4239-4251.

Smith,D.M., Chang,S.C., Park,S., Finley,D., Cheng,Y., and Goldberg,A.L. (2007). Docking of the proteasomal ATPases' carboxyl termini in the 20S proteasome's alpha ring opens the gate for substrate entry. Mol. Cell *27*, 731-744.

Smith,P.G. and Bradley,R. (2003). Bovine spongiform encephalopathy (BSE) and its epidemiology. Br. Med. Bull. *66*, 185-198.

Sokolowski,F., Modler,A.J., Masuch,R., Zirwer,D., Baier,M., Lutsch,G., Moss,D.A., Gast,K., and Naumann,D. (2003). Formation of critical oligomers is a key event during conformational transition of recombinant syrian hamster prion protein. J. Biol. Chem. *278*, 40481-40492.

Solforosi,L., Criado,J.R., McGavern,D.B., Wirz,S., Sanchez-Alavez,M., Sugama,S., DeGiorgio,L.A., Volpe,B.T., Wiseman,E., Abalos,G., Masliah,E., Gilden,D., Oldstone,M.B., Conti,B., and Williamson,R.A. (2004). Cross-linking cellular prion protein triggers neuronal apoptosis in vivo. Science *303*, 1514-1516.

Somerville,R.A. and Ritchie,L.A. (1990). Differential glycosylation of the protein (PrP) forming scrapie-associated fibrils. J. Gen. Virol. *71 (Pt 4)*, 833-839.

Soto,C. and Castilla,J. (2004). The controversial protein-only hypothesis of prion propagation. Nat. Med. *10 Suppl*, S63-S67.

Spencer,M.D., Knight,R.S., and Will,R.G. (2002). First hundred cases of variant Creutzfeldt-Jakob disease: retrospective case note review of early psychiatric and neurological features. BMJ *324*, 1479-1482.

Spraker,T.R., Zink,R.R., Cummings,B.A., Sigurdson,C.J., Miller,M.W., and O'Rourke,K.I. (2002). Distribution of protease-resistant prion protein and spongiform encephalopathy in free-ranging mule deer (Odocoileus hemionus) with chronic wasting disease. Vet. Pathol. *39*, 546-556.

Stahl,N., Baldwin,M.A., Teplow,D.B., Hood,L., Gibson,B.W., Burlingame,A.L., and Prusiner,S.B. (1993). Structural Studies of the scrapie prion protein using mass spectrometry and amino acid sequencing. Biochemistry *32*, 1991-2002.

Stahl,N., Borchelt,D.R., Hsiao,K., and Prusiner,S.B. (1987). Scrapie prion protein contains a phosphatidylinositol glycolipid. Cell *51*, 229-240.

Stahl,N., Borchelt,D.R., and Prusiner,S.B. (1990). Differential release of cellular and scrapie prion proteins from cellular membranes by phosphatidylinositol-specific phospholipase. Biochemistry *29*, 5405-5412.

Stephenson,D.A., Chiotti,K., Ebeling,C., Groth,D., DeArmond,S.J., Prusiner,S.B., and Carlson,G.A. (2000). Quantitative trait loci affecting prion incubation time in mice. Genomics *69*, 47-53.

Stewart,R.S., Piccardo,P., Ghetti,B., and Harris,D.A. (2005). Neurodegenerative illness in transgenic mice expressing a transmembrane form of the prion protein. J. Neurosci. *25*, 3469-3477.

Sunyach,C., Jen,A., Deng,J., Fitzgerald,K.T., Frobert,Y., Grassi,J., McCaffrey,M.W., and Morris,R. (2003). The mechanism of internalization of glycosylphosphatidylinositol-anchored prion protein. EMBO J. *22*, 3591-3601.

Supattapone,S. (2004). Prion protein conversion in vitro. J. Mol. Med. *82*, 348-356.

Swietnicki,W., Petersen,R.B., Gambetti,P., and Surewicz,W.K. (1998). Familial mutations and the thermodynamic stability of the recombinant human prion protein. J. Biol. Chem. *273*, 31048-31052.

Tahiri-Alaoui,A., Gill,A.C., Disterer,P., and James,W. (2004). Methionine 129 variant of human prion protein oligomerizes more rapidly than the valine 129 variant: implications for disease susceptibility to Creutzfeldt-Jakob disease. J. Biol. Chem. *279*, 31390-31397.

Tai,H.C. and Schuman,E.M. (2008). Ubiquitin, the proteasome and protein degradation in neuronal function and dysfunction. Nat. Rev. Neurosci. *9*, 826-838.

Tanaka,K., Ii,K., Ichihara,A., Waxman,L., and Goldberg,A.L. (1986). A high molecular weight protease in the cytosol of rat liver. I. Purification, enzymological properties, and tissue distribution. J. Biol. Chem. *261*, 15197-15203.

Tanaka,M., Machida,Y., Niu,S., Ikeda,T., Jana,N.R., Doi,H., Kurosawa,M., Nekooki,M., and Nukina,N. (2004). Trehalose alleviates polyglutamine-mediated pathology in a mouse model of Huntington disease. Nat. Med. *10*, 148-154.

Tanida,I., Minematsu-Ikeguchi,N., Ueno,T., and Kominami,E. (2005). Lysosomal turnover, but not a cellular level, of endogenous LC3 is a marker for autophagy. Autophagy. *1*, 84-91.

Taraboulos,A., Raeber,A., Borchelt,D.R., Serban,D., and Prusiner,S.B. (1992). Synthesis and trafficking of prion proteins in cultured cells. Mol. Biol. of the Cell *3*, 851-863.

Taraboulos,A., Scott,M., Semenov,A., Avraham,D., Laszlo,L., and Prusiner,S.B. (1995). Cholesterol depletion and modification of COOH-terminal targeting sequence of the prion protein inhibit formation of the scrapie isoform. J. Cell Biol. *129*, 121-132.

Tarcsa,E., Szymanska,G., Lecker,S., O'Connor,C.M., and Goldberg,A.L. (2000). Ca2+-free calmodulin and calmodulin damaged by in vitro aging are selectively degraded by 26 S proteasomes without ubiquitination. J. Biol. Chem. *275*, 20295-20301.

Tattum,M.H., Cohen-Krausz,S., Thumanu,K., Wharton,C.W., Khalili-Shirazi,A., Jackson,G.S., Orlova,E.V., Collinge,J., Clarke,A.R., and Saibil,H.R. (2006). Elongated oligomers assemble into mammalian PrP amyloid fibrils. J. Mol. Biol. *357*, 975-985.

Taylor,D.R. and Hooper,N.M. (2007). The low-density lipoprotein receptor-related protein 1 (LRP1) mediates the endocytosis of the cellular prion protein. Biochem. J. *402*, 17-23.

Taylor,D.R., Watt,N.T., Perera,W.S., and Hooper,N.M. (2005). Assigning functions to distinct regions of the N-terminus of the prion protein that are involved in its copper-stimulated, clathrin-dependent endocytosis. J. Cell Sci. *118*, 5141-5153.

Taylor,J.P., Hardy,J., and Fischbeck,K.H. (2002). Toxic proteins in neurodegenerative disease. Science *296*, 1991-1995.

Taylor,J.P., Tanaka,F., Robitschek,J., Sandoval,C.M., Taye,A., Markovic-Plese,S., and Fischbeck,K.H. (2003). Aggresomes protect cells by enhancing the degradation of toxic polyglutamine-containing protein. Hum. Mol. Genet. *12*, 749-757.

Telling,G.C., Tremblay,P., Torchia,M., DeArmond,S.J., Cohen,F.E., and Prusiner,S.B. (1997). N-terminally tagged prion protein supports prion propagation in transgenic mice. Protein Science *6*, 825-833.

Thellung,S., Florio,T., Corsaro,A., Arena,S., Merlino,M., Salmona,M., Tagliavini,F., Bugiani,O., Forloni,G., and Schettini,G. (2000). Intracellular mechanisms mediating the neuronal death and astrogliosis induced by the prion protein fragment 106-126. Int. J. Dev. Neurosci. *18*, 481-492.

Tilly,G., Chapuis,J., Vilette,D., Laude,H., and Vilotte,J.L. (2003). Efficient and specific down-regulation of prion protein expression by RNAi. Biochem. Biophys. Res. Commun. *305*, 548-551.

Tobler,I., Gaus,S.E., Deboer,T., Achermann,P., Fischer,M., Rulicke,T., Moser,M., Oesch,B., McBride,P.A., and Manson,J.C. (1996). Altered circadian activity rhythms and sleep in mice devoid of prion protein. Nature *380*, 639-642.

Trevitt,C.R. and Collinge,J. (2006). A systematic review of prion therapeutics in experimental models. Brain *129*, 2241-2265.

Turk,E., Teplow,D.B., Hood,L.E., and Prusiner,S.B. (1988). Purification and properties of the cellular and scrapie hamster prion proteins. Eur. J. Biochem. *176*, 21-30.

Turnbull,S., Tabner,B.J., Brown,D.R., and Allsop,D. (2003). Quinacrine acts as an antioxidant and reduces the toxicity of the prion peptide PrP106-126. Neuroreport *14*, 1743-1745.

Vanik,D.L., Surewicz,K.A., and Surewicz,W.K. (2004). Molecular basis of barriers for interspecies transmissibility of mammalian prions. Mol. Cell *14*, 139-145.

Vassallo,N. and Herms,J. (2003). Cellular prion protein function in copper homeostasis and redox signalling at the synapse. J. Neurochem. *86*, 538-544.

Venkatraman,P., Wetzel,R., Tanaka,M., Nukina,N., and Goldberg,A.L. (2004). Eukaryotic proteasomes cannot digest polyglutamine sequences and release them during degradation of polyglutamine-containing proteins. Mol. Cell *14*, 95-104.

Verhoef,L.G., Lindsten,K., Masucci,M.G., and Dantuma,N.P. (2002). Aggregate formation inhibits proteasomal degradation of polyglutamine proteins. Hum. Mol. Genet. *11*, 2689-2700.

Vey,M., Pilkuhn,S., Wille,H., Nixon,R., DeArmond,S.J., Smart,E.J., Anderson,R.G.W., Taraboulos,A., and Prusiner,S.B. (1996). Subcellular colocalization of the cellular and scrapie prion proteins in caveolae-like membranous domains. Proc. Natl. Acad. Sci. USA *93*, 14945-14949.

Voges,D., Zwickl,P., and Baumeister,W. (1999). The 26S proteasome: a molecular machine designed for controlled proteolysis. Annu. Rev. Biochem. *68:1015-68.*, 1015-1068.

Vollmert,C., Windl,O., Xiang,W., Rosenberger,A., Zerr,I., Wichmann,H.E., Bickeboller,H., Illig,T., and Kretzschmar,H.A. (2006). Significant association of a M129V independent polymorphism in the 5' UTR of the PRNP gene with sporadic Creutzfeldt-Jakob disease in a large German case-control study. J. Med. Genet. *43*, e53.

Wadia,J.S., Schaller,M., Williamson,R.A., and Dowdy,S.F. (2008). Pathologic Prion Protein Infects Cells by Lipid-Raft Dependent Macropinocytosis. PLoS ONE *3*, e3314.

Wadsworth,J.D. and Collinge,J. (2007). Update on human prion disease. Biochim. Biophys. Acta *1772*, 598-609.

Wadsworth,J.D., Joiner,S., Fox,K., Linehan,J.M., Desbruslais,M., Brandner,S., Asante,E.A., and Collinge,J. (2007). Prion infectivity in variant Creutzfeldt-Jakob disease rectum. Gut *56*, 90-94.

Wadsworth,J.D., Joiner,S., Hill,A.F., Campbell,T.A., Desbruslais,M., Luthert,P.J., and Collinge,J. (2001). Tissue distribution of protease resistant prion protein in variant Creutzfeldt-Jakob disease using a highly sensitive immunoblotting assay. Lancet *358*, 171-180.

Wadsworth,J.D., Joiner,S., Linehan,J.M., Cooper,S., Powell,C., Mallinson,G., Buckell,J., Gowland,I., Asante,E.A., Budka,H., Brandner,S., and Collinge,J. (2006). Phenotypic heterogeneity in inherited prion disease (P102L) is associated with differential propagation of protease-resistant wild-type and mutant prion protein. Brain *129*, 1557-1569.

Wang,J., Wang,C.E., Orr,A., Tydlacka,S., Li,S.H., and Li,X.J. (2008). Impaired ubiquitin-proteasome system activity in the synapses of Huntington's disease mice. J. Cell Biol. *180*, 1177-1189.

Wang,Q.J., Ding,Y., Kohtz,D.S., Mizushima,N., Cristea,I.M., Rout,M.P., Chait,B.T., Zhong,Y., Heintz,N., and Yue,Z. (2006). Induction of autophagy in axonal dystrophy and degeneration. J. Neurosci. *26*, 8057-8068.

Wang,S., Herndon,M.E., Ranganathan,S., Godyna,S., Lawler,J., Argraves,W.S., and Liau,G. (2004). Internalization but not binding of thrombospondin-1 to low density lipoprotein receptor-related protein-1 requires heparan sulfate proteoglycans. J. Cell Biochem. *91*, 766-776.

Wang,X., Wang,F., Sy,M.S., and Ma,J. (2005). Calpain and other cytosolic proteases can contribute to the degradation of retro-translocated prion protein in the cytosol. J. Biol. Chem. *280*, 317-325.

Ward,H.J., Everington,D., Croes,E.A., Alperovitch,A., Delasnerie-Laupretre,N., Zerr,I., Poser,S., and van Duijn,C.M. (2002). Sporadic Creutzfeldt-Jakob disease and surgery: a case-control study using community controls. Neurology *59*, 543-548.

Warner,R.G., Hundt,C., Weiss,S., and Turnbull,J.E. (2002). Identification of the heparan sulfate binding sites in the cellular prion protein. J. Biol. Chem. *277*, 18421-18430.

Webb,J.L., Ravikumar,B., Atkins,J., Skepper,J.N., and Rubinsztein,D.C. (2003). Alpha-Synuclein is degraded by both autophagy and the proteasome. J. Biol. Chem. *278*, 25009-25013.

Weissmann,C. and Aguzzi,A. (1997). Bovine spongiform encephalopathy and early onset variant Creutzfeldt-Jakob disease. Curr. Opin. Neurobiol. *7*, 695-700.

Wenzel,T. and Baumeister,W. (1995). Conformational constraints in protein degradation by the 20S proteasome. Nat. Struct. Biol. *2*, 199-204.

Westergard,L., Christensen,H.M., and Harris,D.A. (2007). The cellular prion protein (PrP(C)): its physiological function and role in disease. Biochim. Biophys. Acta *1772*, 629-644.

Whitby,F.G., Masters,E.I., Kramer,L., Knowlton,J.R., Yao,Y., Wang,C.C., and Hill,C.P. (2000). Structural basis for the activation of 20S proteasomes by 11S regulators. Nature. *408*, 115-120.

White,A.R., Collins,S.J., Maher,F., Jobling,M.F., Stewart,L.R., Thyer,J.M., Beyreuther,K., Masters,C.L., and Cappai,R. (1999). Prion protein-deficient neurons reveal lower glutathione reductase activity and increased susceptibility to hydrogen peroxide toxicity. Am. J. Pathol. *155*, 1723-1730.

White,A.R., Enever,P., Tayebi,M., Mushens,R., Linehan J, Brandner S, Anstee,D., Collinge J, and Hawke,S. (2003). Monoclonal antibodies inhibit prion replication and delay the development of prion disease. Nature *422*, 80-83.

White,M.D., Farmer,M., Mirabile,I., Brandner,S., Collinge,J., and Mallucci,G.R. (2008). Single treatment with RNAi against prion protein rescues early neuronal dysfunction and prolongs survival in mice with prion disease. Proc. Natl. Acad. Sci. U. S. A *105*, 10238-10243.

Wickner,R.B. (1997). A new prion controls fungal cell fusion incompatibility. Proc. Natl. Acad. Sci. USA *94*, 10012-10014.

Wickner,R.B., Edskes,H.K., Shewmaker,F., and Nakayashiki,T. (2007). Prions of fungi: inherited structures and biological roles. Nat. Rev. Microbiol. *5*, 611-618.

Wilesmith,J.W., Ryan,J.B., and Atkinson,M.J. (1991). Bovine spongiform encephalopathy: epidemiological studies on the origin. Vet. Rec. *128*, 199-203.

Wilesmith,J.W., Wells,G.A., Cranwell,M.P., and Ryan,J.B. (1988). Bovine spongiform encephalopathy: epidemiological studies. Vet. Rec. *123*, 638-644.

Will,R.G., Ironside,J.W., Zeidler,M., Cousens,S.N., Estibeiro,K., Alperovitch,A., Poser,S., Pocchiari,M., Hofman,A., and Smith,P.G. (1996). A new variant of Creutzfeldt-Jakob disease in the UK. Lancet *347*, 921-925.

Williams,E.S. (2005). Chronic wasting disease. Vet. Pathol. *42*, 530-549.

Williams,E.S. and Miller,M.W. (2002). Chronic wasting disease in deer and elk in North America. Rev. Sci. Tech. *21*, 305-316.

Williams,E.S. and Young,S. (1980). Chronic wasting disease of captive mule deer: a spongiform encephalopathy. J. Wildl. Dis. *16*, 89-98.

Windl,O., Dempster,M., Estibeiro,P., and Lathe,R. (1995). A candidate marsupial *PrP* gene reveals two domains conserved in mammalian PrP proteins. Gene *159*, 181-186.

Windl,O., Giese,A., Schulz-Schaeffer,W., Zerr,I., Skworc,K., Arendt,S., Oberdieck,C., Bodemer,M., Poser,S., and Kretzschmar,H.A. (1999). Molecular genetics of human prion diseases in Germany. Hum. Genet. *105*, 244-252.

Wopfner,F., Weidenhofer,G., Schneider,R., von Brunn,A., Gilch,S., Schwarz,T.F., Werner,T., and Schatzl,H.M. (1999). Analysis of 27 mammalian and 9 avian PrPs reveals high conservation of flexible regions of the prion protein. J. Mol. Biol. *289*, 1163-1178.

Wroe,S.J., Pal S, Siddique,D., Hyare,H., Macfarlane,R., Joiner S, Linehan J, Brandner S, Wadsworth J, Hewitt,P., and Collinge J (2006). Clinical presentation and pre-mortem diagnosis of variant Creutzfeldt-Jakob disease associated with blood transfusion: a case report. Lancet *368*, 2061-2067.

Yamamoto,A., Cremona,M.L., and Rothman,J.E. (2006). Autophagy-mediated clearance of huntingtin aggregates triggered by the insulin-signaling pathway. J. Cell Biol. *172*, 719-731.

Yedidia,Y., Horonchik,L., Tzaban,S., Yanai,A., and Taraboulos,A. (2001). Proteasomes and ubiquitin are involved in the turnover of the wild-type prion protein. EMBO J. *20*, 5383-5391.

Zanusso,G., Petersen,R.B., Jin,T., Jing,Y., Kanoush,R., Ferrari,S., Gambetti,P., and Singh,N. (1999). Proteasomal degradation and N-terminal protease resistance of the codon 145 mutant prion protein. J. Biol. Chem. *274*, 23396-23404.

Zhang,C.C., Steele,A.D., Lindquist,S., and Lodish,H.F. (2006). Prion protein is expressed on long-term repopulating hematopoietic stem cells and is important for their self-renewal. Proc. Natl. Acad. Sci. U. S. A *103*, 2184-2189.

Zwickl,P., Baumeister,W., and Steven,A. (2000). Dis-assembly lines: the proteasome and related ATPase-assisted proteases. Curr. Opin. Struct. Biol. *10*, 242-250.

Zwickl,P., Grziwa,A., Puhler,G., Dahlmann,B., Lottspeich,F., and Baumeister,W. (1992). Primary structure of the Thermoplasma proteasome and its implications for the structure, function, and evolution of the multicatalytic proteinase. Biochemistry *31*, 964-972.

8 PUBLICATIONS RELATING TO THIS THESIS

Kristiansen, M.*, Deriziotis, P.*, Dimcheff, D.E., Jackson, G.S., Ovaa, H., Naumann, H., Clarke, A.R., van Leeuwen, F.W.B., Menéndez-Benito, V., Dantuma, N.P., Portis, J.L., Collinge, J., and Tabrizi, S.J. **2007**. Disease-associated prion protein oligomers inhibit the 26S proteasome. *Molecular Cell* 27:175-188. * *denotes equal first author*

Deriziotis, P., and Tabrizi, S.J. **2008**. Prions and the proteasome. *Biochimica et Biophysica Acta, Molecular Basis of Disease* 1782:713-722.

Mead, S., Poulter, M., Uphill, J., Beck, J., Whitfield, J., Webb, T.E., Campbell, T., Adamson, G., Deriziotis, P., Tabrizi, S.J., Hummerich, H., Verzilli, C., Alpers, M.P., Whittaker, J.C., Collinge, J. **2009**. Genetic risk factors for variant Creutzfeldt-Jakob disease: a genome-wide association study. *Lancet Neurology* 8:57-66